

2

AFWAL-TR-85-2003

LITHIUM CELL REACTIONS



W. Clark, F. Dampier
R. McDonald, A. Lombardi
D. Batson, T. Cole

GTE LABORATORIES, INC.
40 SYLVAN ROAD
WALTHAM, MASSACHUSETTS 02254

FEBRUARY 1985

FINAL REPORT FOR PERIOD DECEMBER 1981 - DECEMBER 1984

APPROVED FOR PUBLIC RELEASE; DISTRIBUTION UNLIMITED

DTIC
ELECTE
JUN 3 1985
S B D

AERO PROPULSION LABORATORY
AIR FORCE WRIGHT AERONAUTICAL LABORATORIES
AIR FORCE SYSTEMS COMMAND
WRIGHT PATTERSON AIR FORCE BASE, OHIO 45433-6563

AD-A154 429

DTIC FILE COPY

NOTICE

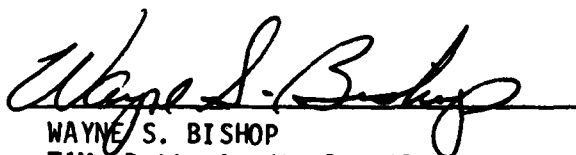
When Government drawings, specifications, or other data are used for any purpose other than in connection with a definitely related Government procurement operation, the United States Government thereby incurs no responsibility nor any obligation whatsoever; and the fact that the government may have formulated, furnished, or in any way supplied the said drawings, specifications, or other data, is not to be regarded by implication or otherwise as in any manner licensing the holder or any other person or corporation, or conveying any rights or permission to manufacture use, or sell any patented invention that may in any way be related thereto.

This report has been reviewed by the Office of Public Affairs (ASD/PA) and is releasable to the National Technical Information Service (NTIS). At NTIS, it will be available to the general public, including foreign nations.

This technical report has been reviewed and is approved for publication.



RICHARD A. MARSH
Batteries/Fuel Cells
Energy Conversion Branch
Aerospace Power Division



WAYNE S. BISHOP
TAM, Batteries/Fuel Cells
Energy Conversion Branch
Aerospace Power Division

FOR THE COMMANDER



JAMES D. REAMS
Chief, Aerospace Power Division
Aero Propulsion Laboratory

"If your address has changed, if you wish to be removed from our mailing list, or if the addressee is no longer employed by your organization please notify AFWAL/POOC, W-PAFB, OH 45433 to help us maintain a current mailing list".

Copies of this report should not be returned unless return is required by security considerations, contractual obligations, or notice on a specific document.

UNCLASSIFIED

SECURITY CLASSIFICATION OF THIS PAGE

REPORT DOCUMENTATION PAGE

1a. REPORT SECURITY CLASSIFICATION UNCLASSIFIED			1b. RESTRICTIVE MARKINGS NONE			
2a. SECURITY CLASSIFICATION AUTHORITY			3. DISTRIBUTION/AVAILABILITY OF REPORT Approval for Public release; distribution unlimited			
2b. DECLASSIFICATION/DOWNGRADING SCHEDULE						
4. PERFORMING ORGANIZATION REPORT NUMBER(S)			5. MONITORING ORGANIZATION REPORT NUMBER(S) AFWAL-TR-85-2003			
6a. NAME OF PERFORMING ORGANIZATION GTE LABORATORIES INC.		6b. OFFICE SYMBOL (If applicable) N/A	7a. NAME OF MONITORING ORGANIZATION Aero Propulsion Laboratory (AFWAL/POOC) AF Wright Aeronautical Laboratories			
6c. ADDRESS (City, State and ZIP Code) 40 SYLVAN ROAD WALTHAM, MA 02254			7b. ADDRESS (City, State and ZIP Code) Wright Patterson AFB Ohio 45433-6563			
8a. NAME OF FUNDING/SPONSORING ORGANIZATION AFWAL		8b. OFFICE SYMBOL (If applicable) AFWAL/POOC-1	9. PROCUREMENT INSTRUMENT IDENTIFICATION NUMBER F33615-81-C-2070			
8c. ADDRESS (City, State and ZIP Code) Aero Propulsion Laboratory WPAFB, OHIO 45433			10. SOURCE OF FUNDING NOS.			
11. TITLE (Include Security Classification) LITHIUM CELL REACTIONS			PROGRAM ELEMENT NO. 62203 F	PROJECT NO. 3145	TASK NO. 22	WORK UNIT NO. 96
			12. PERSONAL AUTHOR(S) W. CLARK, F. DAMPIER, R. McDONALD, A. LOMBARDI, D. BATSON AND T. COLE			
13a. TYPE OF REPORT FINAL		13b. TIME COVERED FROM DEC 81 TO DEC 84	14. DATE OF REPORT (Yr., Mo., Day) 1985 February		15. PAGE COUNT 223	
16. SUPPLEMENTARY NOTATION N/A						
17. COSATI CODES			18. SUBJECT TERMS (Continue on reverse if necessary and identify by block number)			
FIELD 1001	GROUP 1002	SUB. GR. 1003	BATTERIES, LITHIUM BATTERIES, PRIMARY BATTERIES, THIONYL CHLORIDE BATTERIES, ELECTROCHEMICAL REACTIONS, NON RECHARGEABLE BATTERIES.			
19. ABSTRACT (Continue on reverse if necessary and identify by block number) The objectives of Part I of this program were to (i) investigate reactions occurring in the Li/SOCl ₂ cell for a range of specified test conditions and (ii) to perform analyses to identify reactants, intermediates and products generated by the chemical and electrochemical reactions occurring in the cell and to assess their impact upon safety and performance. The stoichiometry of the SOCl ₂ reduction reaction was investigated in 0.6 Ahr prototype cells by extracting the cells five times with pure SOCl ₂ , after discharge then analyzing the combined extracts for SO ₂ by quantitative IR spectroscopy. The cells had high electrolyte-to-carbon mass ratios comparable to those in commercial cells. The multiple SOCl ₂ extraction procedure was developed to recover the SO ₂ discharge product adsorbed on the high surface area carbon electrode. <i>Originator Suggested keywords include:</i>						
20. DISTRIBUTION/AVAILABILITY OF ABSTRACT UNCLASSIFIED/UNLIMITED <input checked="" type="checkbox"/> SAME AS RPT. <input type="checkbox"/> DTIC USERS <input type="checkbox"/>			21. ABSTRACT SECURITY CLASSIFICATION UNCLASSIFIED			
22a. NAME OF RESPONSIBLE INDIVIDUAL RICHARD A. MARSH			22b. TELEPHONE NUMBER (Include Area Code) 513-255-6235		22c. OFFICE SYMBOL AFWAL/POOC-1	

DD FORM 1473, 83 APR

EDITION OF 1 JAN 73 IS OBSOLETE

UNCLASSIFIED
SECURITY CLASSIFICATION OF THIS PAGE

19. continued

The SO₂ analysis results obtained using the above procedure are in good agreement with the generally accepted reaction for the Li/SOCl₂ cell



An average of 86.4% of the theoretically expected SO₂ was found with a standard deviation of 6.3% for three cells discharged at 23°C, 5 mA/cm² to a 0.05V cutoff. From tests with undischarged control cells, it is estimated that approximately 14 ± 3% of the SO₂ produced during cell discharge would be retained after five extractions due to SO₂ adsorption on the carbon and capillary effects.

From the results of SO₂ analyses for the extracted discharged cells, it has been concluded that SOCl₂ reduction intermediates with half lives greater than approximately one hour are not formed during discharge at 23°C. Furthermore, from the constant current electrolysis and voltammetry studies that were carried out during the project at 23°C and -20°C in DMF, it was concluded that SOCl₂ reduction intermediates with lifetimes from 0.1 to 17 hours are not formed in significant quantities. The above findings suggest that a number of theories reported in the literature concerning long lived unstable SOCl₂ reduction intermediates and their hazards in cells are now highly unlikely.

Quantitative infrared measurements of the SO₂ concentrations in neutral and acid SOCl₂ electrolytes to which about 2M SO₂ was added have shown that approximately 24% and 45% of the SO₂ reacts after 24 hours in the two electrolytes, respectively. Voltammetric studies in DMF gave similar results and support the existence of the following solvation reaction suggested in the literature by Barbier and co-workers based on Raman data.



Lithium dendrite short circuits and corrosion were investigated during charging and during the overdischarge of carbon limited (CL) cells by in-situ microphotography and other techniques.

During the overdischarge of prototype CL cells at current densities from 1.0 to 30 mA/cm², no signs of negative potential transients indicative of short circuits occurred. Analysis of the amount of Li remaining on the anode at the end of overdischarge showed that 99.5% of the overdischarge current was conducted via an electronic pathway through the Li dendrites. However, during charging tests in 0.8 Ahr prototype cells at from 1.0 to 20 mA/cm² low resistance Li dendrite shorts that could overheat cells and cause thermal runaway were not formed. Explanations are given to account for the behavior of the Li dendrites during charging and Cl overdischarge.

FOREWORD

This report describes work performed by GTE Laboratories, Waltham under U.S. Air Force Contract No. F33615-81-C-2070. The report covers the work performed from May, 1983 to December, 1984. The contract was administered by the Air Force Aero Propulsion Laboratory, Wright-Patterson Air Force Base, Ohio, Mr. Richard A. Marsh, Project Engineer.

The Contract Manager was Dr. W.D.K. Clark, Manager of the Power Sources Department at GTE Laboratories, Inc. The experimental work on Section 1.0 was performed by Dr. F. W. Dampier who was the Principal Investigator. Assistance in carrying out the experimental work was provided by Mr. A. Lombardi and Mr. T. Cole.

The experimental work on Section 2.0 was carried out under subcontract by GTE Government Systems Corporation, Strategic Systems Division, Power Systems Operation, Waltham, Massachusetts. Dr. R. C. McDonald was the Principle Investigator for the work on Task III and was assisted by Mr. D. Batson, Project Engineer.

DTIC
ELECTE
S JUN 3 1985 **D**
B

Accession For	
NTIS GRA&I	<input checked="" type="checkbox"/>
DTIC TAB	<input type="checkbox"/>
Unannounced	<input type="checkbox"/>
Justification	
By	
Distribution/	
Availability Codes	
Dist	Avail and/or Special
A-1	



TABLE OF CONTENTS

Part 1

	<u>Page</u>
1. INVESTIGATION OF CHEMICAL, ELECTROCHEMICAL AND PARASITIC REACTIONS IN LITHIUM-THIONYL CHLORIDE CELLS	1
1.1 INTRODUCTION	1
1.2 INVESTIGATION OF THIONYL CHLORIDE REDUCTION IN A SUPPORTING ELECTROLYTE BY VOLTAMMETRY AND COULOMETRY	2
1.2.1 Low Temperature Electrolysis with Voltammetric Analysis	2
1.2.1.1 Background	2
1.2.1.2 Experimental	3
1.2.1.3 Results	7
1.2.1.4 Discussion and Recommendations	18
1.2.2 Voltammetry of Neutral and Acid Electrolyte with Added SO ₂	19
1.2.2.1 Background	19
1.2.2.2 Neutral SOCl ₂ Electrolyte With Added SO ₂	20
1.2.3 Voltammetry of Acid SOCl ₂ Electrolyte with Added SO ₂	28
1.3 INVESTIGATION OF THE ADSORPTION OF SULFUR DIOXIDE FROM SOCl ₂ ELECTROLYTES BY THE CARBON CATHODE	29
1.3.1 Background	29
1.3.2 Experimental Procedure	32
1.3.2.1 Infrared Cells and Instrumentation	32
1.3.2.2 Preparation of SO ₂ /SOCl ₂ Electrolyte Solutions	34
1.3.2.3 Procedure for the Adsorption Measurements	35
1.3.3 Results and Discussion	37
1.3.3.1 Infrared Analysis Calibration for Sulfur Dioxide	37
1.3.3.2 Reaction of SO ₂ with SOCl ₂ Electrolytes	39
1.3.3.3 Sulfur Dioxide Adsorption Results	49

TABLE OF CONTENTS

1.4 INVESTIGATION OF REACTIONS OCCURRING DURING THE OVERDISCHARGE OF LITHIUM-THIONYL CHLORIDE CELLS	56
1.4.1 Carbon Limited Overdischarge	56
1.4.1.1 Background	56
1.4.1.2 In Situ Photography of Overdischarged Cells	59
1.4.1.3 Voltammetry of Electrolyte From Carbon Limited Cells Overdischarged at -40°C	72
1.4.1.4 Prototype Cell Overdischarge Results	75
1.4.2 Anode Limited Overdischarge	86
1.4.2.1 Background	86
1.4.2.2 Voltammetry Results	89
1.5 INVESTIGATION OF REACTIONS OCCURRING DURING CHARGING OF LITHIUM THIONYL-CHLORIDE CELLS	101
1.5.1 Background	101
1.5.2 Microphotography	104
1.5.2.1 Experimental	104
1.5.2.2 Results	104
1.5.3 Prototype Cell Charging Tests	115
1.5.3.1 Experimental	115
1.5.3.2 Results	115
1.6 INVESTIGATION OF THIONYL CHLORIDE REDUCTION IN PROTOTYPE CELLS BY MULTIPLE EXTRACTION AND INFRARED ANALYSIS	117
1.6.1 Background	117
1.6.2 Experimental	118
1.6.3 Results and Discussions	122
1.6.4 Recommendations for Future Work	134
1.7 CONCLUSIONS FOR PART I	136

Part 2.

2. Introduction	142
2.1 Experimental	144
2.1.1 Component Preparation	144

TABLE OF CONTENTS

2.1.2 Testing	146
2.2 Results	147
2.2.1 D Cells	147
2.2.2 Manometer Cells	148
2.3 Discussion	148
2.3.1 Crane Paper Binder	148
2.3.2 Teflon Binder	149
2.3.3 Excess AlCl ₃	149
2.3.4 Texas and Quebec Acetylene Blacks	150
2.3.5 Pressure Studies	150
References	218

LIST OF FIGURES

<u>Figure</u>	<u>Page</u>
1. Low Temperature Electrolysis Cell with Voltammetry Electrodes.	4
2. Purge Gas Distribution System for Low Temperature Voltammetry Cell . . .	5
3. Cyclic Voltammogram of 0.1M TBAPF ₆ in DMF on Pt Electrode at 23°C and -20°C, Background, Scan rate 200 mV/second.	8
4. Voltammograms of 5.1 μl of 1.8M LiAlCl ₄ /SOCl ₂ in .1M TBAPF ₆ /DMF at -20°C	9
5. Voltammograms of 10 mg of 1.8M LiAlCl ₄ /SOCl ₂ in 0.1M TBAPF ₆ /DMF at 0°C.	10
6. Voltammograms of 5.0 μl of 2.73M SO ₂ /1.64M LiAlCl ₄ /SOCl ₂ in .1M TBAPF ₆ /DMF at 200 mV/second.	12
7. Voltammograms of 8.5 mg of 1.8M LiAlCl ₄ /SOCl ₂ in .1M TBAPF ₆ /DMF after electrolysis at -20°C, on a 4 cm ² Pt cathode at 0.50 mA/cm ² , to n = 1.95.	14
8. Cell Potential during 0.50 mA/cm ² constant current electrolysis at -20°C of 5.82 mM SOCl ₂ in 0.1M TBAPF ₆ /DMF at a 4 cm ² Pt cathode.	15
9. Voltammograms after -20°C storage of 8.5 mg of 1.8M LiAlCl ₄ /SOCl ₂ in 0.1M TBAPF ₆ /DMF after electrolysis at -20°C, on a 4 cm ² Pt cathode	16
10. Voltammograms at 25°C after -20°C and 25°C storage of 8.5 mg of 1.8M LiAlCl ₄ /SOCl ₂ in 0.1M TBAPF ₆ /DMF after electrolysis	17

11. Voltammograms of 12 mg of 1.8M LiAlCl ₄ , 2.7M SO ₂ /SOCl ₂ in 10 ml of 0.1M TBAPF ₆ /DMF at 25°C After Various Periods of Storage,	21
12. Decline in the SOCl ₂ Concentration during 25°C Storage for a 1.8M LiAlCl ₄ /SOCl ₂ Electrolyte Initially Containing 2.88M SO ₂ Measured by Voltammetry*.	23
13. Voltammograms of ≈ 8 mg of Distilled SOCl ₂ with 2.8M SO ₂ in 10 ml of 0.1M TBAPF ₆ /DMF at 25°C, scan rate 200 mV/second.	24
14. Voltammetry Currents For Peak III at Approximately -1.4V During 23°C Storage for 1.8M LiAlCl ₄ /SOCl ₂ - 2.7M SO ₂ and SOCl ₂ - 2.8M SO ₂ Samples	25
15. Voltammograms of ≈ 8 mg of 2.0M AlCl ₃ , 0.10M LiCl/SOCl ₂ Acid Electrolyte with 1.65M SO ₂ in 10 ml of 0.10M TBAPF ₆ /DMF at 25°C, Scan rate 200 mv/second.	30
16. IR Absorption of SO ₂ /SOCl ₂ Electrolyte Showing Baseline Technique, Polystyrene Reference Sample, and CaF ₂ Linearity Cutoff.	33
17. Infrared Spectra of 1.8M LiAlCl ₄ /SOCl ₂ with Increasing Amounts of SO ₂	38
18. Calibration Curve Relating IR Absorbance to SO ₂ Concentration in 2.0M AlCl ₃ , 0.1M LiCl/SOCl ₂	40
19. The Decline in SO ₂ Concentration with Time in 1.8M LiAlCl ₄ /SOCl ₂ at 23°C With and Without Carbon-4% Teflon Cathode Material	41
20. The Decline in SO ₂ Concentration with Time in 2.0M AlCl ₃ , 0.10M LiCl/SOCl ₂ at 23°C With and Without Carbon-4% Teflon Cathode Material	42

21. Infrared Spectra of 1.8M LiAlCl ₄ /SOCl ₂ Containing 1.0M SO ₂ Before and After 4.0 Hours Storage at 23°C.	45
22. Infrared Spectra of 1.8M LiAlCl ₄ /SOCl ₂ Containing 1.0M SO ₂ Before and After 147 Hours Storage at 23°C.	46
23. Lithium Dendrites on the Cathode of a Carbon Limited Li/SOCl ₂ Cell Overdischarged at -40°C after 2 Hours on OCP at 23°C	61
24. Cell Overdischarged at -40°C After 3.5 Hours on OCP at 23°C.	63
25. Cell Overdischarged at -40°C After 23 Hours on OCP at 23°C.	63
26. Overdischarge of a Li/SOCl ₂ Cell at 23°C, 5.0 mA/cm ² .*	66
27. Lithium Dendrites After 2.0 Hours Overdischarge at 5.0 mA/cm ² . For the Cell Described by Figures 26, 28-30. Magnification 21 X	68
28. Lithium Dendrites After 6.75 Hours Overdischarge at 5.0 mA/cm ² at the Same Spot as Shown in Figure 27. Magnification 21 X	68
29. Pulses in the Cell Potential During the Overdischarge of an Electrolyte Flooded Li/SOCl ₂ Cell at 5.0 mA/cm ² , 23°C*	69
30. Lithium Dendrites After 23.3 Hours Overdischarged at 5.0 mA/cm ² . For the Cell Described by Figures 26-28, 30. Magnification 21 X	71
31. Voltammograms of 5 μl of SOCl ₂ Electrolyte from a Carbon Limited Cell Overdischarge 380% at -40°C, 1 mA/cm ²	73
32. Behavior of a Carbon Limited Li/SOCl ₂ Cell During Discharge and Overdischarge at 5.0 mA/cm ² , 23°C.*	77

33. Behavior of a Carbon Limited Li/SOCl ₂ Cell During Discharge and Overdischarge at 1.0 mA/cm ² at 23°C.	78
34. High Rate Overdischarge of Carbon Limited Li/SOCl ₂ Cells at -20°C. . .	79
35. Voltammograms for 3.5 μl of Distilled SO ₂ Cl ₂ in 10 ml of 0.1M TBAPF ₆ /DMF at 23°C at a Platinum Electrode,	90
36. Calibration Curve Relating Peak Current By Voltammetry to the SO ₂ Cl ₂ Concentration in 0.1M TBAPF ₆ /DMF Supporting Electrolyte at 23°C . .	92
37. Voltammograms for 4.4 mM Distilled SO ₂ Cl ₂ in 0.1M TBAPF ₆ /DMF at 23°C at a Pt Electrode, Scan Rate 200 mV/second	94
38. Voltammograms for 7.44 mg 0.9M LiAlCl ₄ /50% SOCl ₂ - 50% SO ₂ Cl ₂ and ≈ 3.7 mg 1.8 LiAlCl ₄ /SOCl ₂ in DMF.	95
39. Voltammograms for 13.2 mM Distilled SO ₂ Cl ₂ with Approximately 80 mM Added SO ₂ in 0.1M TBAPF ₆ /DMF at 23°C	97
40. Behavior of a Lithium Limited Cell During Discharge and Overdischarge at 5 mA/cm ² , 23°C (Cell No. 63)	98
41. Voltammograms of 8.36 mg of SOCl ₂ Electrolyte from a Lithium Limited Cell Overdischarged 5200% at 23°C, 5 mA/cm ²	99
42. Lithium Dendrites Attached to the Lithium Electrode of Cell 1 After 1.35 Ahr Discharge and 0.67 Ahr Charge Followed by Three Hours Storage, 14 X Magnification	107
43. Lithium Dendrites Shown in Figure 42 but with 10 Minutes Charging at 4.0 mA/cm ² . 14 X Magnification (Note new growth at tips)	107

44. Lithium Dendrites Shown in Figure 43 After 22 Hours Storage Followed by 10 Minutes Charging at 4.0 mA/cm ² . 14 X Magnification.	108
45. Lithium Dendrites in Contact with the Carbon Electrode After 4 Hours of Charge at 10 mA/cm ² , Magnification 7X for Cell No. 3 Listed in Table 5	111
46. Microphotograph of the Electrodes of Cell 5 Prior to Charging. 7X Magnification	112
47. The Electrode of Cell 5 After 5.0 mAhr/cm ² of Charging at 20 mA/cm ² , 7X Magnification	112
48. The Electrode of Cell 5 After 54 mAhr/cm ² of charging at 20 mA/cm ² , 7X Magnification.	113
49. The Electrode of Cell 5 after 54 mAhr/cm ² of Charging at 20 mA/cm ² , 18 Hours Storage and 4 mAhr/cm ² of Charging at 5 mA/cm ²	113
50. Apparatus for Multiple Extraction of Discharged Li/SOCl ₂ Cells for Soluble Discharge Products	121
51. Manometer Assembly	195
52. Mercury Height Measuring Apparatus	196
53. Teflon Binder Content vs 3.0 Volt Capacity	197
54. Teflon Binder Content vs 0.2 Volt Capacity	198
55. Teflon Binder Content vs Voltage Delay	199
56. Teflon Binder Content vs Min. Voltage	200

57. Excess AlCl ₃ vs 3.0 Volt Capacity	201
58. Excess AlCl ₃ vs 0.2 Volt Capacity	202
59. Excess AlCl ₃ vs Voltage Delay	203
60. Excess AlCl ₃ vs Min. Voltage	204
61. Cell Pressure: Baseline Continuous	205
62. Cell Pressure: Lydall Paper Continuous	206
63. Cell Pressure: SO ₂ Purge Continuous	207
64. Cell Pressure: Low Nitrogen Lithium Continuous	208
65. Cell Pressure: Gulf Carbon Continuous	209
66. Cell Pressure: Baseline Intermittent	210
67. Cell Pressure: Low Nitrogen Lithium Intermittent	211
68. Cell Pressure: Lydall Paper Intermittent	212
69. Cell Pressure: SO ₂ Purge Intermittent	213
70. Cell Pressure: Gulf Carbon Intermittent	214
71. Variation in Ambient Temperature	215
72. Cell Pressure During and After Continuous Discharge	216
73. Averaged, Smoothed Pressure Curved for Each Cell Type	217

LIST OF TABLES

<u>Table</u>	<u>Page</u>
1. Reaction of SO ₂ With 1.8M LiAlCl ₄ /SOCl ₂ and Adsorption by Carbon-4% Teflon Cathode Material	50
2. Reaction of SO ₂ with 2.0M AlCl ₃ , 0.10M LiCl/SOCl ₂ and Adsorption by Carbon-4% Teflon Cathode Material	50
3. Lithium Anode Dissolution and Shorting During the Overdischarge of Prototype Carbon-Limited Li/SOCl ₂ Cells*	76
4. Cell Potentials for Prototype Carbon Limited Li/SOCl ₂ Cells During Extended Overdischarge*	82
5. Conditions and Results of Charging Tests With Li/SOCl ₂ Cells Equipped for In Situ Optical Microscopy*	105
6. Condition and Results of Charging Tests With 0.77 Ahr Prototype Li/SOCl ₂ Cells*	116
7. The Amount of SO ₂ Found by IR Analysis Compared to the Amount Expected for Li/SOCl ₂ Cells Extracted With SOCl ₂ at 23°C	123
8. Discharge Conditions and SOCl ₂ Utilizations for Li/SOCl ₂ Cells Discharged at 25°C and Analyzed for SO ₂	124
9. The Amount of SO ₂ Found by IR Analysis Compared to the Amount Expected for Li/SOCl ₂ Cells Extracted with SOCl ₂ at -20°C	128

10. Discharge Conditions and SOCl_2 Utilizations for Li/SOCl_2 Cells Extracted at -20°C and Analyzed for SO_2	129
11. The Efficiency of SO_2 Extraction from Undischarged Control Cells Filled with a Known Amount of SO_2	131
12. Task A: Fresh Baseline D Cell Results	156
13. Task A: Stored Baseline D Cell Results	157
14. Task A: Fresh Lydall Binderless Results	158
15. Task A: Stored Lydall Binderless Results	159
16. Task A: Fresh PVA Results	160
17. Task A: Stored PVA Results	161
18. Task A: Fresh PVC Results	162
19. Task A: Stored PVC Results	163
20. Task C: Fresh 2% TFE Binder Results	164
21. Task C: Stored 2% TFE Binder Results	165
22. Task C: Fresh 3# TFE Binder Results	166
23. Task C: Stored 3% TFE Binder Results	167
24. Task C: Stored 4% TFE Binder Results	168
25. Task C: Stored 4% TFE Binder Results	169

26. Task C: Fresh 5% TFE Binder Results	170
27. Task C: Stored 5% TFE Binder Results	171
28. Task C: Fresh 6% TFE Binder Results	172
29. Task C: Stored 6% TFE Binder Results	173
30. Task C: Fresh 10% TFE Binder Results	174
31. Task C: Stored 10% TFE Binder Results	175
32. Task D: Fresh .01% Excess AlCl ₃	176
33. Task D: Stored .01% Excess AlCl ₃	177
34. Task D: Fresh .05% Excess AlCl ₃	178
35. Task D: Stored .05% Excess AlCl ₃	179
36. Task D: Fresh .10% Excess AlCl ₃	180
37. Task D: Stored .10% Excess AlCl ₃	181
38. Task D: Fresh 2.00% Excess AlCl ₃	182
39. Task D: 1.00% Excess AlCl ₃	183
40. Task D: 2.00% Excess AlCl ₃	184
41. Task D: Stored 2.00% Excess AlCl ₃	185
42. Task D: Fresh 4.00% Excess AlCl ₃	186

43. Task D: Stored 4.00% Excess AlCl ₃	187
44. Task D: Fresh 8.00% Excess AlCl ₃	188
45. Task D: Stored 8.00% Excess AlCl ₃	189
46. Task E: Fresh Gulf Texas Carbon	190
47. Task E: Stored Gulf Texas Carbon	191
48. Summary of Pressure Results, Continuous Discharge	192
49. Summary of Pressure Results, Intermittent Discharge	193
50. Physical Comparison of the MESP(10,000Ah) and DD(28Ah) Cells	194

1. INVESTIGATION OF CHEMICAL, ELECTROCHEMICAL AND PARASITIC REACTIONS IN LITHIUM-THIONYL CHLORIDE CELLS

1.1 INTRODUCTION

The objectives of Task I of the project were to (i) fully investigate reactions occurring in the Li/SOCl_2 cell for a range of specified test conditions, and (ii) to perform analyses to identify reactants, intermediates and products generated by the chemical and electrochemical reactions occurring in the cell and to assess their impact upon safety and performance.

The extensive experimental results obtained for Task I during the first 18 months of the project have been described in a lengthy interim report (1). The interim report describes the experimental approach and procedures and, therefore, should be read to understand Section 1.0 of the present report.

The objectives of Task II of the project were to perform detailed analyses for impurities that may be present in each reagent and component used in cell construction. Task II also included experimental investigations to provide a detailed parametric assessment of the impact of each impurity upon cell safety and performance. The results obtained during Task II are presented in the interim report (1).

Based on the findings from Task I and II above, Task III involved the establishment of a more thorough understanding of Li/SOCl_2 cell chemistry and the identification and experimental demonstration of any recommendations that may be beneficial to cell safety and performance. The results of the work undertaken during Task III are discussed in Section 2 of the present report.

1.2 INVESTIGATION OF THIONYL CHLORIDE REDUCTION IN A SUPPORTING ELECTROLYTE BY VOLTAMMETRY AND COULOMETRY

1.2.1 Low Temperature Electrolysis with Voltammetric Analysis

1.2.1.1 Background

Earlier investigations using coulometry and voltammetry undertaken at room temperature during the present program (1) gave no indication of the presence of significant quantities of SOCl_2 reduction intermediates with lifetimes from approximately 0.1 to 48 hours. These findings agree with the results at room temperature reported by Attia (2) obtained using an infrared flow cell and those by Williams and co-workers (3) obtained by using ESR spectroscopy. Since SOCl_2 reduction intermediates would be expected to be more stable and to be present at higher concentrations at low temperatures (i.e., $\leq -20^\circ\text{C}$), voltammetry and coulometry investigations were undertaken at low temperatures using techniques similar to those used previously at 23°C .

Unlike infrared spectroscopy which is generally restricted to room temperature studies, coulometry combined with voltammetry is especially suited for low temperature investigations of the reduction mechanism of SOCl_2 . Radical intermediates have been found and investigated at low temperatures by Williams and co-workers (3) using ESR spectroscopy. Voltammetry could provide additional information about SOCl_2 reduction intermediates present at low temperature which ESR measurements do not provide, such as the concentration of intermediates which are not radicals, their lifetimes and reduction potentials.

The voltammetry and coulometry measurements at low temperatures require special degassing precautions because of the greater solubility of oxygen in the DMF electrolyte at low temperatures. Furthermore, as the cell cools, the vapor pressure inside the cell decreases and moist air can be drawn into the cell thereby contaminating the electrolyte. The rate of diffusion of the various electroactive species decreases as the temperature is lowered, thus, the

peak potentials as observed by voltammetry are shifted. The peak potentials therefore have to be redetermined at low temperature for those compounds (e.g., SO_2 , SOCl_2) that are to be determined by voltammetric analysis.

1.2.1.2 Experimental

The two compartment H cell used for the low temperature constant current electrolysis and voltammetry studies is shown in Figure 1. The working, counter, and Ag/AgCl reference electrodes as well as information concerning the electrolysis cathodes, electrolytes, cell design, potentiostat and associated ancillary equipment was described earlier in Section 1.1.2 of the interim report (1). The argon purge gas distribution system required to cool the argon and control its flow into the low temperature two compartment cell is illustrated in Figure 2.

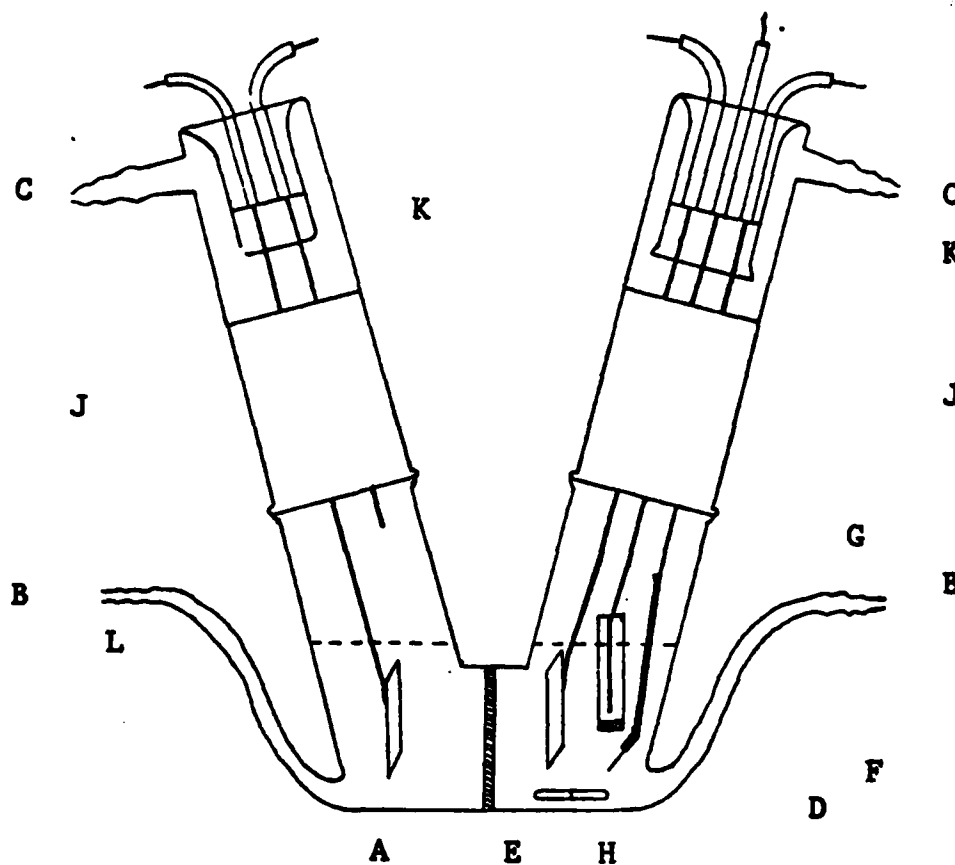


Figure 1: Low Temperature Electrolysis Cell with Voltammetry Electrodes.

A, Platinum counter electrode; B, Argon inlets; C, Argon outlets; D, Teflon Magnetic Stir Bar; E, Platinum constant current electrolysis cathode; F, Voltammetry working electrode; G, Ag/AgCl reference electrode; H, 5 mm Dia. sintered glass frit; I, 20 mm Dia sintered glass frit; J, 24/40 Standard taper joint; K, Glass-to-metal seal; L, Electrolyte level.

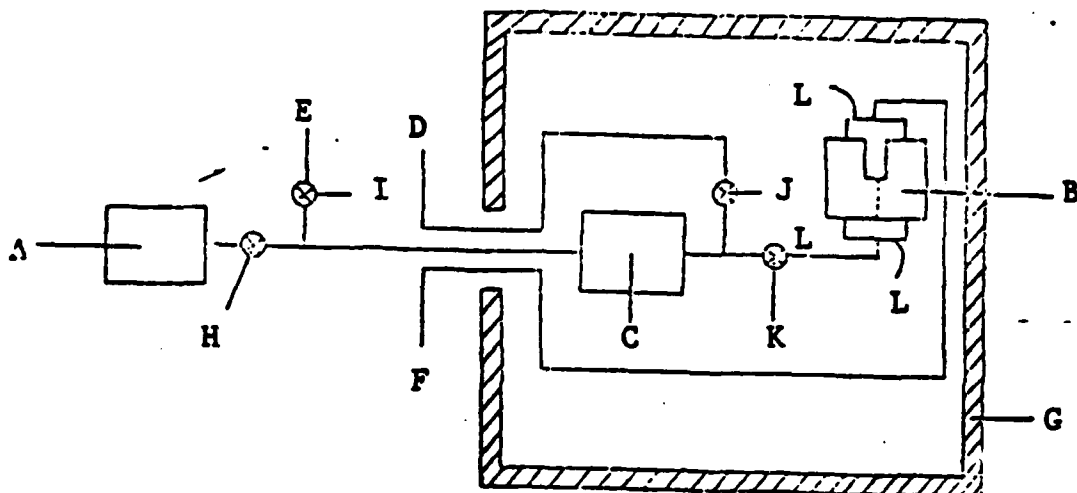


Figure 2: Purge Gas Distribution System for Low Temperature Voltammetry Cell

A, Argon tank and regulator; B, Voltammetry cell as shown in Figure 1; C, Cooling can; D, Purge exhaust outlet; E, Pressure relief exhaust; F, Exhaust-to-flow meter; G, Wall of refrigerated chamber; H, I, J, K, Valves; L, Rubber hose connecting glass tubing inlets and outlets to copper tubing.

In previous constant current electrolysis experiments at room temperature (1), the current was interrupted at specific times during the electrolysis and the standard taper top with the electrolysis cathode and the reference electrode was removed and a second top with a Pt voltammetry working electrode and a Ag/AgCl reference electrode was inserted into the cell. Voltammetric analyses were then carried out, after which the original set of electrolysis electrodes were replaced and the constant current electrolysis continued. This procedure was unsatisfactory for the low temperature electrolysis experiments because opening the cell would allow oxygen to rapidly dissolve in the cold electrolyte and moisture would condense on the cold electrode assemblies even in the dry room. Therefore, for the low temperature electrolysis experiments, the cell was modified so that all four electrodes required for both electrolysis and voltammetry were in the two compartment cell from the start of the electrolysis (cf. Figure 1) thus eliminating the need to open the cell to change electrodes during the course of the electrolysis. The modification primarily involved replacing the 24/40 size top with two glass-to-metal leads with one with three glass-to-metal sealed leads.

The low temperature cell was filled with 0.1M TBAPF₆/DMF in a dry room (< 4% R.H.), deoxygenated with ultra high purity argon (Matheson, 99.999%) and the SOCl₂ sample added with a microliter syringe. The argon inlets and outlets on the cell were capped (i.e., B and C in Figure 1) and the cell transferred into a refrigerated chamber 40.6 x 40.6 x 40.6 cm (Conrad, Inc.). The argon purge system was first flushed with argon by opening Valves H and J (see Figure 2), closing Valve K and adjusting the flow rate which was monitored by a bubbler at Outlet D. The cooling coil (C in Figure 2) was wound from 5.6 m of 0.25 inch copper tubing and was required to insure that the argon entering the cell would be adequately cooled.

After the cooling coil was purged with argon for 30 minutes, Valve K was opened, Valve J closed and the cell connected with argon flowing to prevent contamination by diffusion. The argon flow rate was monitored (F in Figure 2) and adjusted to one bubble/minute so that volatile components (e.g., SOCl₂, SO₂) would not be lost during the constant current electrolysis.

Throughout the electrolysis the stirring rate was monitored by placing an inductor probe connected to an oscilloscope near the spinning magnet. The stirring rate was held constant at 1850 RPM. When a voltammogram was required, the argon flow was stopped and the pressure equalized by carefully opening and closing the pressure relief valve (i.e., I in Figure 2). This step was necessary since a single bubble would cause the potentiostat to pass a large current through the working electrode. In addition, the magnetic stirrer was stopped and the refrigeration unit of the low temperature chamber was shut off to reduce vibrations.

1.2.1.3 Results

The potential range of the DMF supporting electrolyte at -20°C and 23°C without a sample is given in the cyclic voltammograms shown in Figure 3. Analyses were only carried out if preliminary scans of the supporting electrolyte showed that the background current at -20°C was $< 5\mu\text{A}$ from $+1.0$ to -2.25V and $< 10\mu\text{A}$ from -2.25 to -2.50V vs Ag/AgCl . It was found that contamination of supporting electrolyte containing $\text{LiAlCl}_4/\text{SOCl}_2$ with air at -20°C produced a large cathodic peak at -1.45V probably due to oxygen reduction and a large cathodic peak at $+0.415\text{V}$ due to chloride reduction on the return cathodic sweep.

The voltammograms obtained at -20°C for samples of 1.8M $\text{LiAlCl}_4/\text{SOCl}_2$ in DMF supporting electrolyte at sweep rates from 50 to 500 mV/second are given in Figures 4 and 5.

A linear relationship between the peak current and the square root of the sweep rate for the peaks at approximately -0.85V was obtained for the voltammograms at -20°C (cf. Figure 4). The results were fitted to a linear least squares equation and the standard error of estimate was $1.21\mu\text{A}$ or about 3.45% at a peak current of $35\mu\text{A}$. The linear relation between peak height and the square root of sweep rate found for SOCl_2 reduction at -20°C is indicative of a diffusion controlled electrode process (4).

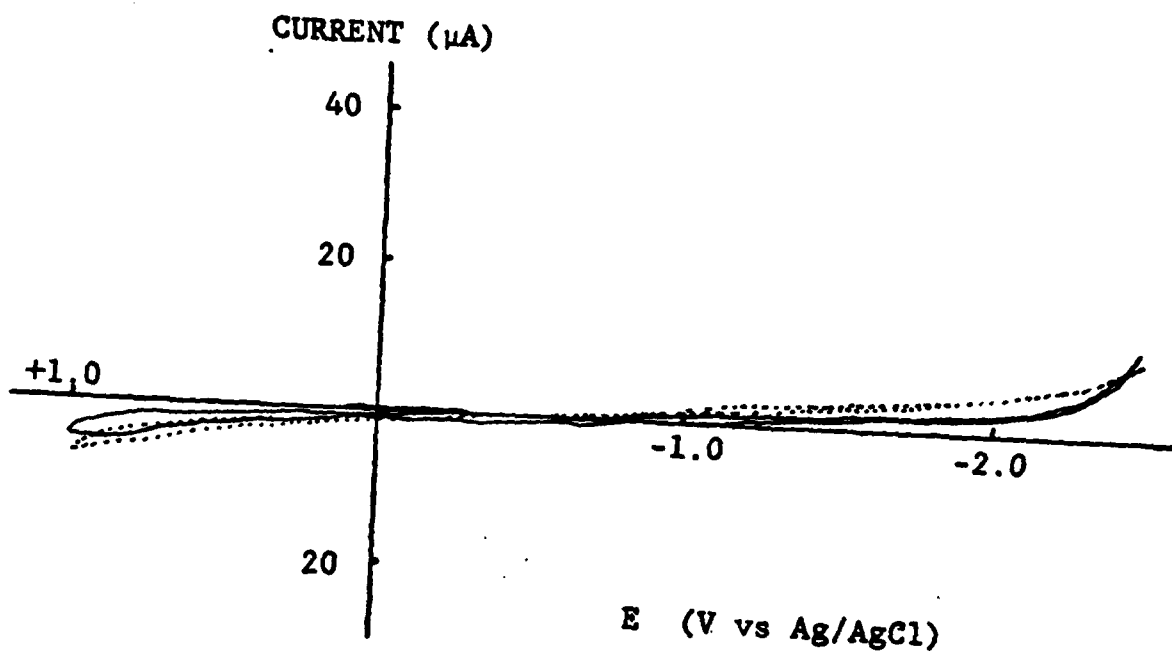


Figure 3: Cyclic Voltammogram of 0.1M TBAPF₆ in DMF on Pt Electrode at 23°C and -20°C, Background, Scan rate 200mV/second.

(——), -20°C
(.....), 23°C

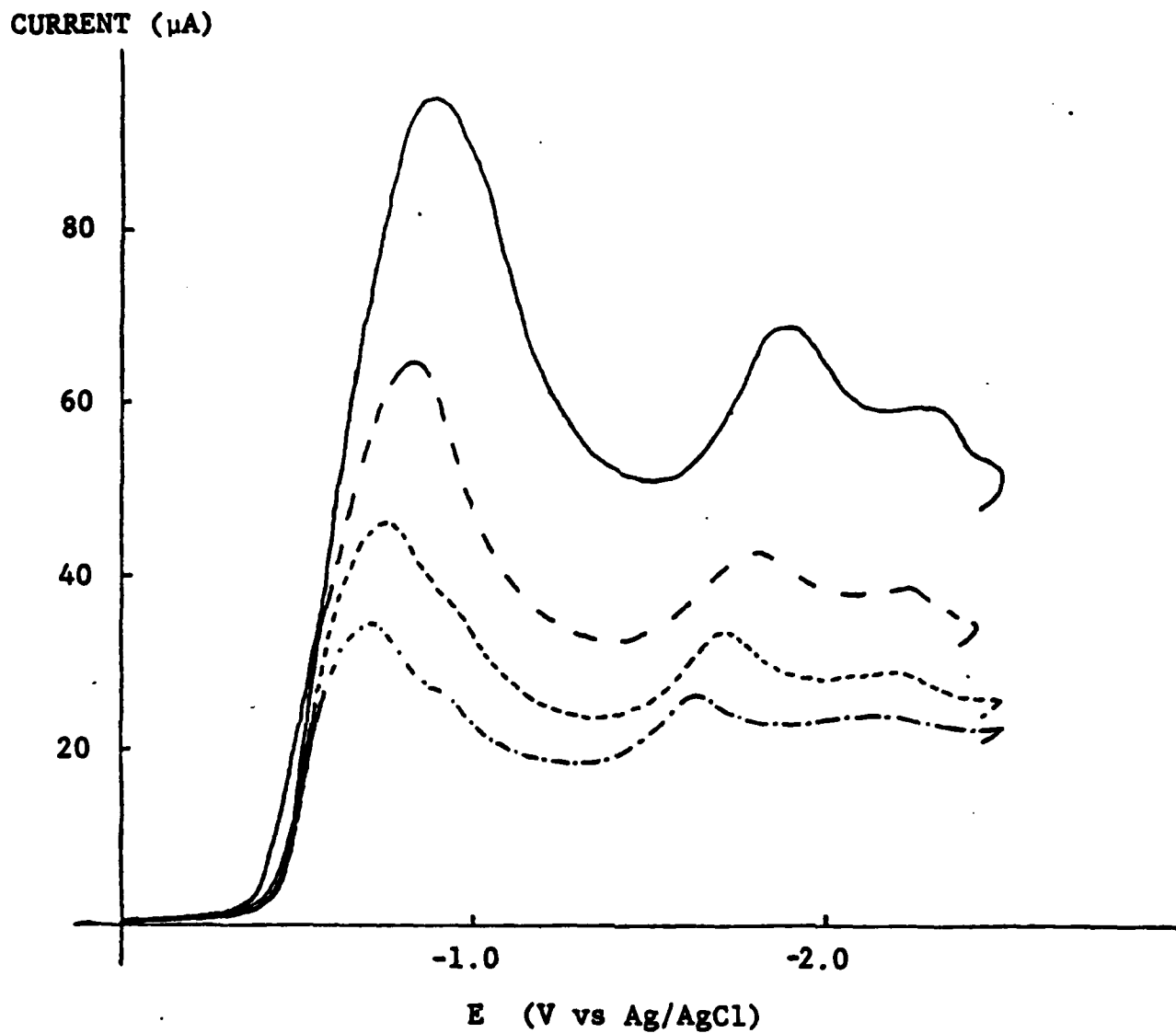


Figure 4: Voltammograms of 5.1 μ l of 1.8M LiAlCl₄/SOCl₂ in .1M TBAPF₆/DMF at -20°C Scan rate effect shown. Return scans not shown.

- (——): Scan at 500mV/second.
- (- - -): Scan at 200mV/second.
- (- - - -): Scan at 100mV/second.
- (- . - . -): Scan at 50mV/second.

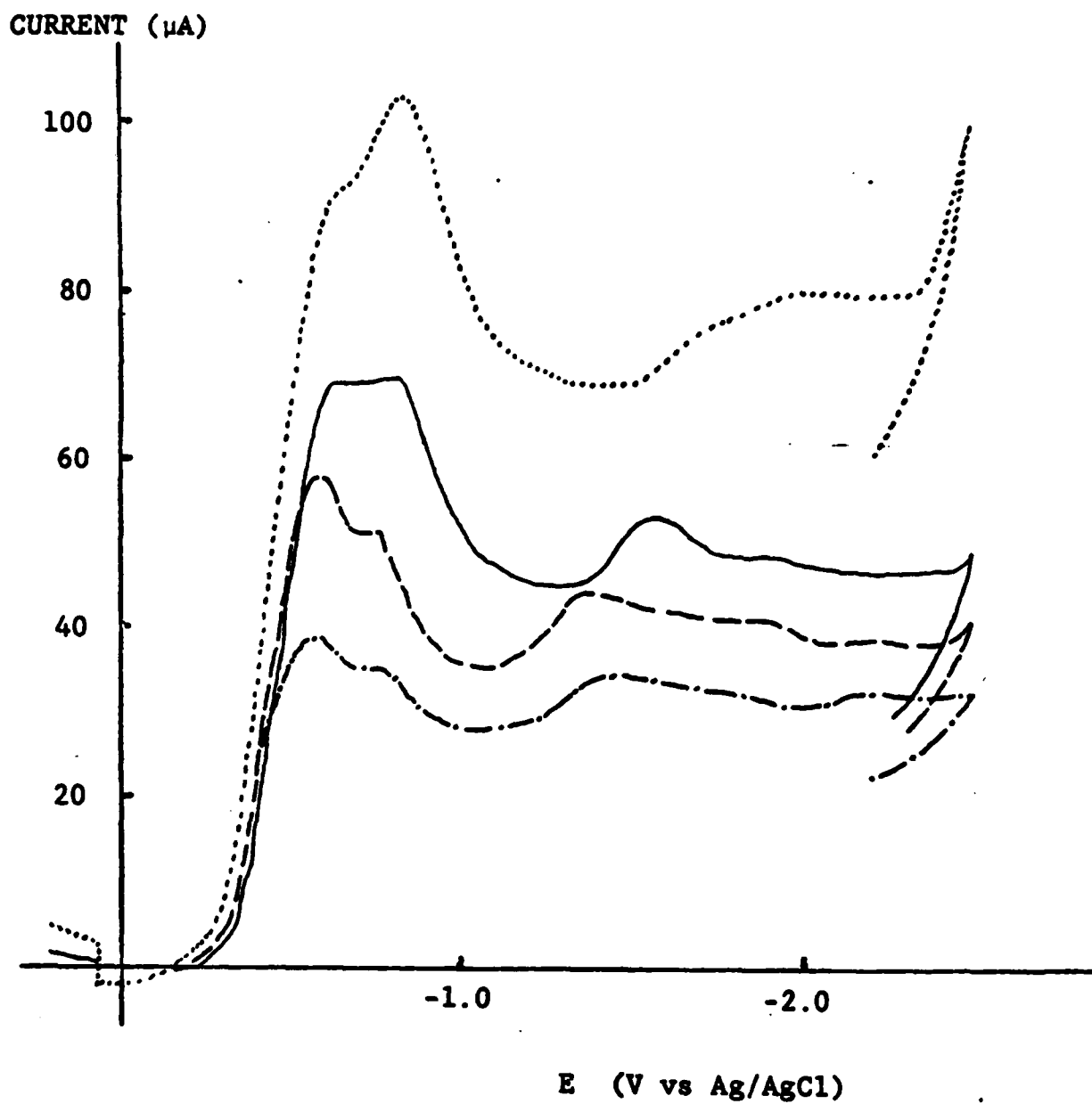


Figure 5: Voltammograms of 10mg of 1.8M $\text{LiAlCl}_4/\text{SOCl}_2$ in 0.1M $\text{TBAPF}_6/\text{DMF}$ at 0°C .

- (.....) Scan Rate, 500mV/second.
- (——) Scan Rate, 200mV/second.
- (— —) Scan Rate, 100mV/second.
- (- . -) Scan Rate, 50mV/second.

The voltammogram for 1.8M LiAlCl₄/SOCl₂ electrolyte at -20°C in Figure 4 at 200 mV/second shows a large peak at -0.865V instead of separate peaks for SOCl₂ and SO₂ as observed at 23°C (1). The voltammograms at 0°C in Figure 5 show a somewhat better resolution of the SOCl₂ and SO₂ peaks. The merging of the SO₂ and SOCl₂ peaks as the temperature was decreased could be entirely due to slower diffusion at the working electrode at low temperatures, or greater solvation of the SO₂ or SOCl₂ by the DMF. However the peaks could appear to merge at low temperature due to the presence of intermediate(s) which reduce at potentials between the reduction potentials of SOCl₂ and SO₂. To resolve this uncertainty, voltammograms were required at -20°C for samples of LiAlCl₄/SOCl₂ electrolyte containing known quantities of SO₂.

Figure 6 shows the voltammograms obtained for 5.1 µl samples of 2.72M SO₂/1.64M LiAlCl₄/SOCl₂ in DMF supporting electrolyte at 20, 5, -25 and then at +30°C. On cooling the sample from 20°C to -25°C, it was observed that the SOCl₂ and SO₂ peaks at -0.75 and -0.95V, respectively, gradually began to merge as the temperature was lowered and were one peak at temperatures from 5 to -25°C. When the cell was warmed to 30°C, the SO₂ peak reappeared, thus the merging of the SO₂ and SOCl₂ peaks is not due to the formation of a stable compound.

Solutions of 15 mM SO₂ in DMF supporting electrolyte were analyzed by LSV at 23, 3 and -40°C using sweep rates of 50, 100, 200, and 500 mV/second. In all cases the peak potential was approximately -0.95V vs Ag/AgCl and the main effect of temperature was to reduce the peak current from approximately 53 µA at 23°C to 42 and 24 µA at 3 and -40°C, respectively, all at 200 mV/second.

The constant current electrolysis at -20°C of approximately 8.5 mg 1.8M LiAlCl₄/SOCl₂ in 10 ml of DMF supporting electrolyte at a 4 cm² Pt cathode was carried out at 0.50 mA/cm² with LSV analysis at n = 1.00 and 1.95 equivalents of charge passed per mole of SOCl₂. The voltammograms obtained at -20°C at the start of the electrolysis and at n = 1.00 and 1.95 equivalents of charge passed/mole of SOCl₂ are shown in Figure 7. The cell potential observed during the constant current electrolysis at -20°C of LiAlCl₄/SOCl₂ plotted versus

CURRENT (μA)

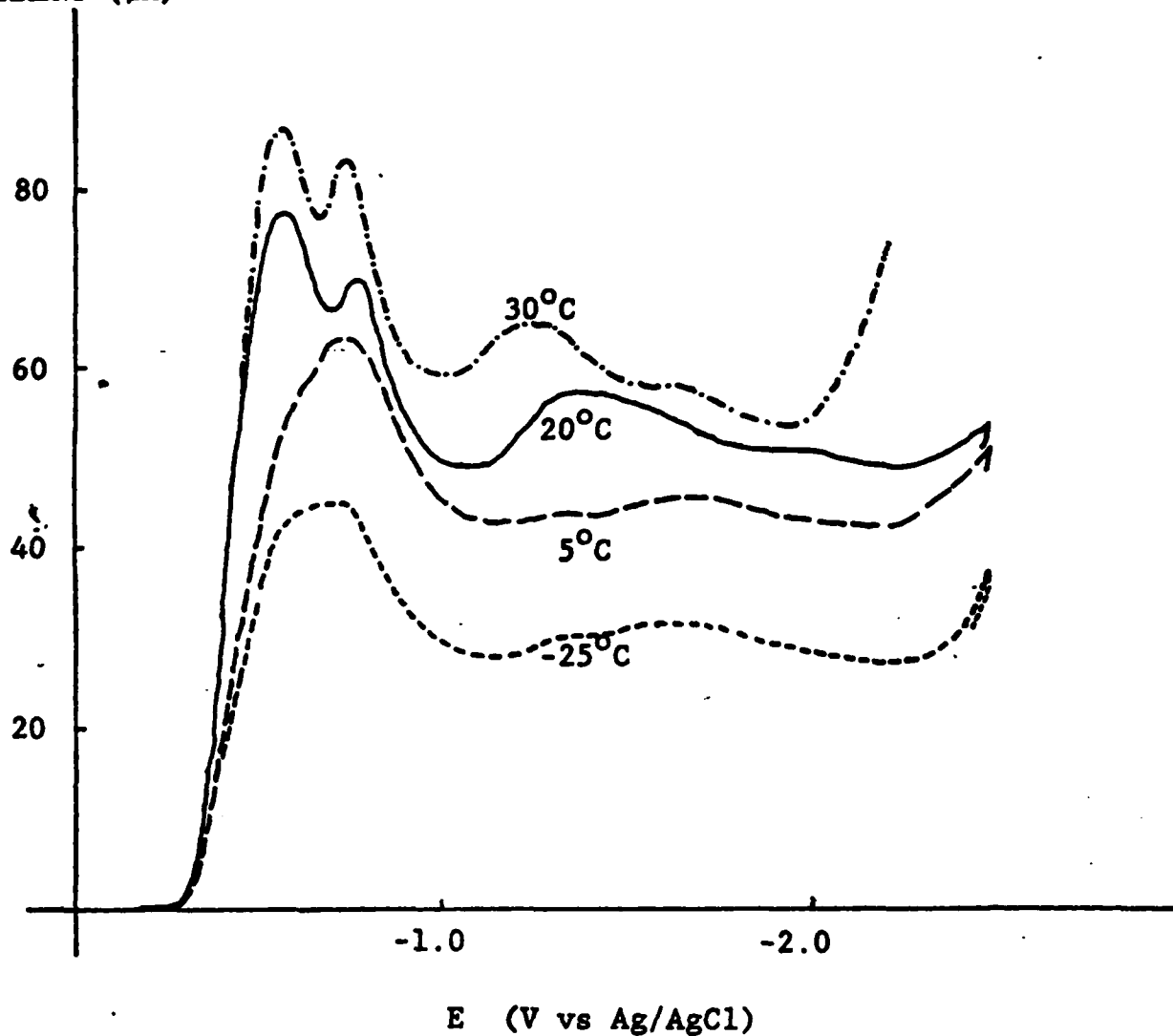
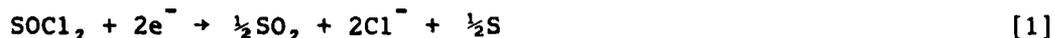


Figure 6: Voltammograms of $5.0\mu\text{l}$ of $2.73\text{M SO}_2/1.64\text{M LiAlCl}_4/\text{SOCl}_2$ in $.1\text{M TBAPF}_6/\text{DMF}$ at 200mV/second . Return scan not shown.

- (—): Scan at $+20^\circ\text{C}$.
- (- -): Scan at $+5^\circ\text{C}$.
- (-----): Scan at -25°C .
- (-·-·-): Scan at $+30^\circ\text{C}$. shown shifted -1.00V .

the charge passed/mole of SOCl_2 , are given in Figure 8. The decline in the electrolysis cell potential between $n = 1.95$ and 2.00 is consistent with the generally accepted (5,6) reaction for the two electron reduction of SOCl_2 .



The voltammograms obtained during the electrolysis at -20°C (cf. Figure 7) show that the SOCl_2 and SO_2 peaks which are merged at the start of the electrolysis begin to separate at $n = 1.00$ and the separation increased as the electrolysis was continued to $n = 1.95$. The increased separation of the two peaks was due to the consumption of SOCl_2 and the generation of SO_2 during the electrolysis. No new peaks were observed during the electrolysis that could indicate the presence of SOCl_2 reduction intermediates or unexpected products.

After electrolysis at -20°C to $n = 1.95$ analyses by linear sweep voltammetry (LSV) were carried out immediately and after 0.5, 1.0, and 17 hours storage at -20°C . The electrolysis cell was then allowed to warm from -20°C to 0.0°C over a period of one hour and an additional LSV analysis carried out followed by scans after one hour storage at 0°C , after the cell had warmed to 20°C over one hour and after 1.5 hours warming from 20°C to 25°C . Finally, LSV analyses were undertaken after 1.5, 3.5, and 69 hours of 25°C storage. The voltammogram obtained after electrolysis to $n = 1.95$ at -20°C and 0.50 and 17 hours of -20°C storage are given in Figure 9. Figure 10 shows the voltammogram obtained after 0, 20, and 25°C storage. The slight increase in the SOCl_2 and SO_2 peaks seen after 17 hours of -20°C storage in Figure 9 are probably due to diffusion of SOCl_2 into the working electrode compartment from the counter electrode compartment during the storage period.

Two other constant current electrolysis experiments at -20°C were carried out to $n = 1.00$ with LSV analyses after storage at -20°C , 0°C , and 25°C and likewise no unusual reaction products were observed.

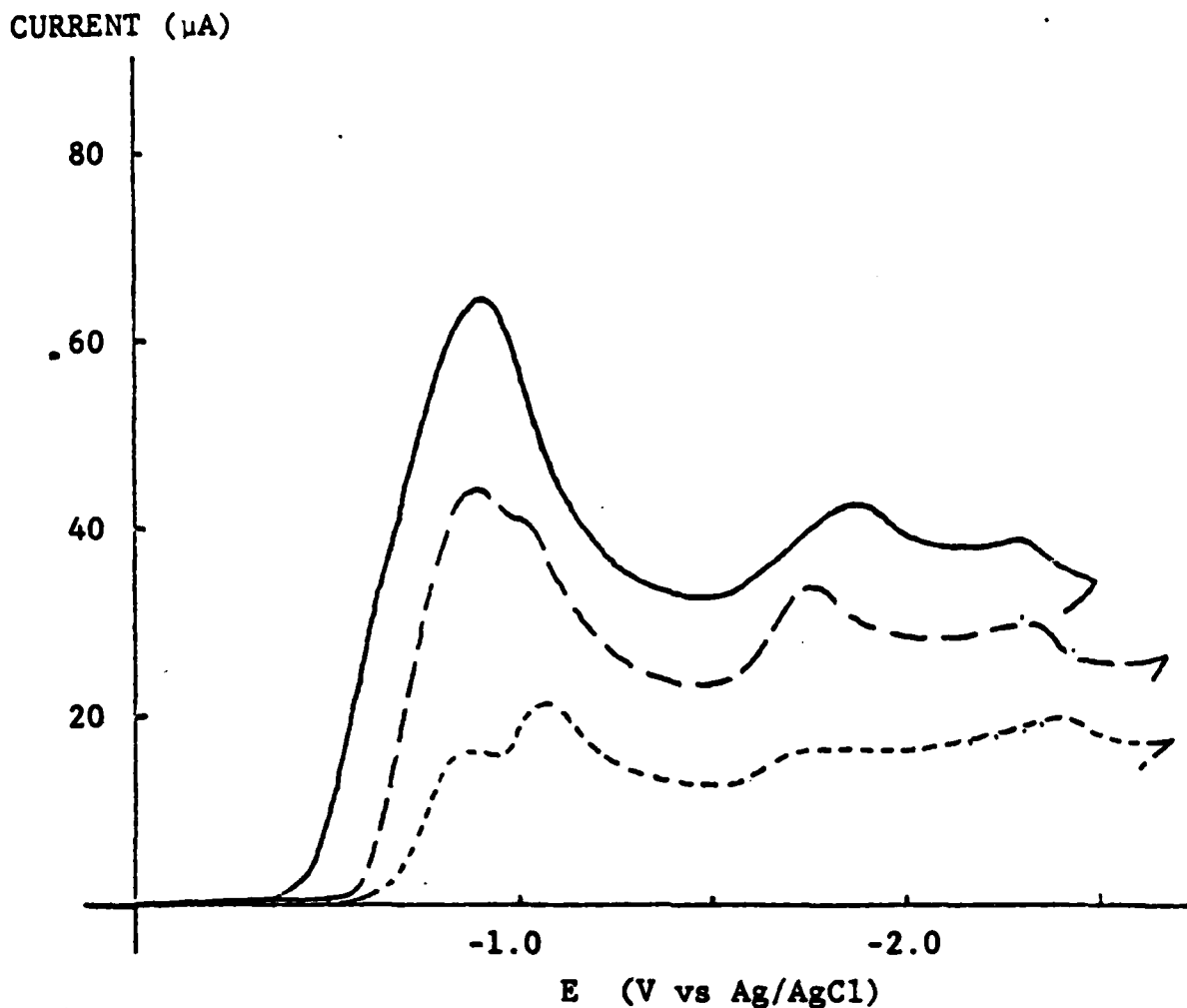


Figure 7: Voltammograms of 8.5mg of 1.8M $\text{LiAlCl}_4/\text{SOCl}_2$ in .1M TBAPF₆/DMF after electrolysis at -20°C, on a 4cm² Pt cathode at 0.50mA/cm², to n = 1.95. Scan rate = 200 mV/second. Return scans not shown.

(—): Scan at n = 0.00, OCP = 0.025V

(- -): Scan at n = 1.00, shown shifted -.463V (to the right)
OCP = 0.100V.

(- . - .): Scan at n = 1.95, shown shifted -.475V (to the right)
OCP = +0.070V

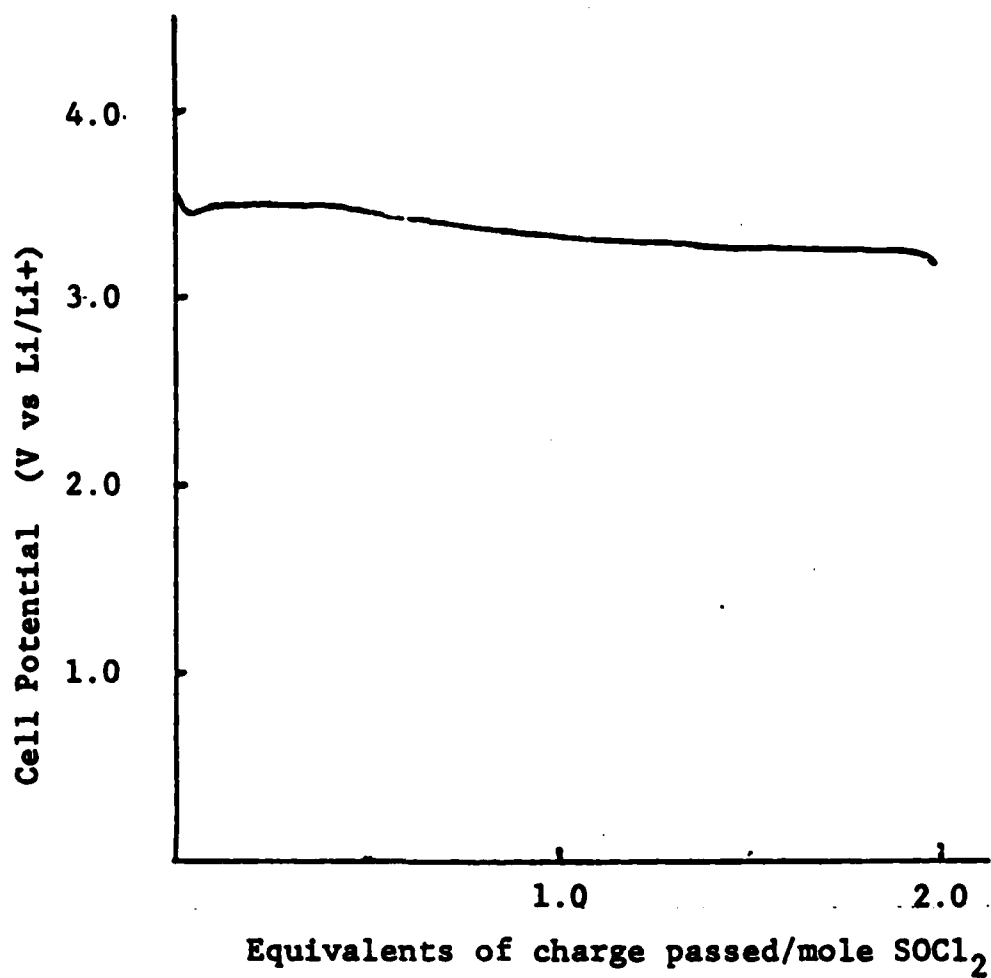


Figure 8: Cell Potential during 0.50mA/cm² constant current electrolysis at -20°C of 5.82mM SOCl₂ in 0.1M TBAPF₆/DMF at a 4cm² Pt cathode.

The sample of 8.5mg of 1.8M LiAlCl₄/SOCl₂ electrolyte was added to 10.0ml of DMF. The cell potential was monitored with a Ag/AgCl reference electrode and the potentials converted to a Li/Li⁺ ref. electrode scale on the basis of Ag/AgCl 3.42V vs Li/Li⁺.

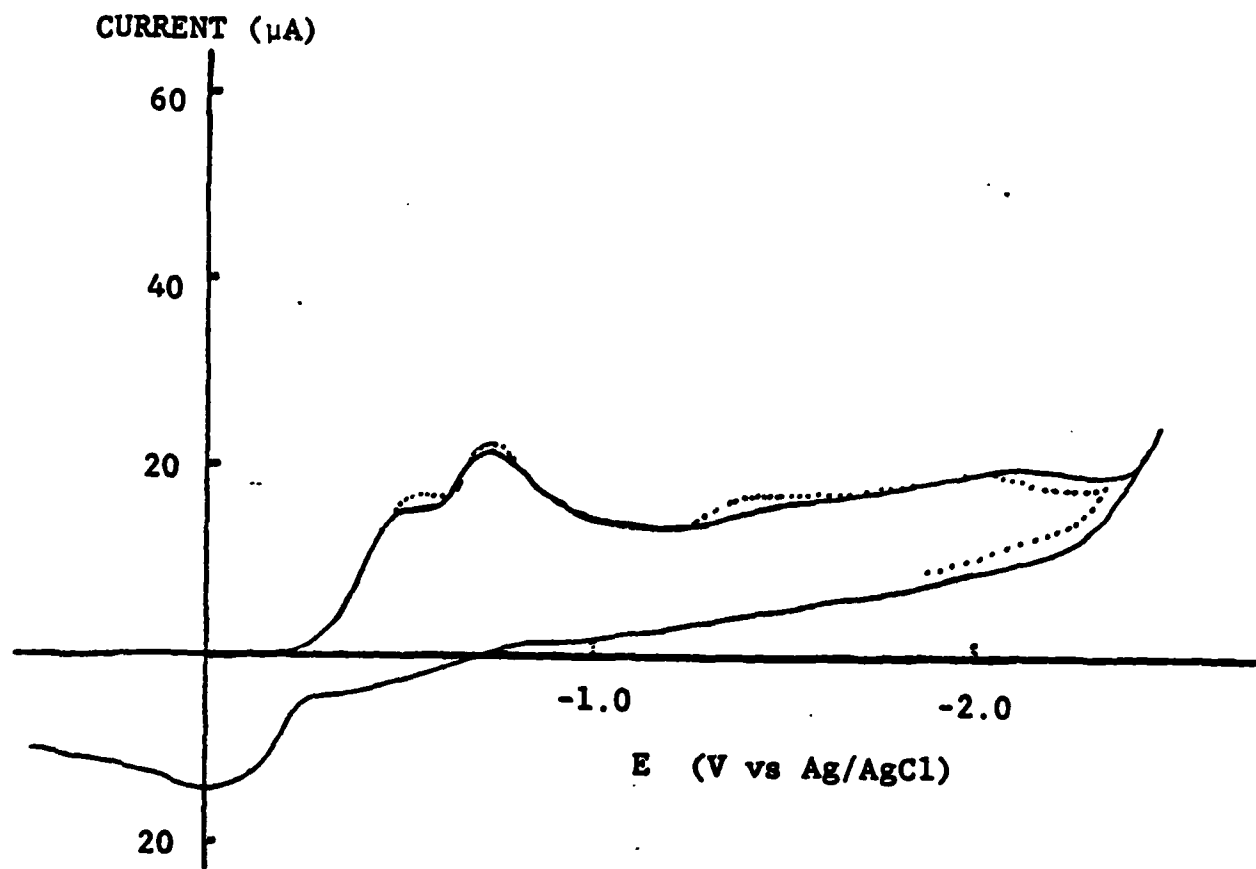


Figure 9: Voltammograms after -20°C storage of 8.5 mg of $1.8\text{M LiAlCl}_4/\text{SOCl}_2$ in $0.1\text{M TBAPF}_6/\text{DMF}$ after electrolysis at -20°C , on a 4 cm^2 Pt cathode at 0.50 mA/cm^2 to $n = 1.95$, scan rate 200 mV/second .

(—), Scan after 0.50 hours -20°C storage, $\text{OCP} = 0.070\text{V}$.

(...), Scan after 17 hours -20°C storage, $\text{OCP} = 0.025\text{V}$.

Drawn shown shifted 0.16V to the right.

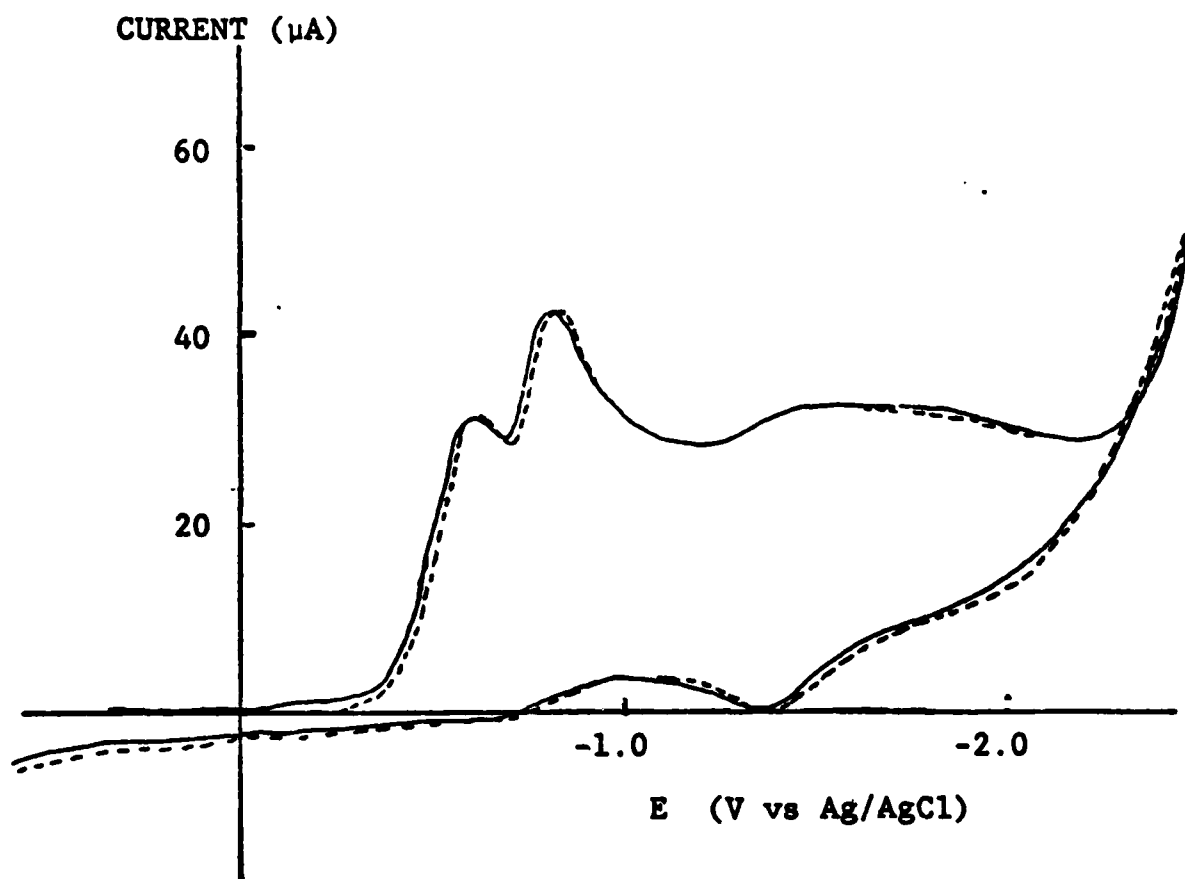


Figure 10: Voltammograms at 25°C after -20°C and 25°C storage of 8.5 mg of 1.8M LiAlCl₄/SOCl₂ in 0.1M TBAPF₆/DMF after electrolysis at -20°C on a 4 cm² Pt Cathode at 0.50 mA/cm² to n = 1.95, Scan Rate 200 mV/second.

- (—), Scan after 17 hours at -20°C, 1 hour warming to 0°C, 1 hour at 0°C, 1 hour warming to 20°C, and 1.5 hours warming from 20°C to 25°C, OCP = 0.075V.
- (.....), Scan after similar storage conditions as above with 3.5 hours additional storage at 25°C. OCP = 0.075V.

1.2.1.4 Discussion and Recommendations

The constant current electrolysis and voltammetry studies that were undertaken at -20°C gave no indication that SOCl_2 reduction at a Pt cathode in DMF yields significant quantities of SOCl_2 reduction intermediates with lifetimes from 0.1 to 17 hours at -20°C . It is possible that reactive SOCl_2 reduction intermediates were formed during electrolysis at -20°C but they reacted rapidly with the DMF supporting electrolyte and, thus, were not detected. However, Williams and co-workers (3) using ESR spectroscopy estimate that the various free radicals formed during the reduction of 1.5M $\text{LiAlCl}_4/\text{SOCl}_2$ at a gold electrode would have a lifetime of \approx six minutes at -46°C and < 10 seconds at 24°C . Since our electrolysis to $n = 1.95$ took 1.55 hours at 0.50 mA/cm^2 , intermediates with a half life of a few minutes at -20°C would react or decompose during the long electrolysis and would not build up to sufficiently large concentrations to be detected by voltammetry. Even if the intermediates were present at low concentrations and did not react with DMF they could have reduction potentials near SOCl_2 or SO_2 and, thus, have been difficult to detect by voltammetry.

Notwithstanding these uncertainties, it was concluded from the electrolysis, voltammetry and ESR data (2) that the concentration of SOCl_2 reduction intermediates formed during the discharge of Li/SOCl_2 cells from -20°C to 25°C is so small that it is unlikely that hazardous reactions could take place in commercial cells. It was also concluded that SOCl_2 is reduced at -20°C following the well established reaction (5,6) involving two electrons/mole of SOCl_2 to form SO_2 , Cl^- and S.

The reduction of SOCl_2 at low temperature could be further investigated by extending the temperature range to -40°C or below. However, the results of this initial exploratory investigation suggest that the effort required for such an extensive study would be more productively utilized at the present time in carrying out several other investigations such as studies of the reactions occurring during overdischarge and charging.

1.2.2 Voltammetry of Neutral and Acid Electrolyte with Added SO₂

1.2.2.1 Background

Earlier during the present program (1) it was found that voltammetric analysis of 1.8M LiAlCl₄/SOCl₂ electrolyte with 3.5M added SO₂ showed signs of substantial SO₂ reaction within four hours and almost complete consumption of the SO₂ within 46 hours at 25°C. The finding was significant because it provided an explanation for the decline of the SO₂ peak during storage after SOCl₂ electrolysis which had earlier been attributed (7) to the slow decomposition of an SOCl₂ reduction intermediate.

From the earlier voltammetry studies, it was not possible to determine the composition of species being produced from the reaction of SO₂ and LiAlCl₄/SOCl₂ in the DMF electrolyte but adducts such as LiAlCl₄•SO₂•SOCl₂ or LiAlCl₄•SO₂•DMF were considered likely products. Because the SO₂ - LiAlCl₄/SOCl₂ reactions observed by voltammetry could involve the DMF supporting electrolyte and, therefore, would not occur in commercial Li/SOCl₂ cells which do not contain organic solvents, quantitative infrared studies of the SO₂ - LiAlCl₄/SOCl₂ reaction were undertaken to determine whether the reaction could occur in batteries. The quantitative infrared studies of the above reaction that were carried out are described later in Section 1.3.2. The IR results showed that SO₂ reacts with 1.8M LiAlCl₄/SOCl₂ in the absence of organic solvents at rates very similar to those found during the initial voltammetry studies. Thus, the SO₂ - LiAlCl₄/SOCl₂ reaction occurs in Li/SOCl₂ batteries and could be of importance relative to high rate discharge, safety and anode corrosion during intermittent discharge and storage.

The infrared spectra obtained during the SO₂ - LiAlCl₄/SOCl₂ reaction only shows the decline of the SO₂ absorption peaks and does not show new peaks which could be used to determine the composition of the products. However, the voltammograms obtained during the reaction of SO₂ with LiAlCl₄/SOCl₂ not only show the decline of the SO₂ concentration with time but very clearly show

the generation of a new product which reduces at approximately $-1.4V$ vs $Ag/AgCl$. Thus, the original voltammetry study of the reaction of SO_2 with $SOCl_2$ electrolyte that was limited to neutral electrolyte was extended to the reaction of SO_2 with acid electrolyte and pure distilled $SOCl_2$, to gain information not provided by quantitative IR about the products of the reaction. Moreover, since both infrared and voltammetric analysis have certain experimental limitations, it would strengthen the data base to have the reaction rate confirmed by two different techniques.

The interpretation of the voltammetry data obtained earlier (1) during the exhaustive electrolysis of $SOCl_2$ acid electrolyte in DMF was restricted because it was not known whether SO_2 reacts with $SOCl_2$ in acid electrolyte and whether DMF would have a role in the reaction. Therefore, the voltammetric studies of the reaction of SO_2 with $SOCl_2$ acid electrolytes to be described in this section were undertaken, among other reasons, to assist in the interpretation of the earlier electrolysis results.

1.2.2.2 Neutral $SOCl_2$ Electrolyte With Added SO_2

The first series of voltammograms obtained earlier (1) in the program in the study of $1.8M LiAlCl_4/SOCl_2$ neutral electrolyte with $3.5M$ of added SO_2 were carried out immediately after the SO_2 was added and after 4, 46, and 120 hours of $25^\circ C$ storage. The voltammograms showed that substantial reaction had occurred after four hours storage. Thus, to reinvestigate the SO_2 reaction more thoroughly voltammetry was carried out after 1, 2, 5, and 22.5 hours of storage. Figure 11 gives the voltammograms obtained for $1.8M LiAlCl_4/SOCl_2$ with $2.7M$ of added SO_2 after 0, 1, 2, 5, and 22.5 hours of storage at $25^\circ C$.

The results in Figure 11 show that the SO_2 peak and to a lesser extent the $SOCl_2$ peak, decline during the first 22.5 hours of storage whereas a third peak at approximately $-1.4V$ increases dramatically in a regular manner during storage. The decline in the $SOCl_2$ peak during storage plotted in terms of the concentration of $SOCl_2$ in the DMF electrolyte as a function of time is given

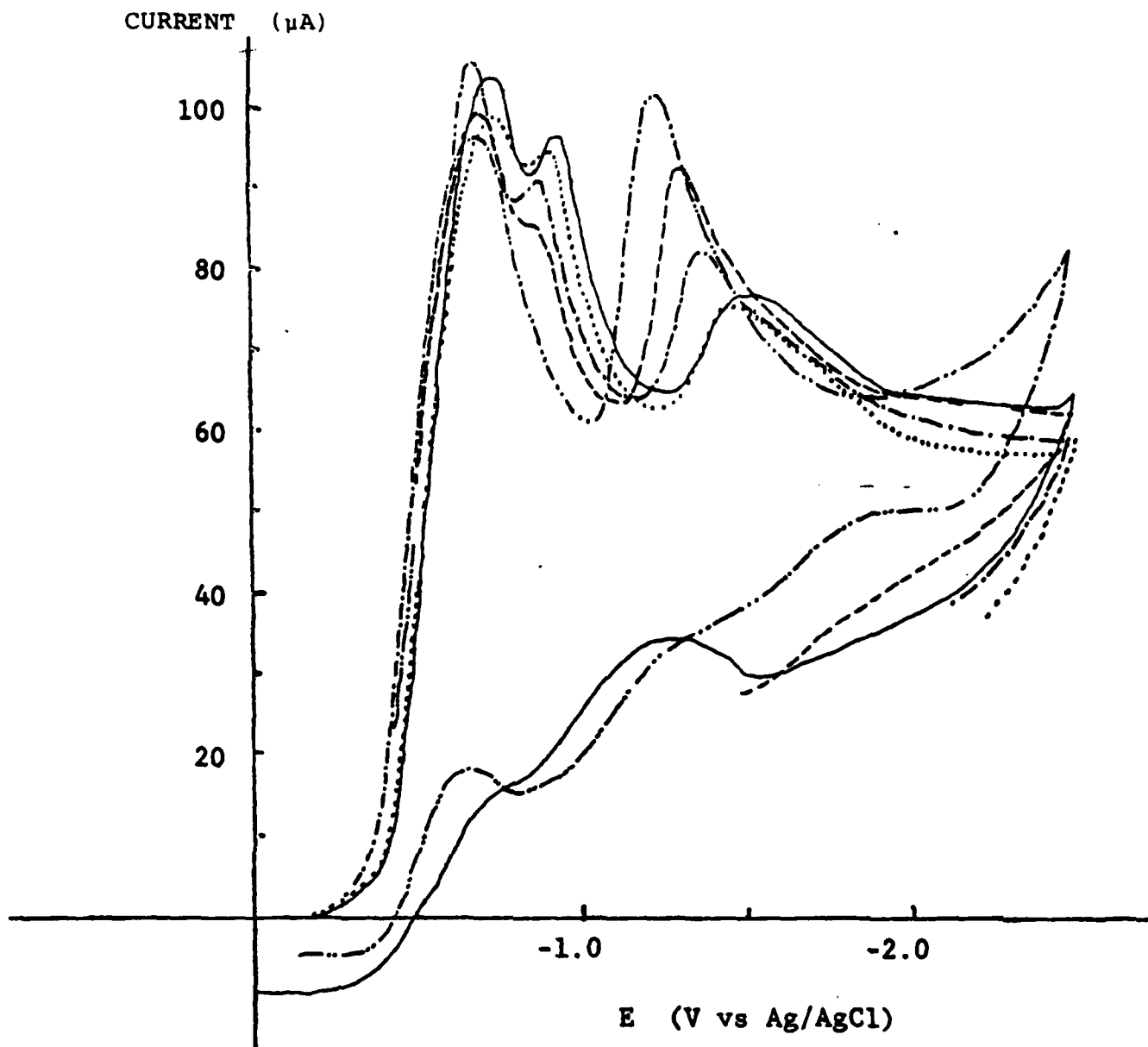


Figure 11: Voltammograms of 12mg of 1.8M LiAlCl_4 , 2.7M $\text{SO}_2/\text{SOCl}_2$, in 10ml of 0.1M $\text{TBAPF}_6/\text{DMF}$ at 25°C After Various Periods of Storage, Scan Rate 200mV/second.

- (——) immediately after electrolyte prepared .
- (.....) after 1 hour of storage
- (- . - .) after 2 hours of storage
- (— —) after 5 hours of storage
- (—.. —) after 22.5 hours of storage

in Figure 12. The SOCl_2 concentrations were obtained from a calibration curve of the SOCl_2 peak currents as a function of the SOCl_2 concentration for samples with a known concentration of SOCl_2 , using the same Pt working electrode as used for the LSV analyses in Figure 11.

Figure 15 shows the rise in the voltammetry currents for Peak III at approximately -1.4V plotted in terms of the storage time. A comparison of Figures 12 and 14 reveals that during five hours storage the SOCl_2 concentration only declines 8.4% (i.e., 7.32 to 6.77mM) whereas the current for Peak III increases 21% (i.e., 76.7 to 93.2 μA). Thus, it is possible that the reaction of one molecule each of SO_2 and SOCl_2 (or LiAlCl_4) produces two or more molecules of a new compound which is reduced giving Peak III. However, the larger current for Peak III could also be accounted for by other phenomenon such as absorption of the product on the platinum working electrode.

The quantitative infrared measurements of the reaction rate of 2.73M SO_2 in 1.8M $\text{LiAlCl}_4/\text{SOCl}_2$, presented later in Figure 19 of Section 1.3.2 show that only 6.7% of the SO_2 reacts after five hours and 26% after 22 hours in the absence of organic solvents at 25°C. Thus, the voltammetry and quantitative infrared results are in remarkably good agreement!

The finding that a portion of the SO_2 of concentrated SO_2 solutions of 1.8M $\text{LiAlCl}_4/\text{SOCl}_2$ electrolyte reacts with the electrolyte very slowly over a 20 hour period may be relevant to certain types of behavior of Li/ SOCl_2 batteries. It is possible that the product of the SO_2 - SOCl_2 electrolyte reaction may be somehow involved in the reactions in which the LiCl film on the Li anode slowly ages (5,8,10) during the first weeks of cell storage, slowly lowering the short circuit current.

Having discussed the most significant and unambiguous results of the voltammetric study of the reaction of SO_2 with neutral electrolyte, some of the unresolved aspects of the study will next be addressed. To follow the course of the SO_2 reaction, it would be useful if the SO_2 peak currents in Figure 11 could be used to calculate the SO_2 concentrations during storage. A baseline

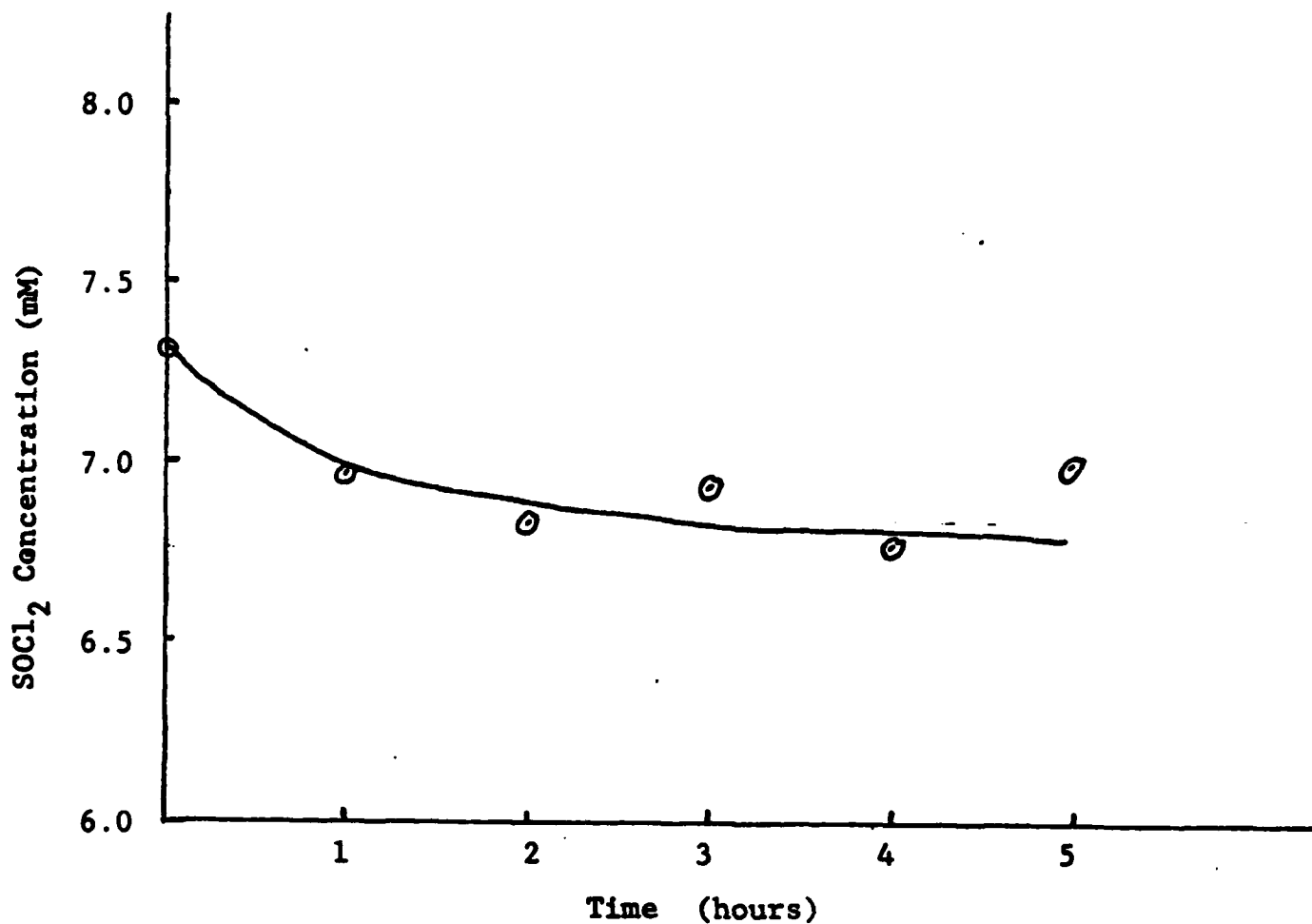


Figure 12: Decline in the SOCl₂ Concentration during 25°C Storage for a 1.8M LiAlCl₄/SOCl₂ Electrolyte Initially Containing 2.88M SO₂ Measured by Voltammetry*.

* For an approximately 12.0 8mg sample of 1.8M LiAlCl₄/SOCl₂ with 2.88M SO₂ added to 10ml of 0.1M TBAPF₆/DMF.

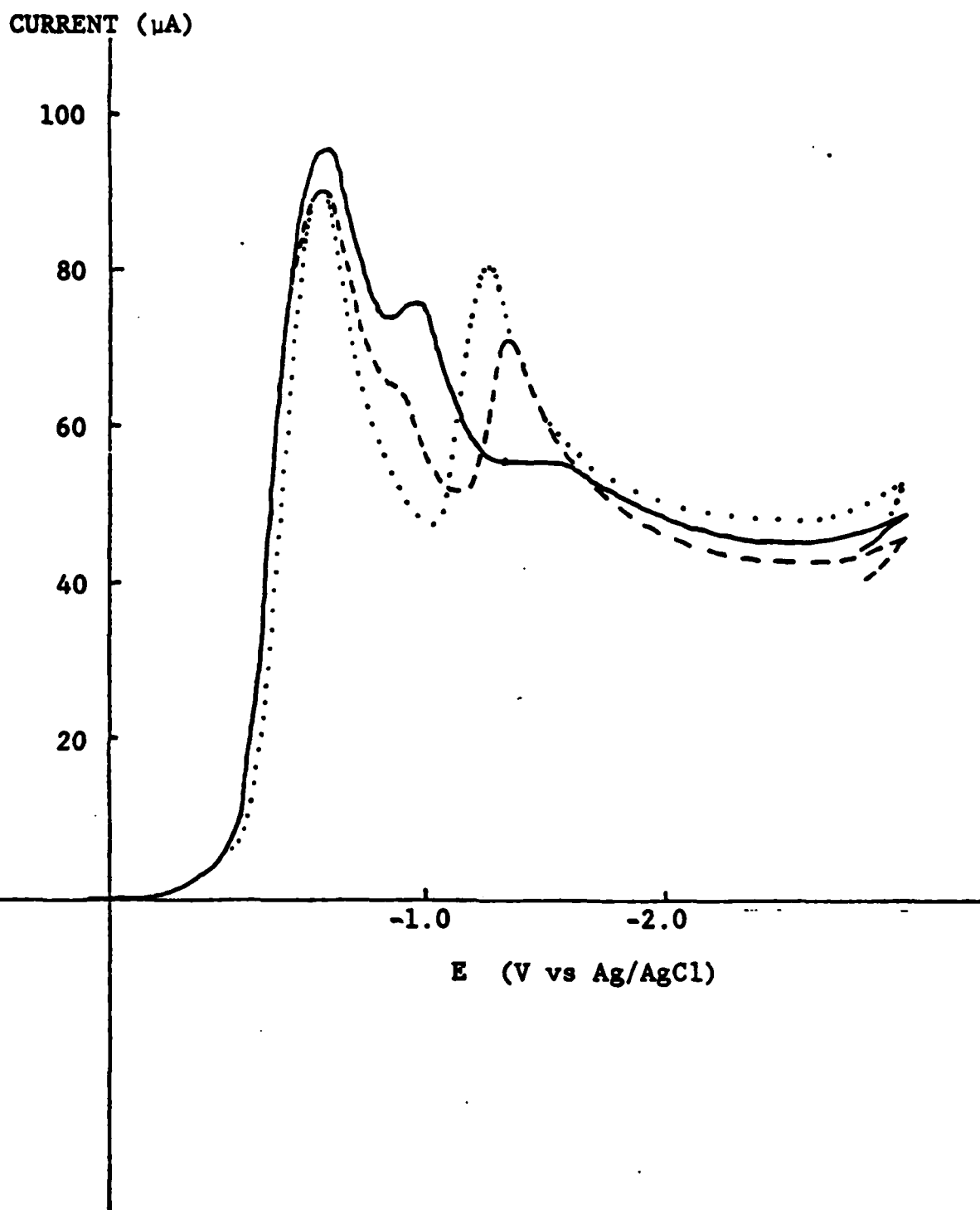


Figure 13: Voltammograms of $\approx 8\text{mg}$ of Distilled SOCl_2 with 2.8 M SO_2 in 10ml of $0.1\text{M TBAPF}_6/\text{DMF}$ at 25°C , scan rate 200mV/second .

- (—) immediately after electrolyte prepared
- (- - -) after 3 hours of storage
- (·····) after 22 hours of storage

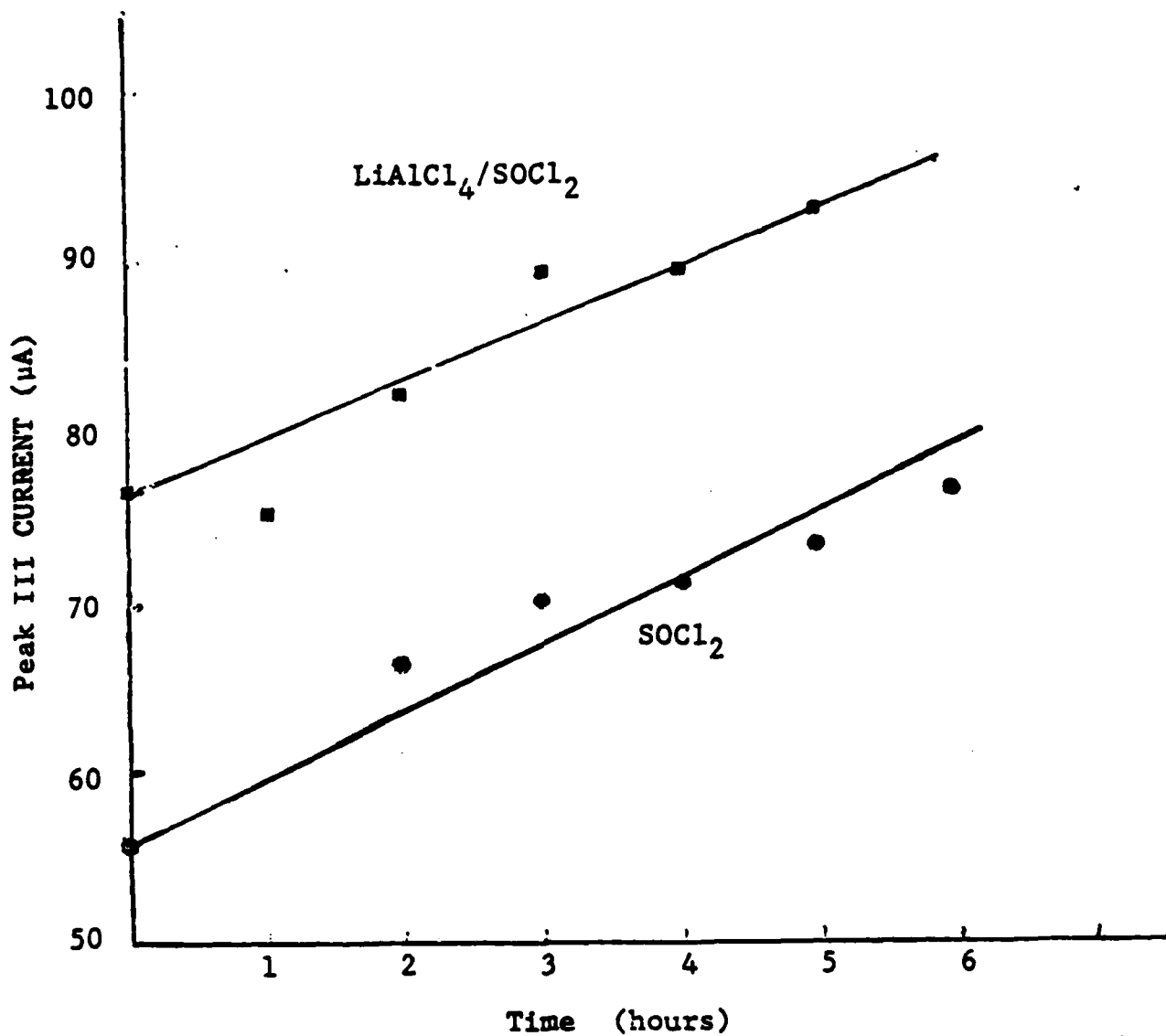
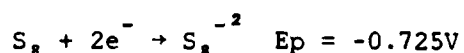


Figure 14: Voltammetry Currents For Peak III at Approximately -1.4V During 23°C Storage for 1.8M LiAlCl₄/SOCl₂ - 2.7M SO₂ and SOCl₂ - 2.8M SO₂ Samples in 0.1M TBAPF₆/DMF Supporting Electrolyte.

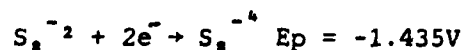
The Concentrations and voltammograms for the two samples are given in detail in the captions for Figures 11 and 13.

curve obtained using a held scan for SOCl_2 as described earlier (see Figure 17 of Ref. 1) was used to calculate the SO_2 peak currents but the precision of the SO_2 concentrations calculated in this manner was so low that it became clear that it would not be possible to calculate reliable values for the SO_2 concentration. It was concluded that voltammetry is not suitable for the present application to measure small changes (i.e., $< 20\%$) of the SO_2 concentration in SOCl_2 electrolytes and that other analytical techniques such as quantitative infrared analysis would be more accurate (see Section 1.3.1.).

The composition of the species produced by the reaction of SO_2 and $\text{LiAlCl}_4/\text{SOCl}_2$ and responsible for Peak III seen at approximately -1.4V in the voltammogram (see Figure 11) is of considerable interest since it would probably accumulate in substantial amounts ($\approx 20\%$) in the electrolyte of commercial cells. On the basis of the limited information presently available, it appears that the -1.4V peak may be due to the reduction of the polysulfide S_8^{-2} which occurs at a peak potential of 1.435V during voltammetry under conditions very similar to those used for the scans presented in Figure 11. Voltammograms for 15 mM sulfur in DMF were obtained earlier in the present program (1) and following the thorough study of the electrochemistry of sulfur reduction in DMSO by Sawyer (11) the reduction of elemental sulfur was concluded to take place as a two electron reduction. The first reduction of elemental sulfur to the polysulfide takes place at -0.725V .



The second reduction wave of sulfur which occurs at -1.435V in DMF was assigned by Sawyer to the two electron reduction of the polysulfide:



The presence of elemental sulfur as a product of the reaction of SO_2 and SOCl_2 electrolyte would help account for the observation that as the Peak III current increases in Figure 11 during storage the SOCl_2 peak current decreases then begins to increase. After 22.5 hours the SOCl_2 peak current increased to

106 μA which is larger than the initial SOCl_2 peak current (i.e., 104 μA). If elemental sulfur was a product of the SO_2 - SOCl_2 electrolyte reaction, then the first reduction peak of sulfur at -0.725V would be hidden under the SOCl_2 peak which occurs at -0.73V in Figure 11. As the sulfur concentration increased, the peak at -0.725V would increase along with Peak III and the SOCl_2 peak current would not decrease as much as expected then increase.

The only alternative assignment for Peak III that can be suggested on the basis of the limited data available is S_2Cl_2 , sulfur monochloride. Bowden and Dey (7) have reported that S_2Cl_2 reduces with a small absorption wave near -1.15V and a large reduction wave at -1.75V in acetonitrile/TBAPF₆ at 500 mV/second. Since S_2Cl_2 gives a very characteristic peak shape, and since Peak III is 300 to 500 mV anodic of the -1.75V peak of S_2Cl_2 , it is doubtful that Peak III is due to S_2Cl_2 .

It is also likely that Peak III may be due to a compound which is only produced in DMF and which is not produced in SO_2 - LiAlCl_4 / SOCl_2 electrolytes free from organic solvents. Thus, discussion about the products of the SO_2 - SOCl_2 electrolyte reaction will be continued later in Section 1.3 after the quantitative infrared studies of the reaction have been presented.

To determine whether LiAlCl_4 takes part in the reaction between SO_2 and LiAlCl_4 / SOCl_2 electrolyte, voltammetric analyses were carried out on samples of distilled SOCl_2 containing 2.8M SO_2 after periods from 0 to 22 hours of storage at 25°C. The voltammograms obtained immediately after the SOCl_2 and SO_2 were mixed and after 3 and 22 hours of storage are shown in Figure 13. The rapid decline in the SO_2 peak and to a lesser extent the SOCl_2 peak during storage is very similar to the behavior seen in Figure 11 for LiAlCl_4 / SOCl_2 to which SO_2 has been added. The increase in the Peak III current during storage for the SOCl_2 - SO_2 sample is compared in Figure 14 with the results obtained for 1.8M LiAlCl_4 / SOCl_2 containing 2.7M of added SO_2 .

From Figure 14, it can be seen that the rate of increase in the Peak III current for the SOCl_2 - SO_2 solutions is approximately the same for the samples

with and without LiAlCl_4 . It was, therefore, concluded that LiAlCl_4 does not take part in the reaction of SO_2 with SOCl_2 electrolytes. However, the SO_2 - SOCl_2 reaction may require the presence of an ionized dissolved salt as a catalyst and the 0.1M TBAPF_6 dissolved in the DMF may, perhaps, serve as a catalyst. Since an ionized salt is required in the supporting electrolyte for voltammetry, it is evident that the possibility that TBAPF_6 functions as a catalyst will have to be determined using another analytical technique such as quantitative infrared analysis.

1.2.3 Voltammetry of Acid SOCl_2 Electrolyte with Added SO_2

The voltammograms obtained for 1.65M SO_2 added to 2.0M AlCl_3 , 0.10M $\text{LiCl}/\text{SOCl}_2$ acid electrolyte after 0, 5.75 and 22 hours of storage at 25°C are shown in Figure 15. The 2.0M AlCl_3 , 0.10M $\text{LiCl}/\text{SOCl}_2$ concentration for the acid electrolyte used in the investigation was the same formulation as used earlier in the constant current electrolysis studies (1) and was chosen based on its favorable characteristics for low temperature reserve cell applications. The rapid decline in the SO_2 peak and the increase in Peak III at approximately -1.3V during storage is very similar to the behavior seen for $\text{LiAlCl}_4/\text{SOCl}_2$ and distilled SOCl_2 to which SO_2 was added as shown previously in Figures 11 and 13, respectively. The Peak III current increased from 44.6 μA immediately after the SO_2 was added to 49.5 μA after 5.75 hours storage which is a somewhat smaller reaction rate than observed earlier for pure SOCl_2 and neutral electrolyte. The lower rate of increase in the Peak III current during storage in the case of acid electrolyte was probably due to the lower initial SO_2 concentration of 1.6M compared to 2.8 and 2.88M SO_2 in the other experiments.

Quantitative infrared measurements of the reaction of 1.6M SO_2 with 2.0M AlCl_3 , 0.10M $\text{LiCl}/\text{SOCl}_2$ are presented later in Figure 20 and confirm the lower reaction rate observed by voltammetry. The infrared measurements also provide strong evidence that the DMF supporting electrolyte is not directly involved in the reaction of SO_2 with SOCl_2 acid electrolyte.

The interpretation of the voltammetry data obtained during the first half of the program (1) involving the exhaustive electrolysis of SOCl_2 acid electrolyte was restricted earlier because previously it was not known whether SO_2 reacted with SOCl_2 acid electrolyte. Now that the rate and extent of reaction of SO_2 with SOCl_2 acid electrolyte has been characterized by both infrared and voltammetric analysis, some of the results of these earlier electrolyses experiments can be better understood. For example, 16 hours after the constant current electrolyses of 8 mg of SOCl_2 acid electrolyte in DMF to $n = 1.12$ at a Pt cathode, the SOCl_2 and SO_2 peaks decreased and the peak at -1.36V increased [see Figure 33, Ref (1)]. The increase in the -1.36V peak during and after the electrolysis of the acid electrolyte could have been understood previously to be due to the formation of a new product or intermediate from the reduction of SOCl_2 . In terms of our new information about the SO_2 - SOCl_2 reaction in acid electrolyte, the increase in the -1.36V peak seen during storage after electrolysis at Pt is clearly due to the product of the SO_2 - SOCl_2 reaction. The growth in the 1.36V peak seen during the course of the electrolysis could also be due to the product of the SO_2 - SOCl_2 reaction but considering the large size of the peak and the relative slowness of the SO_2 - SOCl_2 reaction, it is thought that the -1.36V peak seen at $n = 1.12$ is primarily due to the second reduction peak of elemental sulfur.

1.3 INVESTIGATION OF THE ADSORPTION OF SULFUR DIOXIDE FROM SOCl_2 ELECTROLYTES BY THE CARBON CATHODE

1.3.1 Background

One of the major goals of the project was to investigate the products and intermediates of the electrochemical reduction of SOCl_2 in prototype cells over a broad range of temperature and discharge conditions. During the first half of the project (1) it was found that reduction of SOCl_2 can not be accurately studied in prototype Li/ SOCl_2 cells by chemically analyzing the electrolyte because SO_2 and presumably other products are strongly adsorbed by the carbon cathode. Furthermore, it was found that SO_2 can not be accurately determined

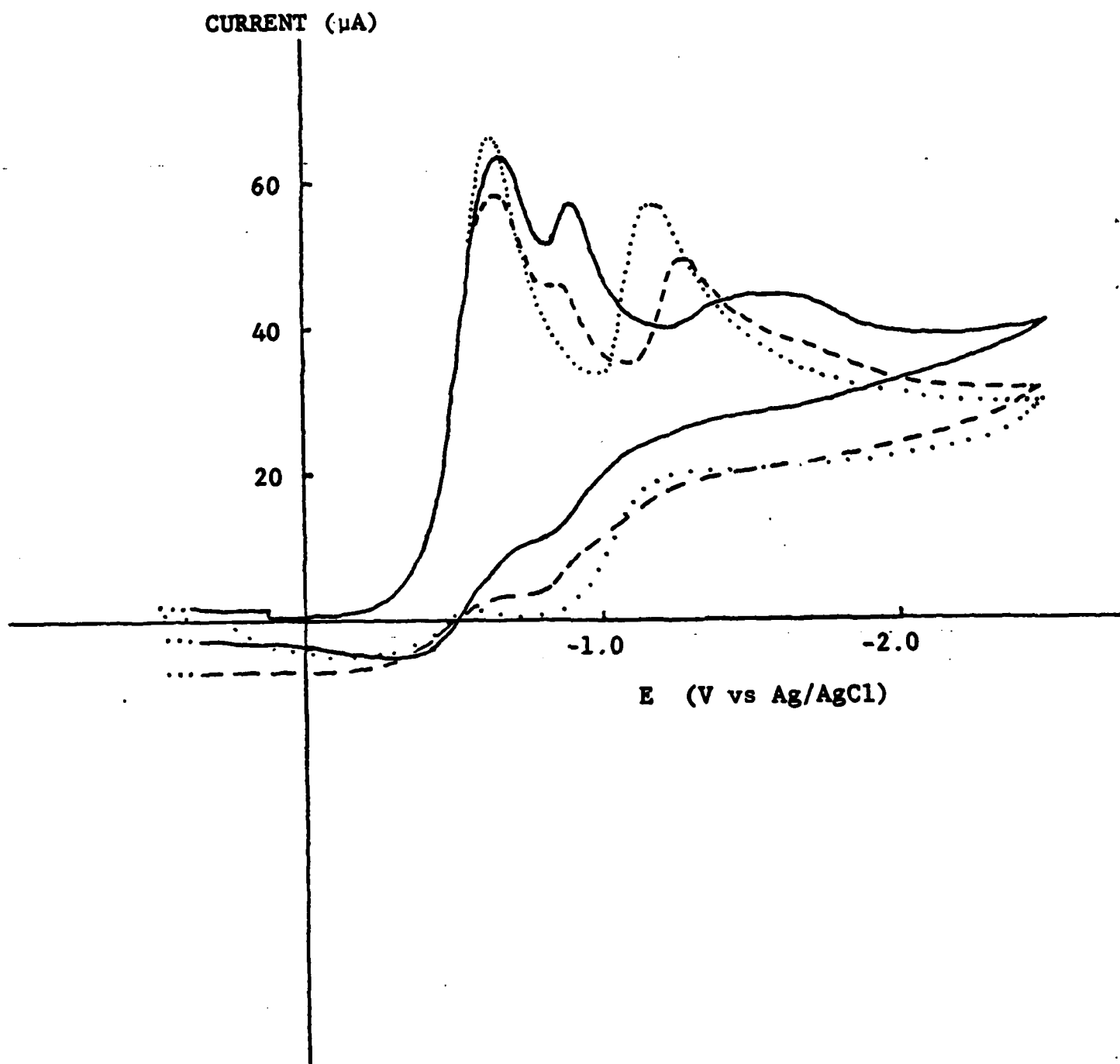


Figure 15: Voltammograms of $\approx 8\text{mg}$ of 2.0M AlCl_3 , 0.10M LiCl/SOCl_2 Acid Electrolyte with 1.65M SO_2 in 10ml of $0.10\text{M TBAPF}_6/\text{DMF}$ at 25°C , Scan rate 200 mv/second .

- (—) immediately after electrolyte prepared
- (- - -) after 5.75 hours of storage
- (. . . .) after 22 hours of storage

by voltammetry in the presence of an excess of SOCl_2 , because the reduction peaks for the two compounds are only 300 mV apart. The results of the exploratory studies carried out during the first half of the project (1) showed that 40% of the SO_2 from a 1.8M $\text{LiAlCl}_4/\text{SOCl}_2$ solution with 2.73M SO_2 was absorbed on Shawinigan carbon black. Based on these exploratory results a more extensive investigation was undertaken that will be presented in this section. The new investigation included adsorption measurements in both neutral and acid SOCl_2 electrolytes for Shawinigan carbon without and with the Teflon binder used in commercial cathodes. Higher ratios of carbon-to-electrolyte weight were used and the results were corrected for the reaction of SO_2 with SOCl_2 electrolyte.

A quantitative understanding of SO_2 adsorption on the carbon cathode of Li/ SOCl_2 cells under well controlled conditions is required to determine whether discharge intermediates are produced in prototype Li/ SOCl_2 cells during discharge. Since the chemical composition of possible intermediates or unusual products are not known, thereby preventing the use of highly specific methods of chemical analysis, the approach chosen was to chemically analyze the cell electrolyte and components for SO_2 after discharge. Any difference between the SO_2 value calculated from the number of coulombs of discharge and the SO_2 value obtained by chemical analysis would be the maximum concentration of intermediate or unexpected products that could be present. To obtain a reliable and accurate estimate of the amount of intermediates produced, it is clear that (i) the chemical analyses (ii) the correction for SO_2 adsorption by the carbon and (iii) the correction for SO_2 reaction with the electrolyte must all be accurate to at least 10%.

Once the extent of SO_2 adsorption by carbon from the SOCl_2 electrolytes is known, the analysis of SO_2 from prototype cells to determine the maximum level of intermediates could be carried out in several ways depending on the results. If the SO_2 adsorption was relatively small, the electrolyte samples could be analyzed for SO_2 and the SO_2 concentrations corrected for SO_2 adsorption by the carbon. However, should it be found that substantial SO_2 is adsorbed by the carbon, it may be necessary to develop new procedures, such as

total disassembly of the cell at low temperatures and separate analysis of the electrolyte and carbon cathode for reduction products. Low temperature extraction or disassembly of the cell would be required to suppress the SO_2 - SOCl_2 electrolyte reaction and SO_2 losses from the electrolyte by Henry's low evaporation effects.

1.3.2 Experimental Procedure

1.3.2.1 Infrared Cells and Instrumentation

The infrared absorption of SO_2 at 1333 cm^{-1} has been found (6) to be the most useful absorption band for the quantitative analysis of SO_2 in SOCl_2 solutions. The selection of a suitable cell requires some care since SOCl_2 electrolytes slowly dissolve window materials such as NaCl causing the pathlength to change and leaving opaque deposits. For the quantitative IR measurements an in-house machined stainless steel cell similar to the Barnes Analytical/Spectra Tech., Inc. demountable liquid cell was used with either NaCl or CaF_2 windows. Pathlengths from 0.125 to 0.02 mm were tested and 0.05 mm was selected as the most suitable. Longer pathlengths gave poor baselines (see Figure 16) due to the broadening of the intense absorption at 1245 cm^{-1} due to SOCl_2 . Shorter pathlength spacers were too fragile to be reused and the pathlength was not reproducible. The NaCl windows (32 x 3 mm) used in the demountable liquid cell were fogged by reaction with the SOCl_2 electrolyte which produced residues that could not be removed by common solvents (except water). Thus, after several hours of use, it was necessary to take the cell apart and abrasively clean and polish the NaCl windows. Besides being time consuming, the process of taking the cell apart and rebuilding it caused the pathlength to change, therefore, a new calibration curve had to be generated after each cell assembly.

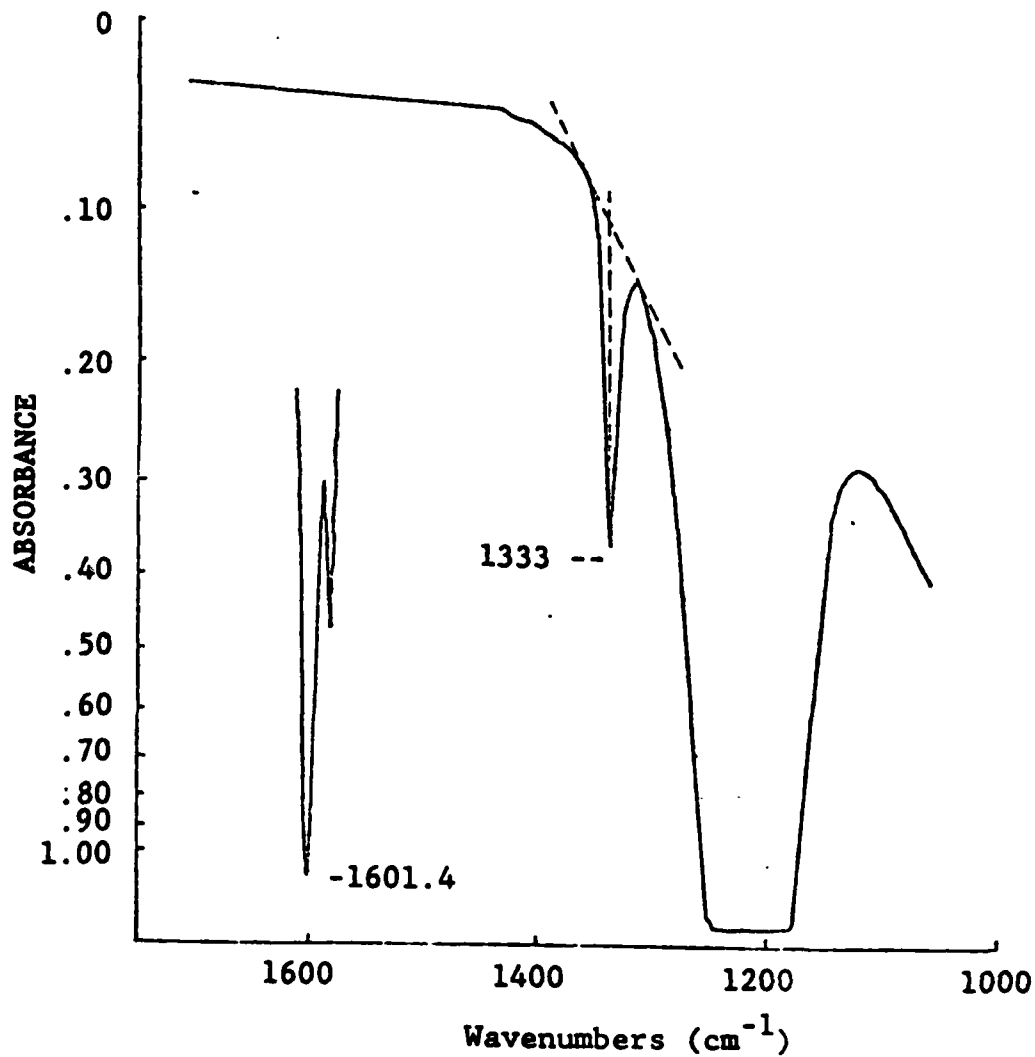


Figure 16: IR Absorption of $\text{SO}_2/\text{SOCl}_2$ Electrolyte Showing Baseline Technique, Polystyrene Reference Sample, and CaF_2 Linearity Cutoff.

(————) Actual Absorbance of Samples
 (-----) Baseline Estimation Technique

Windows of CaF_2 were used for many of the measurements because they are much more stable to attack by AlCl_3 and SOCl_2 and can be more easily cleaned without cell disassembly. Care must be taken when handling CaF_2 windows since they are temperature and shock sensitive. The usable linear transmission region for CaF_2 windows is 1100 cm^{-1} compared to 590 cm^{-1} for NaCl , thus CaF_2 is adequate for quantitative analysis of SO_2 using the 1333 cm^{-1} band. However, during the investigation of the reaction of SO_2 with SOCl_2 electrolyte, the appearance of new bands due to products of the reaction down to at least 450 cm^{-1} was of interest. Thus, many of the IR analyses were carried out with NaCl windows or disposable AgCl cells (0.1 mm pathlength). The disposable AgCl cells were only used to obtain IR spectra for qualitative purposes.

Quantitative analysis of $\text{SO}_2/\text{SOCl}_2$ electrolyte samples for SO_2 was carried out on a Perkin-Elmer Model 621 grating IR spectrophotometer from 1700 cm^{-1} to 1100 cm^{-1} . All instrumental parameters (e.g., scan time, gain and suppression) were held constant once optimized. The baseline to calculate the SO_2 absorption was determined by drawing a line tangent to both sides of the SO_2 peak (see Figure 16). The actual absorption due to SO_2 is thus the peak absorbance at 1333 cm^{-1} minus the baseline absorbance at 1333 cm^{-1} .

1.3.2.2 Preparation of $\text{SO}_2/\text{SOCl}_2$ Electrolyte Solutions

Concentrated standard solutions of SO_2 in neutral and acid SOCl_2 electrolyte were prepared gravimetrically by bubbling anhydrous SO_2 through the SOCl_2 electrolyte and weighing the bubbler tube before and after the SO_2 was added. The bubbler tube was cooled with a dry ice/acetone bath to prevent a weight loss due to SOCl_2 evaporation and to increase the rate of SO_2 dissolution in the electrolyte. At dry ice temperatures, the SO_2 bubbles in the bubbler dissolved before they reached the surface of the electrolyte. The solubility of SO_2 in 1.8M $\text{LiAlCl}_4/\text{SOCl}_2$ is 3.92M at 24°C (12), thus, solutions were prepared with SO_2 concentration below 2.88M SO_2 to minimize SO_2 losses during transfer operations such as pipetting.

The procedure used to prepare the 1.8M LiAlCl₄/SOCl₂ and 2.0M AlCl₃, 0.10M LiCl/SOCl₂ electrolytes was the same as described earlier [i.e., Section 1.1.2 of Ref.(1)]. The residual SO₂ present in the 1.8M LiAlCl₄/SOCl₂ was determined from the infrared spectra and was approximately $8.0 \cdot 10^{-4}$ M or 0.003 Wt%.

All SO₂ used to prepare solutions was purified using the basic procedure described by Burow (13) starting with 99.98% anhydrous SO₂ (Matheson), which was first passed through a bubbler of concentrated H₂SO₄ to remove SO₃, a 36 inch column of Linde 3A molecular sieves, a six-inch column of P₂O₅, then distilled into a flask containing P₂O₅. After storage over P₂O₅ for at least 48 hours, the SO₂ was distilled a second time before use to prepare standard solutions.

Several special precautions had to be taken when concentrated standard or unknown solutions were diluted prior to analysis to avoid losses of SO₂ from the solutions. Pipettes with large tip openings were filled very slowly to minimize losses of SO₂ due to the reduced pressure and turbulence required to fill the pipette. Volumetric flasks were half filled with the diluting SOCl₂ electrolyte before the concentrated sample was added. The SO₂ calibration standards were used immediately, and discarded because dilute solutions of SO₂ in SOCl₂ electrolyte are unstable. Concentrated standard solutions of SO₂/SOCl₂ electrolyte used to prepare the more dilute standards were stored at -67°C or below to prevent SO₂ losses due to the SO₂-SOCl₂ electrolyte reaction. The preparation and transfer of SO₂/SOCl₂ electrolyte solution was carried out either in an argon filled glove box or a dry room maintained at < 4% R.H.

1.3.2.3 Procedure for the Adsorption Measurements

The carbon or carbon/Teflon cathode material samples were vacuum dried at 150°C for 24 hours and added to a 14 cm x 3 cm diameter heavy wall glass tube. The tube was hermetically sealed with a glass cap using a high pressure metal coupling with a thick Teflon gasket. The tube containing the carbon was evac-

uated through a glass vacuum stopcock with a Teflon plug connected to the glass cap. The $\text{SO}_2\text{-SOCl}_2$ electrolyte was pipetted while cool, into the long 10 mm diameter glass filling tube connected to the valve and pulled into the cell by opening the stopcock to the evacuated tube. The stopcock was closed before all the solution had passed through the stopcock in order to prevent air entering the tube and to maintain a partial vacuum. The pressure in the apparatus was held at the electrolyte pressure for one hour, by which time the carbon samples had sunk to the bottom of the tube, indicating that they were completely filled with electrolyte. The stopcock was opened to the dry room atmosphere briefly to equalize the pressure.

The tube was initially filled with 100 ml of the $\text{SO}_2\text{-SOCl}_2$ electrolyte and 5 ml samples for analysis were taken after various time periods by tipping the tube upside down, opening the stopcock and allowing 5 ml of liquid to flow into a 15 ml screw cap test tube. The glass microliter syringe used to fill the demountable infrared cell was not filled in the regular way because the reduced pressure caused by pulling out the plunger would cause SO_2 bubbles to form, resulting in SO_2 losses and errors in the analysis. Instead, the syringe was filled by removing the plunger and filling it with a Pasteur pipet with a large tip opening, then replacing the plunger. The IR cell was filled by inserting the ground glass tip of the glass syringe (without a needle), into the "needle plate" of the demountable cell. The sample must be injected slowly to prevent internal pressure from cracking the windows or forcing the corrosive electrolyte past the gaskets causing the cell to leak and possibly damage the IR spectrometer.

The experimental procedure used to investigate the rate of reaction of SO_2 with SOCl_2 electrolyte was very similar to the one just given for SO_2 absorption except for the carbon cathode material that was not included.

1.3.3 Results and Discussion

1.3.3.1 Infrared Analysis Calibration for Sulfur Dioxide

A typical set of infrared spectra for 1.8M $\text{LiAlCl}_4/\text{SOCl}_2$ electrolyte with increasing amounts of SO_2 are given in Figure 17. The spectra show the substantial decrease in the transmittance of the 1333 cm^{-1} band as the SO_2 concentration was increased from the $8.0 \cdot 10^{-4} \text{ M}$ SO_2 background to 0.117M SO_2 . Because of the strong IR absorbance of SO_2 and the sensitivity of the spectrometer, the maximum upper SO_2 concentration in the SO_2 electrolytes transferred to the IR cells was limited to approximately 0.25M.

The concentrated solutions used for the carbon adsorption studies were generally diluted with SOCl_2 electrolyte by a factor of 25 for the quantitative infrared analysis. The concentrations after dilution were calculated assuming no volume change upon the addition of SO_2 because values of the densities of SOCl_2 electrolyte solutions containing various amounts of SO_2 were not available over the complete concentration range required.

From literature values (14) of the densities of 1.5M AlCl_3 , 0.15M LiCl , 0.15M SOCl_2 solutions, with and without 0.5M SO_2 (i.e., $\rho = 1.678$ and 1.688 g/ml at 20°C ., respectively), it is estimated that the systematic errors caused by neglecting density changes varied from 0.59% for 0.50M SO_2 to approximately 3.3% for 2.8M SO_2 solutions. Thus neglecting the density changes could cause systematic errors in the absolute values of the SO_2 concentrations found by the analysis but the decreased SO_2 concentrations observed during storage due to SO_2 adsorption by carbon and the reaction of SO_2 with SOCl_2 electrolyte are real and are influenced to a much lesser extent by the lack of a density correction. This is because the amount of reaction or adsorption on carbon is the difference of two concentrations over a given period of time and the density corrections tend to cancel out.

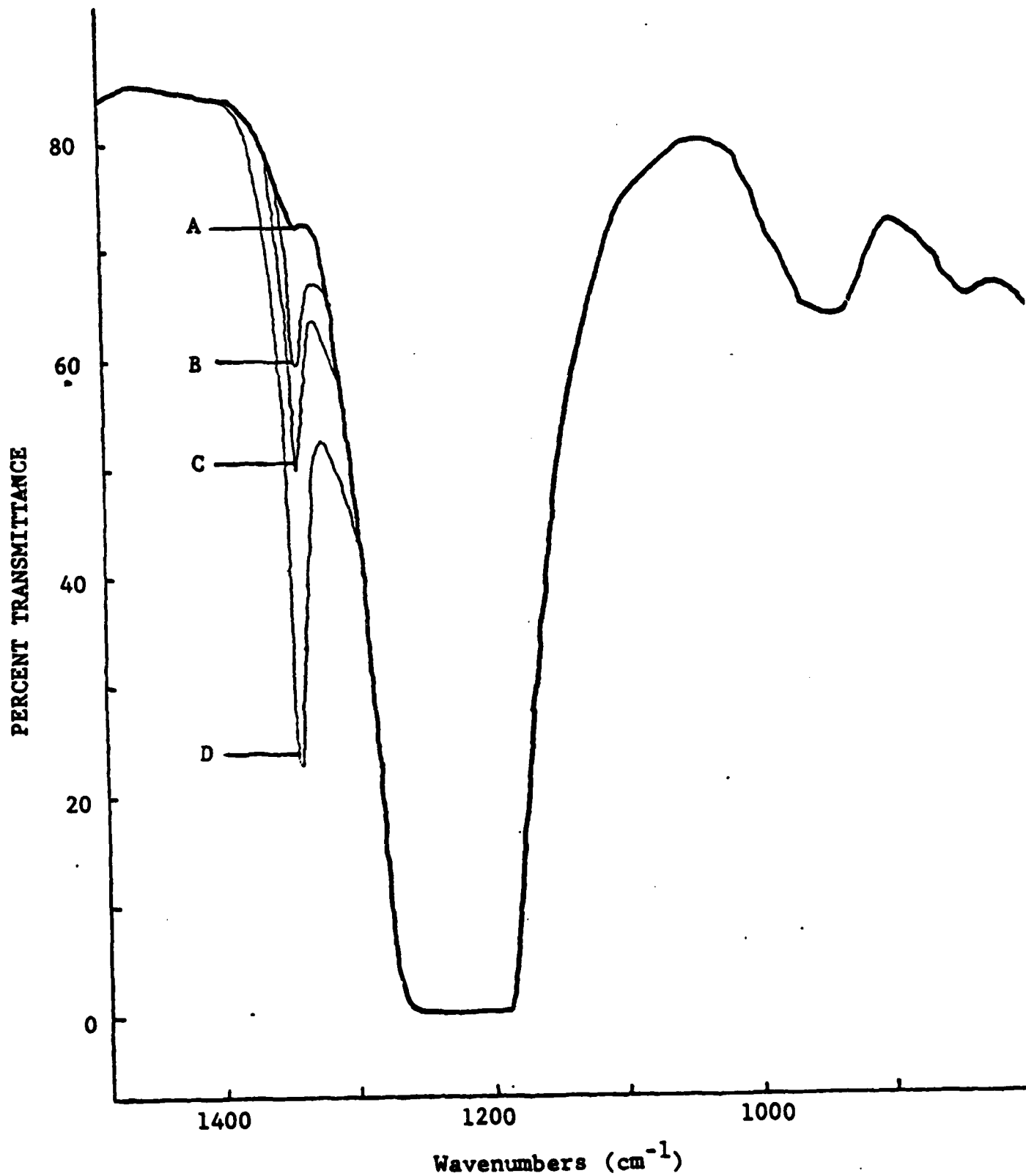


Figure 17: Infrared Spectra of 1.8M LiAlCl₄/SOCl₂ with Increasing Amounts of SO₂

A, Without Added SO₂; B, 0.0256M SO₂; C, 0.0601M SO₂; D, 0.117M SO₂; Spectra Obtained With 0.13mm Pathlength NaCl Cell.

Figure 18 shows a typical Beer's law calibration curve for the IR absorbance at 1333 cm^{-1} as a function of the SO_2 concentration in 2.0M AlCl_3 , 0.1M LiCl/SOCl_2 acid electrolyte. The standard error of estimate to the least squares linear equation

$$A = 1.421 C + 0.0131$$

(where A is the absorbance at 1333 cm^{-1} and C the SO_2 concentration) for the data in Figure 18 was 0.00516 or $\pm 2.8\%$ at 0.111M SO_2 . Thus, SO_2 can be determined in SOCl_2 electrolytes by quantitative IR spectroscopy with excellent accuracy if the numerous precautions discussed earlier are followed.

Calibration curves were generated for both neutral and acid electrolyte, as well as each time the IR cells were disassembled for cleaning as discussed earlier. Since a tight work schedule was required to calibrate a cell and also analyze samples at regular time intervals during a carbon adsorption experiment, time usually permitted no more than three or four concentrations for each of the calibration curves that were required.

1.3.3.2 Reaction of SO_2 with SOCl_2 Electrolytes

The rate of reaction of SO_2 with neutral and acid SOCl_2 electrolyte is given in Figures 19 and 20, respectively, where the SO_2 concentration is plotted as a function of the storage period. The decline in the SO_2 concentration due to the reaction of SO_2 with SOCl_2 electrolyte in the absence of carbon is indicated by the solid line curve in each figure. The numerical values of the SO_2 concentrations plotted in Figures 19 and 20 as determined by quantitative infrared analysis are listed in Tables 1 and 2.

A comparison of the results obtained in neutral and acid SOCl_2 electrolyte indicate that the SO_2 - SOCl_2 electrolyte reaction proceeds somewhat faster in

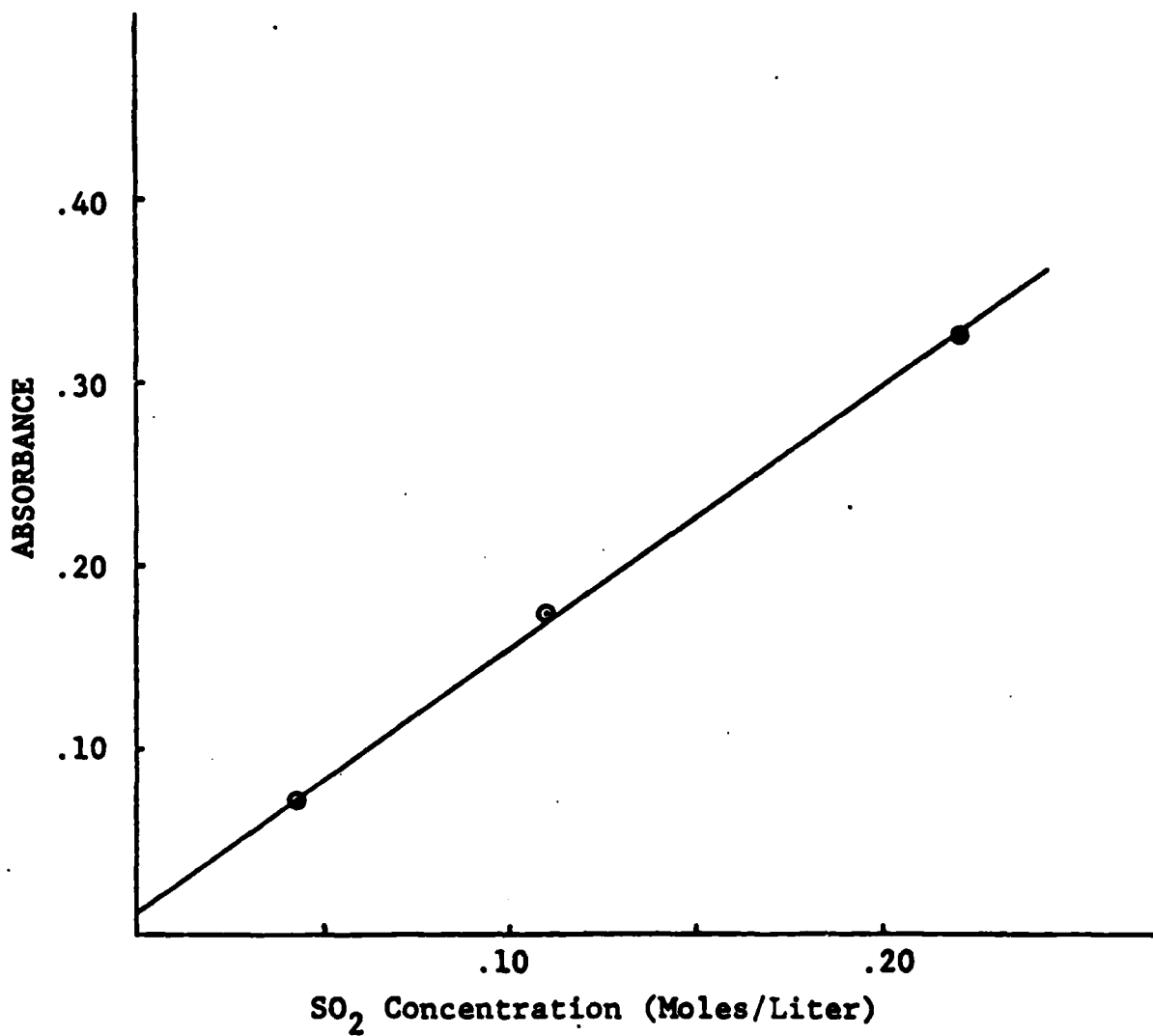


Figure 18: Calibration Curve Relating IR Absorbance to SO₂ Concentration in 2.0M AlCl₃, 0.1M LiCl/SOCl₂

The Spectra were obtained using a 0.05 mm pathlength CaF₂ Cell.

The absorbences plotted were at 1333 cm⁻¹.

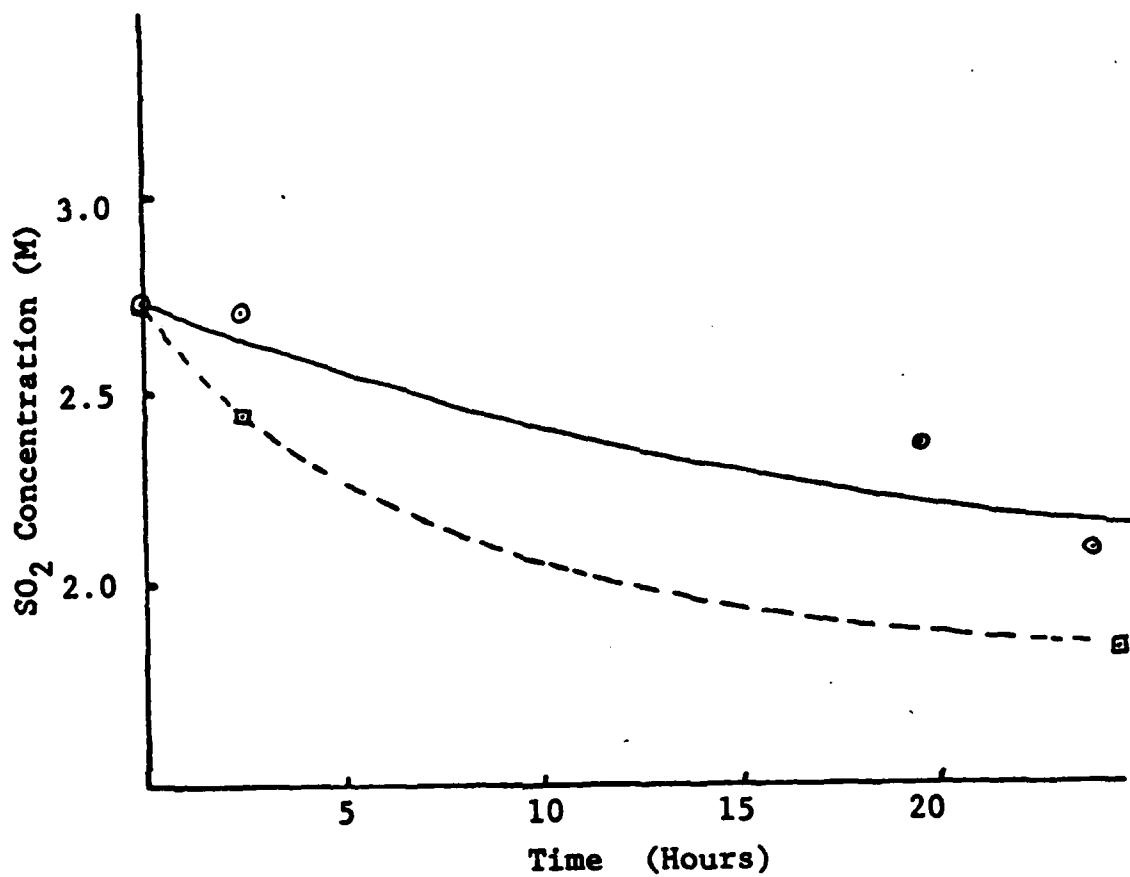


Figure 19: The Decline in SO_2 Concentration with Time in $1.8\text{M LiAlCl}_4/\text{SOCl}_2$ at 23°C With and Without Carbon-4% Teflon Cathode Material

(————), no carbon present

(- - - -), 0.050 g carbon-Teflon cathode material per ml electrolyte

The SO_2 concentrations are listed in Tables 1 and 2.

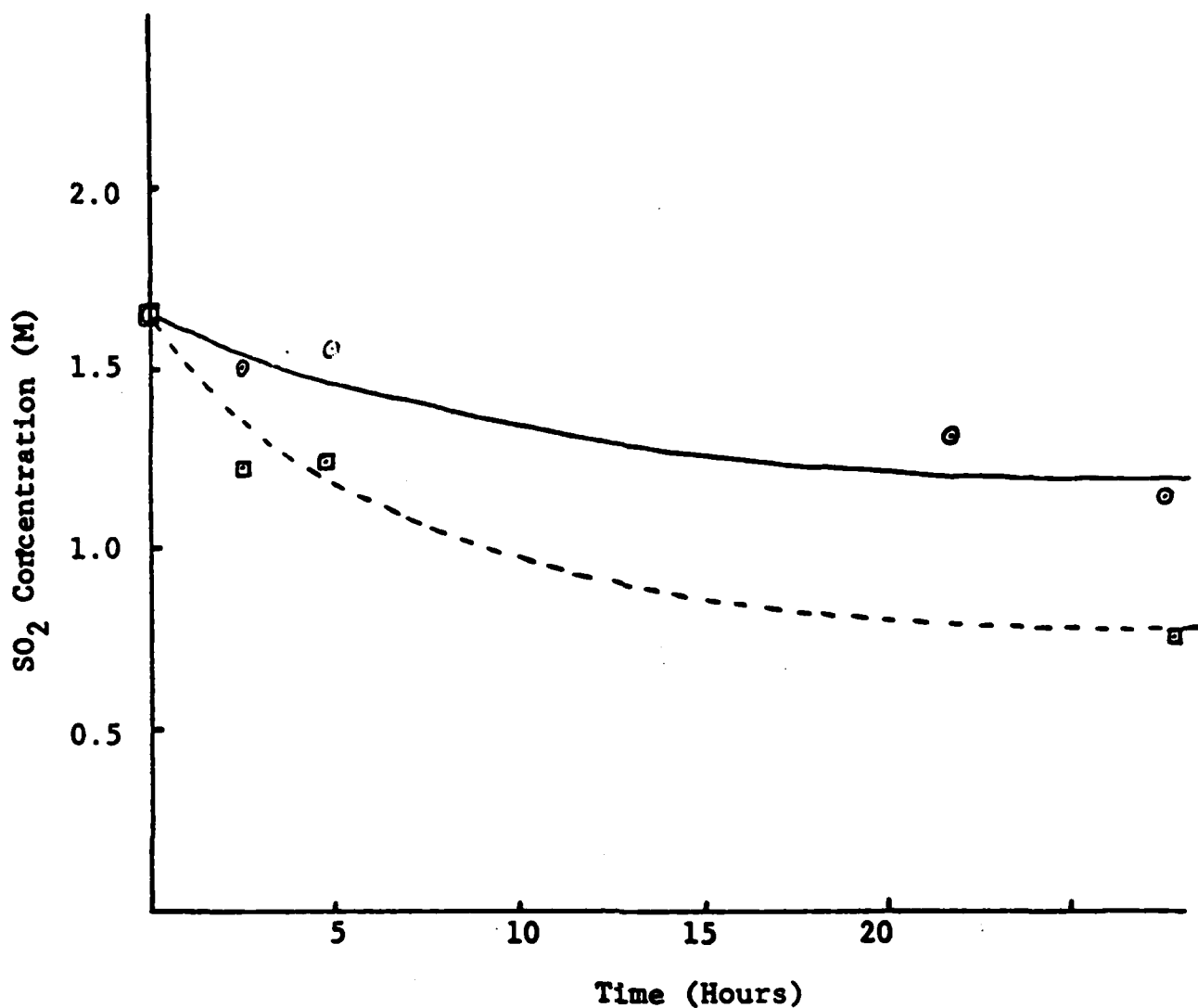


Figure 20: The Decline in SO₂ Concentration with Time in 2.0M AlCl₃, 0.10M LiCl/SOCl₂ at 23°C With and Without Carbon-4% Teflon Cathode Material

(———), no carbon present

(- - - -), 0.050 g carbon-Teflon cathode material per ml acid electrolyte

The SO₂ concentrations are listed in Tables 1 and 2.

acid electrolyte where 31% of the initial SO_2 was consumed after 26 hours compared to 24% of the initial SO_2 consumed after 24 hours in neutral electrolyte. The initial SO_2 concentration in the SOCl_2 acid electrolyte was lower than the initial SO_2 concentration in the experiment with neutral electrolyte (i.e., 1.64 vs 2.73 m/l) thus the reaction rate may actually be greater in acid electrolyte than the data suggests. The initial SO_2 concentration was lower in the acid electrolyte only because no attempt was made to prepare solutions with identical SO_2 concentrations in both electrolytes.

The amount of reaction is noteworthy and it is clear that the existence of the reaction must be taken into account in any investigation of the stoichiometry of the reduction of SOCl_2 or studies of SO_2 adsorption on carbon in SOCl_2 electrolyte. The amount of SO_2 consumed by the reaction in even 20 hours at 23°C is substantial enough (i.e., 10 to 20%) that it can not be neglected and a correction would have to be made. To make such a correction, one would

require accurate experimental values concerning the rate constant for the SO_2 - SOCl_2 electrolyte reaction for the temperature, time period, electrolyte composition and SO_2 concentrations under consideration.

The reaction rate and extent of reaction of SO_2 with acid and neutral SOCl_2 electrolytes found by quantitative infrared analysis correlate remarkably well with those found by voltammetry for dilute SOCl_2 solutions in DMF as discussed earlier in Section 1.2.2. The voltammetry studies showed the growth of a new peak at -1.4V during storage (see Figure 14) which corresponded to the decline in the SO_2 peak. Because voltammetry can not be used to determine the chemical composition of the products of the SO_2 - SOCl_2 electrolyte reaction, a qualitative infrared study was undertaken with AgCl cells which have a usable transmission region down to 450 cm^{-1} .

The IR spectra obtained after 0.0, 4.0, and 147 hours of storage for 1.8M $\text{LiAlCl}_4/\text{SOCl}_2$ solutions containing 1.0M SO_2 are shown in Figures 21 and 22. A comparison of these IR spectra during increasing periods of storage does not reveal any new absorption peaks which could be due to the products of the

SO₂-SOCl₂ electrolyte reaction. The SO₂ peak at about 1165 cm⁻¹ noticeably changed from a small peak to a small shoulder during the first four hours of storage. The peaks between 1000 cm⁻¹ and 750 cm⁻¹ changed slightly, but not in a consistent or recognizable manner. The gap in the spectra after four hours storage in Figure 21 at approximately 600 cm⁻¹ was an instrumental artifact which rarely occurs at that point as the instrument automatically pauses and changes gratings. The SO₂ peak at 1333 cm⁻¹ doesn't decrease during storage in Figures 21 and 22 because the SO₂ solutions examined were much more concentrated than those used for quantitative IR measurements for SO₂.

The absence of new peaks in the IR spectra during storage of SO₂-LiAlCl₄/SOCl₂ solutions could possibly occur because the new peaks are hidden by the absorption bands of SOCl₂ at 1225 and 2420 cm⁻¹. Raman spectroscopic studies of 1.5M LiAlCl₄/SOCl₂ with approximately 2.4M SO₂ reported by P. Barbier and co-workers (15) show a new band at 1157 cm⁻¹ which is consistent with our voltammetric results that indicate the formation of a new compound. This new band was assigned (15) to the S-O stretching vibrational mode of SO₂ molecules bonded to a Li cation. Since Barbier and co-workers (15) do not give an explanation for their assignment, it is not possible at this time to predict which infrared bands would correspond to the 1157 cm⁻¹ band in the Raman. Depending on the symmetry of the new species it is possible that no new infrared bands would appear.

From quantitative measurements of the Raman spectra for different amounts of SO₂ in 1.45M LiAlCl₄/SOCl₂, Barbier et al (15) have postulated that the following reaction occurs when SO₂ is added to LiAlCl₄/SOCl₂:



where the equilibrium constant is 6.2. They calculate that for a 1M LiAlCl₄/SOCl₂ solution with 2M SO₂ the concentration of the new Li (SO₂, SOCl₂) AlCl₄ species would be 0.4M. Thus, 20% of the available SO₂ reacts to form the new species which compares well with our infrared results (see Figure 19) for 2.73M SO₂ in 1.8M LiAlCl₄/SOCl₂ where 24% of the SO₂ reacted after 24 hours.

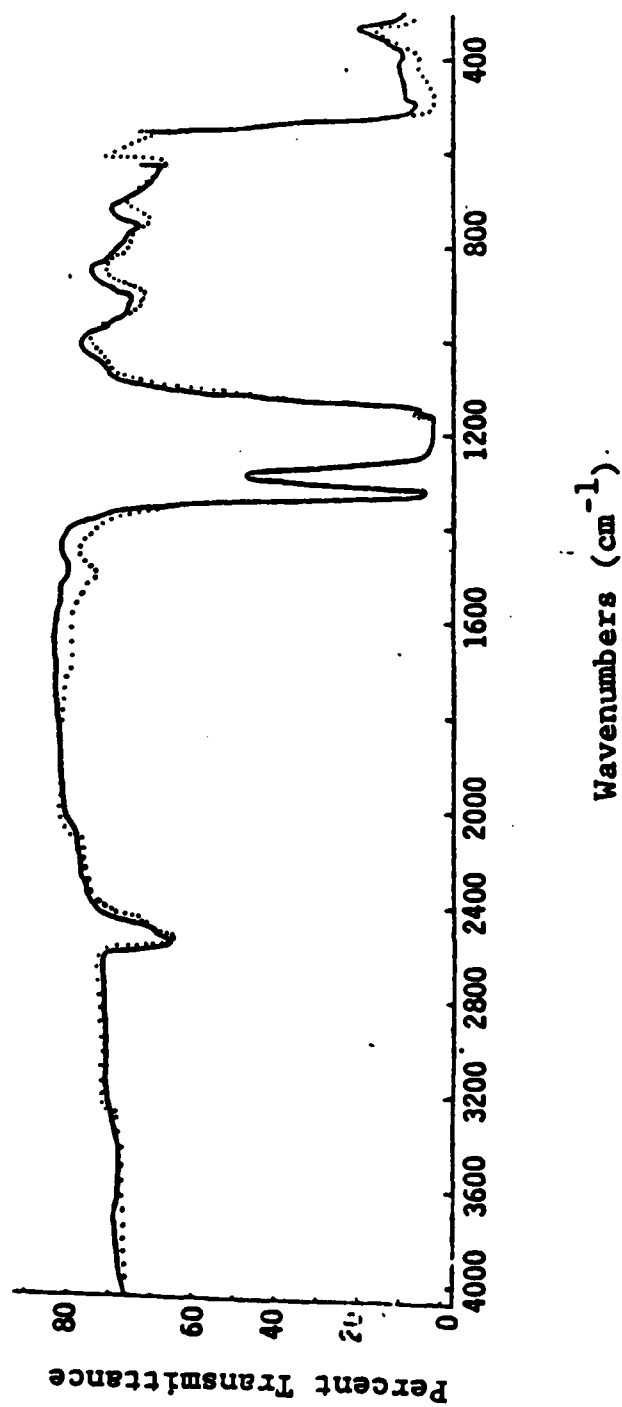


Figure 21: Infrared Spectra of 1.8M LiAlCl₄/SOCl₂ Containing 1.0M SO₂ Before and After 4.0 Hours Storage at 23°C. (0.1mm Pathlength AgCl Cell)

(.....) 0.0 hours storage
(————) 4.0 hours storage

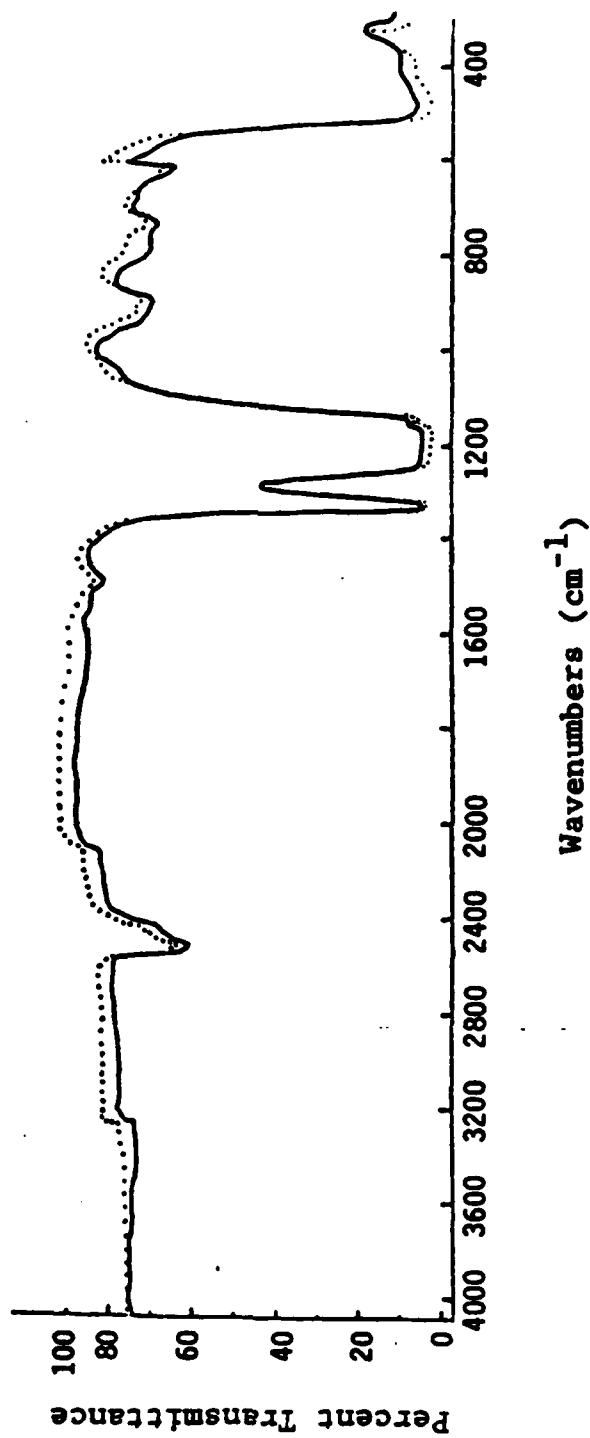


Figure 22: Infrared Spectra of 1.8M $\text{LiAlCl}_4/\text{SOCl}_2$ Containing 1.0M SO_2 Before and After 147 Hours Storage at 23°C. (0.1mm Pathlength AgCl Cell)

(.....) 0.0 hours storage
 (————) 147 hours storage

It is not stated whether the Raman spectra were obtained immediately after the solutions were prepared or after they had been allowed to stand for a long enough period for the SO_2 to react. The Raman spectra were generated with an argon laser light source, thus, it is possible that the spectra were obtained over an extended period (e.g., 12 hours) using signal averaging techniques to increase the signal-to-noise ratio.

Because the basis for the Raman assignments for the new 1157^{-1} band was not discussed by Barbier et al (15), the chemical composition of the product of the SO_2 - SOCl_2 electrolyte reaction still remain unresolved. It is possible, for example, that SO_2 slowly reacts with SOCl_2 electrolyte to form $\text{SO}_2 \cdot \text{AlCl}_3$, or $\text{SO}_2 \cdot \text{LiAlCl}_4$ adducts. In terms of the relevance of the results to Li/ SOCl_2 battery technology, if the product were a weakly bound solvation complex, it would probably be of very little importance. However, the voltammetry results indicate that the product of the SO_2 - SOCl_2 electrolyte reaction is a moderately bonded species which suggests that it may be of some practical importance.

The voltammetry peak for the product of the SO_2 - SOCl_2 electrolyte reaction at -1.40V vs Ag/AgCl is about 0.490V more cathodic than SO_2 (see Section 1.2.2) which indicates that the SO_2 becomes much more difficult to reduce after it has reacted. The peak potentials obtained during voltammetry occur at very high current densities and can not be used in thermodynamic calculations that require reversible potentials measured with a negligible current for solutions with a known concentration of the species of interest. However, assuming that the peak currents correlate roughly with the thermodynamic half cell potentials, which is a fairly safe assumption, the 490 mV difference between the two peaks would indicate that the free energy of the reaction between SO_2 and SOCl_2 electrolyte is about 11 Kcal/mole. This value is about what one would expect for an adduct or a complex but greater than the free energy involved in the simple solvation of an ion. For example, the total van der Waals forces between Cl_2 , CO and H_2O molecules are 5, 2.09, and 11.30 Kcal/mole, respectively, (16). By comparison, the energy of the O-O and O-Cl covalent bonds are 34 and 49 Kcal/mole (16).

The $\text{Li}(\text{SOCl}_2, \text{SO}_2)^+$ complex ion species postulated by Barbier et al is not unreasonable because it is very likely that the Li^+ is very strongly solvated in $\text{SOCl}_2, \text{SO}_2$ solutions. As far as is known, the transference number for Li^+ in $\text{LiAlCl}_4/\text{SOCl}_2$ solutions has not been published but from work in aprotic organic electrolytes one could estimate by analogy that it is probably less than 0.4. Keller and co-workers (17) found that the Li^+ in transference numbers in 1M $\text{LiClO}_4/\text{propylene carbonate}$ and 1M $\text{LiClO}_4/\text{acetonitrile}$ were 0.19 and 0.32, respectively.

To unequivocally determine the chemical composition of the product of the $\text{SO}_2\text{-SOCl}_2$ electrolyte reaction, it is clear that further Raman and infrared studies will be required with the emphasis placed on an exact quantitative model to account for the observed vibrational spectra. In addition, measurements of the reaction heat and other types of analytical measurements may be required to determine the exact composition of the product. Once the composition is known, a variety of kinetic and solubility studies and possibly Li^+ transference number measurements may be required to characterize the properties of the product in SOCl_2 electrolytes.

If it is found that the product of the $\text{SO}_2\text{-SOCl}_2$ electrolyte reaction is a strongly bound complex of SO_2 to Li^+ or the $\text{AlCl}_3\cdot\text{SO}_2$ or $\text{LiAlCl}_4\cdot\text{SO}_2$ adducts, the results could lead to important improvements in the performance of Li/SOCl_2 batteries. For example, if SO_2 reacts with LiAlCl_4 to form $\text{AlCl}_3\cdot\text{SO}_2$ adduct and LiCl , it could cause the equilibrium of neutral electrolyte in cells to shift acidic during discharge. This slightly acidic environment could cause Li anode corrosion losses in cells stored for long periods with intermittent discharge during storage. The SO_2 complex or adducts may also be present at higher concentrations at low temperature and an understanding of their composition and structure may be very useful for the selection of low temperature catalysts and the design of cathodes for low temperature applications.

Relative to high rate battery applications, if the $\text{AlCl}_3\cdot\text{SO}_2$ adduct or SO_2 complex formed in acid electrolyte reduces the reactivity of AlCl_3 towards

LiCl formed in the cathode during discharge, it could cause increased polarization and reduced capacity. Changing the cell chemistry to inhibit the SO₂ adduct or complex formation would, in principle, greatly improve the high rate performance.

The above examples demonstrate how an understanding of the chemistry of the SO₂-SOCl₂ electrolyte reaction with some certainty would allow one to justify and undertake further types of programs to improve Li/SOCl₂ battery performance with more certainty as to the outcome. Further elaboration of the benefits of knowing the composition of the products of the SO₂-SOCl₂ electrolyte reaction will have to be postponed until more information is available concerning the possible composition and properties of the product.

1.3.3.3 Sulfur Dioxide Adsorption Results

The amount of SO₂ adsorbed by carbon-4% Teflon cathode material from neutral and acid SOCl₂ electrolytes at 23°C at various times after the addition of the SO₂ are listed in Tables 1 and 2. The concentrations of SO₂ in the solutions with and without the carbon-Teflon cathode material are plotted as a function of time in Figures 19 and 20. The SO₂ adsorption measurements showed that 12% and 41% of the SO₂ was adsorbed on the carbon cathode material from neutral and acid SOCl₂ electrolytes, respectively, after approximately 24 hours. Thus the amount of SO₂ adsorbed on the carbon is substantial and it is clear that the amount of SO₂ produced during the discharge of prototype Li/SOCl₂ cells can not be accurately determined by simply draining electrolyte samples from the cells and analyzing the samples for SO₂.

A comparison of the SO₂ concentration curves as a function of time, with and without carbon in Figures 19 and 20 shows a remarkable similarity in the shape of the curves which was unexpected. One would expect the adsorption equilibria to be reached rather quickly (i.e., < 1.0 hour) and that the total SO₂ ad-

Table 1

Reaction of SO_2 with 1.8M $\text{LiAlCl}_4/\text{SOCl}_2$ and Adsorption by Carbon-4% Teflon Cathode Material

Time (Hrs)	Without Carbon			With Carbon**		
	SO_2 (m/l)*	SO_2 Reacted (m/l)*	SO_2 Reacted (%)	SO_2 (m/l)*	SO_2 Adsorbed (m/l)**	SO_2 Adsorbed (%)**
0	2.73	0	0	2.73	0	0
2.5	2.71	0.02	0.7	2.44	0.27	10.0
19.0	2.46	0.27	9.9	2.35	0.11	4.5
24.0	2.08	0.65	2.4	1.83	0.25	12.0

Table 2

Reaction of SO_2 with 2.0M AlCl_3 , 0.10M $\text{LiCl}/\text{SOCl}_2$ and Adsorption by Carbon-4% Teflon Cathode Material

Time (Hrs)	Without Carbon			With Carbon**		
	SO_2 (m/l)*	SO_2 Reacted (m/l)*	SO_2 Reacted (%)	SO_2 (m/l)*	SO_2 Adsorbed (m/l)**	SO_2 Adsorbed (%)**
0	1.64	0	0	1.64	0	0
2.5	1.50	0.14	8.5	1.28	0.22	14.6
5	1.55	0.09	5.4	1.25	0.30	19.3
20	1.30	0.34	20.7	1.18	0.12	9.2
26	1.13	0.51	31.1	0.66	0.47	41.5

+ SO_2 adsorbed at a particular reaction time is:
(SO_2 without carbon) - (SO_2 with carbon)

** For 0.050 g carbon-4% Teflon cathode material/ml SOCl_2 electrolyte; the results are plotted in Figures 19 and 20.

** The percent SO_2 adsorbed in Column 7 was calculated from the ratio of the SO_2 adsorbed in Column 6 at a given time over the amount of unreacted SO_2 at that time in Column 2.

* Concentrations in moles/liter uncorrected for volume changes.

sorbed would decrease with time as the SO_2 reacted with the SOCl_2 electrolyte and the adsorption equilibria shifted. The similar rate of the reaction and adsorption processes indicated by the curves suggest that the SO_2 may not be adsorbed on the carbon but instead it is the product of the SO_2 - SOCl_2 electrolyte reaction that is adsorbed. Alternatively, it is possible that the carbon just catalyzes the SO_2 - SOCl_2 electrolyte reaction. This matter is discussed further in Section 1.6.3 in connection with the data in Table 2 which firmly establishes that SO_2 is strongly adsorbed on carbon, especially at low temperature.

Should these alternative reactions become of practical importance, further experimental studies could be carried out. For example, the carbon could be extracted with an inert solvent after an "adsorption" experiment and the extract analyzed. Although some uncertainties exist concerning the SO_2 "adsorption" phenomenon, we will continue to refer to the process as SO_2 adsorption throughout this report because we believe it is the most likely process and to prevent the discussion from becoming needlessly abstract and confusing.

Adsorption and the Analysis of Prototype Cells. - The SO_2 adsorption results described in Tables 1 and 2 were carried out under electrolyte flooded conditions with a ratio of 0.050 g carbon cathode material/ml of SOCl_2 electrolyte. However, practical Li/ SOCl_2 cells have only a slight excess of electrolyte. Therefore, the amount of SO_2 that would be adsorbed on the carbon would be much greater than the values listed in Tables 1 and 2. For example, cathode limited spiral wound C size cells typically (9) have a ratio of 0.14 g of carbon cathode material/ml of electrolyte whereas AA size Li/ SOCl_2 bobbin cells (18) have ratios as high as 0.18 g carbon cathode/ml electrolyte.

Using the above ratios for prototype cells, one can calculate that the carbon would adsorb from 2.8 to 3.6 times more SO_2 than the values listed in Tables 1 and 2 obtained with a larger excess of electrolyte. Thus, samples of electrolyte drained from discharged prototype cells would give erroneously low values for the SO_2 concentration when analyzed. Such low values have been reported in the literature by Schlaijker and co-workers (6), and were attributed to

(SO)_n intermediates. The correct SO₂ concentration can not be obtained by correcting for the amount of SO₂ adsorbed because adsorption data is not available for carbon cathodes at various states of discharge. Presumably the carbon surface available for adsorption would decrease during discharge as the surface became covered with LiCl crystals and possibly adsorbed elemental sulfur. Since it is not likely that accurate SO₂ adsorption data for discharged cathodes will be available for some time, it was concluded that the most practical way to determine the amount of SO₂ produced during discharge would be to drain the electrolyte, extract the cell a number of times with an inert solvent and analyze the combined solutions for SO₂. Work that was undertaken to find a suitable solvent and to develop the multiple extraction technique is described later in Section 1.6.

From quantitative infrared measurements with an IR flow cell connected to a Li/SOCl₂ cell, Attia and co-workers (2) have shown that the SO₂ produced during discharge corresponds to 0.17 moles SO₂/Faraday at 1.0 and 5.0 mA/cm² at room temperature. This compares favorably with the 0.25 moles SO₂/Faraday expected on the basis of the generally accepted (5, 6, 19) equation for the discharge reaction:



The 32% difference between their experimental value and the theoretical value may be due to (i) errors in the quantitative IR analysis, (ii) reaction of SO₂ with the SOCl₂ electrolyte, (iii) adsorption of SO₂ by the carbon cathode, (iv) the formation of long lived intermediates or unknown side reactions. Their carbon mass-to-electrolyte volume ratio was not given directly but from their discharge capacities and assuming 1.52 Ahr/g of carbon 10% Teflon mix at 5 mA/cm² we have calculated that their cells (e.g., Cell SC-69) had a ratio of approximately 0.0087 g carbon mix/ml SOCl₂ electrolyte. Since prototype spiral wound Li/SOCl₂ cells typically (9) contain 0.14 g of carbon mix/ml of electrolyte, the infrared flow cell contained approximately 16 times more electrolyte than used in practical cells. Thus, it is doubtful that the 32% short fall in the SO₂ concentration can be entirely attributed to SO₂ adsorption on the carbon.

The infrared flow cell measurements (2) have provided perhaps the most accurate and convincing data published to date that shows the SOCl_2 is reduced as described by equation [1] without the generation of any long lived (e.g., > 1 hour) intermediates. As such, the work represents a significant achievement. However, the infrared in-situ flow cell measurements were carried out with approximately 16 times excess SOCl_2 electrolyte and to only $n = 0.042$ equivalents of charge passed per mole of SOCl_2 , in which case only 2.1% of the SOCl_2 was reduced.

It is clear that much further work is required to determine the reduction reaction for SOCl_2 in practical cells with only a slight excess of electrolyte where much greater SO_2 adsorption occurs and at least 70% of the SOCl_2 is reduced. In commercial cells, in which most of the SOCl_2 is reduced, the concentration of SO_2 , sulfur, LiAlCl_4 , and the SO_2 - SOCl_2 electrolyte reaction product would become appreciable and could effect the reaction mechanism for SOCl_2 reduction. At high rates, the very short lived intermediates that have been observed at low temperatures by Williams and co-workers (3) could be stabilized by adsorption on the carbon to a much greater extent in practical cells with high carbon-to-electrolyte ratios. Such cells would in many cases probably have excess carbon that would not be completely covered with LiCl by the end of discharge and, therefore, would be able to adsorb intermediates.

The concentrations of products and intermediates would also be higher during overdischarge or charging in prototype cells with high carbon-to-electrolyte ratios which could lead, in principle, to the accumulation of hazardous products. It is recommended that overdischarge and charging should be fully investigated in Li/SOCl_2 prototype cells with high carbon-to-electrolyte ratios using the multiple extraction techniques described in Section 1.6 followed by both IR and Raman analysis.

In view of the finding by the in-situ infrared flow cell measurements that the experimental SO_2 concentration is 32% below the theoretical value, additional work should be carried out to account for the missing SO_2 .

The Molecular Mechanism of SO₂ Adsorption. - From available information about the surface area of the carbon cathode mixture and the amount of SO₂ adsorbed, it is possible to calculate the number of layers or fractions of a layer of SO₂ molecules adsorbed on the carbon surface. Such information regarding adsorption is of value in understanding catalysis and possibly in selecting catalysts for Li/SOCl₂ high rate cells.

Following the nomenclature of Adamson (20) for the adsorption of a solute species from a solution onto an adsorbent, the fraction of the surface occupied is given by:

$$\theta = \frac{n_2^S}{n^S} \quad [2]$$

where n_2^S is the number of moles of solute adsorbed per gram of adsorbent and n^S is the number of moles of adsorption sites per gram of adsorbent. The quantity n^S is given by

$$n^S = \frac{\Sigma}{N\sigma^0} \quad [3]$$

where Σ is the surface area per gram of adsorbent, N , Avogadro's number and σ^0 is the area of the adsorbed molecule. Next, from ΔC_2 , the change in the solute concentration in moles/liter following adsorption, one can obtain n_2^S from the relation

$$n_2^S = \frac{\Delta C_2 V}{m} \quad [4]$$

where m is the grams of adsorbent, and V , the total volume of solution. Substituting Eq. 3 and Eq. 4 into Eq. 2, the fraction of the surface occupied is then given by:

$$\theta = \frac{C_2 V N \sigma^0}{m \Sigma} \quad [5]$$

For SO₂ adsorption onto the carbon-4% Teflon cathode material used in the adsorption measurements, it is known that Σ is approximately 36 m²/g from BET

surface area measurements and that σ° , the cross sectional area of an SO_2 molecule is approximately $10.4 \cdot 10^{-20} \text{ M}^2$. This value of σ° was calculated based on a S-O bond distance (21) of $1.43 \cdot 10^{-10} \text{ M}$, a O-S-O bond angle of 119.5° (22) and an oxygen atomic radius of $0.55 \cdot 10^{-10} \text{ M}$ (23).

Taking the case for SO_2 adsorption onto carbon-4% Teflon in 1.8M $\text{LiAlCl}_4/\text{SOCl}_2$ after 24 hours where from Table 1 $\Delta C_2 = 0.25 \text{ m/l}$, using Eq. 5, it can be calculated that $\theta = 8.74$ where $m = 2.0 \text{ g}$ and $V = 0.0401$. Thus, assuming that uncomplexed SO_2 is adsorbed, the film of adsorbed SO_2 on the carbon material would be approximately eight SO_2 layers thick. A similar calculation for SO_2 adsorbed in acid electrolyte onto carbon-4% Teflon after 26 hours (where from Table 2, $\Delta C = 0.47 \text{ m/l}$) shows that the adsorbed SO_2 film would be 16.4 SO_2 layers thick.

Multilayer adsorption from solution has been observed for a number of systems and has been discussed by Adamson (Pg. 407, Ref. 20). He concludes that: "in solutions two potentially adsorbing components are present, and there is really no good reason to suppose that multilayer adsorption of a solute occurs with complete exclusion of solvent. In other words, the situation might more profitably be regarded as one of a phase separation induced by the interaction with the solid surface or as a capillary effect".

Multilayer SO_2 adsorption on the carbon electrode may inhibit the reduction of SOCl_2 during high rate discharge of Li/SOCl_2 cells, especially at low temperature. It is possible that the soluble organo metallic catalysts (24-26) that have proven so effective in high rate Li/SOCl_2 cells may mediate charge transfer through the multiple layers of SO_2 adsorbed on the carbon. However, the soluble catalysts may also effect mass transfer of Cl^- , Li^+ and other species in the SO_2 adsorption layer and change the morphology of the growing LiCl crystallites in a manner which increases high rate discharge performance. Driscoll and Szpak (27,28) have recently identified several LiCl crystal morphologies in carbon cathodes from Li/SOCl_2 cells discharged in acid SOCl_2 electrolyte but the most beneficial LiCl morphologies and the mechanisms causing such morphologies remain to be investigated.

1.4 INVESTIGATION OF REACTIONS OCCURRING DURING THE OVERDISCHARGE OF LITHIUM-THIONYL CHLORIDE CELLS

1.4.1 Carbon Limited Overdischarge

1.4.1.1 Background

Overdischarge or reversal of Li/SOCl₂ cells through series string discharge or constant current discharge with an external power supply can result in thermal runaway depending on the design of the cell. Considerable evidence (29-33) indicates that carbon* limited cells may undergo thermal runaway during high rate reversal and that the anode limited design is preferred(44-47). However, the subject remains a matter of some controversy (19,34). The electrolyte limited design is hazardous (33) but the thermal problems associated with electrolyte limitation can be avoided by providing cells with a slight excess of electrolyte and a hermetic closure. Thus the issue of the preferred design to withstand overdischarge becomes a choice between the carbon and lithium limited designs.

Situations where overdischarge of carbon limited cells have resulted in thermal runaway with venting or "explosions" have been reported widely (29-31). For example, the behavior of the temperature and potential as a function of time during overdischarge at constant currents of 0.5 and 0.25A (i.e., 0.55 mA/cm²) have been reported by Dey (29,30) for spiral wound carbon**limited D

* The terminology carbon limited instead of cathode limited is used to avoid confusion between electrolyte and carbon limitation since SOCl₂ is both the cathode material and the electrolyte solvent.

** It was not stated explicitly that the D cells were carbon limited but from the Li anode dimensions it was calculated that the Li anode volume was 8.357 cm³ and the Li anode capacity 17.2 Ahr. The 45 g of electrolyte (Pg 29, ref. 30) could provide 30.6 Ahr. From Figure 9 of ref. 30 a D size cell delivered 11.8 Ahr to 3.00V at 0.1A (0.22 mA/cm²). Thus their D cells were carbon limited.

cells. It was found that the potentials become slightly negative (i.e., -0.3 to -0.5V) on overdischarge and oscillated just before the cells "exploded". The cell overdischarged at 0.25 A "exploded" when the cell had been overdischarged 12.7% (i.e., 6.5 hrs) at which time the cell wall temperature was 39°C.

During overdischarge of carbon limited cells the electrode reaction at the Li anode continues to be the oxidation of Li metal to Li ions. However, the carbon cathode becomes totally passivated with LiCl upon reversal and instead of the reduction of SOCl_2 , the cathode reaction changes to the reduction of Li cations. ions from the electrolyte to form Li dendrites on the surface of the carbon electrode that grow out into the solution (35,36). In principle, on further overdischarge, the Li anode will eventually become depleted of Li and the carbon limited cell will become both carbon and lithium limited.

The precise reaction that occurs during overdischarge that leads to thermal runaway in high rate Li/ SOCl_2 cells is not known although a variety of likely reactions have been suggested (19,29,30,33,37-39). On overdischarge the Li dendrites growing towards the Li anode could make contact with the anode and short circuit the cell. The Li dendrites would then heat up and could react exothermically with sulfur deposited on the dendrites (30,33) or melt and react with the SOCl_2 electrolyte (30), carbon (38) or other cell components.

During a recent investigation of Li deposition in Li/ SOCl_2 cells (35,36) carried out at GTE Laboratories for the Naval Surface Weapons Center (NSWC), it was found that Li deposits as fine filaments. The Li dendrites were examined by scanning electron microscopy (SEM) and were observed to be made up of a coiled spaghetti-like structure of Li filaments with a diameter of $4 \cdot 10^{-3}$ mm. The morphology of the Li filaments was very similar for cells overdischarged at 2, 5 and 20 mA/cm² at 25°C. Thus it was concluded that the Li dendrites would have such a high electrical resistance that they could not carry a large enough current to reach the melting point of Li (i.e., 180.5°C) when Li dendrite shorting occurred.

To learn about the reactions between Li dendrites and other cell components during dendrite shorting brought about by overdischarge, in situ studies of dendrite shorting were undertaken using optical microphotography. The results of the in situ observations of dendrite shorting are discussed in Section 1.4.1.2. The in situ optical studies of Li dendrites were carried out in special cells without separators that contained up to 30 times excess SOCl_2 electrolyte to facilitate the microphotography. Therefore, to determine the influence of the separator and closer inter-electrode spacing on Li dendrite shorting during carbon limited overdischarge, additional tests were carried out in 0.3 Ahr cells with separators that closely resembled practical cells. The results of the dendrite shorting experiments carried out in the above cells are described later in Section 1.4.1.4.

Incidents have been reported (40) in which 5 Ahr carbon limited (41) prototype Li/ SOCl_2 cells that were overdischarged at -40°F vented violently when they were allowed to warm to room temperature. To investigate cell reversal during such conditions, carbon limited Li/ SOCl_2 cells were investigated at -40°C during our earlier NSWC Study (35,36). It was found that when carbon limited cells are overdischarged at -40°C then allowed to warm to room temperature, the Li dendrites only become detached from the cathode between 3.5 and 16 hrs after the cell has warmed up. The detached Li dendrites then dissolved in the electrolyte which was puzzling since they are usually very stable. For example, Li dendrites deposited on the cathode of carbon limited cells at 25°C are stable for over 300 hrs after the end of discharge.

The stability of the Li dendrites for over three hours after the cell had warmed up to 25°C from -40°C is an indication that the species attacking the Li builds up slowly as is the case with the product of the SO_2 - SOCl_2 electrolyte reaction (see Figure 19). The $(\text{OClS})_2$ dimer intermediate postulated by the group at JPL (3) has a lifetime of only five minutes at -40°C and 10 seconds at 25°C and thus could not account for such a slow reaction.

In Section 1.4.1.3 work is described in which carbon limited cells were overdischarged at -40°C , then the corrosion and detachment of the Li dendrites

photographed over a period of 24 hrs. There is a need for a photographic record to document the reaction rate since previously our only evidence was two qualitative observations at 3.5 and 19 hours (35). The solid product that was produced and settled to the bottom of the cell as the Li dendrites dissolved was collected and analyzed since the composition of this compound could indicate the composition of the unknown compound in solution responsible for the unusual high rate of corrosion of the Li deposits.

Work was also undertaken to analyze by voltammetry the electrolyte from carbon limited cells overdischarged at -40°C containing only a slight excess of SOCl_2 electrolyte. The voltammetry results are discussed in Section 1.4.1.3.

Even though a lithium limited design is preferred to reduce the possibility of thermal runaway during overdischarge, information about carbon limited overdischarge is of vital importance because lithium limited cells can become carbon limited under certain operating conditions such as low temperature discharge. Carbon limited overdischarge in a nominally lithium limited cell can also occur if a low rate cell with a low cathode area is discharged at high rate. Thus, information about the processes leading to thermal runaway in carbon limited cells during overdischarge would be extremely useful in order to decide which design changes or chemical modifications to adopt in order to decrease the possibility of thermal runaway in lithium limited Li/SOCl_2 cells during electrical abuse.

1.4.1.2 In Situ Photography of Overdischarged Cells

Low Temperature Overdischarge. The cell used for the in situ photography of Li dendrite corrosion at 23°C after overdischarge at -40°C was similar to the cell described previously (35,36). The electrodes consisted of a single 3.5×3.0 cm Shawinigan carbon black -10% Teflon cathode 3.5 mm thick positioned between two 3.5×3.0 cm Li anodes, 1.7 mm thick. The cathode and two lithium anodes were parallel with 6 mm separation. Since the electrodes were held

rigidly in place with thick Ni lead wires, no separators were required, thus allowing an unobstructed view of all electrode surfaces. The electrode assembly was contained in a 5.5 cm diameter cylindrical glass cell (see Figure 23) with a flat 4.0 cm diameter optical glass window positioned to allow in-situ optical microscopy of the lithium dendrites. The cells were vacuum filled with 1.8M $\text{LiAlCl}_4/\text{SOCl}_2$.

A carbon limited cell of the above design with approximately 150 ml of neutral electrolyte was discharged at -40°C at 1 mA/cm^2 for 224 mAh/cm^2 to 0.00V then overdischarged 336 mAh/cm^2 at 1 mA/cm^2 . The cell was then stored on open circuit for 31 hours at 25°C and nine color photographs were taken of the dissolution of the Li dendrites, four of which are shown in Figures 23-25.

Figure 23 shows two views of the Li dendrites on the carbon electrode after two hours on open circuit. The Li growth was uniform across the carbon surface and not confined to the edges of the carbon. Although the Li deposits appear white in Figure 23 and 24, as though they were covered with a LiCl film, they were actually a very bright, reflective metallic color similar to clean Li foil. The Li deposit from the carbon cathode that appears to touch the right Li anode near the top, about $1/4$ of the distance down in Figure 23 would appear to have adequate contact to short the cell but no short was observed. The difficulty of forming Li dendrite short circuits will be discussed later in this section.

After about four hours, it was observed both visually and photographically that the electrolyte turned from yellow to green. The green color intensified

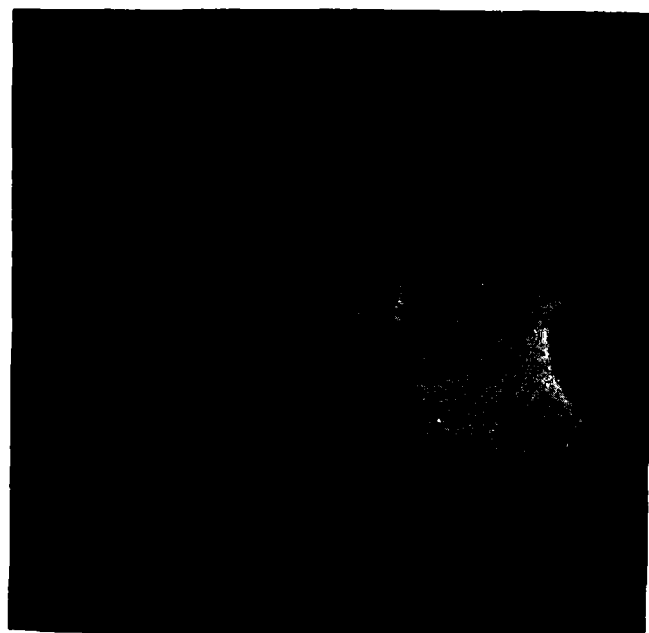


Figure 23: Lithium Dendrites on the Cathode of a Carbon Limited Li/SOCl_2 Cell Overdischarged at -40°C after 2 Hours on OCP at 23°C (Side and Top Views of the 5.5 cm Diameter Cell)

during continued storage. Figure 24 taken after 3.5 hours on open circuit showed some corrosion and detachment of the Li dendrites and the first sign of a precipitate settling out on the bottom of the cell. After six hours on open circuit the metallic Li dendrites began to turn grey and white. Other photographs revealed that the Li dendrites dissolved most rapidly in the period between 7 and 28 hours during which time approximately 80% of the dendrites dissolved. A comparison of Figures 24 and 25 taken after 3.5 and 23 hours as open circuit at 23°C, respectively, shows the dissolution of a large portion of the Li dendrites and the buildup of white precipitate on the bottom of the cell. Particularly noticeable, in Figure 25 is the dissolution of the Li dendrites on the left side of the cathode, on the surface of the electrolyte and on the leads.

The white salt formed from the Li dendrites was collected and washed with several aliquots of pure SOCl_2 to remove LiAlCl_4 and sulfur. The precipitate was then dried under vacuum at 150°C. An infrared spectra of a KBr pellet with the white precipitate was taken and it showed only the strong absorption at 1650 cm^{-1} characteristic of LiCl and none of the peaks expected for lithium dithionite (42). A portion of the white precipitate was added to water and about 5% insoluble matter (B) remained. Titration of the solution with 0.017M AgNO_3 (Mohr method) indicated that the soluble portion of the white salt is 98% LiCl if the cation is assumed to be Li^+ . A gravametric analysis of the solution by precipitation of AgCl indicated that the white salt was 99.0% ($\pm 0.5\%$) LiCl if the cation is again assumed to be Li^+ .

The insoluble matter (B) was rinsed with hot water, acetone, THF, and CS_2 but was unaffected. Addition of 25 ml chromic acid turned the solution green, indicating that the material could be oxidized. The remaining material appeared to be mostly particles and Teflon as seen under a microscope at 50 X.

Other tests were carried out which showed that the electrolyte from the over-discharged cell contained less than one to five ppm dissolved nickel. Thus the green color must be due to some other substance such as polysulfides produced by reduction of sulfur.

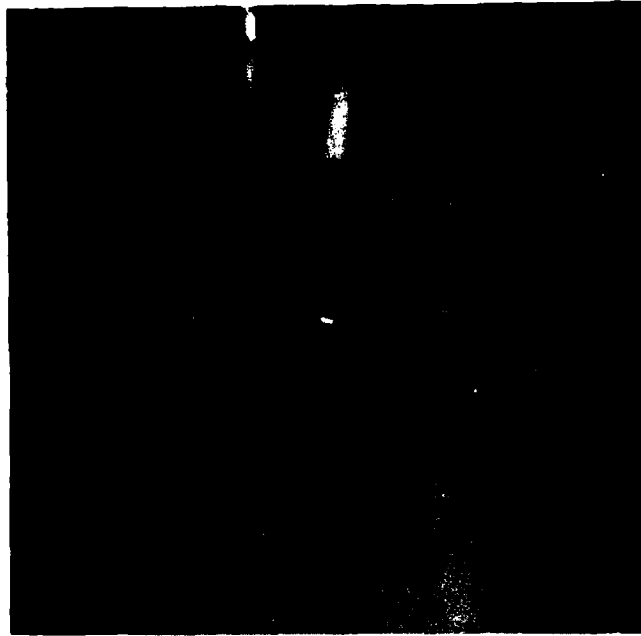


Figure 24: Cell Overdischarged at -40°C After 3.5 Hours on OCP at 23°C . See Caption for Figure 23.



Figure 25: Cell Overdischarged at -40°C After 23 Hours on OCP at 23°C .

Since cells discharged at -40°C contain especially high concentrations of SO_2 which could react to produce lithium dithionite ($\text{Li}_2\text{S}_2\text{O}_4$), measurements were undertaken to determine the solubility of $\text{Li}_2\text{S}_2\text{O}_4$ in SOCl_2 . Anhydrous $\text{Li}_2\text{S}_2\text{O}_4$ used for the tests was synthesized in house because the compound is not commercially available. The solubility of the 90% purity material was less than $7.0 \cdot 10^{-4}$ M in SOCl_2 at 23°C .

Overdischarge tests at -40°C with two additional carbon limited cells very similar to the one just described indicated that the corrosion rate of the Li deposits depend on the discharge capacity of the cell and the electrolyte volume. As the capacity of the cell is reduced, the concentration of the discharge products responsible for corrosion at 23°C is also reduced and the corrosion rate of the Li dendrites is lowered.

The second and third cells overdischarged at -40°C used the same cell design as described earlier and shown in Figure 23 with single 3.0×3.5 cm cathodes. For these cells the cathodes were 1.0 mm and 1.7 mm thick compared to 1.7 mm in the first cell. The second cell with the 1.0 mm thick cathode yielded a discharge capacity of 31 mAhr/cm² at -40°C at 2 mA/cm² to 0.0V, after which it was overdischarged to 332 mAhr/cm² at 10 mA/cm². A total of 11 photographs were taken of the cell over a period of 96 hours at 23°C on open circuit and no sign of dendrite dissolution was observed. A third cell with a 1.7 mm cathode was discharged at 1 mA/cm² at -40°C and yielded 140 mAhr/cm² to 0.00V. The cell was then overdischarged 30.5 hours at 1 mA/cm² and 40.5 hours at 10 mA/cm² at -40°C because the cell would not support the higher current density until the Li dendrites were formed. A series of 14 color photographs were taken of the cell during 28.9 hours of open circuit storage at 25°C . The photographs revealed a similar process of Li dendrite corrosion, detachment from the cathode surface and dissolution as described earlier in connection with Figures 23-25. However, the rate of Li dendrite dissolution was somewhat slower. The cell used for the investigation of cell reversal contained about 150 ml of SOCl_2 electrolyte which was about 50 times more electrolyte than would be used in a commercial cell of similar capacity. The large excess of electrolyte was required to facilitate the observation of the Li dendrites.

The dissolution of the Li dendrites was not observed in the second cell overdischarged at -40°C because the capacity was five times less than in the third cell and thus the soluble discharge products were diluted to a greater extent. Such electrolyte volume effects are of considerable importance because in commercial cells with a small volume of SOCl_2 electrolyte the concentrations of reactive discharge products after -40°C overdischarge could be much higher and could lead to a thermal runaway reaction with the high surface area Li dendrites.

Reviewing all the experimental results, it was concluded that Li dendrites deposited at -40°C are more reactive towards the electrolyte than those deposited at 25°C because of the greater amount of SO_2 in the SOCl_2 electrolyte at -40°C . At -40°C , the reaction of SO_2 with SOCl_2 electrolyte proceeds much more slowly and the SO_2 concentration becomes greater. Furthermore, the solubility of SO_2 in SOCl_2 electrolyte is greater at -40°C , which is significant in cells like those used in the present work with a large head space. It is well known that voltage delay at the Li anode in Li/ SOCl_2 cells can be reduced by adding SO_2 to the electrolyte which increases the rate of Li corrosion at the anode. It is thought that the corrosion of Li dendrites deposited at -40°C is caused by the same phenomenon. By some unknown process high concentrations of SO_2 reduce the effectiveness of the LiCl film on the Li surface by preventing SOCl_2 from reacting with Li.

To gain additional information about the concentration of various chemical species in cells overdischarged at -40°C , a 0.3 Ahr Li/ SOCl_2 cell of a practical configuration with only a slight excess of neutral SOCl_2 electrolyte was overdischarged at 40°C and a sample of electrolyte from the cell analyzed by linear sweep voltammetry in DMF supporting electrolyte. The voltammetry results for the cells overdischarged at -40°C are discussed in Section 1.4.1.3.

Lithium Dendrite Shorting. - Lithium dendrite shorting during overdischarge of a carbon limited cell was investigated using the 5.5 cm diameter cell with the optical glass window described earlier. The cell was first discharged at 2.5 mA/cm^2 to 0.0V yielding a capacity of 1.03 Ahr then overdischarged at 5.0 mA/cm^2 at a potential of -0.92V vs Li (see Figure 26.). Figure 27 shows the

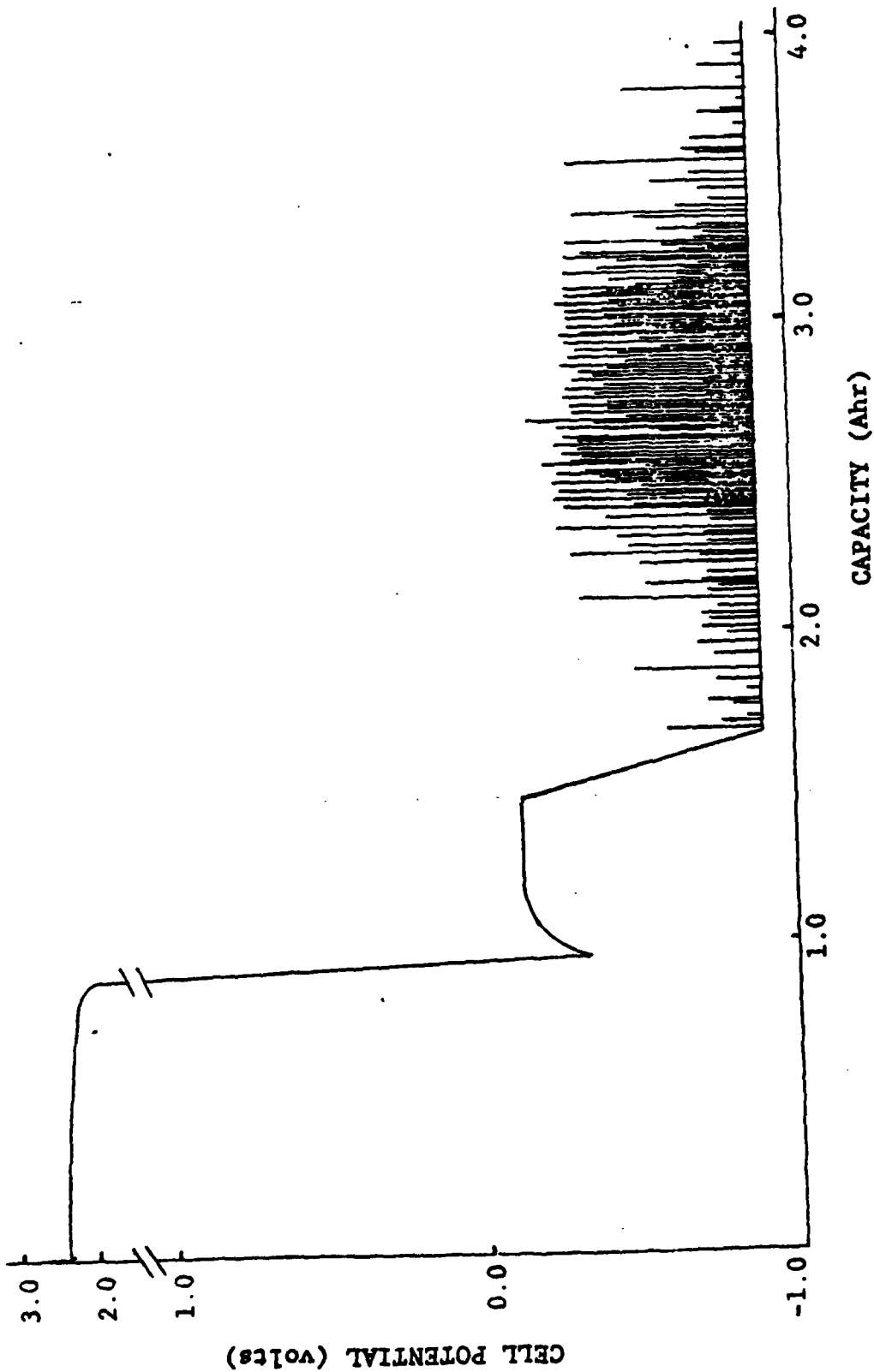


Figure 26: Overdischarge of a Li/SOCl₂ Cell at 23°C, 5.0 mA/cm² *

* The cell did not contain a separator, was flooded with electrolyte and was discharged at 2.5mA/cm². The overdischarge current density was increased to 10mA/cm² at 1.7Ahr.

Li dendrite growth after 2.0 hrs of overdischarge. The carbon electrode is on the left and the Li electrode is the large white mass extending from the center bottom almost to the right edge of the microphotograph. The Li electrode was bent sharply in an "L" shape towards the cathode to cause the dendrites to grow preferentially and short circuit within easy view of the microscope. In the exact center of Figure 27 the edge of the Exmet screen of the Li electrode can be seen that was exposed due to anodic dissolution of the Li.

The growth of the Li dendrites after 6.75 hours of overdischarge is shown in Figure 28 which is a microphotograph of the exact same spot at 21 X magnification as shown in Figure 27. By 6.75 hours no electrical shorts had occurred even though the Li dendrites had grown across the inter-electrode gap and all around the exposed edge of the Ni Exmet current collector of the Li anode.

The current density was then increased to 10 mA/cm^2 and the first transient short circuit (< 2 seconds) appeared after a total of 6.87 hours of overdischarge. No other shorts occurred for three hours (until 1.33 Ahr overdischarge) but thereafter they occurred more frequently but randomly until the maximum frequency was reached at approximately 2.17 Ahr overdischarge (see Figure 26). The shorts were all of less than two seconds duration, and were of high resistance, lowering the cell potential to no lower than -0.24V from the -0.92V value (see Figure 29). The potential of the cell during overdischarge was monitored with a high speed Gould Model 2200 S recorder, operating at chart speeds up to 50 mm/second . The use of this high speed recorder may be one reason why we were able to observe that the shorts were of a transient duration, an important observation that has not been reported previously to our knowledge.

The shape of the cell potential versus time curves during the transient short circuits as recorded on the high speed recorder has a very unusual and characteristic shape which occurred uniformly for a large majority of all the transients that were recorded at the highest chart speeds. The time of the transients and the minimum cell potential changed somewhat but the shape remained uniform (see Figure 29). The fast drop in cell potential is to be expected as



Figure 27: Lithium Dendrites After 2.0 Hours Overdischarge at 5.0 mA/cm². For the Cell Described by Figures 26, 28-30. Magnification 21 X

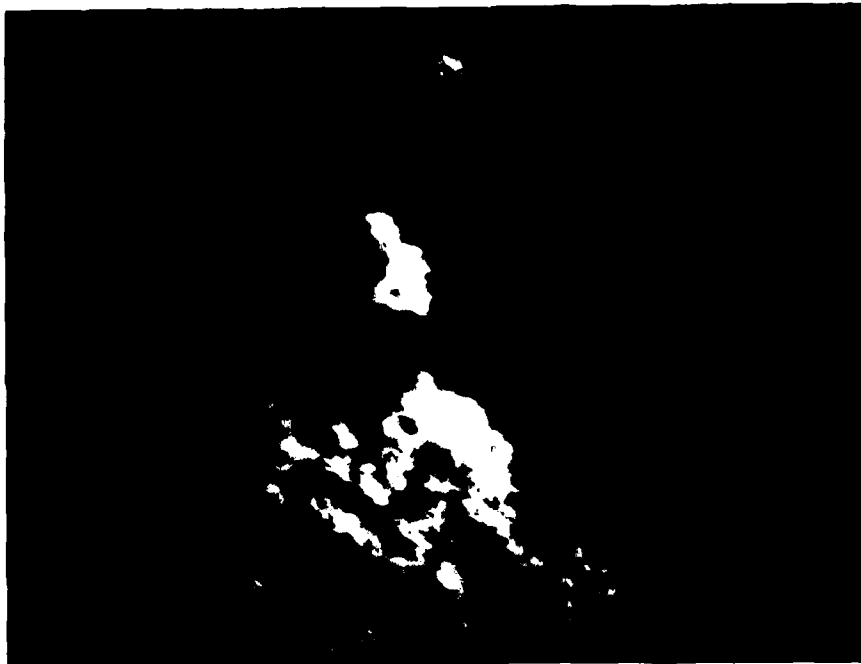


Figure 28: Lithium Dendrites After 6.75 Hours Overdischarge at 5.0 mA/cm² at the Same Spot as Shown in Figure 27. Magnification 21 X

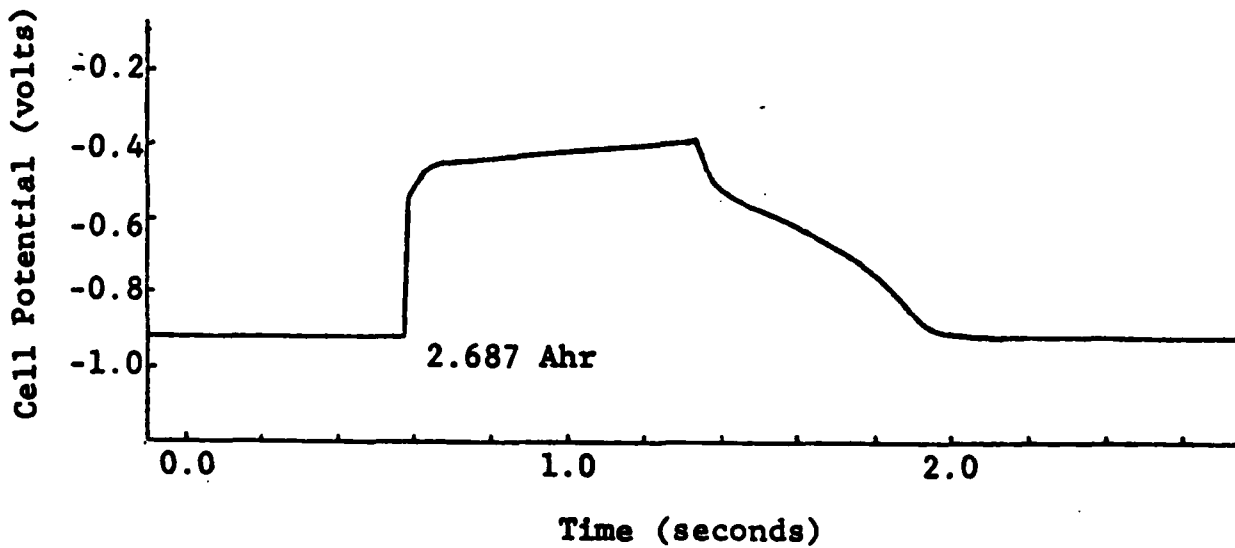
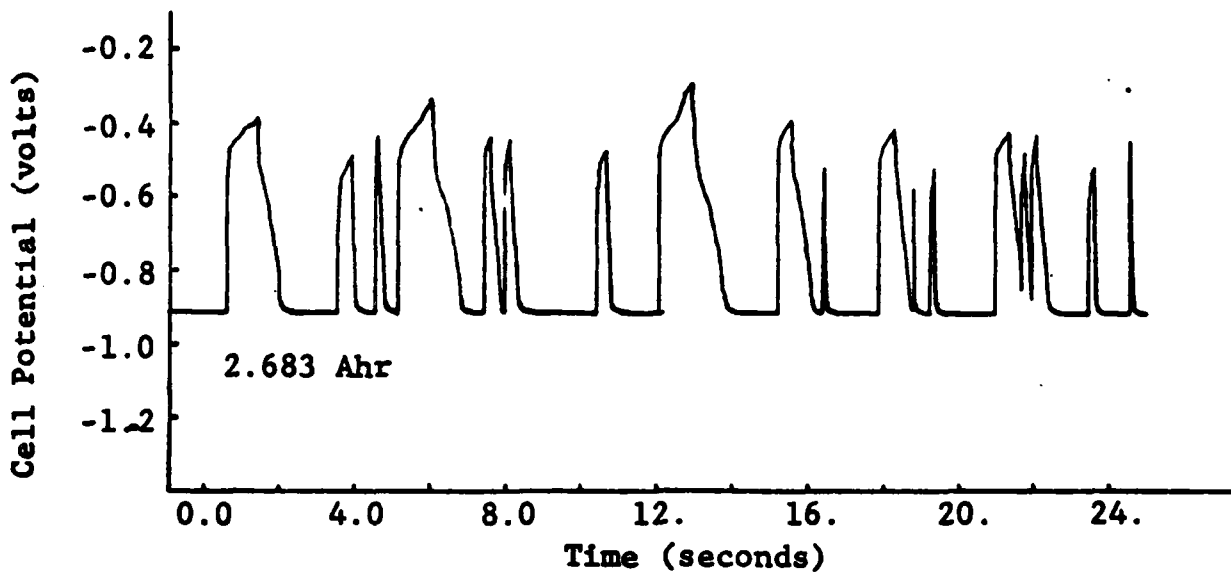


Figure 29: Pulses in the Cell Potential During the Overdischarge of an Electrolyte Flooded Li/SOCl₂ Cell at 5.0mA/cm², 23°C*

* The positions of the pulses in Figures 29A and 29B are shown approximately at 2.683 and 2.687Ahr in Figure 26.

the initial contact of the Li dendrite with the Li anode is made. Previously it had been thought that the Li dendrite might heat up and suddenly melt, causing a very rapid return to the original operating potential. However, recent data indicates that it is very unlikely that Li dendrites melt during the short circuits brought about by overdischarge.

It is known from earlier scanning electron microscope studies that Li is deposited on the cathode in SOCl_2 cells during overdischarge in the form of dendrites made up of a steel wool type structure of Li filaments with a diameter of $4 \cdot 10^{-3}$ mm. In the present cell, it is clear that one such small filament couldn't support a 0.21A short circuit current. Thus, the slow 0.7s return of the potential to the operating potential is probably caused by innumerable small filaments of various lengths heating up, reacting faster with the SOCl_2 , and corroding until they break apart. In view of the small diameter and large surface area of the Li filaments, it is doubtful that their temperature would rise high enough to melt Li, considering that they would be surrounded by SOCl_2 electrolyte, which would rapidly conduct the heat away. Several other factors, such as the contact resistance between the dendrite tip and the Li anode could perhaps account for the slow decline of the transient but will not be evaluated here.

Figure 30 shows the Li dendrites touching the Li anode screen after 23.3 hours of overdischarge at a magnification of 21X at a point close to those shown in Figures 27 and 28 but not identical as before. The Li dendrites were growing from the carbon electrode on the left towards the Li anode on the right. The photo shows the appearance of the dendrites after about 16 hours of shorting but at a time when the frequency and the resistance of the shorts was beginning to markedly decrease. The Ni Exmet screen of the Li anode bent towards the cathode was depleted of Li and it may be that the Li dendrites make poorer contact and therefore shorts with Ni than with the Li foil of the anode.

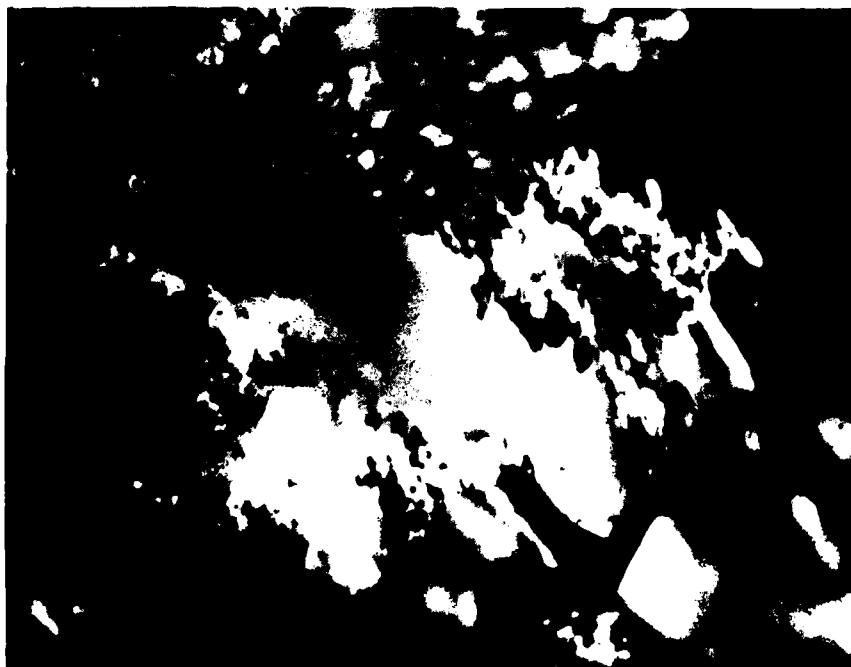


Figure 30: Lithium Dendrites After 23.3 Hours Overdischarged at 5.0 mA/cm².
For the Cell Described by Figures 26-28, 30. Magnification 21 X

1.4.1.3 Voltammetry of Electrolyte From Carbon Limited Cells Overdischarged at -40°C

The Li/SOCl_2 cells that were overdischarged at -40°C utilized two 3.5×2.5 cm Li anodes, 0.76 mm thick on either side of a similar size carbon cathode 1 mm thick. The cathode was separated from the anode by three layers of Crane glass fiber paper 0.17 mm thick. The cell package was contained in a 1.0 inch I.D. thick walled Pyrex glass tube with two Teflon half cylinders to restrict the amount of electrolyte required to immerse the electrodes. A glass top with glass-to-metal feed throughs was attached to the tube containing the electrode package using a metal coupling with a Teflon flat gasket and the cell was vacuum filled with 5 ml of 1.8M $\text{LiAlCl}_4/\text{SOCl}_2$ electrolyte. Details of the cell design have been discussed earlier in Section 1.2.2 of Reference 1.

The above cell was discharged at -40°C at $2 \text{ mA}/\text{cm}^2$ for 11.3 hours (0.203 Ahr) then overdischarged at $1 \text{ mA}/\text{cm}^2$ for 101 hours (0.909 Ahr) also at -40°C . The potential was continuously recorded and no potential transients indicative of the Li dendrite shorts were observed during overdischarge.

At the end of overdischarge, the electrolyte from the overdischarged cell was transferred in the dry room to a 250 ml Erlenmeyer flask that contained 100 ml of anhydrous DMF at -40°C . The electrode package was rinsed in the cell with DMF at -40°C and the rinse added to the Erlenmeyer flask and the volume brought up to 150 ml. Exactly 0.30 ml of this solution of the overdischarged SOCl_2 electrolyte in DMF was then added to 9.7 ml of degassed 0.1M $\text{TBAPF}_6/\text{DMF}$ supporting electrolyte at 23°C in the voltammetry cell. Thus the overall dilution of the SOCl_2 electrolyte was 1:970.

The voltammograms that were obtained immediately after the overdischarged electrolyte was added to the voltammetry cell and after 1.5 and 17 hours of storage at 25°C are given in Figure 31. The voltammogram obtained immediately after the sample was added to the cell shows the expected peaks for SOCl_2 and SO_2 at -0.72 and -0.95V , respectively. The SO_2 peak is larger than for

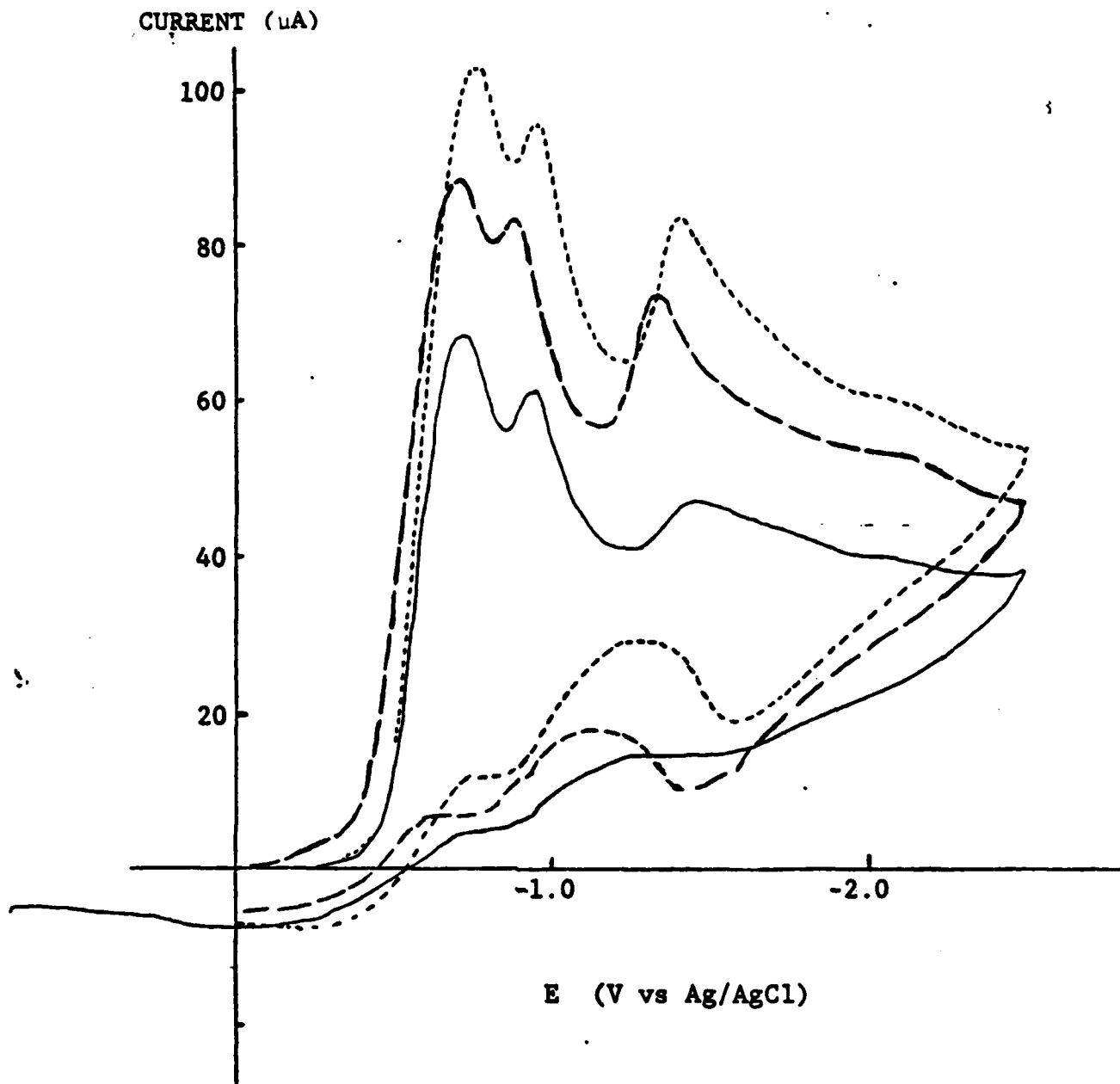


Figure 31: Voltammograms of 5 μl of SOCl_2 Electrolyte from a Carbon Limited Cell Overdischarge 380% at -40°C , 1 mA/cm^2 .

The 5 μl electrolyte sample at -40°C was dissolved in 0.1M TBAPF₆/DMF. The scan rate was 200 mV/second.

(—), immediately after sample added to DMF in cell.

(. . . .), after 1.5 hours storage, 23°C .

(- - -), after 17 hours storage, 23°C .

samples of fresh SOCl_2 electrolyte (see Figure 11 of Ref. 1) as would be expected since SO_2 is produced during discharge. No new peaks were observed which is consistent with the finding by Williams and co-workers (3) that the OClS radical has a lifetime of < 10 seconds at 24°C .

The substantial rise in the SOCl_2 peak from $68.8 \mu\text{A}$ to $103.2 \mu\text{A}$ after 1.5 hours of storage at 23°C is quite remarkable and its cause is not yet known. The increase in the SOCl_2 peak current was not due to warming of the 10 ml of DMF electrolyte chilled by the addition of 0.3 ml of sample at -40°C because calculations show that the 10 ml of electrolyte would at most be cooled by 0.55°C neglecting the mass of the cell and transfer pipette. However a 15°C change in electrolyte temperature causes only a 18.2% reduction in the SOCl_2 peak current (see Figure 6) which is small compared to the 34.1% reduction that was observed. The increase in the SOCl_2 peak current during the first 1.5 hours of 23°C storage could be due to recombination of some intermediate formed during overdischarge at -40°C to form SOCl_2 . More likely possible causes of the low SOCl_2 peak are either poor mixing of the cold 0.3 ml sample in the cell or some type of low temperature solvation between the SOCl_2 electrolyte and DMF.

The rise in the peak at 1.4V during the first 1.5 hours of storage is clearly due to an increase in the concentration of the products of the SO_2 - SOCl_2 electrolyte reaction as discussed in Section 1.2.3. The cause of the decrease in the SOCl_2 peak current during the period from 1.5 to 17 hours storage is currently unknown. It is not due to the SO_2 - SOCl_2 electrolyte reaction or diffusion into the counter electrode compartment because standard samples containing 2.7M SO_2 stored 22 hours did not exhibit such large changes (see Figure 11). Thus some unknown product of overdischarge could be either reacting with the SOCl_2 (or DMF) electrolytes or somehow passivating the Pt working electrode.

To analyze SOCl_2 electrolyte from prototype Li/ SOCl_2 cells overdischarged at -40°C by voltammetry, it is clear that additional voltammetry should be carried out at 25°C and at temperatures below -20°C . However, the resolution of

SOCl_2 , SO_2 and presumably other compounds at -20°C in the voltammograms is very poor as shown in Figure 6. These resolution problems could perhaps be overcome by lowering the scan rate from 200 to 50 mV/second or lower to make up for the slower diffusion (see Figures 4 and 5) but considerable work would be required to obtain new calibration curves for SO_2 , SOCl_2 and the rate of the SO_2 - SOCl_2 electrolyte reaction at -40°C or other temperatures selected for investigation.

It is concluded from the present work that the electrolyte from prototype Li/ SOCl_2 cells overdischarged at low temperatures should be analyzed by quantitative infrared spectroscopy and that further voltammetry measurements should be postponed. Once the concentrations of the species produced during low temperature overdischarge have been determined by infrared analysis then voltammetry could be used to characterize the electrochemical properties of any new species that are found to be present at significant concentrations.

1.4.1.4 Prototype Cell Overdischarge Results

The seven prototype cells that were overdischarged used the same design as described in Section 1.4.1.3 but with somewhat smaller 2.0 x 3.0 cm electrodes. The cells contained a single carbon cathode 1 mm thick, a separator and two Li anodes in a 1.0 inch I.D. glass tube with two Teflon half cylinders to restrict the electrolyte volume. The objective of the overdischarge tests in prototype cells was to determine the effect of separators and restricted electrolyte volume on Li dendrite shorting over a range of temperatures and discharge rates.

The discharge and overdischarge capacities, current densities, temperatures and other results for the seven cells that were overdischarged are listed in Table 3. The behavior of the potential during discharge and extended overdischarge for four of the cells are shown in Figures 32-34.

Table 3

Lithium Anode Dissolution and Shorting During the Overdischarge of
 Prototype Carbon-Limited Li/SOCl₂ Cells*

Cell No.	Temp. (°C)	Current Density (mA/cm ²)	Over-		Discharge Capacity (Ahr)	Percent Over-Discharge (%)	Lithium Anode	
			Discharge Capacity (Ahr)	Discharge Capacity (Ahr)			Capacity (Ahr)	Dissolution (%)
51	23	5.0	20.0	0.26	7690	1.7	-	
52	23	5.0	14.8	0.25	5940	1.70	40	
53	23	1.0	12.5	0.23	5500	1.7	-	
54	-20	5.0	19.0	0.237	8000	1.7	29.5	
55	-20	10.0	8.17	0.15	5440	1.801	28	
56	-20	20.0	33.5	0.23	14500	1.725	22.9	
57	-20	30.0	24.9	0.27	9200	1.774	24.3	

* None of the cells showed negative transients in the potential indicative of lithium dendrite shorts. All the cells used a single sheet of 0.007 inch thick Crane glass separator between the electrodes except for Cell 51 which had three layers.

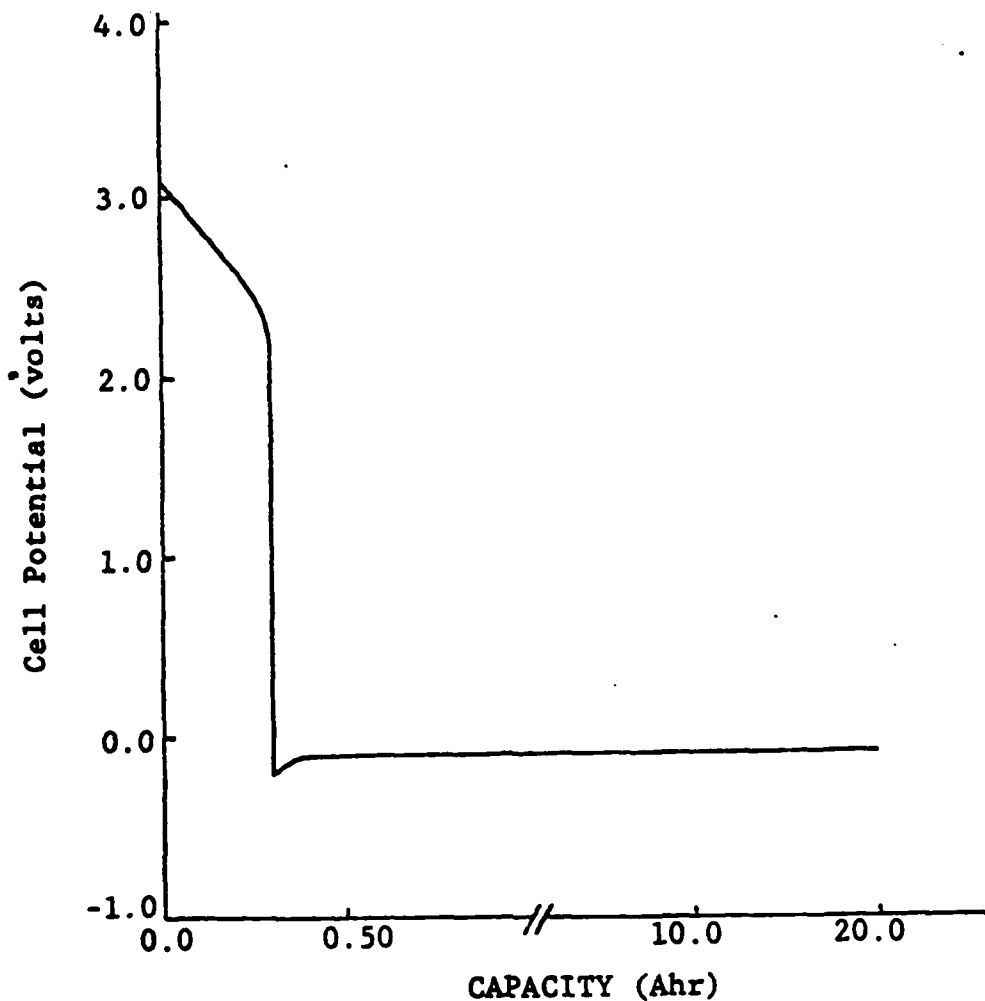


Figure 32: Behavior of a Carbon Limited Li/SOCl₂ Cell During Discharge and Overdischarge at 5.0mA/cm², 23°C.*

* Cell 51 contained three layers of 0.007 inch thick glass fiber separator paper and only a slight excess of 1.8M LiAlCl₄/SOCl₂ Electrolyte. The two Li anodes and cathode measured 2.0 x 3.0cm.

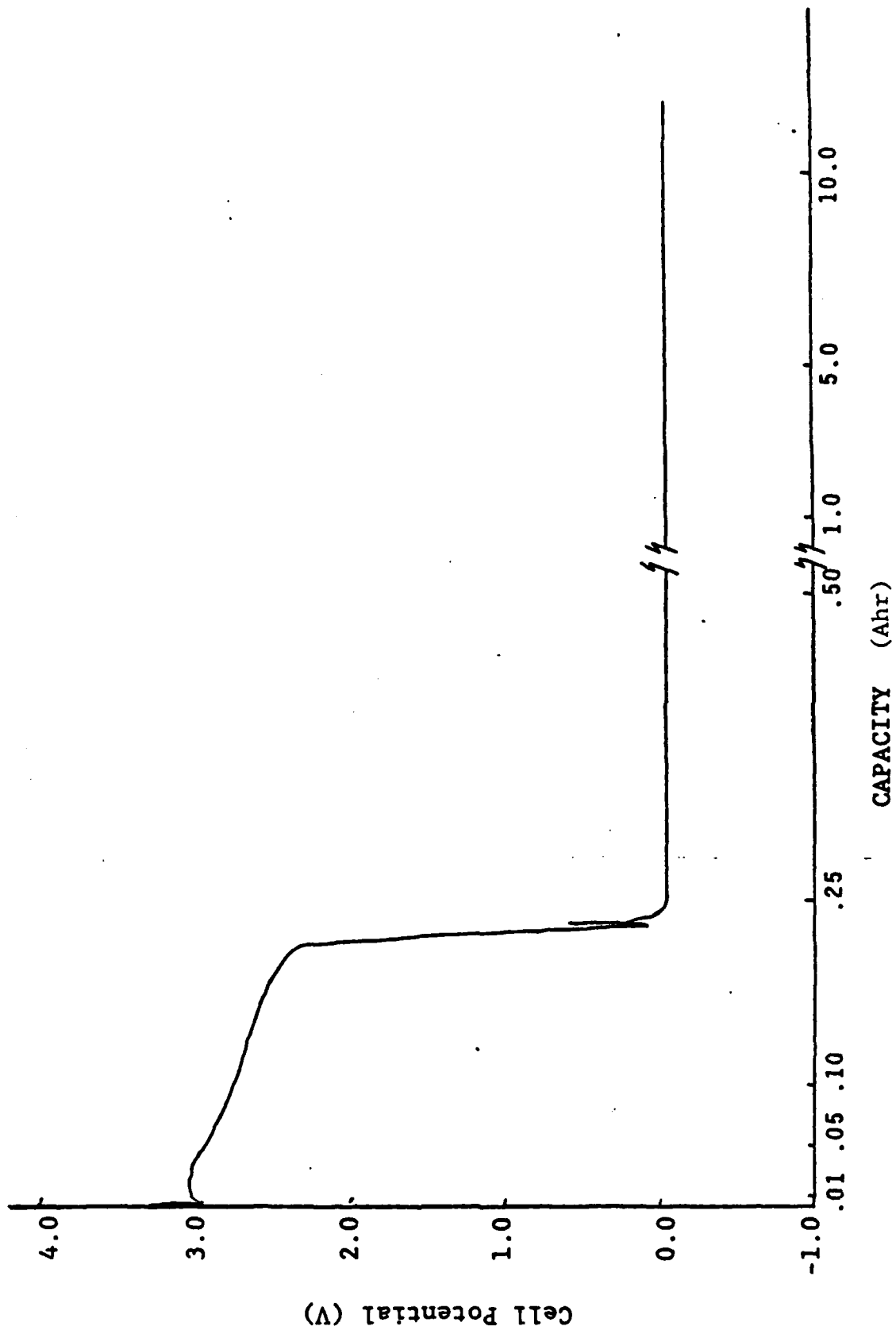
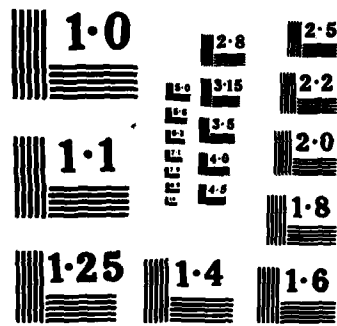


Figure 33: Behavior of a Carbon Limited Li/SOCl_2 Cell During Discharge and Overdischarge at $1.0 \text{ mA}/\text{cm}^2$ at 23°C . Additional information about Cell 53 is given in Tables 3 and 4.



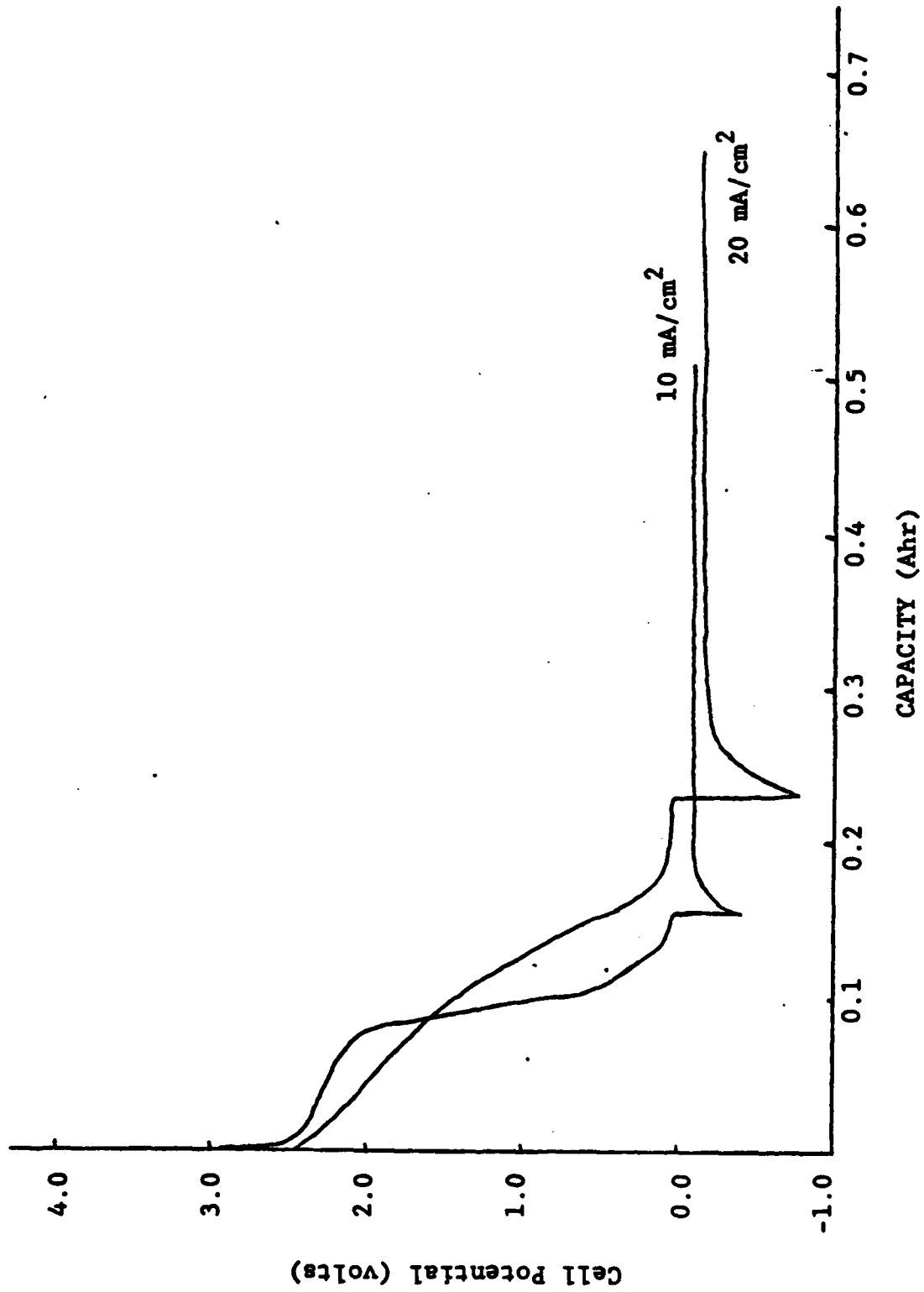


Figure 34: High Rate Overdischarge of Carbon-Limited Li/SOCl₂ Cells at -20°C. Further information about Cells 55 and 56 discharged at 10 and 20 mA/cm², respectively, is given in Table 3.

None of the cells listed in Table 3 showed negative transient pulses in the potentials during overdischarge indicative of lithium dendrite shorting. Such transients were discussed earlier in connection with Figures 26 and 29 for electrolyte flooded cells with widely spaced electrodes without separators.

At the end of overdischarge the cells were disassembled and the lithium anodes cleaned and weighed to determine the amount of lithium that was consumed. The lithium anode capacities and the amount of lithium consumed is listed for each of the cells in Table 3. All of the cells were overdischarged to at least 8 Ahr yet the lithium anodes only had theoretical capacities between 1.7 and 1.8 Ahr. Furthermore, the cell potentials during overdischarge were no more negative than -0.40V and did not shift to potentials more negative than -3.5V indicative of lithium depletion at the anode. Thus it is clear that the cells were at no time anode limited and that a majority of the current passed through the cell during overdischarge by an electronic pathway and not via an ionic pathway that could lead to excessive and possibly hazardous Li dendrite formation.

It was also observed when the cells were disassembled that the Li dendrites had grown through the separator paper to the extent that the separator paper could not be removed without damaging the cathode. No signs of excessive heating such as burn marks were observed on any of the electrodes or separators.

The small amount of lithium that was anodically dissolved during extended overdischarge suggests that the Li dendrite shorting occurred fairly early during overdischarge and that most of the current passed through the cell via an electronic pathway through the Li dendrites. For example, for Cell 56, the results in Table 3 show that although the cell was overdischarged 33.5 Ahr only 22.9% of the 1.725 Ahr capacity of the Li anode was utilized or 0.395 Ahr. Since 0.23 Ahr of Li was consumed during discharge only 0.165 Ahr of Li was used during the 33.5 Ahr of overdischarge. Thus only $0.165/33.5$ or 0.49% of the overdischarge current was conducted via the ionic pathway. Similar calculations could be carried out for the other cells listed in Table 3.

The cell potentials during overdischarge at 5 mA/cm^2 were approximately -0.06 to -0.11V which at first would appear to indicate the absence of a short circuit and to be inconsistent with the high degree of electronic conductivity indicated by the very low lithium utilizations. However, resistance measurements have shown that the cell potential is almost entirely due to the IR drop across the porous carbon in the cathode.

Several cell potentials during overdischarge are given in Table 4 for each of the seven prototype cells that were overdischarged. The potentials quickly reached steady state values that showed little change during the long overdischarge period. The electrical resistance of the carbon on the 1 mm thick porous carbon cathodes was determined by pressing a $2.0 \times 3.0 \text{ cm}$ piece of Ni foil on a similar size carbon cathode at a pressure of 40 g/cm^2 and measuring the resistance with a standard digital ohm meter between the Ni plate and the lead to the Exmet grid of the cathode. The total resistance was six ohms, thus the specific resistance was 36 ohm cm^{-1} at 23°C between the surface of the cathode and the Ni Exmet grid in the center of the cathode.

For a cell with two $2.0 \times 3.0 \text{ cm}$ Li electrodes on either side of the $2.0 \times 3.0 \text{ cm}$ carbon cathode such as those described in Table 3, the contact resistance would therefore be three ohms if the electrodes were in direct contact without a separator. If the cell was being overdischarged at 5 mA/cm^2 the total cell current would be 60 mA and the IR drop across the three ohm resistance of the carbon layers of the cathode would give a potential of 0.180V by Ohm's law. From Table 4 it can be seen that the cell potentials for Cells 51 and 52 during overdischarge at 4 mA/cm^2 were only -0.09 and -0.06 , respectively. It is thought that these unusually low potentials were achieved because some of the Li dendrites grew from the exposed Ni Exmet grid on the edges of the cathode to the Li anode to form a low resistance path.

One would expect that the formation of the low resistance shorts between the exposed ends of the Ni grid and the Li would have resulted in negative transients in the cell potential, but the exact mechanism of the shorting process remains somewhat of a mystery. Perhaps the fine (i.e., $\pm \mu\text{m}$ diameter) Li

Table 4

Cell Potentials for Prototype Carbon Limited
Li/SOCl₂ Cells During Extended Overdischarge*

Cell No.	Current Density (mA/cm ²)	T (°C)	Overdischarge Time, t (hrs)	Capacity At t (Ahr)	Cell Potential at t (V)
51	5.0	25	97.67	6.13	-0.09
51	5.0	25	333.5	20.3	-0.09
52	5.0	25	0.33	0.020	-0.11
52	5.0	25	7.45	0.447	-0.07
52	5.0	25	31.13	1.86	-0.06
52	5.0	25	247.53	14.85	-0.06
53	1.0	25	1.20	0.01	-0.05
53	1.0	25	17.02	0.20	-0.05
53	1.0	25	1028	12.34	-0.42
54	5.0	-20	0.45	0.027	-0.111
54	5.0	-20	2.0	0.12	-0.092
54	5.0	-20	28	1.68	-0.0858
54	5.0	-20	196	11.76	-0.0810
54	5.0	-20	318	19.08	-0.0793
55	10.0	-20	0.10	0.01	-0.273
55	10.0	-20	0.54	0.06	-0.109
55	10.0	-20	3.04	0.36	-0.090
56	20.0	-20	0.10	0.02	-0.402
56	20.0	-20	0.54	0.13	-0.168
56	20.0	-20	3.04	0.73	-0.141
57	30.0	-20	1.78	0.641	-0.159
57	30.0	-20	69.31	24.95	-0.140

* All the cells used a single layer of 0.007 inch thick Crane glass separator between the electrodes except for Cell 51 which had three layers. Additional information about the cells is given in Table 3.

filaments making up the dendrites formed a large number of durable short circuit paths over a period of from ten to thirty minutes thereby gradually increasing the conductivity of the short circuit and lowering the cell potential in a continuous and gradual manner without transients. It is possible that the shorter inter-electrode distance in the prototype cells and the presence of a separator to support the frail Li dendrites makes them less likely to increase slightly in temperature due to IR heating, corrode, break apart and terminate the short circuit abruptly, resulting in a potential transient.

It has been noted earlier in the literature (34) that carbon limited cells can be overdischarged for long periods of time during which the charge input greatly exceeded the Li originally present in the cell. Similar to the present work no transients in the potential were noted and a short circuit mechanism was proposed to account for the low Li utilization. However, quantitative data were not given concerning the Li utilization or the proportion of the current carried by an electronic pathway during overdischarge.

The results of the overdischarge tests described in this section tend to suggest that carbon limited cells form Li dendrite shorts by a benign mechanism and that overdischarge does not constitute a specific hazard. This impression was reinforced by observations during cell disassembly which revealed no sign of overheating such as burn marks. However, spiral wound D size cells have been reported (29,30) to "explode" when overdischarged 12.7% at which time the cell wall temperature was only 39°C. Other situations where the overdischarge of carbon limited cells has resulted in thermal runaway have been widely reported (29-31).

Various chemical reactions and processes have been proposed (29,30,38) to account for thermal runaway in carbon limited cells during overdischarge. Of the various explanations, we think evidence is growing stronger that thermal runaway occurs due to the reaction of sulfur which has precipitated from the electrolyte with the high surface area Li dendrites. The reaction of sulfur with Li is highly energetic



[6]

with a free energy, $\Delta F = -120$ Kcal/mole of Li_2S . Differential thermal analysis (DTA) measurements (30,37) have shown that the $\text{Li} + \text{S}$ reaction has a strong exothermic transition and undergoes thermal runaway at 153°C . Sulfur normally does not react with the Li anode because the Li is passivated by a LiCl film and the sulfur is dissolved in the SOCl_2 electrolyte. However, it has recently been found by scanning electron microscope studies (35,36) that the Li dendrites formed in Li/SOCl_2 cells during overdischarge are fine filaments (i.e., $4 \mu\text{m}$ diameter) coiled in a spaghetti-like structure with an extremely high surface area. During overdischarge it is possible that some of these fine Li dendrites covered with a layer of precipitated sulfur or near a large sulfur crystal could either mechanically break or be corroded and the fresh Li surface could come in contact with solid sulfur and begin to react. Alternatively, the Li dendrites could undergo a substantial temperature rise due to IR heating during short circuit and react with nearby sulfur crystals initiating a thermal runaway reaction.

In 1978 it was proposed (30) that discharged carbon limited cells could undergo thermal runaway due to reaction of Li with unstable SOCl_2 reduction intermediates such as SO which were believed to exist. Recent infrared, ESR and electrochemical studies of electrolyte from discharged Li/SOCl_2 cells (1-3) have shown no evidence for the existence of long lived intermediates. Thus exothermic reactions of discharge intermediates can be ruled out as a cause of thermal runaway for carbon limited cells during overdischarge.

Assuming that thermal runaway in carbon limited cells occurs during overdischarge due to a reaction of solid sulfur with the high surface area Li dendrites, then it is not surprising that the 0.25 Ahr prototype cells used in the present investigation did not show signs of excessive heating or undergo thermal runaway. First, the cells contained a somewhat higher electrolyte to carbon cathode mass ratio than commercial cells and it is likely that the electrolyte volume was large enough so that all the sulfur produced from the discharge reaction dissolved*. Thus no solid sulfur was present to react with

* The solubility of sulfur in $1.8\text{M LiAlCl}_4/\text{SOCl}_2$ is 1.328M at 24°C (43).

the Li dendrites. Second, even if an exothermic reaction occurred, thermal runaway did not take place probably because of the small size of the cell and the excellent heat transfer properties of the prismatic configuration.

Because overdischarged carbon limited cells can explode with only a 15°C temperature rise before the explosion, it appears that the chemical reactions responsible for thermal runaway can be identified and safely studied in small laboratory prismatic cells. This is in contrast to thermal runaway brought about by short circuit in high rate cells which is caused by both poor heat transfer and exothermic chemical reactions and which can only be investigated effectively in high rate cells at least as large as C size. Thus it appears that it will probably be much easier to study thermal runaway in overdischarged cells than short circuit in high rate cells. Since small cells may be adequate to identify the cause of thermal runaway during carbon limited overdischarge, the investigation could progress more rapidly to yield designs to eliminate the thermal runaway hazard.

It is therefore recommended that additional overdischarge tests should be carried out with small carbon limited prismatic cells with small electrolyte-to-carbon mass ratios at temperatures from 25°C to approximately 60°C. The electrolyte and components from the overdischarged cells should be analyzed for unusual products that could be generated from exothermic side reactions such as Li_2S and the cell components inspected for burn marks or other signs of excessive heating. If small exothermic reactions can not be detected then additional tests in somewhat larger multiple cathode prismatic cells could be carried out.

It is also recommended that DTA measurements of the properties of lithium dendrites and sulfur should be carried out since earlier measurements did not use finely divided Li. Information is also needed concerning the chemical and electrical behavior of compressed slurries of Li dendrites in SOCl_2 neutral electrolyte while high current densities are passed through the slurry. The use of metal tabs on the anode and cathode to localize Li dendrite growth and prevent thermal runaway as described in a recent patent (41) should also be

thoroughly investigated since little information has been published about this promising design modification.

1.4.2 Anode Limited Overdischarge

1.4.2.1 Background

As discussed earlier in Section 1.4.1.1 most of the results currently available indicate that anode limited Li/SOCl₂ cells are less likely to undergo thermal runaway during high rate overdischarge than carbon or electrolyte limited cells (44-47). GTE (44,45) and Honeywell (46) have carried out overdischarge tests with large anode limited cells with capacities up to 16,500 Ahr and incidents involving thermal runaway were not experienced with any of the cells. Union Carbide (47) carried out safety tests on over 8,000 cylindrical cells slightly smaller than a standard 'AA' size and no safety problems or hazards were identified as a result of the tests.

During the overdischarge of anode (i.e., lithium) limited cells, the electrode reaction at the carbon cathode continues to be the reduction of SOCl₂ to produce SO₂, Cl⁻, and S as described by Equation [1]. However, the LiAlCl₄/SOCl₂ electrolyte is oxidized at the bare nickel anode screen as soon as the lithium is consumed by anodic dissolution. The predominant reaction of LiAlCl₄/SOCl₂ electrolyte oxidation at the anode substrate is:



The AlCl₃ and Cl₂ produced can then react further with the SOCl₂ discharge products SO₂ and S



The dissolved chlorine produced by reaction [7] could also undergo reduction at the carbon cathode where it would be reduced in preference to SOCl_2 .



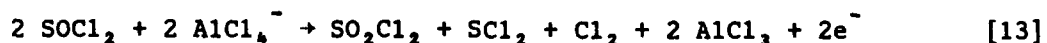
The existence and relative importance of the side reactions of Equations [10], [11], [12] under various conditions of charging are still a subject of active research that will be discussed further in this section.

The AlCl_3 , produced by oxidation of the SOCl_2 electrolyte at the anode screen diffuses to the carbon cathode where it reacts with LiCl inside the cathode produced by the reduction of SOCl_2 and Cl_2 (i.e., Equation [12]). For every equivalent of charge passed, one mole of AlCl_3 will be produced at the anode substrate and one mole of LiCl will be produced at the cathode by the reduction of SOCl_2 , SO_2Cl_2 or Cl_2 that will eventually react to form soluble LiAlCl_4 . Thus the carbon cathode will not be filled up with LiCl and become passivated but will remain active indefinitely, provided that the cell has sufficient electrolyte. Electrolyte is consumed during anode limited overdischarge because the S and SO_2 produced by the reduction of SOCl_2 are not regenerated.

The above qualitative description of the reactions occurring during anode limited overdischarge generally agrees with the electrochemical behavior and the early exploratory infrared and voltammetric analysis of the electrolyte (19,34). However, the explosions of several anode limited spiral wound "C" size cells overdischarged at 1 mA/cm^2 reported by Abraham and Mank (34) and the claims by Salmon et al (50) that chlorine monoxide, Cl_2O , a highly oxidized explosive compound is produced has stimulated further research (2,49). This research has used a variety of very sensitive techniques such as in situ electron spin resonance (ESR), infrared spectroscopy and mass spectroscopy to determine the composition of all the minor products and intermediates formed during anode limited overdischarge. No new compounds such as Cl_2O were detected. The investigations were generally semi-quantitative and quantitative analytical data has yet to be obtained to accurately describe the stoichiome-

try of the reactions occurring during anode limited overdischarge at even one set of standard conditions at room temperature. Ultimately, to be assured that no hidden safety hazards exist, it will be necessary to know the reaction stoichiometry during anode limited overdischarge over a broad range of conditions of temperature, rate, and overdischarge time for both flooded and electrolyte limited cells.

Attia and co-workers (2) using an "in situ" IR flow cell detected SOCl^+ , SO_2Cl_2 and species giving rise to absorptions at 1070 cm^{-1} and 665 cm^{-1} that were interpreted as indirect evidence for Cl_2 or SCl_2 formation. They obtained direct evidence for SCl_2 formation on anode limited overdischarge by mass spectroscopy. Carter et al (49) used gas chromatography (GC), atomic adsorption, IR and ESR spectroscopy to analyze the electrolyte during and after anode limited overdischarge. They found by ESR that ClO_2 is not present in sufficient concentrations to be observed. Their analytical results agreed well with those reported earlier by Abraham and Mank (34) and they proposed a similar overall cell reaction for the oxidation of $\text{LiAlCl}_4/\text{SOCl}_2$.



They proposed that there is no safety hazard due to intermediates or products formed by the oxidation of $\text{LiAlCl}_4/\text{SOCl}_2$ during anode limited overdischarge. They limited their conclusions however to flooded cells at room temperature.

It is now thought (51) that the explosions of spiral wound anode limited Li/SOCl_2 cells that were observed by Abraham and Mank (34) during overdischarge were caused by intermittent electrical contact between the anode screen and dislodged lithium rather than unstable oxidation products. Schlijker has noted (19) that the proper design and construction of anode limited Li/SOCl_2 cells is essential to their successful use and that the lithium must be applied to the screen such that it does not become detached during discharge.

At GTE Laboratories, voltammetric analyses of the electrolyte from overdischarged anode limited cells were carried out during the present contract. A

quantitative infrared study was not undertaken because we were aware of the infrared studies underway at other laboratories (2,49) and our low temperature extraction technique was not yet sufficiently developed to avoid the carbon adsorption problem. It was also thought that voltammetry data would complement the IR, ESR and GC results and could perhaps detect and describe certain properties of species not observed by other techniques.

Since SO_2Cl_2 was expected as an oxidation product of $\text{LiAlCl}_4/\text{SOCl}_2$ electrolyte, it was first necessary to determine whether SO_2Cl_2 could be determined quantitatively by voltammetry in DMF supporting electrolyte. Thus a number of DMF solutions containing known amounts of SO_2Cl_2 were analyzed by voltammetry and a calibration curve generated. Next, samples containing mixtures of SO_2Cl_2 - SOCl_2 or SO_2Cl_2 were analyzed by voltammetry to determine whether such mixtures could be analyzed quantitatively. Finally a close packed anode limited Li/SOCl_2 cell with a carbon cathode capacity of 0.6 Ahr was overdischarged for an extended time period and the electrolyte analyzed by voltammetry in DMF supporting electrolyte. The voltammetry results are discussed in the following section.

1.4.2.2 Voltammetry Results

- Preliminary Calibration and Standardization. - Figure 35 gives the voltammograms for 4.4 mM of distilled SO_2Cl_2 $\text{TBAPF}_6/\text{DMF}$ supporting electrolyte at sweep rates from 200 to 1,000 mV/second. At the highest sweep rate of 1,000 mV/second the SO_2Cl_2 peak at -0.74V shows a pronounced broadening into at least two peaks. The new peaks seen at 1,000 mV/second are clearly due to SO_2Cl_2 reduction intermediates which have a long enough lifetime (approximately 0.17 seconds) that they can be observed at the higher sweep rate.

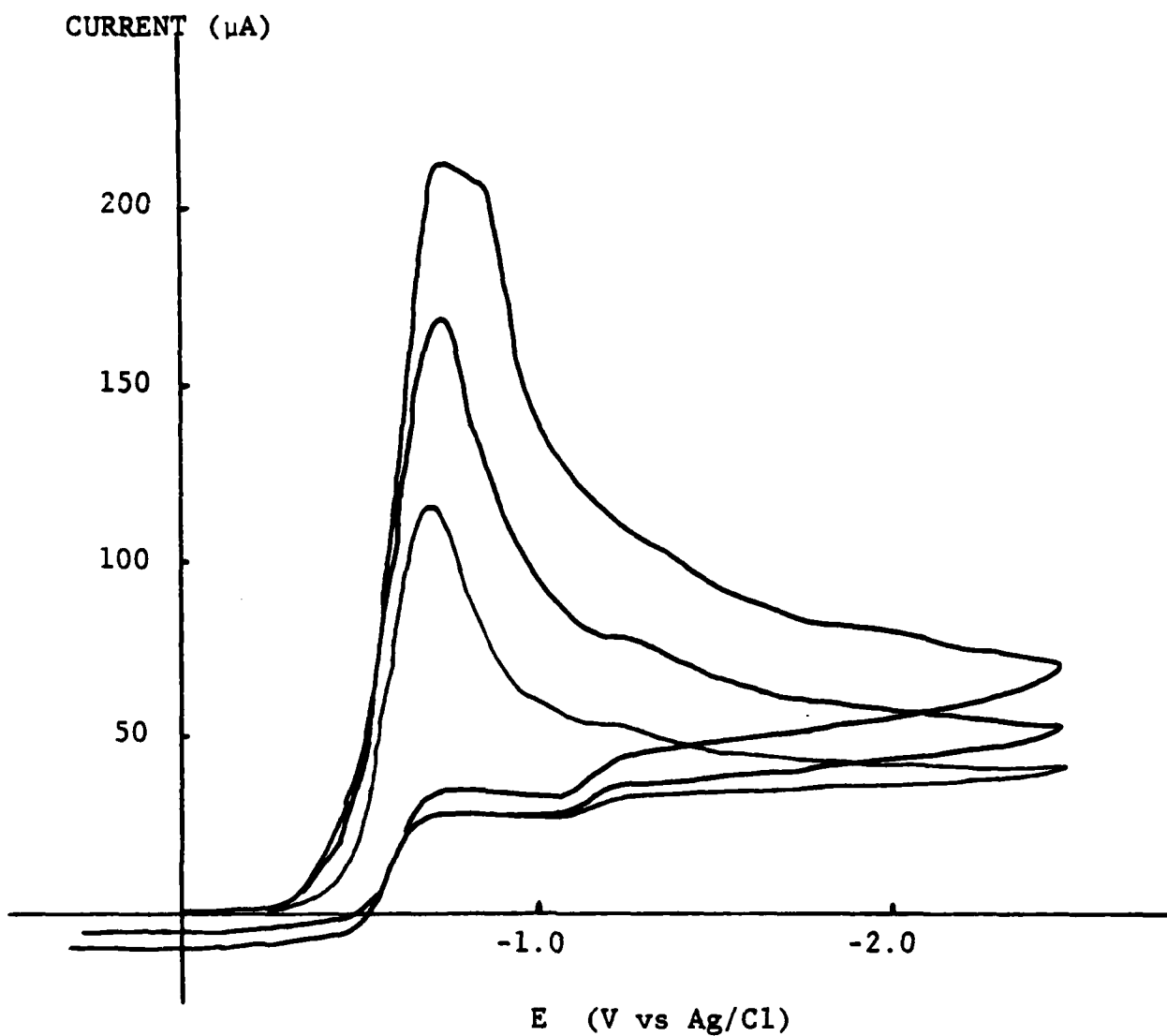
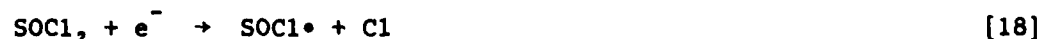


Figure 35: Voltammograms for 3.5 μl of Distilled SO_2Cl_2 in 10 ml of 0.1M $\text{TBAPF}_6/\text{DMF}$ at 23°C at a Platinum Electrode, Scan Rates 200, 500 and 1000 mV/second. The DMF Solution was 4.4 mM in SO_2Cl_2 .

The overall reaction for the electro-reduction of SO_2Cl_2 was reported by Klinedinst (52) to be:



The mechanism for the cathodic reduction of SO_2Cl_2 was investigated by Blomgren and co-workers (53) by voltammetry of 1M $\text{LiAlCl}_4/\text{SOCl}_2$ without an electrochemically inert supporting electrolyte. The principle steps of their projected mechanism for the reduction of SO_2Cl_2 were:



Thus the cause of the second peak at approximately -0.86V in the voltammogram at 1,000 mV/second in Figure 35 may be due to reactions [16], [17], or [18]. Further work to assign reactions to the various peaks in the -0.74 to -0.86V region was not undertaken because a determination of the details of the reduction mechanism of SO_2Cl_2 were outside the scope of the project.

Figure 36 gives a calibration curve of the SO_2Cl_2 peak currents at 200 mV/second versus the SO_2Cl_2 concentration. The SO_2Cl_2 calibration curve shows that SO_2Cl_2 can be determined quantitatively by voltammetry in DMF supporting electrolyte.

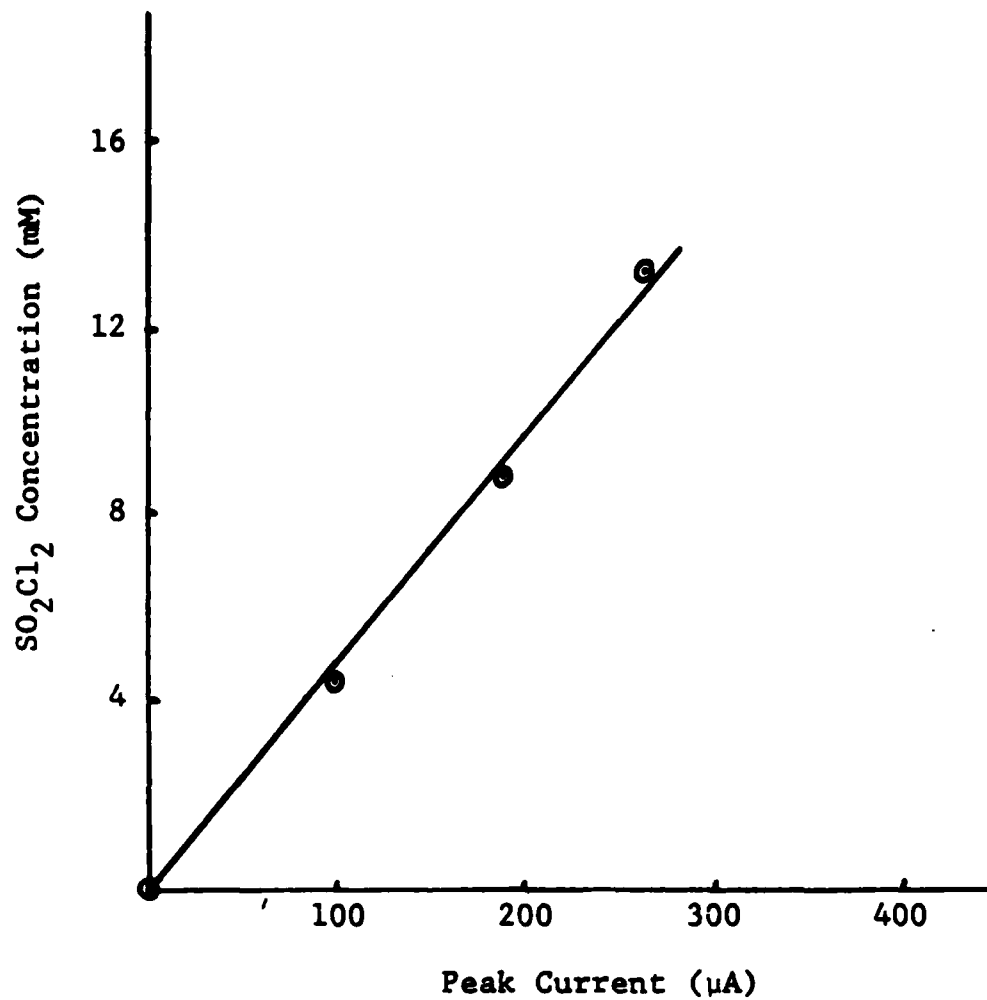


Figure 36: Calibration Curve Relating Peak Current By Voltammetry to the SO_2Cl_2 Concentration in 0.1M $\text{TBAPF}_6/\text{DMF}$ Supporting Electrolyte at 23°C

The stability of SO_2Cl_2 in DMF supporting electrolyte was of interest because storage tests of electrolyte from overdischarge anode limited cells were planned to determine the existence and lifetimes of any unstable species produced during overdischarge. Figure 37 shows the voltammograms obtained immediately after the SO_2Cl_2 was added to the DMF electrolyte and after 16.5 and 24.5 hours storage at 23°C. The SO_2Cl_2 peak at -0.725V shifted to -0.525V during the first 16.5 hours of storage and the shift is most likely due to a shift in the reference electrode caused by a reaction of AgCl with SO_2Cl_2 . The peak current for the SO_2Cl_2 peak didn't change during the first 16.4 hours of storage within the limits of experimental error. Thus SO_2Cl_2 is sufficiently stable in DMF supporting electrolyte to permit long lived unstable compounds to be determined. After 16.5 hours of storage a new small peak appears at -1.05V vs Ag/AgCl which increased in size after 24.5 hours storage. This peak is 525 mV more cathodic than the SO_2Cl_2 peak and correcting for the shift of the SO_2Cl_2 peak during storage the new peak would appear at -1.350V on a corrected scale. The new peak is clearly not due to SO_2 or SOCl_2 but may be due to a reaction of SO_2 produced by reaction [17] with the $\text{SO}_2\text{Cl}_2/\text{TBAPF}_6/\text{DMF}$ solution



similar to the reactions discussed in Sections 1.2.2 and 1.3.3.2.

The voltammogram obtained for 7.44 mg of 0.9M $\text{LiAlCl}_4/50\text{V}\% \text{SO}_2\text{Cl}_2 - 50\% \text{SOCl}_2$ in 10 ml DMF electrolyte is given in Figure 38. It shows that SO_2Cl_2 and SOCl_2 give a single peak and that the two compounds can not be distinguished by our conventional voltammetric procedures. Since it is doubtful that an accurate voltammetric procedure could be developed to analyze for SO_2Cl_2 in the presence of SOCl_2 without a great deal of effort, it is clear that some other technique such as quantitative IR spectroscopy will be required to analyze for SO_2Cl_2 in SOCl_2 electrolyte.

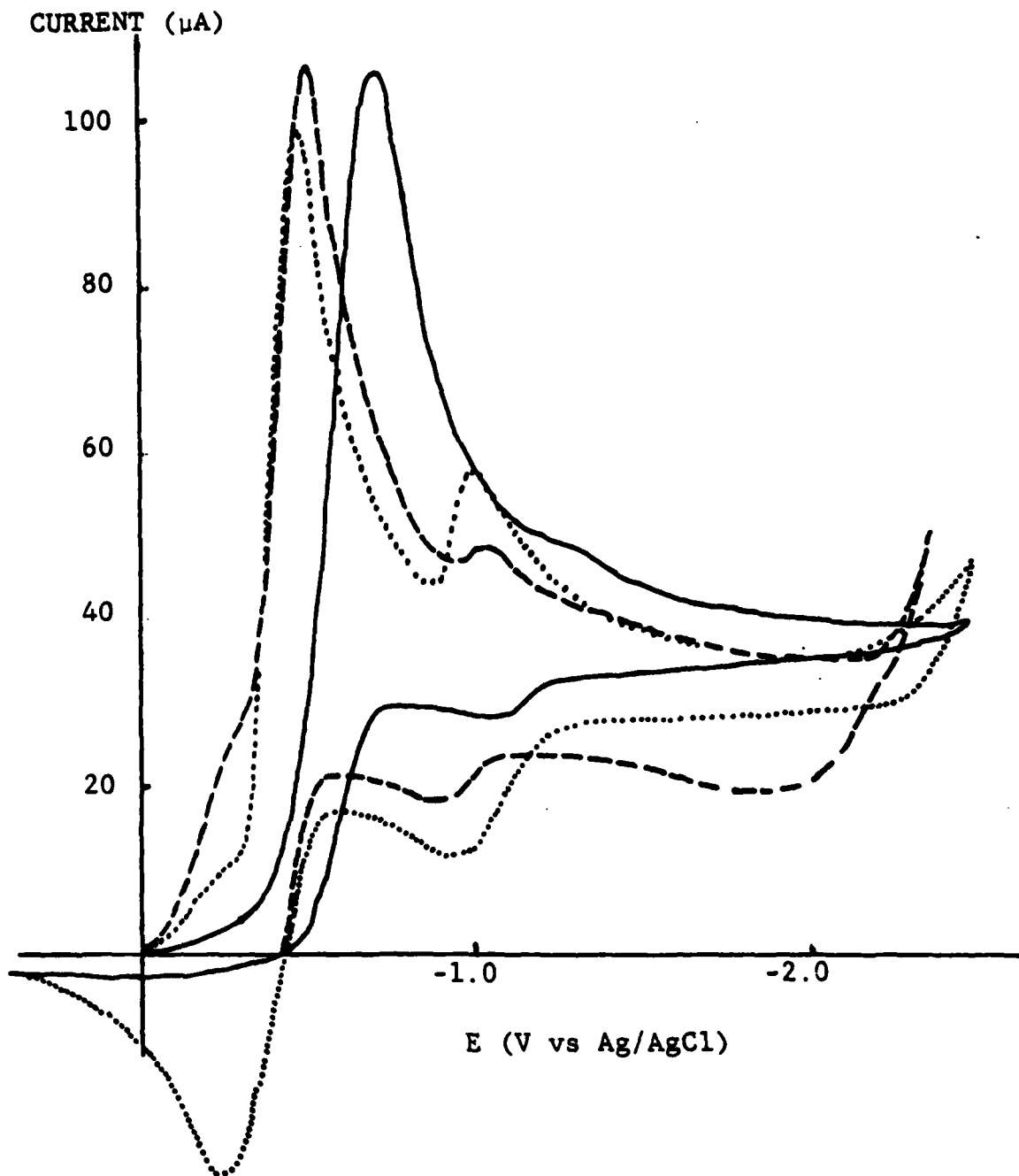


Figure 37: Voltammograms for 4.4 mM Distilled SO_2Cl_2 in 0.1M $\text{TBAPF}_6/\text{DMF}$ at 23°C at a Pt Electrode, Scan Rate 200 mV/second

(—), Immediately
 (- - -), After 16.5 Hours Stand
 (.....), After 24.5 Hours Stand

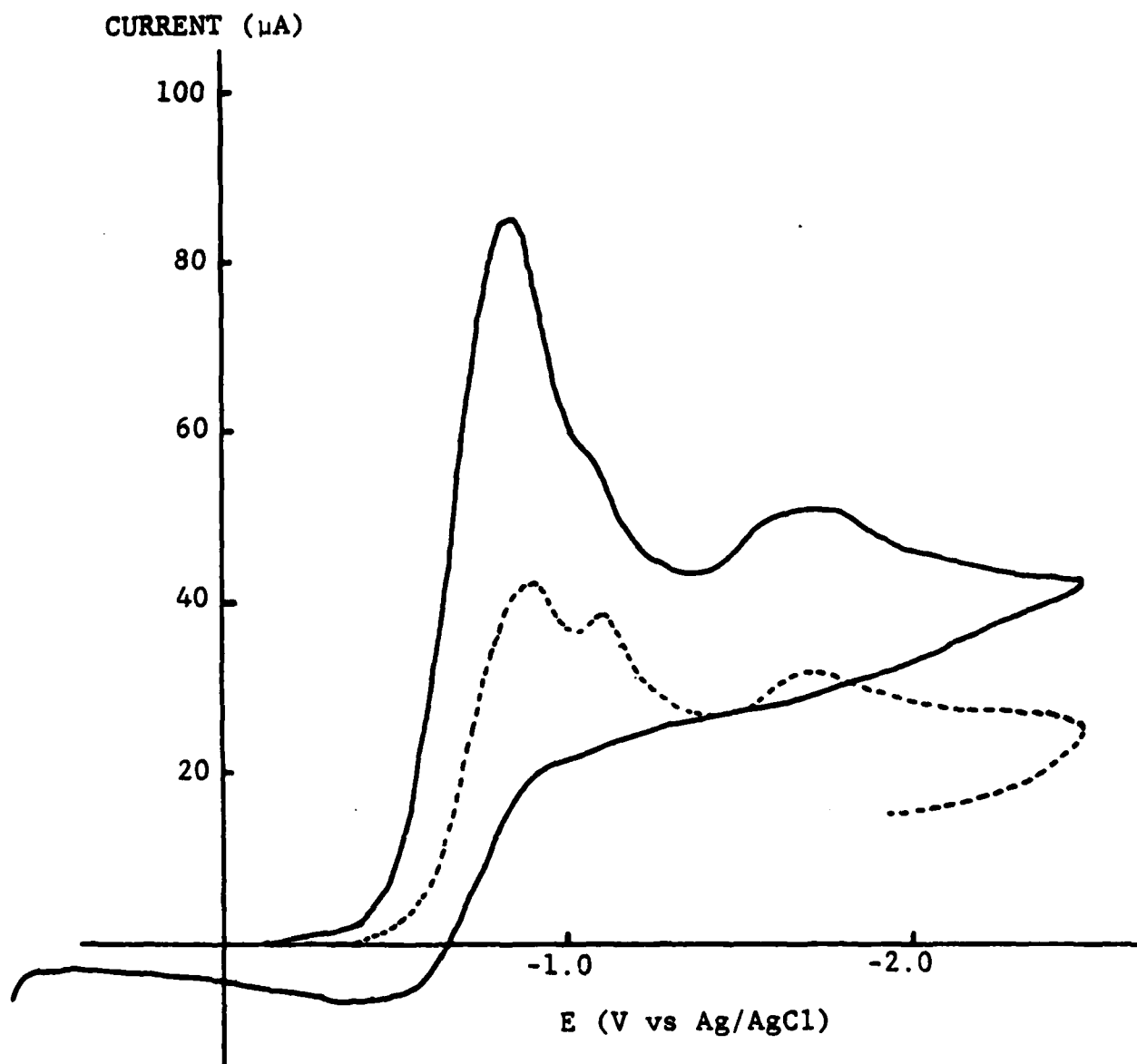


Figure 38: Voltammograms for 7.44 mg 0.9M LiAlCl_4 /50% SOCl_2 - 50% SO_2Cl_2 and = 3.7 mg 1.8 LiAlCl_4 / SOCl_2 in DMF. Scan Rate 200 mV/second

(——) 7.44 mg 1.8M LiAlCl_4 /50 Volume % SOCl_2 -50V% SO_2Cl_2
 (- - - -) 3.7 mg 1.8M LiAlCl_4 / SOCl_2

The voltammograms obtained for 13.2 mM SO_2Cl_2 in DMF electrolyte with 80 mM added SO_2 are given in Figure 39. The peaks at -0.643V and -1.01V due to SO_2Cl_2 are clearly distinguished. The peak at -1.34V is possibly due to the reaction of SO_2 with the $\text{SO}_2\text{Cl}_2/\text{TBAPF}_6/\text{DMF}$ electrolyte shown in reaction [19] discussed earlier.

- Analysis of Electrolyte From Overdischarged Anode Limited Li/SOCl₂ Cells - A prototype Li/SOCl₂ cell with a nominal carbon cathode capacity of 0.64 Ahr was constructed using two 2.0 x 3.0 cm carbon cathodes, 1 mm thick and three Li anodes with 2.0 x 3.0 cm 5 Ni10-2/0 Exmet grids. The Li anodes contained 0.0737 g (equivalent to 0.284 Ahr) of 0.010 in thick Li foil pressed on the Ni grid in the shape of an "X" pattern. The electrodes were separated with three layers of 0.17 mm thick Crane glass fiber separator and the cell was filled with 7.58ml 1.8M LiAlCl₄/SOCl₂ electrolyte. The cell package was contained in a 1.0 inch I.D. thick walled Pyrex glass tube with two Teflon half cylinder spacers to restrict the amount of electrolyte required to immerse the electrodes. Details of the cell design have been discussed earlier in Section 1.2.3 of Reference 1.

The prototype Li/SOCl₂ cell was discharged then overdischarged at 5 mA/cm², 23°C. A plot of the cell potential during discharge and overdischarge for the anode limited cell is given in Figure 40. The cell discharged for 2.7 hours to deliver 0.324 Ahr to 0.00V after which it was overdischarged 140.8 hours (i.e., 16.9 Ahr). Thus, the cell was overdischarged 5216% of the 0.324 Ahr Li electrode capacity or 2640% of the 0.64 Ahr cathode capacity.

An 8.36 mg sample of the electrolyte from the above overdischarged cell was transferred to 10 ml of DMF electrolyte and the voltammograms that were obtained are shown in Figure 41. Scans were obtained immediately after the end of overdischarge and after the sample had been allowed to stand for 16 hours in the voltammetry cell. The voltammograms obtained immediately after the end of overdischarge show peaks at -0.86V, -1.08V and -1.81V which are due to SOCl₂, SO₂ and the second reduction peak of sulfur. The peak positions and

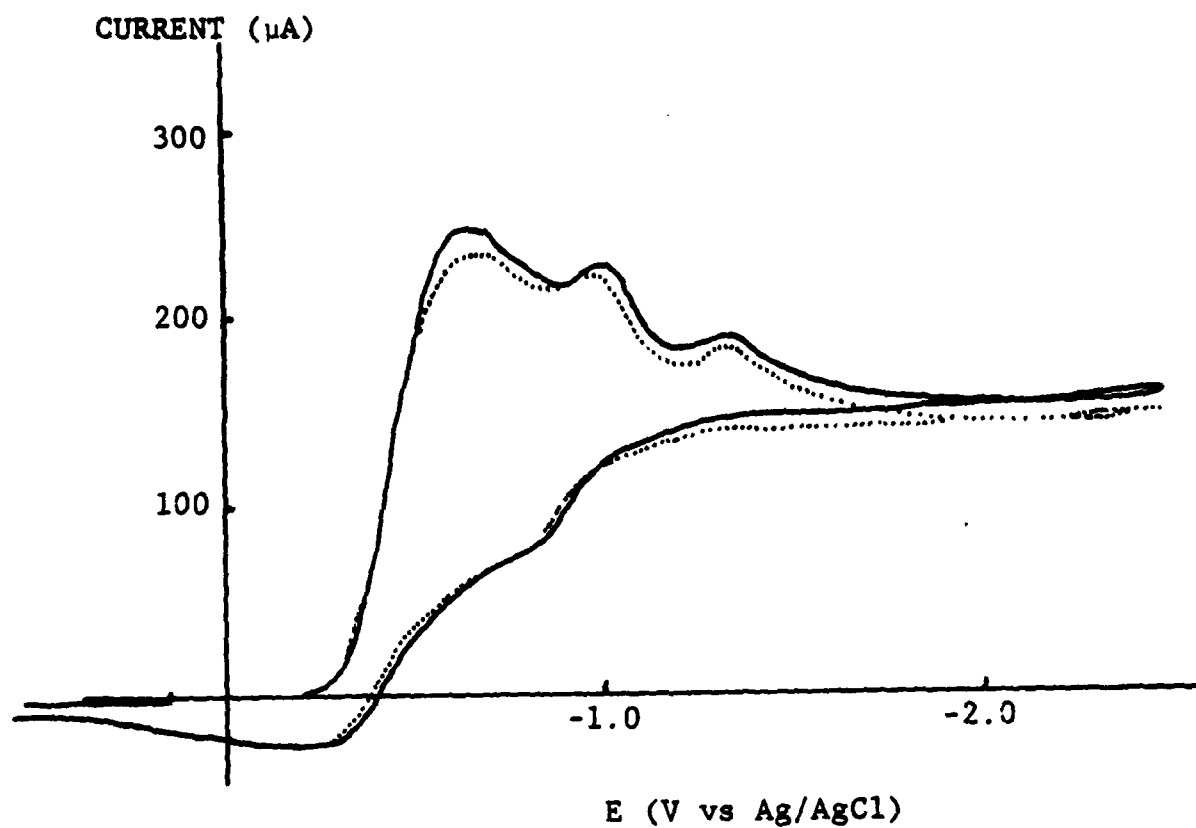


Figure 39: Voltammograms for 13.2 mM Distilled SO_2Cl_2 , with Approximately 80 mM Added SO_2 in 0.1M $\text{TBAPF}_6/\text{DMF}$ at 23°C
Scan Rate 200 mV/second.

(—), Immediately
(. . . .), 4 Hours Stand

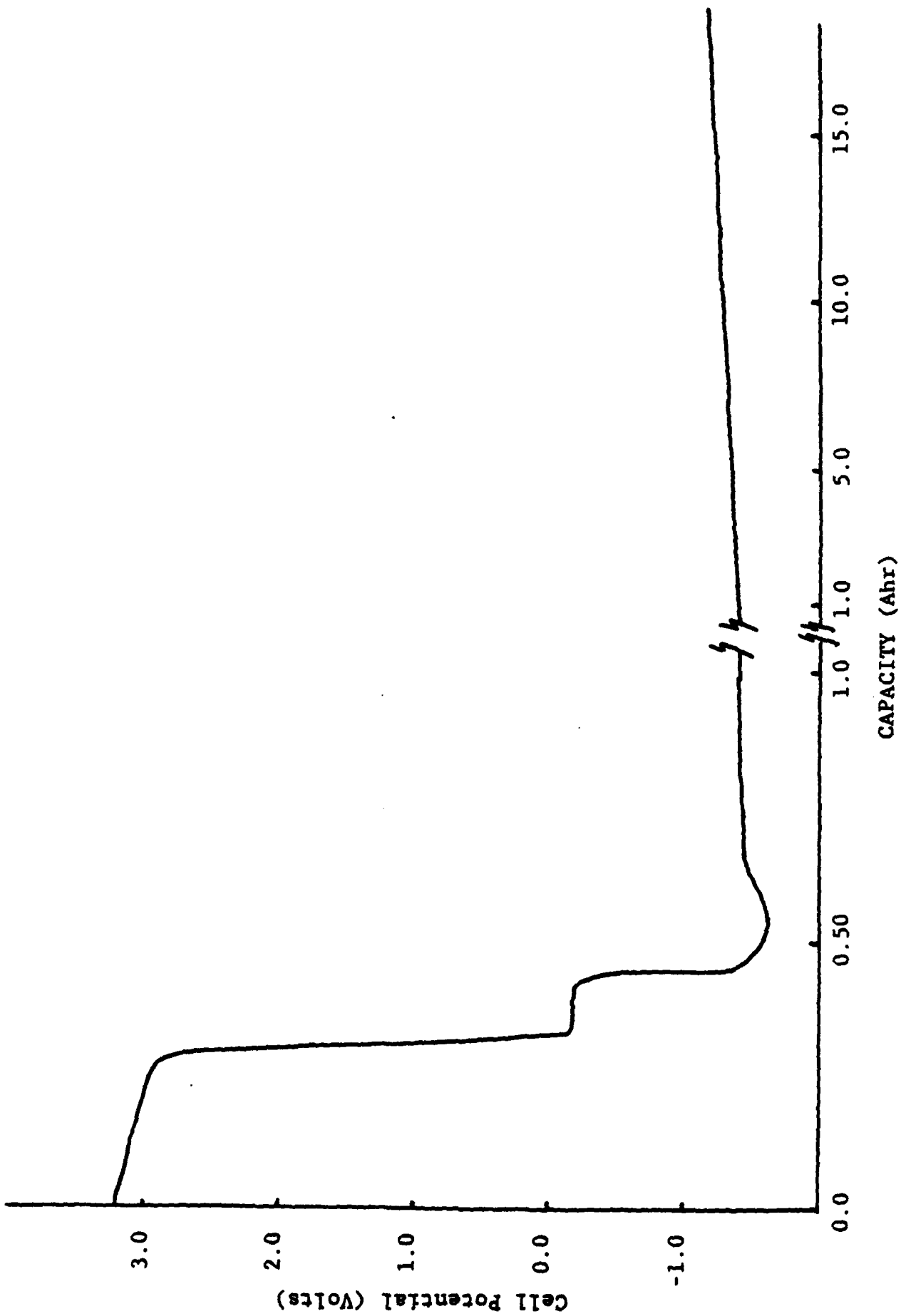


Figure 40: Behavior of a Lithium Limited Cell During Discharge and Overdischarge at 5 mA/cm², 23°C (Cell No. 63)

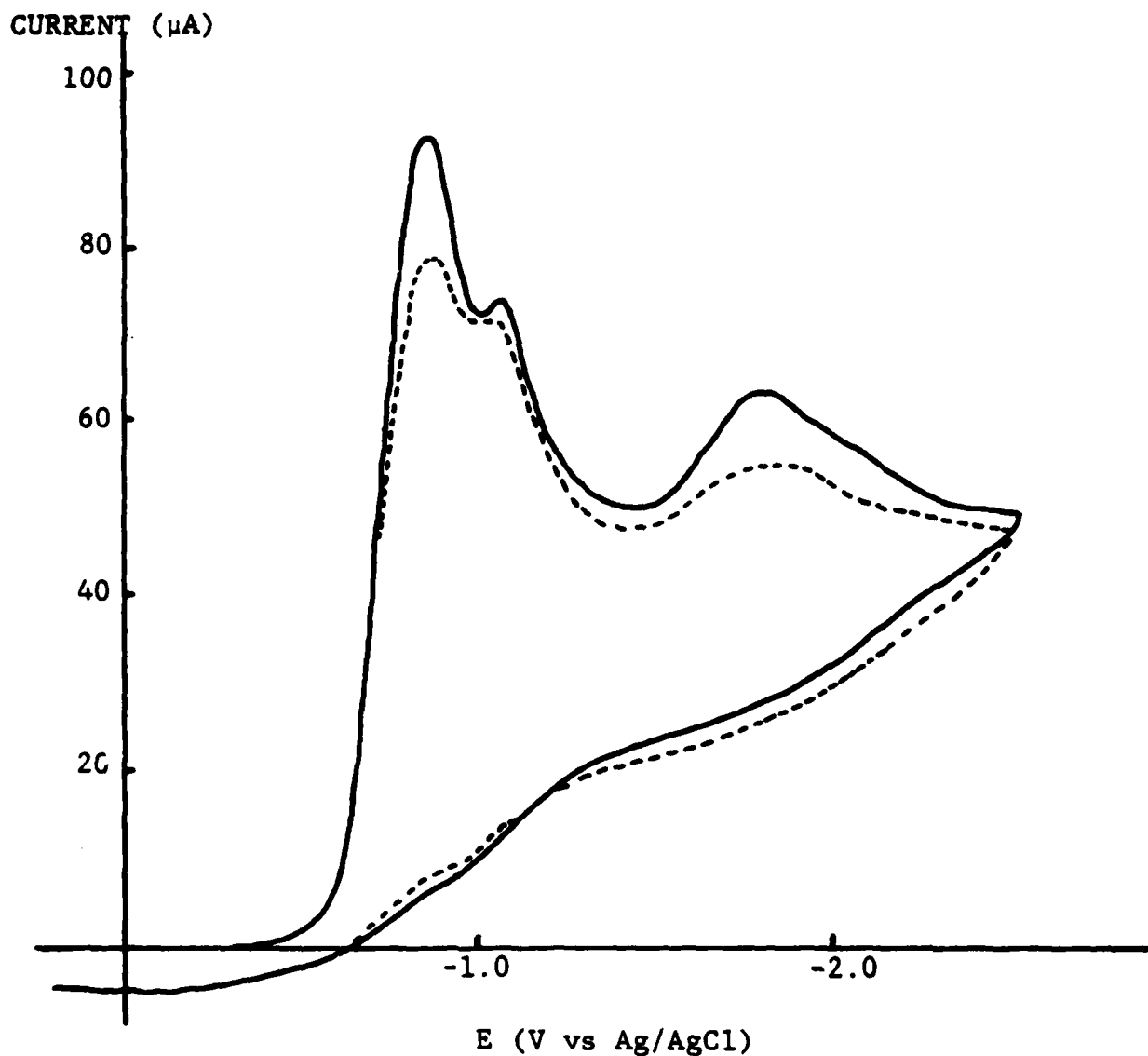


Figure 41: Voltammograms of 8.36 mg of SOCl_2 Electrolyte from a Lithium Limited Cell Overdischarged 5200% at 23°C , 5 mA/cm^2

The 8.36 mg of electrolyte sample from Cell 63 was dissolved in 10 ml of $0.1\text{M TBAPF}_6/\text{DMF}$. The scan rate was 200 mV/second .

(———), Immediately after sample added to DMF in cell.

(- - - -), After 16 hours storage at 23°C .

heights are very similar to those in the voltammograms obtained for the same concentration of 1.8M LiAlCl₄/SOCl₂ (see Figure 2, Ref. 1) except that the SO₂ peak is somewhat smaller than for SOCl₂ electrolyte. The SOCl₂ and SO₂ peaks appear at -0.75V and -0.95V vs Ag/AgCl respectively for 1.8M LiAlCl₄/SOCl₂ but often shift slightly due to the condition of the surface of the Pt working electrode. The separation of the SOCl₂ and SO₂ peaks is very characteristic and is 214 mV in Figure 41 compared to the usual 200 mV average separation. No new peaks in the region of + 0.45V due to the reduction of Cl₂ or at -1.15V or -1.75V vs Ag/AgCl due to the reduction of sulfur monochloride, S₂Cl₂ were observed. The assignments for the reduction potentials of S₂Cl₂ are those of Bowden and Dey (7) at 500 mV/second in TBAPF₆/acetonitrile supporting electrolyte. It is possible that Cl₂ was not observed because it is either reduced at the carbon cathode or reacts with SO₂ to form SO₂Cl₂.

It was concluded that oxidation products of LiAlCl₄/SOCl₂ that were observed by other laboratories using infrared and mass spectroscopy (2,49) were not observed by voltammetry due to the poor resolution of the technique and its lack of sensitivity for SO₂ and other compounds in the presence of excess SOCl₂. The concentrations of the various oxidation products and the products of reactions [10] and [11] most likely change during the course of anode limited discharge and it would be valuable if the concentrations could be followed during the overdischarge. Such information would be very useful to determine for example whether Cl₂ is primarily reduced at the carbon electrode or reacts with SO₂ to form SO₂Cl₂. Knowing the extent of each reaction, one would then have an improved data base on which to evaluate the safety hazards of anode limited overdischarge.

To analyze the electrolyte from overdischarged anode limited cells, it is clear that the multiple extraction technique followed by FT-IR analysis of the electrolyte would provide data of the desired accuracy and resolution. It is possible that part of the reason that the electrolyte oxidation products were not detected by voltammetry was because our prototype cell had a high carbon-to-electrolyte volume ratio and the products were adsorbed on the carbon. The multiple extraction technique described in Section 1.6 would also eliminate such adsorption problems.

1.5 INVESTIGATION OF REACTIONS OCCURRING DURING CHARGING OF LITHIUM THIONYL-CHLORIDE CELLS

1.5.1 Background

Charging of Li/SOCl₂ cells of a variety of designs has been widely investigated by a number of organizations. Discharged and fresh lithium limited D size bobbin type cells were charged at GTE Products Corp. (32,44) at currents up to 100 mA for two to eight hours and no rupture, leakage, bulging or explosion was experienced with any of the cells. Charging tests at 40A for 100 hours with three 10 Kahr cells by GTE (45) showed only a small pressure increase to = 18 psig and a temperature increase to 66°C. Similar results with no instances of thermal runaway or venting were found by Honeywell during charging tests with 16.5 Kahr cells (46). However, Zupancic and co-workers (47) at Union Carbide found that 1.25 Ahr Li/SOCl₂ cells slightly smaller than a 'AA' size cell underwent a high pressure gas release through a vent assembly on the cell when charged at greater than 100 mA for a discharged cell and 1.0A for an undischarged cell. The vent operated in the 2.7MPa (400 psi) range.

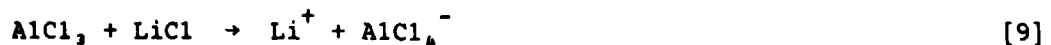
When Li/SOCl₂ cells are charged, lithium is electrodeposited at the lithium negative electrode. Present analytical results (34) indicate that the predominant reaction at the carbon electrode is



The Cl₂ can then react with the Li electrode



and the AlCl₃ can react with the LiCl film on the Li electrode.



For each equivalent of charge passed during "charging" one equivalent of Li is deposited and one equivalent each of Cl₂ and AlCl₃ is generated. The metallic Li then reacts with the Cl₂ and AlCl₃ to regenerate the LiAlCl₄ that was electrolyzed during charging. This sequence of reactions has been postulated (34) to account for the observation that Li/SOCl₂ cells could be charged for very long periods in which the total coulombs passed considerably exceeded the amount of SOCl₂ or Li originally present in the cell. Such cells could then be discharged to yield capacities equivalent to those obtainable from fresh cells.

Abraham and Mank (34) identified SO₂Cl₂, SO₂ and SCl₂ in the electrolyte of Li/SOCl₂ cells that were "charged". Cells that were discharged prior to charging would contain SO₂ and S which could react with the chlorine and aluminum chloride produced at the carbon electrode during charging



Sulfur dichloride (SCl₂) is normally somewhat unstable (48) thus it is peculiar that it has been observed in both "charged" and overdischarged anode limited cells (49).

It was noted earlier that small Li/SOCl₂ cells that have been discharged vent when charged at currents ten times smaller than those required to cause fresh cells to vent (47). It is not known whether discharged cells vent simply due to the effect of moderate heating and the pressure of SO₂ produced as a discharge product or due to exothermic chemical reactions involving either SO₂Cl₂, S₂Cl₂ or Li. It is also possible that in discharged cells Cl₂ and AlCl₃ would be more likely to be consumed by reactions such as [10], [11] and [9] (LiCl in the carbon pores) in the vicinity of the carbon electrode, therefore allowing greater growth or buildup of Li dendrites at the lithium electrode. The morphology of the Li deposits could be effected by the composition of the electrolyte.

In view of the exothermic nature of the reaction of Li with Cl_2 , SO_2Cl_2 and other oxidation products and the potentially hazardous effects of Li dendrite shorts, an investigation was undertaken of the growth and reactions of Li dendrites during charging. Previously very little attention had been given to exothermic reactions that could occur at Li dendrites during charging and clearly this was a subject that merited investigation. Of particular interest was the rate of corrosion of the Li dendrites produced during charging by AlCl_3 and Cl_2 and shape changes and energetic chemical reactions that occur when the Li dendrites reach the carbon electrode surface causing a short circuit.

Charging of primary Li/ SOCl_2 cells involves less hazard than overdischarge of carbon limited cells. Charging does not cause thermal runaway and it can be prevented by the inclusion of a diode in the circuit. However, charging is a matter of some concern in the design of reserve batteries where charging can occur via the common electrolyte fill path between a series stack of cells. In large, high rate reserve batteries, charging is thought in some cases to produce dendrite shorts resulting in thermal runaway.

There is some similarity between the products produced during oxidation of $\text{LiAlCl}_4/\text{SOCl}_2$ in overdischarged anode limited cells and those produced during "charging". However, in anode limited overdischarge, the oxidation occurs at the bare grid of the Li anode which is usually nickel whereas during charging the oxidation occurs at a high surface area carbon electrode. In charging the Cl_2 can attack the Li electrode whereas during anode limited overdischarge no metallic Li is present and the chlorine could either be reduced at the carbon electrode, undergo reactions [10] and [11] or other reactions currently under investigation (2,49). Thus the chemical stability of high surface area Li dendrites in an electrolyte containing SOCl_2 oxidation products is a potentially hazardous situation unique to charging. This was an additional factor in selecting the investigation of the deposition and stability of Li dendrites during charging as the focus of our study of cell reactions during charging.

1.5.2 Microphotography

1.5.2.1 Experimental

Lithium dendrite deposition during cell charging at 25°C was investigated by in-situ microphotography using the same 5.5 cm diameter cylindrical glass cell with a flat 4.0 cm diameter optical glass window shown in Figure 23 and described in Section 1.4.1.2 in connection with the cell reversal studies.

The electrodes measured 3.0 x 3.5 cm. For two cells (Cells 1 and 3) 2.8 mm thick Shawinigan carbon black cathodes with 10% Teflon were used and for three cells nickel sheet cathodes 1 mm thick were used to investigate whether low resistance short circuits could be formed. The two Li electrodes on either side were parallel to the cathode for Cells 1 and 3 and for the first part of the experiment for Cell 4. However, to stimulate the formation of Li dendrite short circuits during charging, the two Li electrodes were bent into an "L" shape towards the cathode with the narrow inter-electrode gap on the side next to the window and microscope. The inter electrode gap was reduced primarily to reduce the tendency of the upward convection currents and Li dendrite buoyancy to break off the Li dendrites before they were long enough to form shorts. The gap was not decreased to increase the current density because the Li dendrites have a very high surface area and probably grow with maximum current density at the dendrite tips (35).

1.5.2.2 Results

The discharge and charge conditions tested with the Li/SOCl₂ cells equipped for in-situ optical microscopy are listed in Table 5 with some of the short circuit results.

The first cell tested with a carbon electrode (i.e., Cell 1) was used to investigate the corrosion rate of the Li dendrites during storage after charging.

Table 5

Conditions and Results of Charging Tests with Li/SOCl₂ Cells
Equipped for In-Situ Optical Microscopy*

Cell No.	Cathode Material	Pre-Discharge Capacity (Ahr) [†]	Charge Current Density (mA/cm ²)	Charge Capacity (Ahr)	Dendrite Bridging	Short Circuits
1	C	1.34	4	0.67	Not Attempted	None
3	C	0.068	10	0.84	Touching	None
4	Ni	0	20	2.5	0.3mm Gap	None
5	Ni	0	20	3.6	Touching	None

* The cells were flooded with 1.8M LiAlCl₄/SOCl₂ electrolyte.

† Cell 3 was discharged at 1 mA/cm².

The cell was discharged at 1 mA/cm^2 , 23°C to a depth of 128 mAh/cm^2 (about 30% of the total cathode capacity) then charged at 4 mA/cm^2 for four hours. The cell was left on open circuit for three hours and Figure 42 shows one of the dendrites growing 3.5 mm out of the Li anode at 14 X magnification. The dendrite was photographed after 1.0, 2.0, and 3.0 hours on OCV and no shape changes greater than $\pm 0.05 \text{ mm}$ were observed. When charging was begun again after three hours on open circuit, the new Li growth occurred almost exclusively at the tip of the dendrite (see Figure 43) showing that it had not become electrically isolated due to corrosion. This observation has safety implications because the Li dendrites would, in principle, be capable of causing short circuits even after three hours storage if the cell was subjected to vibrations or shock. However, results for overdischarged carbon limited cells discussed in Section 1.4.1.2 indicate that Li dendrites are not capable of sustaining high enough currents to melt but rather corrode until they break the short circuit.

When Cell 1 was stored 22 hours and then charged ten minutes, the Li deposited at the surface of the Li electrode (see Figure 44) and not at the tip of the Li dendrite as occurred after three hours of storage (see Figure 43). After 22 hours of storage, the Li dendrites had turned grey and had become coated with a smooth layer of LiCl .

The low rate of corrosion of the Li dendrites by the oxidation products of SOCl_2 produced during charge may not be as low in practical cells as described above because the in-situ cells were flooded with 150 ml of electrolyte. This is approximately 50 times more electrolyte than would be used in a commercial cell with the same capacity and therefore the concentration of the SOCl_2 oxidation products were greatly reduced which probably lowered the Li corrosion rate.

Next, three cells were tested (i.e., Cells 3-5 in Table 5) to investigate the shape changes and reactions that occur during charging as the Li dendrite tips approach and touch either the carbon electrode surface or the Ni grids or leads of the carbon electrode. The electrical transients caused by any Li



Figure 42: Lithium Dendrites Attached to the Lithium Electrode of Cell 1 After 1.35 Ahr Discharge and 0.67 Ahr Charge Followed by Three Hours Storage, 14 X Magnification



Figure 43: Lithium Dendrites Shown in Figure 42 but with 10 Minutes Charging at 4.0 mA/cm². 14 X Magnification (Note new growth at tips)



Figure 44: Lithium Dendrites Shown in Figure 43 After 22 Hours Storage
Followed by 10 Minutes Charging at 4.0 mA/cm^2 . 14 X
Magnification. Note shiny new growth at base of lithium electrode
to the right.

dendrite short circuits and the electrical impedance changes in the cells were also monitored.

Ten microphotographs were taken at 7X magnification of Cell 3 during the charging period. Figure 45 shows that the Li dendrites clearly touched the carbon at a large number of points between the Li and carbon electrodes, but no shorting occurred since sudden drops in the cell potential were not observed at any time. The fine structure of the Li dendrites is obscured in Figure 45 because the exposure time was increased to make the dark edge of the carbon electrode more clearly visible. The dashed line with eight white segments running vertically down the center of the photograph are the exposed edges of the Exmet grid in the carbon electrode.

The A.C. impedance of Cell 3 at 1000 Hz was 2.42 ohms in the early stages of dendrite growth and was only 2.00 ohms with the Li dendrites in contact with the carbon cathode. Such a high "short circuit" resistance is not unexpected since carbon electrodes 1.0 mm thick are known to have a resistance of 36 ohm cm^{-1} (see Section 1.4.1.4) and the carbon electrode used in Cell 3 was 2.8 mm thick. Thus, the minimum resistance for Cell 3 if the entire area of both electrodes were shorted would be greater than 1.71 ohms. At one point during the charging of Cell 3 a Li dendrite touching the carbon electrode broke off and left a sizable Li dendrite attached to the carbon electrode. This observation suggests that the Li dendrite had probably grown some distance into the carbon electrode or at the very least was in good mechanical contact with the carbon.

Cells 4 and 5 contained nickel foil positive electrodes to simulate Li dendrite growth towards the Ni cathode frames and leads in commercial cells. Cell 5 was charged for 35 hours at 20 mA/cm^2 , over which period, 52 microphotographs at magnification from 7X to 21X were taken. Figures 46 and 47 show the electrodes of Cell 5 just prior to charging and after 5.0 mAhr/cm^2 of charging at 20 mA/cm^2 . Although the Li dendrites appeared to touch the Ni positive electrode after 54 mAhr/cm^2 of charging at 20 mA/cm^2 (see Figure 48), the cell potential did not drop during charging. Thus it was concluded that

cell shorting did not occur. Even when the current density was reduced to 5 mA/cm², to reduce the shear forces on the Li dendrites, caused by the convective upward movement of the electrolyte at the Ni electrode surface, Li dendrite shorts still did not occur.



Figure 45: Lithium Dendrites in Contact with the Carbon Electrode After 4 Hours of Charge at 10 mA/cm^2 , Magnification 7X for Cell No. 3 Listed in Table 5

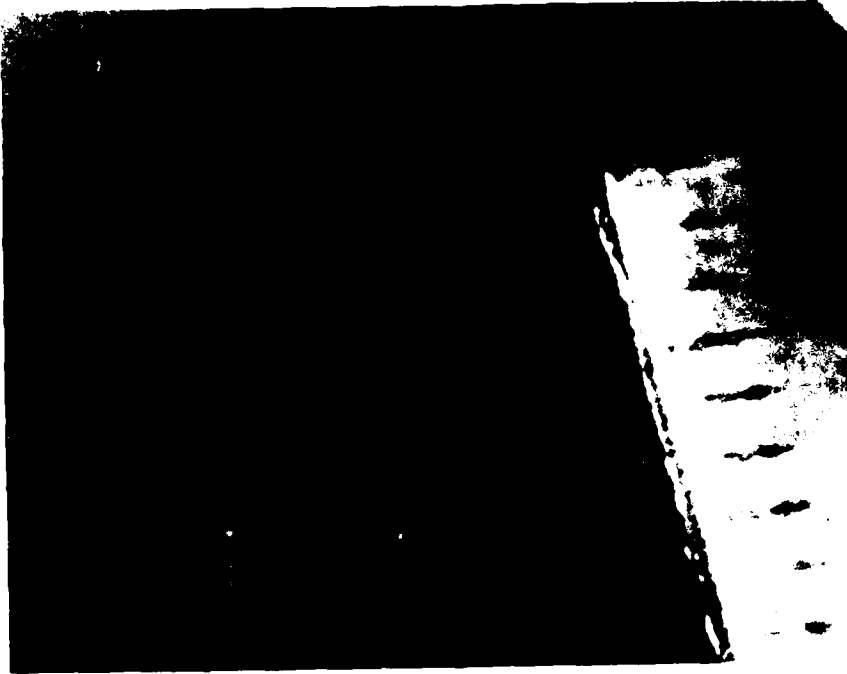


Figure 46: Microphotograph of the Electrodes of Cell 5 Prior to Charging. 7X Magnification



Figure 47: The Electrode of Cell 5 After 5.0 mAh/cm² of Charging at 20 mA/cm², 7X Magnification



Figure 48: The Electrode of Cell 5 After 54 mAh/cm² of charging at 20 mA/cm²,
7X Magnification.



Figure 49: The Electrode of Cell 5 after 54 mAh/cm² of Charging at 20 mA/cm²,
18 Hours Storage and 4 mAh/cm² of Charging at 5 mA/cm².

From the above results, it appears that Li dendrite shorts are difficult to form during the charging of Li/SOCl₂ cells, because as the Li dendrites growing out of the Li anode approach very close to the cathode, their tips are rapidly corroded by AlCl₃ and Cl₂ produced at the cathode during charging. The concentrations of AlCl₃ and Cl₂ increase the closer the Li dendrite tips approach the cathode. The corrosion of Li dendrites during charging contrasts sharply with the situation during the overdischarge of cathode limited cells, where Li dendrites growing from the carbon electrode, advance toward the Li electrode and a high concentration of Li ions. Thus, the cell chemistry during cathode limited overdischarge promotes the growth of Li dendrite shorts which may lead to hazardous heating problems.

During the cell charging studies with Cell 5 it was noticed that the Li dendrites growing toward the Ni electrode would begin to twist upward as they grew toward the Ni cathode and then break off just before they would have touched. It is thought that this upward distortion of the Li dendrites was due to two forces, the upward motion of the convection current near the Ni electrode and the buoyancy of Li in SOCl₂ electrolyte which has a density of 1.7 g/cm³ vs 0.534 g/cm³ for Li.

To determine whether a Li dendrite short could be formed if the upward convective forces were reduced, Cell 5 was charged at 5 instead of 20 mA/cm². After the 20mA/cm² charging experiments with Cell 5 the cell was allowed to stand overnight and the long dendrites detached by shaking the cell. A new growth of dendrites was then deposited by charging the cell at 5 mA/cm². Figure 49 shows a long narrow Li dendrite that grew toward the Ni electrode and touched the electrode without shorting just before the photograph was taken. However, it was bent upward by the convection and buoyancy forces as shown in Figure 49 before a high magnification photo of the dendrite could be taken.

No major difference in the Li growth morphology was observed when the current density was lowered from 20 to 5 mA/cm². The Li dendrites in Figure 49 are spear shape compared to those in Figure 48 only because not as much charge was passed.

The cells used for the microphotography studies of dendrite shorting did not contain separators and had large inter-electrode separations. Since the separators and much smaller inter-electrode separations found in commercial cells could prevent dendrites breaking due to buoyancy and connection forces, it was thought that short circuits might occur more frequently during charging in commercial cells. Further work in which prototype Li/SOCl₂ cells were charged and monitored for short circuits is discussed in the next section.

1.5.3 Prototype Cell Charging Tests

1.5.3.1 Experimental

The three prototype cells that were charged were of the same design as described in Section 1.4.1.3 but used a somewhat smaller cathode 2.0 x 3.0 cm, 2.8 mm thick containing 10% Teflon. The cells utilized two Li anodes on either side of the cathode separated by a single layer of 0.007 inch thick Crane glass fiber separator. The cells were gravity filled with standard 1.8M LiAlCl₄/SOCl₂ electrolyte. The charging was carried out at constant current and the potential was continuously monitored with a strip chart recorder.

1.5.3.2 Results

The charge capacities, current densities and some of the results for the three prototype cells that were charged are listed in Table 6. No negative transients in the cell potentials were observed at any time during charging and on that basis it was concluded that low resistance Li dendrite short circuits were not formed during any of the charging tests. High resistance shorts to the carbon electrode may have been formed as discussed earlier relative to the in-situ charging experiments.

Table 6

Condition and Results of Charging Tests with
0.77 Ahr Prototype Li/SOCl₂ Cells*

Cell No.	Current Density (mA/cm ²)	Charge Capacity (Ahr)	Short Circuits
6	1.0	1.416	None
7	5.0	6.75	None
8	20.	5.94	None

* The cells contained cathode with a nominal capacity of 0.77 Ahr but they were not discharged prior to charging. The electrolyte was 1.8M LiAlCl₄/SOCl₂.

The amount of current conducted through the cell by electronic pathways couldn't be determined by chemical analysis as in the case of carbon limited overdischarge because of the series of regenerative reactions that occur during charging.

1.6 INVESTIGATION OF THIONYL CHLORIDE REDUCTION IN PROTOTYPE CELLS BY MULTIPLE EXTRACTION AND INFRARED ANALYSIS

1.6.1 Background

Investigation of the stoichiometry of the discharge reaction of the Li/SOCl₂ cell is difficult because the products of SOCl₂ reduction (i.e., SO₂ and S) are adsorbed on the high surface area carbon electrode. Furthermore, SO₂ produced during the discharge undergoes a solvation reaction with the LiAlCl₄/SOCl₂ electrolyte thereby consuming approximately 10% of the SO₂ within 19 hours and complicating the IR analysis for SO₂. The absorption of SO₂ and its reaction with LiAlCl₄/SOCl₂ electrolyte were discussed earlier in some detail in Section 1.3. Difficulties caused by SO₂ absorption on the carbon electrode when voltammetry was used to analyze the electrolyte from discharged 0.6 Ahr Li/SOCl₂ cells were described previously in Section 1.2 of the interim report (1).

The adsorption of SO₂ and other discharge products on the carbon electrode leads to a very difficult electrolyte sampling problem in prototype cells with a low electrolyte-to-carbon volume ratio where as much as 75% of the SOCl₂ is reduced by the end of discharge. To overcome this sampling problem, a multiple SOCl₂ extraction technique was developed which involved extracting a discharged 0.6 Ahr, Li/SOCl₂ cell five times with 20 ml of distilled SOCl₂ using a specially designed glass apparatus with three Teflon stopcocks and two 120 ml glass reservoirs. One glass reservoir held the distilled SOCl₂ and the other reservoir the combined extracts which were cooled to -60°C during the extraction to prevent the SO₂-SOCl₂ electrolyte reaction. At the end of the fifth extraction, the combined extracts were warmed to 23°C and analyzed for SO₂ by quantitative IR spectroscopy.

Several other techniques such as a three compartment electrolysis cell and extraction of prototype cells with DMF were used to investigate the reduction of SOCl_2 in prototype cells but all were limited by serious chemical problems which prevented their successful application. The multiple SOCl_2 extraction technique was thoroughly tested and it is clearly the most direct, accurate, and reliable method developed to date to recover all the reaction products of prototype Li/SOCl_2 cells so that the cell reaction stoichiometry can be determined with high accuracy.

During the present investigation the electrolyte extract was only analyzed for SO_2 because accurate analyses (54,55) have already established the reaction stoichiometry for the other discharge products (i.e., LiCl and S). Our plan was to indirectly determine the concentration of any long lived SOCl_2 reduction intermediates by the size of any shortfalls between the actual SO_2 concentration determined by analysis and the 0.25 moles of $\text{SO}_2/\text{Faraday}$ of discharge expected theoretically on the basis of Eq. [1].

1.6.2 Experimental

The glass apparatus and Li/SOCl_2 prototype cell used to investigate the stoichiometry of thionyl chloride reduction by multiple extraction and infrared analysis is shown in Figure 50. The volume of the extract and distilled SOCl_2 reservoirs were each approximately 120 ml and the three glass stopcocks utilized Teflon shafts (Fisher & Porter). The Li/SOCl_2 prototype cells that were extracted contained an electrode package of two carbon cathodes 2.0 x 3.0 cm, 1.0 mm thick and three lithium electrodes 2.0 x 3.0 cm, 1.12 mm thick. The cathodes were separated from the anodes by three layers of Crane glass fiber paper 0.17 mm thick. The cell package was contained in a 1.0 inch I.D. thick walled Pyrex glass tube with two Teflon half cylinders to restrict the amount of electrolyte required to immerse the electrodes. A glass top with glass-to-metal feed throughs was attached to the tube containing the electrode package using a metal coupling with a Teflon flat gasket and the cell was vacuum filled with approximately 4.0 ml of 1.8M $\text{LiAlCl}_4/\text{SOCl}_2$ electrolyte. The pre-

cise amount of electrolyte added to fill each cell until the tops of the cathodes were just covered was determined by weighing the cells before and after filling. Details of the cell design have been discussed earlier in Section 1.2.2 of Reference 1.

Cell assembly as well as the following operations were all performed in either a dry room (R.H. < 4.0%) or in an argon filled glove box. The extraction apparatus was evacuated and the SOCl_2 reservoir (i.e., C in Figure 50) was filled with 100.0 ml of freshly distilled SOCl_2 . Prior to discharge, the outlet tube of the cell was hermetically sealed to the extraction apparatus using a Swagelok tube fitting (G in Figure 50) and securely clamped in a frame. Reservoir B was evacuated with stopcock E closed when the cell and the extraction apparatus were connected. The vacuum in Reservoir B was later used to assist in draining the cell and to keep air bubbles from interfering with the transfer of SOCl_2 through the tubes connecting the reservoirs and the cell. At the end of discharge Stopcocks E and F were opened and the entire assembly was then tipped so that the electrolyte remaining in the cell could flow into the extract reservoir (B in Figure 50). Often the residual electrolyte was entirely trapped in the electrode package and electrolyte could not be recovered during the first cell drain. Next, Stopcock E was closed, the apparatus was lifted so that the SOCl_2 reservoir was slightly raised above the level shown in Figure 50 and Stopcock D was briefly opened to permit approximately 20 ml of SOCl_2 to flow into the drained cell. Reservoir B was then immersed in a dry ice-acetone bath in a small Dewar flask to retard the SO_2 - SOCl_2 electrolyte reaction. At the end of the first five minute extraction, the dry ice-acetone bath was removed, Stopcock E was opened and the cell tipped so the electrolyte in the cell could be drained into the extract reservoir (B in Figure 50). After the extract had been drained, the cell was filled with a second 20 ml aliquot of pure SOCl_2 and the whole process repeated until a total of five extractions had been completed. The extraction times for the five extractions were 5, 10, 15, 30, and 30 minutes, respectively.

The combined extracts were then allowed to warm to near room temperature, the extraction apparatus was disconnected from the cell by loosening the tube fit-

ting G, and approximately 30 ml of the extract was poured to a 50 ml screw cap Erlenmeyer flask. A Lauer taper microliter syringe without a needle was then filled with the SOCl_2 extract and the demountable liquid infrared cell was filled by inserting the Lauer taper glass fitting directly into the lower fitting on the infrared cell. The infrared cell was equipped with CaF_2 windows and the quantitative infrared analysis for SO_2 using the 1333 cm^{-1} absorbance was carried out using a Nicolette Model 20DX Fourier transform infrared spectrometer (FT-IR).

The procedure used to prepare the standard $\text{SO}_2/\text{LiAlCl}_4/\text{SOCl}_2$ solutions and to calibrate the IR Cell before each run has been described in some detail earlier in Section 1.3.2. However, the $\text{SO}_2/\text{LiAlCl}_4/\text{SOCl}_2$ stock solutions used to prepare the more dilute SO_2 calibration standards contained only 0.069M $\text{LiAlCl}_4/\text{SOCl}_2$ to take into account the approximate 1:25 dilution of the $\approx 4 \text{ ml}$ of 1.8M $\text{LiAlCl}_4/\text{SOCl}_2$ electrolyte in the prototype cell by the 100 ml of SOCl_2 used to extract the cell.

An early series of SOCl_2 extractions of discharged cells were carried out using a modification of the above procedure in which the extractions were carried out while the entire apparatus was in a cold chamber at -20°C . The extract reservoir was not further cooled with a dry ice-acetone bath. The Teflon stopcocks tended to leak as the cell was cooled to -20°C because the thermal expansion coefficient for Teflon is larger than for glass. This difficulty was overcome by tightening the stopcocks several times during the initial cooling period and loosening them several times as the apparatus was warmed to room temperature.

It was found that cooling the entire apparatus to -20°C during the extraction yielded a recovery of 30% less SO_2 than if the extraction was carried out at 23°C . A series of control experiments indicated that the reduced recovery of SO_2 obtained by the -20°C extraction was due to the greater adsorption of SO_2 on the carbon electrode at -20°C as expected from theory. The data on which these conclusions are based will be presented in the next section.

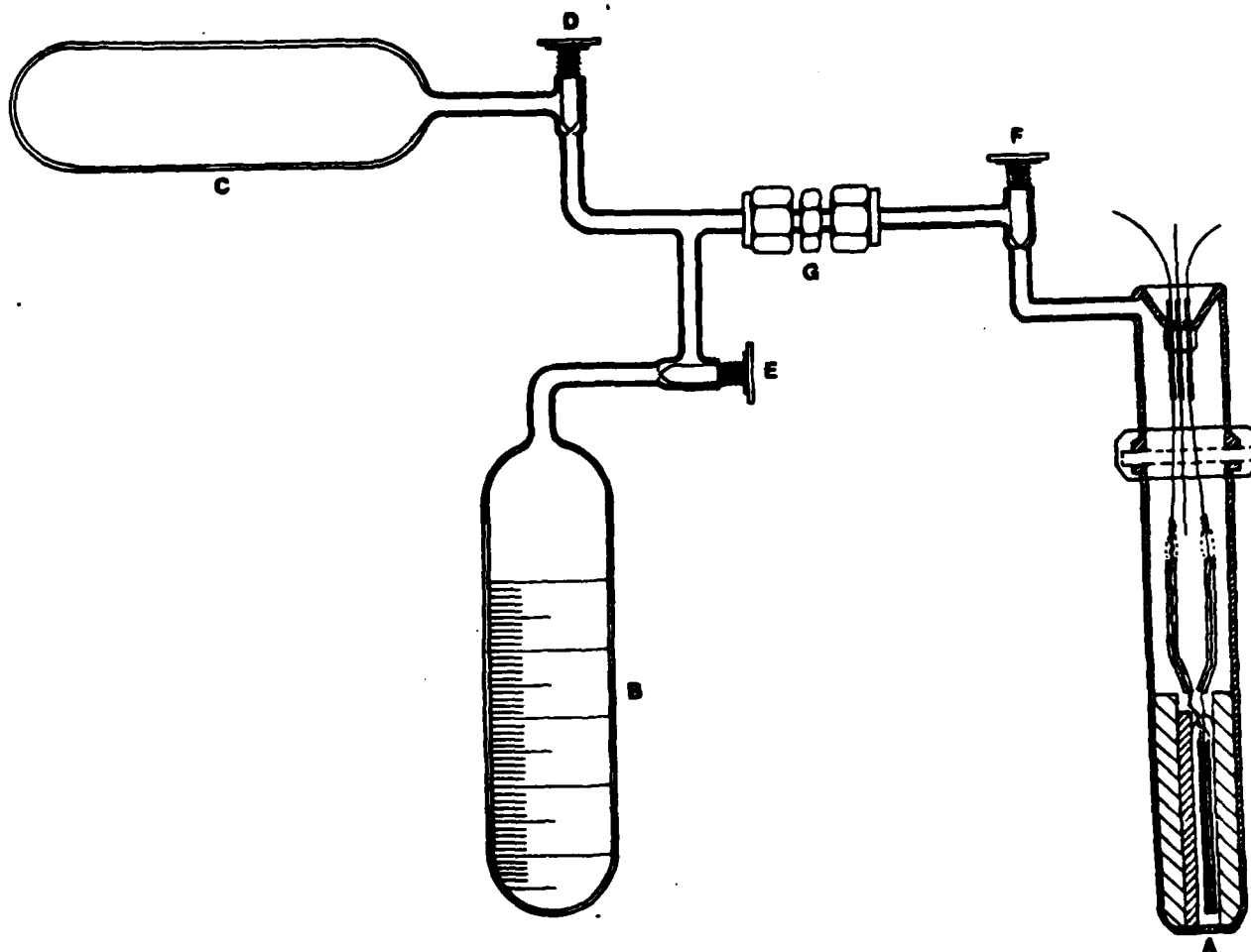


Figure 50: Apparatus for Multiple Extraction of Discharged Li/SOCl₂ Cells for Soluble Discharge Products A, 0.6 Ahr Li/SOCl₂ Cell; B, Extract Reservoir; C, Reservoir for Distilled SOCl₂; D, E, F, Glass Stopcocks with Teflon Shafts; G, Swagelok Tube Fitting

1.6.3 Results and Discussions

The results of the quantitative IR analyses for the amounts of SO_2 contained in the electrolyte extracted from the prototype Li/SOCl_2 cells discharged at 23°C are compared in Table 7 with the amount of SO_2 expected based on Eq. 1 and the amount of charge passed. The discharge conditions, initial electrolyte volumes and SOCl_2 utilization to cutoff for the above cells are listed in Table 8. Table 7 shows that an average of 86.4% of the theoretically expected SO_2 was found with a standard deviation of 6.3% for the three cells discharged at 23°C , $5 \text{ mA}/\text{cm}^2$. From the results in Table 11 for undischarged prototype control cells that were filled with SOCl_2 electrolyte containing a known amount of SO_2 , then extracted and analyzed, it is estimated that the remaining 13.8% of the SO_2 can be fully accounted for by experimental error and other factors. The data obtained from the control cell extraction experiments will be discussed later in this section.

The reproducibility and close agreement between the measured and expected values of SO_2 found in the electrolyte extracted from the discharged prototype cells is an important advance in at least two ways. First, it establishes the stoichiometry of the Li/SOCl_2 cell reaction at 23°C for the first time in practical cells with large carbon-to-electrolyte mass ratios during discharges in which a large portion of the SOCl_2 is consumed. Second, it demonstrates that the multiple SOCl_2 extraction technique is a very effective method for obtaining electrolyte samples from practical Li/SOCl_2 cells that could be used in the future to investigate cells of any size discharged over a wide range of temperature and rate conditions.

Previous investigators of the Li/SOCl_2 cell reaction either observed a very large scatter in their SO_2 results (6,54) most likely due to sampling problems related to adsorption or used electrolyte flooded cells (2,57-59) which limited their SOCl_2 utilization. For example, Attia and co-workers (2) using an IR flow cell with 16 fold excess electrolyte found 68% of the SO_2 expected in discharged cells on the basis of Eq. [1] (i.e., $0.17\text{M SO}_2/\text{Faraday}$). However,

Table 7

The Amount of SO₂ Found by IR Analysis Compared to
The Amount Expected for Li/SOCl₂ Cells Extracted
with SOCl₂ at 23°C

Cell Number ⁺	SOCl ₂ Utilization To Cutoff (%)	Amount SO ₂ Found (mM)	Amount SO ₂ Expected [*] (mM)	Percent of Theoretical SO ₂ Found (%)
74	18.0	3.72	4.23	88.0
75	8.35	1.847	2.015	91.7
76	14.2	2.80	3.53	79.5

⁺ The discharge conditions and electrolyte volumes for the cells are given in Table 7.

^{*} The amount of SO₂ expected was calculated from the number of equivalents of charge² passed during discharge and the value of 0.25 moles of SO₂/equivalent of charge for the amount of SO₂ expected on the basis of Eq. (1).

Table 8

Discharge Conditions and SOCl_2 Utilizations for
 Li/SOCl_2 Cells Discharged at 25°C and Analyzed for SO_2

Cell Number	Current Density (mA/cm^2)	Electrolyte Volume (ml)	Cutoff Potential (V)	Discharge Time (hrs)	Capacity (Ahr)	SOCl_2 Utilization to Cutoff ⁺ (%)
74	5.0	3.68	0.05	3.45	0.414	18.0
75	5.0	4.14	0.05	1.80	0.216	8.35
76	5.0	4.27	0.05	3.15	0.378	14.2

⁺ The SOCl_2 utilization to cutoff is the percentage of SOCl_2 in the electrolyte which should have been reduced based on the number of equivalents of charge passed during the discharge. The calculation assumes 2.0 equivalents of charge are required per mole SOCl_2 reduced.

because of the large excess of electrolyte in their IR flow cell, only 2.1% of the SOCl_2 was consumed by the end of discharge compared to utilization of up to 22% achieved during the present investigation.

Firmly establishing the stoichiometry of the Li/SOCl_2 cell reaction for the first time in prototype cells has a number of important practical benefits. Now that it is clear that the cell reaction of the Li/SOCl_2 cell at room temperature is



a number of theories concerning long lived unstable SOCl_2 reduction intermediates and unknown discharge products (5,7,30) can be put aside and further research can be more productively focused on techniques to improve cell safety and performance. Previously, it has been postulated (Pg 195, Ref 30) that the occasional spontaneous explosion of partially discharged high rate cells on storage was due to long lived intermediates such as SO or the reaction of Li with sulfur. Since the presence of long lived SOCl_2 reduction intermediates can now be ruled out, it appears that such explosions in high rate cells are due either to short circuits related to faulty cell assembly or design or to the lithium-sulfur reaction. Likewise, incidents of violent venting that have been reported (40) when carbon limited Li/SOCl_2 cells were overdischarged at -40°C then allowed to warm to room temperature that were attributed to the decomposition of long lived intermediates now appear to be due to the reaction of Li dendrites with SOCl_2 (see Section 1.4.1.2).

Establishing the stoichiometry of the Li/SOCl_2 cell reaction in prototype cells has important benefits relative to future work to improve the performance of high rate cells, to decrease voltage delay and to decrease Li anode corrosion losses during storage and intermittent discharge. It has been postulated (25,56) that the organometallic catalysts used to increase the capacity and reduce polarization in high rate Li/SOCl_2 cells, form adducts with discharge intermediates such as SO that increase the rate of charge transfer and modify the reduction mechanism. The present study indicates that the ex-

istence of substantial amounts of intermediates with lifetimes less than approximately one hour is unlikely which is in agreement with the ESR measurements of Williams and co-workers (3) that indicate the presence of small concentrations of intermediates such as OClS with lifetimes less than ten seconds at 24°C . The details of the mechanism for the electrochemical reduction of SOCl_2 are not yet fully understood but other processes such as LiCl , SO_2 and S adsorption on the carbon electrode surface may be the key limiting process (27,28) instead of charge transfer. The possible role of soluble catalysts in facilitating charge transfer of Cl^- and Li^+ through a layer of SO_2 adsorbed on the surface of the carbon electrode is discussed in Section 1.3.3.3. A knowledge of exactly which step in the SOCl_2 reduction process is limiting may be very helpful in the selection of the next generation of catalysts for high rate Li/SOCl_2 cells.

The minimum half life of SOCl_2 reduction intermediates that could be detected by the present series of extraction experiments is approximately one hour based on the 1.80 hour discharge time of Cell 75 and the estimated accuracy of the experimental procedure. It is expected that with certain improvements in the prototype cell design and the experimental technique that would allow cells to be discharged at high rates ($> 50 \text{ mA/cm}^2$) that it may be possible to determine whether intermediates with lifetimes as short as approximately ten minutes are formed. Because ESR can only be used to detect intermediates that are free radicals, the present multiple extraction technique combined with quantitative FT-IR analysis for SO_2 is the only method that has been demonstrated which can determine whether intermediates that are not free radicals are formed during SOCl_2 reduction in prototype cells. The various improvements in the prototype cell design and experimental technique recommended for any future high rate stoichiometry studies will be discussed later in this section.

The results in Table 7 represent the most reproducible and reliable results obtained for the stoichiometry of the Li/SOCl_2 cell reaction for prototype cells after the extraction conditions were semi-optimized. It was found that the multiple SOCl_2 extractions should be carried out at 23°C rather than at

-20°C. Extraction at -20°C causes the SO₂ to be too strongly adsorbed on the carbon cathode material and difficult to extract. The results of the quantitative IR analysis for the amount of SO₂ contained in the electrolyte extracted at -20°C from discharged cells are listed in Table 9. These initial exploratory measurements provided the necessary information to semi-optimize the extraction and discharge conditions. The discharge conditions, initial electrolyte volumes and SOCl₂ utilizations to cutoff for the cells extracted with SOCl₂ at -20°C are listed in Table 10.

Of the five cells discharged at 23°C, 5 mA/cm² listed in Tables 9 and 10, it was found that the two cells discharged to a 0.05V cutoff (i.e., Cells 59 and

Table 9
 The Amount of SO₂ Found by IR Analysis Compared to
 The Amount Expected for Li/SOCl₂ Cells Extracted
 with SOCl₂ at -20°C

Cell Number ⁺	Discharge Temperature (°C)	Current Density (mA/cm ²)	SOCl ₂ Utilization to Cutoff ⁺ (%)	Amount SO ₂ Found (mM)	Amount SO ₂ Expected* (mM)	Percent of Theoretical SO ₂ Found (%)
59	23	5	22.8	3.29	5.32	61.9
60	0	1.5	17.2	1.72	5.46	31.5
61	23	5	16.3	2.72	3.84	59.1
65	23	5	19.7	1.70	3.92	43.4
66	23	5	16.7	1.19	3.572	33.3
67	23	5	13.2	0.98	3.50	28.0
68	-20	1.5	6.2	0.818	3.815	21.4

⁺ The discharge conditions and electrolyte volumes for the cells are given in Table 9.

^{*} The amount of SO₂ expected was calculated from the numbers of equivalents of charge passed during discharge and the value of 0.25 moles of SO₂/equivalent of charge for the amount of SO₂ expected on the basis of Eq. (1).

Table 10

Discharge Conditions and SOCl_2 Utilizations for
 Li/SOCl_2 Cells Extracted at -20°C and Analyzed for SO_2

Cell Number	Discharge Temperature ($^\circ\text{C}$)	Current Density (mA/cm^2)	Electrolyte Volume (ml)	Cutoff Potential (V)	Discharge Time (hrs)	Discharge Capacity (Ahrs)	SOCl_2 Utilization to Cutoff ⁺ (%)
59	23	5	4.0	0.05	4.75	0.57	22.8
60	0	1.5	5.47	0.05	16.25	0.585	17.2
61	23	5	4.05	0.05	3.41	0.41	16.3
65	23	5	3.41	1.45	3.50	0.42	19.7
66	23	5	3.66	-0.10	2.55	0.383	16.7
67	23	5	4.55	2.00	3.13	0.376	13.2
68	-20	1.5	5.37	0.00	11.37	0.49	6.2

⁺ The SOCl_2 utilization to cutoff is the percentage of SOCl_2 in the electrolyte which should have been reduced based on the number of equivalents of charge passed during the discharge. The calculation assumes 2.0 equivalents of charge are required per mole SOCl_2 reduced.

61) gave the highest amounts of SO_2 , compared to the amount of SO_2 expected. The 61.9 and 59.1% of theoretical SO_2 found for Cells 59 and 61, respectively, discharged to a 0.05V cutoff are substantially higher than the 43.4, 28.0 and 33.3% of theoretical SO_2 found for Cells 65, 67, and 66 discharged to 1.45, 2.00 and -1.00V cutoffs, respectively. It is thought that the higher amounts of SO_2 were found for cells discharged to the lower 0.05V cutoff because the SO_2 adsorbed on the cathode material was desorbed near the end of discharge due to displacement by LiCl and S . This explanation was first postulated by Schlaijker and co-workers (6) who also observed rapid increases in the SO_2 concentration in the electrolyte of Li/SOCl_2 cells towards the end of discharge. To minimize the effect of errors caused by SO_2 adsorption on the carbon cathode material, it was decided to discharge all the cells described in Table 7 to a 0.05V cutoff.

It is likely that the effect of the depth of discharge on the amount of SO_2 extracted from prototype cells is much more pronounced when the cells are extracted at low temperatures (i.e., -20°C) when SO_2 is more strongly adsorbed. Thus the effect of the cutoff potential may not be as important for cells extracted using the room temperature extraction technique. Further studies of the effect of depth of discharge on the extraction efficiency for SO_2 will be required for any future studies of the stoichiometry of the Li/SOCl_2 cell reaction at low temperature.

The amounts of SO_2 found in prototype cells discharged at 0 and -20°C at 1.5 mA/cm^2 are also listed in Table 9 where they are compared with the amount theoretically expected. At 0 and -20°C only 31.5 and 21.4% of the theoretically expected SO_2 was found. It is possible that the products of the cell reaction are different for low temperature discharge but based on the findings of the experiments with undischarged control cells presented in Table 11, it is thought that the amount of SO_2 found for the cells discharged at 0 and -20°C was low because it was more strongly adsorbed on the carbon.

At the end of low temperature discharge, the carbon electrode gives less capacity and much of the interior region is not completely filled with LiCl .

Table 11

The Efficiency of SO₂ Extraction From Undischarged
Control Cells Filled with a Known Amount of SO₂

Cell Number	Initial SO ₂ Concentration (m/l)	Electrolyte Volume* (m/l)	Extraction Temperature (°C)	Percent SO ₂ Recovered (%)	Comments
69	0.70	4.4	23,-20	75.3	Complete Cell First Two Extractions at 23°C, Next three at -20°C*
70	0.70	4.0	-20	72.1	Complete Cell ⁺⁺
71	0.98	4.2	23	95.2	No Hemi-cylindrical Spacers
72	0.98	4.0	23	91.1	No Carbon on Grids

** All electrolytes contained either 0.70 or 0.98M SO₂ dissolved in 1.8M LiAlCl₄/SOCl₂. The cells were stored 1.7 hours at 23°C after filling before the first extraction was begun.

* The initial drain and first extraction after 18 minutes for Cell 69 were at 23°C, the next three extractions at -20°C were after 30, 15 and 15 minutes.

++ The extraction times for Cell 70 at -20°C were 48, 15, 15, 15, and 15 minutes, respectively. The cell was cooled 48 minutes at -20°C before the initial drain.

The SO_2 produced during discharge would diffuse both out of the cathode and into the interior of the cathode where it would be strongly adsorbed on the carbon. In principle, at the end of low temperature discharge the surface layers of the carbon cathode would be almost sealed with a passivating skin of LiCl and the SO_2 adsorbed on the carbon in the interior would be especially difficult to extract at -20°C during the limited time period of the extraction procedure. In any future studies of the stoichiometry of the Li/SOCl_2 cell reaction at low temperature, it is possible that more complete extractions may be achieved by developing improved extraction procedures or simply by room temperature extraction of cells discharged at low temperature.

The results of the control tests in which undischarged prototype cells were filled with $1.8\text{M LiAlCl}_4/\text{SOCl}_2$ electrolyte containing a known amount of SO_2 then extracted and analyzed for SO_2 are presented in Table 11. These control experiments somewhat unexpectedly turned out to be of crucial importance in semi-optimizing the extraction conditions and understanding both the room and low temperature discharge analysis results for SO_2 .

The most important finding of the control tests is that the SO_2 extraction efficiency can be raised from approximately 72 to 91% by carrying out the multiple extractions at room temperature instead of at -20°C . The lower extraction efficiency for the -20°C extractions is most likely due to the increased adsorption of SO_2 by the carbon electrode at low temperatures. The implications of these results on the extraction procedure and our understanding of the SO_2 analyses for cells discharged at low temperatures has been discussed earlier in this section.

Initially draining the control cell at 23°C before carrying out the remainder of the extractions at -20°C produced only a small increase in the extraction efficiency from 72.1 to 75.3% comparing Cells 69 and 70 in Table 11. However, the accuracy of the quantitative IR analysis was approximately 3% at best so many duplicate tests would be required to substantiate this and other small effects.

In an earlier discussion of our initial exploratory studies of SO_2 adsorption on carbon, some reservations were expressed that SO_2 may not be adsorbed on carbon in SOCl_2 electrolyte but instead carbon may just catalyze the SO_2 - SOCl_2 electrolyte reaction. The large decrease in the amount of SO_2 extracted as the temperature is decreased found during the control experiments with prototype cells now firmly establishes that SO_2 is strongly adsorbed on carbon, especially at low temperature. Because SO_2 is strongly adsorbed on carbon, it now appears that the results of numerous investigations carried out during the last ten years involving electrolyte samples drained from Li/SOCl_2 cells must be re-interpreted taking into account this new information. In the future, investigators will either have to correct for adsorption or use extraction techniques when electrolyte samples from Li/SOCl_2 cells are required.

To determine the amount of SO_2 trapped by capillary action in the narrow space between the hemi-cylindrical shims and the glass (see Figure 42, Ref 1) and in other cell components, a standard control cell was tested with all components except the carbon cathode mixture. The SO_2 analysis for the cell (cf. Cell 72, Table 11) showed that 91.1% of the SO_2 was recovered. Another control cell was tested which contained the standard carbon electrodes and all cell components except the hemi-cylindrical shims, and 95.2% of the SO_2 added to the cell was recovered (cf. Cell 71, Table 11). The cells were stored 1.7 hours at 23°C after filling to correct for the SO_2 - SOCl_2 electrolyte reaction that would occur during a $5 \text{ mA}/\text{cm}^2$ discharge lasting approximately 3.4 hours. From the above results, it was concluded that the shims and other cell parts (excluding the carbon) retain about 8.9% and the carbon adsorbs about 4.8% of the added SO_2 . Thus for cells containing all the cell components, including all shims and carbon cathodes, one would expect that the total amount of SO_2 retained after five extractions at 23°C would be the sum of 8.9 and 4.8% or 13.7%.

For prototype Li/SOCl_2 cells discharged at $5 \text{ mA}/\text{cm}^2$, 23°C it was noted earlier that an average of 86.4% of the SO_2 expected was recovered after extraction for three cells (cf. Table 7). The average 13.8% of the SO_2 that was not recovered for the discharged cells compares very well with the 13.7% SO_2 that is

expected to be retained in the prototype cells based on the results from Control Cells 71 and 72.

Rather than calculating that 13.7% of the SO_2 would be retained in a control cell containing all components, it would improve the accuracy of the Li/SOCl_2 cell stoichiometry experiments if several control cells containing all components could be tested. Not only would the necessary factor for the amount of SO_2 retained in the cell after extraction be obtained directly but the standard deviation for a series of at least four control tests would provide valuable information about the accuracy and reproducibility of the extraction and quantitative FT-IR analysis procedures.

These crucial control experiments as well as many other very valuable stoichiometry experiments with discharged cells were not carried out because the schedule for the present contract was completed. Some of the valuable SO_2 stoichiometry experiments on discharged Li/SOCl_2 cells that could be carried out with the extraction and quantitative FT-IR analysis procedure that has now been demonstrated are described in the next section.

1.6.4 Recommendations for Future Work

A precise knowledge of the stoichiometry and discharge products of the Li/SOCl_2 cell reaction during discharge conditions such as high rate or low temperature would be valuable to improve the performance of the system. The stoichiometry of the cell reaction at low temperature could probably be determined using the present extraction procedure if the extractions were carried out at room temperature and if the procedure was optimized to improve the extraction efficiency. It is recommended that at least three determinations and three control tests be undertaken at each set of low temperature discharge conditions.

To investigate the stoichiometry of the Li/SOCl_2 cell reaction during high rate discharge, the prototype cells (cf. Figure 50) will have to be redesigned

so that the electrolyte-to-carbon electrode mass ratio can be decreased substantially to increase the SOCl_2 utilization to cutoff. The cathodes in high rate cells are not fully utilized and the carbon in the cathode interior can, in principle, adsorb large amounts of SO_2 , which could be difficult to extract. The electrolyte-to-carbon mass ratio could be decreased by redesigning the prototype cell to replace the three shims used in the present cell with a solid Teflon cylindrical cell case with a precisely machined rectangular slot for the cell package. Thinner cathodes would also reduce the amount of carbon available to adsorb SO_2 at the end of discharge. The results of the stoichiometry studies with high rate cells besides providing information about the possible existence of reduction intermediates with half lives as short as ten minutes should also provide valuable data concerning the effect of cell design on SO_2 adsorption by the carbon cathode material.

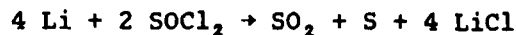
Once the stoichiometry of the Li/SOCl_2 cell reaction has been successfully characterized at high rate in $\text{LiAlCl}_4/\text{SOCl}_2$ neutral electrolyte then additional studies can be carried out in SOCl_2 acid electrolyte without and then with several types of catalysts. An understanding of the effect of SOCl_2 reduction catalysts on the cell reaction at high rate will undoubtedly provide much valuable information that could be applied to the design of high rate cells and the selection of more effective catalysts. Taking into account that each electrolyte-catalyst combination would require duplicate tests at perhaps five rates, each at three to five temperatures, it is evident that an enormous area remains to be investigated.

During the present study the stoichiometry of the Li/SOCl_2 cell was determined in electrolyte limited cells to SOCl_2 utilizations up to 22%. To fully understand the chemical reactions taking place in commercial cells it will ultimately be necessary to investigate the stoichiometry in cells in which at least 75% of the SOCl_2 is reduced by the end of discharge. In such cells, the electrolyte would contain large amounts of dissolved SO_2 and sulfur and the discharge reaction and processes could change causing unexpected effects on cell behavior. The stoichiometry of the Li/SOCl_2 cell reaction could be investigated in prototype cells in which up to 75% of the SOCl_2 is consumed by

the end of discharge using the SOCl_2 multiple extraction and FT-IR techniques developed during the present study. However, to carry out such measurements, the electrolyte-to-carbon mass ratio would have to be reduced by eliminating the three Teflon shims and reducing the electrolyte volume using the design modifications mentioned earlier in this section.

1.7 CONCLUSIONS FOR PART I

The stoichiometry of the Li/SOCl_2 cell reaction has been established for prototype cells discharged at 23°C , $5 \text{ mA}/\text{cm}^2$ using multiple SOCl_2 extractions and quantitative FT-IR analysis for SO_2 . The amount of SO_2 found for 0.6 Ahr prototype cells discharged at the above conditions is in agreement with the generally accepted cell reaction



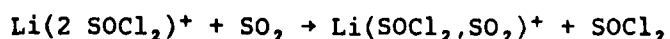
An average of 86.4% of the theoretically expected SO_2 was found with a standard deviation of 6.3% for the three cells discharged at 23°C , $5 \text{ mA}/\text{cm}^2$ to a 0.05V cutoff. From tests with undischarged control cells that were filled with SOCl_2 electrolyte containing a known amount of SO_2 , then extracted and analyzed, it is estimated that 13.7% of the SO_2 produced during cell discharge would be retained after five 23°C extractions with distilled SOCl_2 due to SO_2 adsorption on the carbon and capillary action in the cathode structure.

The average 13.8% of the SO_2 that was not recovered for the discharged cells compares well with the 13.7% SO_2 that is expected to be retained based on the control cell results. Further SO_2 extractions and analyses of discharged and control cells are recommended to statistically define the accuracy of the measurements more precisely.

During the above measurements, the electrolyte volume of the prototype cells was limited and up to 22% of the SOCl_2 was consumed during discharge. This is a significant advance compared with previous studies using IR flow cells in which only 2.1% of the SOCl_2 was reduced during discharge.

From the results of the multiple extraction discharge tests, it has been concluded that SOCl_2 reduction intermediates with half lives greater than approximately one hour are not formed during discharge at 23°C . This estimate is based on the 1.80 hour discharge time for the cells discharged at 5.0 mA/cm^2 and the accuracy of the experimental procedure. Furthermore, from the constant current electrolysis and voltammetry studies that were carried out at 23°C and -20°C in DMF using a Pt cathode, it was concluded that SOCl_2 reduction intermediates with lifetimes from 0.1 to 17 hours are not formed in significant quantities. The above finding, that long lived SOCl_2 reduction intermediates are not formed during the discharge of Li/ SOCl_2 cells, leads to the conclusion that a number of theories reported in the literature concerning long lived unstable SOCl_2 reduction intermediates can be put aside. It has been suggested, for example, that the occasional spontaneous explosion of partially discharged high rate cells on storage was due to long lived intermediates such as SO or the reduction of Li with sulfur. Since the presence of long lived SOCl_2 reduction intermediates can now be ruled out, it appears that such explosions in high rate cells are due either to short circuits related to faulty cell construction or to the lithium-sulfur reaction. Likewise, incidents of violent venting that have been reported when carbon limited Li/ SOCl_2 cells were overdischarged at -40°C then allowed to warm to room temperature that were attributed to the decomposition of long lived intermediates now appear to be due to the reaction of Li dendrites with SOCl_2 .

Quantitative infrared measurements of the SO_2 concentration in 1.8M LiAlCl₄/ SOCl_2 electrolyte to which 2.73M SO_2 was added have shown that 9.9 and 24% of the SO_2 reacts after 19 and 24 hours, respectively. Similar measurements in 2.0M AlCl₃, 0.10M LiCl/ SOCl_2 acid electrolyte to which 1.64M SO_2 was added showed that 26.1 and 45.1% of the SO_2 reacted after 20 and 26 hours, respectively. Voltammetric studies of SO_2 - SOCl_2 electrolytes in DMF showed similar reaction rates for both neutral and acid electrolytes. The SO_2 reaction with SOCl_2 electrolytes was also investigated by Barbier and co-workers (15) using Raman spectroscopy. From their Raman data they have postulated that the following reaction occurs



where the equilibrium constant is 6.2.

The voltammetry peak for the product of the SO_2 - SOCl_2 electrolyte reaction is about 0.490V more cathodic than SO_2 . Assuming that the peak currents correlate roughly with the thermodynamic half cell potentials, then the 490 mV difference between the two peaks would indicate that the free energy of the reaction between SO_2 and SOCl_2 electrolyte is about 11 Kcal/mole. This value is about what one would expect for an adduct or a complex but greater than the free energy involved in the simple solvation of an ion. On this basis it has been concluded that it is unlikely that the SO_2 - SOCl_2 electrolyte reaction generates enough heat to cause a safety hazard. However, further studies of the SO_2 - SOCl_2 electrolyte reaction involving calorimetric and analytical measurements are recommended. Such studies may lead to important performance improvements in cells discharged at high rate and/or low temperature.

During the present investigation, it was found that 12% and 41% of the SO_2 present in neutral and acid SOCl_2 electrolytes, respectively, is adsorbed on the carbon cathode mixture after approximately 24 hours. The above values were corrected for the SO_2 - SOCl_2 electrolyte reaction and were for 0.050 g of carbon cathode material/ml of SOCl_2 electrolyte at 23°C. Additional experiments at low temperature with undischarged Li/ SOCl_2 cells that were extracted five times with pure SOCl_2 showed that SO_2 is adsorbed even more strongly at low temperatures. Since the SO_2 - SOCl_2 electrolyte reaction is suppressed at low temperatures, it is clear that SO_2 is adsorbed on the carbon-4% Teflon cathode material and that carbon does not just catalyze the SO_2 - SOCl_2 electrolyte reaction.

From the work carried out during the present contract the importance of SO_2 adsorption on the carbon electrode has been demonstrated in Li/ SOCl_2 cells for the first time both qualitatively and quantitatively. From these findings, it has been concluded that the results of numerous investigations carried out during the last ten years involving electrolyte samples drained from cells will have to be re-interpreted taking into account the large sampling errors

due to SO_2 adsorption onto the carbon. In the future, investigators will either have to correct for adsorption or use extraction techniques when electrolyte samples from Li/SOCl_2 cells are required.

From our values for the amount of SO_2 adsorbed onto carbon and the surface area of the carbon cathode mixture, it has been calculated that approximately 8 and 16 molecular layers of SO_2 would be adsorbed on the carbon in neutral and acid SOCl_2 electrolytes, respectively. Multilayer SO_2 adsorption on the carbon electrode may limit the reduction of SOCl_2 during high rate discharge of Li/SOCl_2 cells, especially at low temperature. It is possible that the soluble organo-metallic catalysts that have proven so effective in high rate Li/SOCl_2 cells may mediate charge transfer through the multiple layers of SO_2 adsorbed on the carbon.

Carbon limited (CL) 10.6 Ahr prototype Li/SOCl_2 cells with a single layer of glass fiber separator were overdischarged up to 145 times the initial discharge capacity at current densities from 1.0 to 30 mA/cm^2 and no sign of negative potential transients indicative of short circuits were observed in the discharge curves. The lithium remaining on the lithium anodes after discharge and overdischarge was determined and only approximately 22-30% of the Li was consumed. Knowing the amount of Li consumed during discharge, it was calculated that only 0.49% of the overdischarge current was conducted via an ionic pathway and the remainder was conducted via an electronic pathway due to Li dendrite shorts. From these results, it was concluded that CL Li/SOCl_2 cells form Li dendrite shorts during overdischarge by a benign mechanism that probably does not constitute a specific safety hazard.

From results obtained during the present and earlier projects, it has been concluded that the incidents of explosions reported during the overdischarge of CL cells are most likely due to the reaction of sulfur which has precipitated from the electrolyte with the high surface area Li dendrites. It is recommended, that additional tests should be carried out to determine whether increasing the electrolyte-to-carbon mass ratio would increase the volume of the electrolyte sufficiently to prevent sulfur from precipitating out of the

electrolyte during discharge and reacting with the Li dendrites. Differential scanning calorimetry (DTA) measurements with Li dendrites and sulfur in SOCl_2 electrolytes and the evaluation of metal tabs on the anode and cathode to localize the Li dendrite growth are also recommended.

From in-situ photographic studies of the Li dendrites formed during overdischarge of CL, Li/ SOCl_2 cells at -40°C , it was found that Li dendrites detach from the electrode and dissolve at 23°C in the electrolyte in the period between 7 and 28 hours after the end of overdischarge. The product formed when the detached Li dendrites dissolved was analyzed and found to be LiCl. It was concluded that the SO_2 produced during overdischarge at -40°C modifies the LiCl film at 23°C so that SOCl_2 reacts with the Li dendrites as the cell is warmed to room temperature. It is well established that the addition of SO_2 to Li/ SOCl_2 cells increases Li corrosion and reduces voltage delay (5,60).

The electrolyte from overdischarged prototype 0.6 Ahr anode limited cells was analyzed by linear sweep voltammetry in DMF supporting electrolyte. The voltammograms obtained immediately after the end of overdischarge and after 16 hours were very similar to those obtained for the same concentration of 1.8M $\text{LiAlCl}_4/\text{SOCl}_2$ in DMF except that the SO_2 peak was somewhat smaller. Calibration tests showed that SO_2Cl_2 is stable in DMF and can be determined quantitatively by voltammetry. However, it was found that SOCl_2 and SO_2Cl_2 cannot be distinguished by voltammetry in DMF. It was concluded that the oxidation products that were observed by other laboratories using infrared and mass spectroscopy were not observed by voltammetry due to the poor resolution of the technique and its lack of sensitivity for SO_2 and other compounds in the presence of excess SOCl_2 . To analyze the electrolyte from prototype anode limited cells, it is clear that the multiple SOCl_2 extraction technique followed by quantitative FT-IR analysis for the oxidation products of the electrolyte would provide data of the desired accuracy to evaluate the safety hazards of anode limited overdischarge.

An investigation of cell charging with 0.77 Ahr Li/ SOCl_2 prototype cells utilizing a single layer of glass fiber separator showed no negative transients

in the cell potential at any time indicative of Li dendrite shorts. The cells were subjected to charging to at least twice the discharge capacity at current densities from 1.0 to 20.0 mA/cm² at 23°C. It was concluded that low resistance Li dendrite shorts that could overheat and cause thermal runaway were not formed during any of the charging tests.

Cell charging was studied, with an emphasis on the processes of Li dendrite shorting, by in-situ microphotography in cells without separators. Both carbon and nickel positive electrodes were investigated and again negative transients in the cell potential indicative of Li dendrite shorts were not observed at any time over a range of test conditions. From the in-situ microscopy it was concluded that Li dendrite shorts are probably very difficult to form during the charging of Li/SOCl₂ cells, because as the Li dendrites growing out of the Li anode approach very close to the carbon electrode, their tips are rapidly corroded by AlCl₃ and Cl₂ produced at the carbon electrode during charging. The concentrations of AlCl₃ and Cl₂ increase the closer the Li dendrite tips approach the cathode.

Part 2

INVESTIGATION AND DEMONSTRATION OF RECOMMENDATIONS TO IMPROVE Li/SOCl₂ CELL PERFORMANCE AND SAFETY

2.0 INTRODUCTION

Following the recommendations made in the conclusion of the Interim Report (1), certain key MESP* materials were investigated for their impact on load voltage, voltage delay, capacity and cell pressure. D and DD cells were used as test vehicles because of convenient size and cell characteristics.

The study has two parts: 1) additives in D cells evaluated for their effect on load voltage, voltage delay, and shelf life; 2) additives in DD cells fitted with hermetically sealed manometers to measure load voltage and cell pressure on continuous or intermittent discharge.

The polyvinyl alcohol content was investigated because of a concern that the organic binder may react with electrolyte and, in turn, effect either of the electrodes to produce voltage delay or pressure by reduction of the alcohol group to hydrogen. Cells were tested with the normal Crane polyvinyl alcohol paper, binderless paper and cells with binderless paper and PVA or PVC added to the electrolyte. PVC is of interest because it is the most likely reactive product of polyvinyl alcohol and the SOCl₂ electrolyte.

D cells were tested with varying amounts of teflon binder. This was done because of a suspicion that the Triton x surfactant or its pyrolysis

*Minuteman Extended Survival Power

products might effect voltage delay. We were also interested to see what effect on cell capacity and cathode manufacturability the binder content has.

Excess aluminum chloride over that required to make a balanced LiAlCl_4 electrolyte has been shown to react with lithium to produce metallic aluminum, lithium aluminum alloy and LiCl under certain conditions. It is, therefore, of interest to determine the effect of small excesses of AlCl_3 on cell performance at low discharge rates.

Recently, a new source of acetylene black has become available from Gulf, produced at the Bayside, Texas plant. Preliminary analytical studies show that the Texas and Quebec carbons are of comparable purity and physical structure. In the present study, we evaluate the effect of this new carbon on cell performance.

Lastly we wish to investigate cell parameters which may have some impact on cell pressure. We chose DD cells in order to produce the most pressure for a cylindrical cell. These were fitted with closed-end manometers, hermetically sealed to measure relative pressure increases. Some cells were discharged continuously and some intermittently to distinguish between gas evolution on and off load. The intermittent discharge duty cycle was chosen to be similar to that used under the old -0033 contract pressure studies on 10,000 Ah MESP cells.

Five cell conditions were investigated in the manometer DD cells:

1. baseline cells constructed with the same types of materials and processes as used in Henderson on MESP cells;
2. cells using Lydall binderless paper so that any hydrogen gas produced from polyvinyl alcohol binder is excluded;

3. cells which were SO₂ purged in an attempt to exclude trapped and chemisorbed gasses from the high surface area carbon cathode;
4. cells using specially selected low nitrogen lithium supplied by Lithcoa to evaluate the extent of pressure from N₂ released during discharge;
5. cells constructed with Gulf carbon to look for any additional pressure from contaminants not picked up in our normal carbon analysis.

2.1 EXPERIMENTAL

2.1.1 Component Preparation

All D cells were assembled by Power Systems Operation's (PSO) manufacturing group, to proven quality standards. The assembly of cells, having components not used in the standard D cell, such as Lydall separators, various Teflon/carbon blends and Gulf Texas carbon, was directly supervised by the development engineering group.

All DD manometer cells were assembled by PSO's manufacturing group. The manometers were assembled per Figure 51. All the manometers were treated with High Vacuum Leak Sealant from Space Systems, Inc., due to the high number of leaks detected at the glass-to-metal feed-through joint. The manometers were filled with Fischer Scientific technical grade mercury and flame sealed prior to activation.

For cells with binderless paper, all Crane and Mead papers were replaced with Lydall separators. Lydall separator contains no binder.

The PVA-spiked electrolyte was prepared using a sample of the actual binder used by the manufacturer of Crane glass paper. This was used

because information on the chemical content of the binder used in Crane glass paper was unobtainable. It is known that a significant amount of polyvinyl acetate is present in this binder.

To prepare the spiked electrolyte a large sample of binder material was weighed and added to 1.8 molar $\text{LiAlCl}_4/\text{SOCl}_2$ solution. This was then refluxed for 48 hours. The solution was then filtered of all solid particles. The remaining binder material was then weighed again. There was no appreciable weight loss, which suggests the binder has low solubility in the electrolyte solution.

The PVC electrolyte was prepared by adding a large sample of polyvinyl chloride powder to 1.8 molar $\text{LiAlCl}_4/\text{SOCl}_2$ solution. This mix was then refluxed for 48 hours and tested by infrared qualitative spectrometry for trace organic compounds. The scan showed a significant peak in the wavelength range corresponding to organic compounds (CH stretch).

The excess AlCl_3 electrolytes were prepared by adding an appropriate amount, by weight, to dry aluminum chloride to 1.8 molar $\text{LiAlCl}_4/\text{SOCl}_2$ solution and refluxing for 24 hours.

The carbon blends using various teflon contents were prepared by standard manufacturing techniques. These entail blending the carbon/water and alcohol mix with the appropriate amount of teflon suspension mix.

The Gulf Texas carbon cathodes were prepared by the standard manufacturing technique employed in all bobbin-type cells.

The low nitrogen lithium used in the DD manometer cells was purchased from Lithium Corporation of America. This lot (Lot # MR07808) was verified by Lithcoa to contain less than 60 ppm N_2 . Typical production runs at Foote and Lithcoa run around 200 ppm.

2.1.2 Testing

All D cell testing was performed at GTE's Building 9 in Waltham, MA, the cells being discharged at room temperature on a fixed resistance load at 1 mA/cm^2 . The discharge capacities were measured to 3.0V and 0.20V on a Digitec 3000 Datalogger. Capacity measurements were verified by hand calculation, using voltage recordings, where results deviated far from expected results. Voltage delay was measured directly using a strip chart recorder.

Fresh cells were left on OCV for 24 hours prior to start of discharge. Storage cells were stored at 55°C for 30 days in a Blue-M chamber. The cells were removed and left at room temperature for 24 hours prior to the start of discharge.

The continuous discharge manometer cells were allowed to stand on OCV for 48 hours prior to start of discharge to equilibrate pressure in the cell and manometer. The cells were discharged on a fixed resistance load at 1 mA/cm^2 at room temperature. Voltage, current and room temperature were recorded on a Fluke Datalogger. The mercury height, the distance from the meniscus to the inside surface of the glass tube end, was measured every 24 hours, using the apparatus shown in Figure 52.

The intermittent discharge manometer cells were allowed to stand on OCV for 48 hours prior to the first 24 hour discharge. The discharge schedule for intermittent discharge is as follows:

48 hours stand after activation
24 hours at 1 mA/cm²
7 days on OCV
24 hours at 1 mA/cm²
35 days on OCV
24 hours at 1 mA/cm²
21 days on OCV
Continuous discharge at 1 mA/cm²

2.2 RESULTS

2.2.1 D Cells

The electrochemical performance results of the 180 D cells, fresh and after one month storage at 55°C, are summarized in Tables 12 - 47. The voltage delay time to continuous three volts or above and the minimum voltage during the voltage delay are reported. Integrated Amp-hour capacities to 3.0 volts and approximately 0.2 volts are given so that practical capacity and virtual capacity in these lithium limited cells can be prepared. Standard deviation ("one sigma") are provided to indicate the experimental scatter.

In the two studies of Teflon binder and excess AlCl₃ it is useful to examine the dependance on these two variables of voltage delay and capacity. These are presented in Figures 53 - 60. Standard deviation for the voltage delays are included while those for capacity can be read from Tables 12 - 47. No attempts were made to fit parametric equations on smoothing functions to this plotted data.

2.2.2 Manometer Cells

The manometer DD cells all delivered in excess of 26 Ah with no significant voltage delays and consistent load voltages. The variation in calculated cell pressures is shown for continuously and intermittently discharged cells in Figures 61 - 65 and Figures 66 - 70 respectively. Vertical arrows indicate the points in time where one of the four discharges took place. Measurable pressure increases can be seen at these points. Other pressure excursions were associated with the room temperature variation which was within $\pm 7^{\circ}\text{F}$.

Some important averaged pressure parameters are shown in Tables 48 and 49 for cell on and off load. Maximum pressure and pressure following complete discharge are tabulated.

2.3 DISCUSSION

2.3.1 Crane Paper Binder

The fresh cells built with binderless paper behaved for the most part like those with binder paper. After 55°C storage the two sets are still roughly comparable. This result does not support earlier findings that after two and six months at room temperature the binder paper inhibits voltage delay. Furthermore, the addition of the Crane paper binder to cells with binderless paper decreases capacity slightly after one month at 55°C and dramatically increases voltage delay. Taken together with the earlier results, it appears now that further study of the influence of this binder is unwarranted. Its effect on electrochemical performance over these short periods of time are too subtle.

When PVC is added, however, to binderless paper cells, all cells have lower voltage delay than those without PVC. The PVC cells have a

slightly lower capacity, but the possible advantages of using PVC, instead of the Crane binder for glass paper, should be pursued. This result also shows that, during the PVA binder doping of electrolyte and subsequent 55°C one-month cell storage, the PVA is not quantitatively converted to PVC. Taken together, the results also suggest that the electrochemical effects of these polymer additives may be very dependant on whether the material is added to the paper as a binder or dispersed in the electrolyte. Polymer effects on the cathode have not been ruled out.

No change in the MESP separator paper or its binder is recommended at this time. The practicality of replacing the current types of binders with PVC should, however, be explored with the paper companies, perhaps under the "Mantech" program.

2.3.2 Teflon Binder

The amount of Teflon binder appears to have no effect on capacity and shelf life up to ten percent, as shown in Figures 53 and 54. However, Figures 55 and 56 do show a pronounced improvement in startup characteristics. The positive effect seems to reach a maximum around four to six percent TFE so there would probably be no significant advantages in changing the current four percent loading in the MESP cathodes. Again, these results suggest further lines of research to see if Triton-X surfactant or its pyrolysis products can be used to improve start up.

2.3.3 Excess $AlCl_3$

Figures 59 and 60 show that a small excess of $AlCl_3$ (0.5 - 1%) has a significant effect on decreasing voltage delay while causing only about a two percent loss in capacity. In Figures 57 and 58, above two percent

excess AlCl_3 , voltage delay again rises. It can thus be concluded from these tests that up to one percent excess AlCl_3 can be tolerated in Li/ SOCl_2 primary cells without catastrophic effects on performance. Control of the excess AlCl_3 with the reflux under lithium chips should be adequate at these levels.

2.3.4 Texas and Quebec Acetylene Blacks

Comparison of capacity and voltage delay before and after one month storage at 55°C for Quebec and Texas carbon reveals no significant differences. Both sources of carbon black should be adequate for primary Li/ SOCl_2 cells such as the MESP.

2.3.5 Pressure Studies

The effect of room temperature variations on manometer readings was significant. Variations of $\pm 2^\circ\text{C}$ resulted in observed cell pressure variations of ± 2 -3 psig depending on state of discharge. Since all of the continuous and most of the intermittent discharge cells were started concurrently, temperature excursion at about 140 and 300 hours (Figure 71) show up as discontinuities in the pressure increase of most cells. In all of the continuous discharge cells the pressure excursion at about 300 hours (78 hours short of complete discharge) is the highest.

In comparing DD pressure results using closed glass manometers with MESP results using pressure transducers, several physical differences must be taken into account.

As shown in Table 50, both the cathode volume per unit of capacity and electrolyte volume per unit capacity are higher in DD cells. Thus there is more carbon surface area and electrolyte volume for absorption and dissolution of SO_2 . Intermittent discharge in baseline MESP cells

resulted in pressure which ranged from 25-30 psig (61) compared with 13-15 psig for DD cells. This difference is also partly due to the fact that DD cells are vacuum filled with electrolyte while MESP cells are gravity filled allowing gas to escape through a second fill port. Most DD cells continued to rise slightly in pressure following discharge but never reached the final pressures observed in MESP cells.

DD cells start out at the beginning of discharge with a significantly lower void volume to capacity ratio. At end of discharge the ratio is about the same for both designs. Therefore, in DD cells the relative increase in void volume during early discharge is much greater and pressures in these cells actually drop somewhat at the beginning.

Another important variable involves the relative availability of metallic lithium surface area. Table 50 shows that the relative surface area available to reduce polyvinyl alcohol from the separator paper and hydrolysis products from the electrolytes is substantially greater in the MESP cell. Thus, the total pressure and rate of pressure increase during open circuit periods on intermittent discharges are expected to be higher in MESP cells.

No significant difference in discharge pressures was seen among classes of continuously discharged cells (Figure 72). The low nitrogen lithium cells experience slightly higher maximum and end of discharge pressures than other cells but the significance of this is doubtful considering the relatively large effects of temperature, cell to cell variations, and, more importantly, the fact that these cells showed slightly lower than average pressures four weeks after complete discharge.

TABLE 50
Physical Comparison of the MESP (10,000Ah) and DD (28Ah) Cells

Ratio	DD Cell	MESP Cell
Void Volume: Capacity		
Initial	0.161 cc/Ah	0.910 cc/Ah
Final	0.661 cc/Ah	0.590 cc/Ah
Interfacial Area: Capacity		
Initial	0.261 cm ² /Ah	0.079 cm ² /Ah
Cathode Volume: Capacity	1.72 cc/Ah	1.61 cc/Ah
Cathode Weight: Capacity	0.482 gm/Ah	0.603 gm/Ah
Electrolyte Volume: Capacity		
Initial	2.39 cc/Ah	2.20 cc/Ah
Final	1.89 cc/Ah	1.70 cc/Ah
Lithium Surface Area: Separator Weight	215.0 cm ² /gm	115.5 cm ² /gm
Electrolyte Volume: Lithium Surface Area	0.753 1.19 cm	0.485 2.00 cm

For intermitently discharged cells, the scatter of observed pressures within one class of cells increases steadily during discharge with an average deviation from the mean in each group of about +1 psi to +2 psi. The apparent scatter in values was least in baseline and binderless paper cells. With this in mind, Figure 73 was prepared after averaging and smoothing each group of pressure readings, and including reading several weeks after discharge.

The SO₂ purged cells now stand out as those with the highest running pressures. Four weeks following complete discharge, these cells remained 8 psi higher in pressure, on the average, than baseline cells. The reason for this unexpected behavior is not clear. Previous measurements of the SO₂ absorption on carbon cathodes indicate that no more than 0.5

gms of the gas would be added to a DD cell by the SO₂ purge in comparison to the 64 gms produced in discharge. Perhaps the SO₂ purge stimulates the release of moisture from the cathodes into the electrolyte causing more hydrolysis products and hydrogen gas. Although the SO₂ purge has been shown to reduce pressure in MESP cells, its utility in cylindricals may be in doubt. Variables such as the number of purge cycles, purge vacuum pressures, and temperature may be important in determining the effectiveness of the procedure.

The intermittently discharged cells containing the low nitrogen lithium also appear to run at higher pressure than baseline cells. The low nitrogen lithium cells were prepared with anodes having 60 ppm N₂ (by Kjeldahl analysis) as compared with typical values of 100-200 ppm N₂. In discussion with the vendor, it appears that only one nitrogen analysis is performed for a relatively large lot of the metal. Since the measurement has some experimental uncertainty and since the nitrogen distribution in one ingot of lithium may be uneven, there is a possibility that the special lot selected for this cell reaction study was actually higher in nitrogen. The vendor has agreed to perform additional analyses on this lot and a control lot to address this question.

Both the SO₂ purged and low N₂ lithium cells appear to be converging on the same pressure, about 34 PSIA, 2000 hours after discharge. This is about 5 PSI higher than the equilibrium pressures observed for the other groups of cells.

The remaining groups of cells (baseline, Lydall Paper, and Gulf Carbon) show a uniform behavior up to the third discharge. This occurred at about 1000 hours for the Binderless Paper and Gulf Carbon cells and at 1200 hours for the baseline cells. At this point the cells with Gulf Carbon and Lydall Binderless Paper experience rises in pressure greater than the

baseline cells. This variation in pressure continues through the end of discharge until about 2000 hours after end-of-discharge when Gulf Carbon, Binderless Paper and baseline cells converge on the same pressure, around 29 PSIA.

2.4 CONCLUSION

None of the material changes or additives investigated for the MESP battery, using the D cell as a model, seriously degrade cell performance. Teflon binder and its trace contaminants and small excesses of AlCl_3 do not seriously impact voltage delay, load voltage, or capacity. The elimination of this separator paper binder does not improve performance but the addition of PVC dispersed in electrolyte does markedly decrease voltage delay after one month storage at 55°C . There is also no significant difference in performance between cells using Texas and Quebec Acetylene Black.

DD cells equipped with mercury manometers are acceptable specimens for studying pressures in Li/SOCl_2 cells. They do, however, develop final pressures about 20 PSI lower than MESP cells. The rate of pressure increase is also qualitatively different for DD and MESP cells. The differences can be explained by examining the differences in cell physical design and balance of materials.

None of the pressure reducing techniques or materials suggested for the MESP cell demonstrated lower pressure in DD cells. Baseline cells, built with materials and techniques analogous to those used in the MESP cell, showed the least pressure during intermittent discharge. Pressure increases are the same in all cells during continuous discharge.

Pressures, 100 days following continuous or intermittent discharge, averaged 29 ± 2 PSIA for all groups of cells with two exceptions. Cells prepared with a special lot of low N_2 lithium or with a three cycle SO_2 purge came to equilibrium at 34 ± 3 PSIA, 100 days after intermittent discharge.

GTELABS/WPAFB CELL REACTION STUDY
 "D" CELL TEST RESULTS

TASK : - CONDITIONS : TESTED FRESH
 ELECTROLYTE : STANDARD (1.8M BALANCED)
 SEPERATOR : STANDARD (CRANE GLASS)
 CARBON : SHAWINIGAN BLACK
 TFE BINDER : STANDARD (4% TFE)

CELL #	VOLTAGE DELAY TO 3.0V (SEC)	MINIMUM VOLTS BEFORE 3.0V	AMPHRS @ 3.0V	AMPHRS @ 0.2V
1020	0	3.50	11.555	12.114
1021	0	3.50	12.507	12.549
1022	0	3.50	11.178	11.269
1023	0	3.40	10.714	12.545
1024	0	3.60	11.880	12.362
GROUP MEAN	0	3.50	11.527	12.168
GROUP STD. DEV.	0	0.070	0.616	0.533

TABLE 12

STELABS/MPFB CELL REACTION STUDY
 "D" CELL TEST RESULTS

TEMP : - CONDITIONS : STORED 1 MO. @ 55.C
 ELECTROLYTE : STANDARD (1.0M BALANCED)
 SEPARATOR : STANDARD (CRANE GLASS)
 CARBON : SHAWINIGAN BLACK
 TFE BINDER : STANDARD (4% TFE)

CELL #	VOLTAGE DELAY TO 3.0V (SEC)	MINIMUM VOLTS BEFORE 3.0V	AMPHRS @ 3.0V	AMPHRS @ 0.2V
1025	31.6	2.50	11.739	12.191
1026	23.4	2.50	12.637	12.740
1027	13.0	2.30	11.950	12.320
1028	15.2	2.30	11.605	12.116
1029	11.0	2.40	11.958	12.215
GROUP MEAN	18.8	2.40	11.994	12.316
GROUP STD. DEV.	8.55	0.10	0.280	0.248

TABLE 13

GIELARS/WFAFB CELL REACTION STUDY
 "D" CELL TEST RESULTS

TEST : W CONDITIONS : TESTED FRESH
 ELECTROLYTE : STANDARD (1.8M BALANCED)
 GENERATOR : LYDALL BINDERLESS
 CARBON : SHAWINIGAN BLACK
 TFE BINDER : STANDARD (4% TFE)

CELL #	VOLTAGE DELAY TO 3.0V (SEC)	MINIMUM VOLTS BEFORE 3.0V	AMPHRS @ 3.0V	AMPHRS @ 0.2V
1100	0	3.40	12.187	12.431
1101	0	3.50	12.182	12.539
1102	0	3.60	12.099	12.415
1103	0	3.40	12.179	12.448
1104	0	3.40	12.214	12.388
GROUP MEAN	0	3.46	12.172	12.443
GROUP STD. DEV.	0	0.089	0.0432	0.0594

TABLE 14

GTELABS/WPAFB CELL REACTION STUDY
 "D" CELL TEST RESULTS

TASK : A CONDITIONS : STORED 1 MO. @ 55.C
 ELECTROLYTE : STANDARD (1.8M BALANCED)
 SEPERATOR : LYDALL BINDERLESS
 CARBON : SHAWINIGAN BLACK
 TFE BINDER : STANDARD (4% TFE)

CELL #	VOLTAGE DELAY TO 3.0V (SEC)	MINIMUM VOLTS BEFORE 3.0V	AMPHRS @ 3.0V	AMPHRS @ 0.2V
1105	27.0	2.65	11.032	12.030
1106	30.0	2.98	11.659	11.982
1107	0	2.90	11.635	12.002
1108	0	2.80	11.615	11.940
1109	0	3.10	11.892	12.040
GROUP MEAN	13.4	2.89	11.727	11.983
GROUP STD. DEV.	18.5	0.172	0.126	0.060

TABLE 15

GTELABS/WPAFB CELL REACTION STUDY
 "D" CELL TEST RESULTS

TEST : A CONDITIONS : TESTED FRESH
 ELECTROLYTE : 1.0M BALANCED WITH FVA
 SEPERATOR : LYDALL BINDERLESS
 CARBON : SHAWINIGAN BLACK
 TFE BINDER : STANDARD (4% TFE)

CELL #	VOLTAGE DELAY TO 3.0V (SEC)	MINIMUM VOLTS BEFORE 3.0V	AMPHRS @ 3.0V	AMPHRS @ 0.2V
1110	0	3.45	11.847	12.521
1111	0	3.50	12.595	12.966
1112	0	3.50	11.470	12.332
1113	0	3.20	11.812	12.195
1114	0	3.40	11.393	12.084
GROUP MEAN	0	3.37	11.823	12.388
GROUP STD.DEV.	0	0.120	0.476	0.343

TABLE 16

GTCLABS/WPAFB CELL REACTION STUDY
 "G" CELL TEST RESULTS

DISP : A CONDITIONS : STORED 1 MO. @ 55.C
 ELECTROLYTE : 1.0M BALANCED WITH PVA
 SEPERATOR : LYDALL BINDERLESS
 CARBON : SHAWINIGAN BLACK
 TFE BINDER : STANDARD (4% TFE)

CELL #	VOLTAGE DELAY TO 3.0V (SEC)	MINIMUM VOLTS BEFORE 3.0V	AMPHRS @ 3.0V	AMPHRS @ 0.2V
1115	315.6	2.96	11.535	11.750
1116	463.2	2.90	11.740	11.700
1117	420.0	---	11.520	11.676
1118	0	---	11.414	11.714
1119	63.0	---	11.320	11.660
GROUP MEAN	252.4	2.93	11.507	11.710
GROUP STD.DEV.	209.8	0.042	0.160	0.048

TABLE 17

STELABS/WP-MFB CELL REACTION STUDY
 "D" CELL TEST RESULTS

TASK : A CONDITIONS : TESTED FRESH
 ELECTROLYTE : 1.0M BALANCED WITH PVC
 SEPERATOR : LYDALL BINDERLESS
 CARBON : SHAWINIGHT BLACK
 TFE BINDER : STANDARD (4% TFE)

CELL #	VOLTAGE DELAY TO 3.0V (SEC)	MINIMUM VOLTS BEFORE 3.0V	AMPHRS @ 3.0V	AMPHRS @ 0.2V
1120	0	3.50	12.042	12.411
1121	0	3.45	11.920	12.368
1122	0	3.55	11.837	12.543
1123	0	3.50	11.721	12.231
1124	0	3.45	11.679	12.255
GROUP MEAN	0	3.49	11.839	12.362
GROUP STD. DEV.	0	0.042	0.148	0.1263

TABLE 18

GTELABS/WPAFB CELL REACTION STUDY
 "D" CELL TEST RESULTS

TASK : A CONDITIONS : STORED 1 MO. @ 55.C

ELECTROLYTE : 1.8M BALANCED WITH PVC

SEPERATOR : LYDALL BINDERLESS

CARBON : SHAWINIGAN BLACK

TFE BINDER : STANDARD (4% TFE)

CELL #	VOLTAGE DELAY TO 3.0V (SEC)	MINIMUM VOLTS BEFORE 3.0V	AMPHRS @ 3.0V	AMPHRS @ 0.2V
1125	0	---	11.202	11.600
1126	1.0	---	11.202	11.700
1127	1.0	---	11.194	12.560
1128	2.0	---	11.260	11.751
1129	2.0	---	11.223	11.765
GROUP MEAN	1.2	---	11.210	11.907
GROUP STD. DEV.	0.837	---	0.030	0.3669

TABLE 19

GTCLABS/WPAFB CELL REACTION STUDY
 "D" CELL TEST RESULTS

TASK : C CONDITIONS : TESTED FRESH
 ELECTROLYTE : STANDARD (1.0M BALANCED)
 SEPERATOR : STANDARD (CRANE GLASS)
 CARBON : SHAWINIGAN BLACK
 TFE BINDER : 2.0 %

CELL #	VOLTAGE DELAY TO 3.0V (SEC)	MINIMUM VOLTS BEFORE 3.0V	AMPHRS @ 3.0V	AMPHRS @ 0.2V
ED01135	0	3.45	12.100	12.100
ED01136	0	3.40	12.539	12.560
ED01137	0	3.60	12.138	12.184
ED01138	0	3.60	12.145	12.260
ED01139	0	3.50	12.184	12.078
GROUP MEAN		3.51	12.221	12.290
GROUP STD. DEV.		0.089	0.100	0.159

TABLE 20

GTELABS/WPAFB CELL REACTION STUDY
 "U" CELL TEST RESULTS

TEST : C CONDITIONS : STORED 1 MO. @ 55.C
 ELECTROLYTE : STANDARD (1.8M BALANCED)
 SEPERATOR : STANDARD (CRANE GLASS)
 CARBON : SHAWINIGAN BLACK
 TFE BINDER : 2.0 %

CELL #	VOLTAGE DELAY TO 3.0V (SEC)	MINIMUM VOLTS BEFORE 3.0V	AMPHRS @ 3.0V	AMPHRS @ 0.2V
ED01140	17.0	2.20	11.921	12.070
ED01141	14.4	2.20	11.411	11.720
ED01142	9.6	2.05	--	11.500
ED01143	31.2	2.10	11.655	11.710
ED01144	60.0	2.25	11.997	12.220
GROUP MEAN	26.44	2.16	11.746	11.844
GROUP STD. DEV.	20.41	0.002	0.267	0.293

TABLE 21

GTCLABS/WPAFB CELL REACTION STUDY
 "D" CELL TEST RESULTS

TASK : C CONDITIONS : TESTED FRESH
 ELECTROLYTE : STANDARD (1.8M BALANCED)
 SEPERATOR : STANDARD (CRANE GLASS)
 CARBON : SHAWINIGAN BLACK
 TFE BINDER : 3.0 %

CELL #	VOLTAGE DELAY TO 3.0V (SEC)	MINIMUM VOLTS BEFORE 3.0V	AMPHRS @ 3.0V	AMPHRS @ 0.2V
ED01145	0	3.50	11.680	11.931
ED01146	0	3.50	12.054	12.150
ED01147	0	3.50	11.880	12.070
ED01148	0	3.50	12.013	12.270
ED01149	0	3.45	12.770	13.160
GROUP MEAN	0	3.49	12.079	12.316
GROUP STD. DEV.	0	0.022	0.413	0.487

TABLE 22

GTELABS/WPAFB CELL REACTION STUDY
 "D" CELL TEST RESULTS

(AS) : C CONDITIONS : STORED 1 MO. @ 55.C
 ELECTROLYTE : STANDARD (1.8M BALANCED)
 SEPERATOR : STANDARD (CRANE GLASS)
 CARBON : SHAWINIGAN BLACK
 TFE BINDER : 3.0 %

CELL #	VOLTAGE DELAY TO 3.0V (SEC)	MINIMUM VOLTS BEFORE 3.0V	AMPHRS @ 3.0V	AMPHRS @ 0.2V
ED01150	14.4	2.15	11.640	11.735
ED01151	14.4	2.20	11.802	11.940
ED01152	38.4	2.45	11.539	11.651
ED01153	68.4	2.40	11.463	11.627
ED01154	18.0	2.30	11.660	11.785
GROUP MEAN	30.72	2.30	11.621	11.740
GROUP STD. DEV.	23.31	0.127	0.129	0.125

TABLE 23

GTELH89/HFARB CELL REACTION STUDY
 "D" CELL TEST RESULTS

TEST : C CONDITIONS : TESTED FRESH
 ELECTROLYTE : STANDARD (1.6M BALANCED)
 SEPERATOR : STANDARD (CRANE GLASS)
 CARBON : SHAWINIGAN BLACK
 TFE BINDER : STANDARD (4% TFE)

CELL #	VOLTAGE DELAY TO 3.0V (SEC)	MINIMUM VOLTS BEFORE 3.0V	AMPHRS @ 3.0V	AMPHRS @ 0.2V
1020	0	3.50	11.553	12.114
1021	0	3.50	12.507	12.549
1022	0	3.50	11.178	11.269
1023	0	3.40	10.714	12.545
1024	0	3.60	11.880	12.362
GROUP MEAN	0	3.50	11.527	12.168
GROUP STD.DEV.	0	0.070	0.616	0.533

TABLE 24

GTELABS/WFA'S CELL REACTION STUDY
 "D" CELL TEST RESULTS

(AS) : C. CONDITIONS : STORED 1 MO. @ 55.C
 ELECTROLYTE : STANDARD (1.8M BALANCED)
 SEPERATOR : STANDARD (CRANE GLASS)
 CARBON : SHAWINIGAN BLACK
 TFE BINDER : STANDARD (4% TFE)

CELL #	VOLTAGE DELAY TO 3.0V (SEC)	MINIMUM VOLTS BEFORE 3.0V	AMPHRS @ 3.0V	AMPHRS @ 0.2V
1025	31.6	2.50	11.739	12.191
1026	23.4	2.50	12.637	12.740
1027	13.0	2.30	11.950	12.320
1028	15.2	2.30	11.685	12.116
1029	11.0	2.40	11.950	12.215
GROUP MEAN	18.8	2.40	11.994	12.316
GROUP STD. DEV.	8.55	0.10	0.200	0.248

TABLE 25

GTELABS/WFAFB CELL REACTION STUDY
 "D" CELL TEST RESULTS

TASK : C CONDITIONS : TESTED FRESH
 ELECTROLYTE : STANDARD (1.8M BALANCED)
 SEPERATOR : STANDARD (CRANE GLASS)
 CARBON : SHAWINIGAN BLACK
 TFE BINDER : 5.0 %

CELL #	VOLTAGE DELAY TO 3.0V (SEC)	MINIMUM VOLTS BEFORE 3.0V	AMPHRS @ 3.0V	AMPHRS @ 0.2V
ED01155	0	3.45	12.111	12.260
ED01156	0	3.50	12.349	12.551
ED01157	0	3.50	11.960	12.127
ED01158	0	3.50	12.061	12.171
ED01159	0	3.45	11.511	11.872
GROUP MEAN	0	3.48	11.998	12.196
GROUP STD. DEV.	0	0.027	0.307	0.245

TABLE 26

GTELABS/WPAFB CELL REACTION STUDY
 "D" CELL TEST RESULTS

TASK : C CONDITIONS : STORED 1 MO. @ 55.C
 ELECTROLYTE : STANDARD (1.0N BALANCED)
 SEPERATOR : STANDARD (CRANE GLASS)
 CARBON : SHAWINIGAN BLACK
 TFE BINDER : 5.0 %

CELL #	VOLTAGE DELAY TO 3.0V (SEC)	MINIMUM VOLTS BEFORE 3.0V	AMPHRS @ 3.0V	AMPHRS @ 0.2V
ED01160	9.6	2.46	11.591	11.607
ED01161	10.8	2.50	11.617	11.606
ED01162	10.8	2.40	11.200	11.643
ED01163	9.6	2.40	11.754	11.856
ED01164	4.3	2.20	12.570	12.959
GROUP MEAN	9.020	2.38	11.706	11.950
GROUP STD.DEV.	2.706	0.191	0.527	0.572

TABLE 27

GTELABS/WPAFB CELL REACTION STUDY
 "D" CELL TEST RESULTS

TASK : C CONDITIONS : TESTED FRESH
 ELECTROLYTE : STANDARD (1.5M BALANCED)
 SEPERATOR : STANDARD (CRANE GLASS)
 CARBON : SHAWINIGAN BLACK
 TFE BINDER : 6.0 %

CELL #	VOLTAGE DELAY TO 3.0V (SEC)	MINIMUM VOLTS BEFORE 3.0V	AMPHRS @ 3.0V	AMPHRS @ 0.2V
ED01165	0	3.45	12.163	12.238
ED01166	0	3.45	12.101	12.253
ED01167	0	3.40	12.741	12.944
ED01168	0	3.50	11.713	11.767
ED01169	0	3.45	12.049	12.187
GROUP MEAN	0	3.45	12.153	12.278
GROUP STD. DEV.	0	0.041	0.372	0.423

TABLE 28

GTELABS/WPAFB CELL REACTION STUDY
 "D" CELL TEST RESULTS

TASK : C CONDITIONS : STORED 1 MO. @ 55.C

ELECTROLYTE : STANDARD (1.0M BALANCED)

SEPERATOR : STANDARD (CRANE GLASS)

CARBON : SHAWINIGAN BLACK

TFE BINDER : 6.0 %

CELL #	VOLTAGE DELAY TO 3.0V (SEC)	MINIMUM VOLTS BEFORE 3.0V	AMPHRS @ 3.0V	AMPHRS @ 0.2V
ED01170	13.2	2.50	11.569	11.712
ED01171	8.4	2.40	11.611	11.637
ED01172	34.8	2.60	10.360	11.359
ED01173	16.0	2.50	11.203	11.539
ED01174	7.2	2.20	11.595	11.679
GROUP MEAN	16.00	2.44	11.269	11.584
GROUP STD. DEV.	11.15	0.152	0.531	0.141

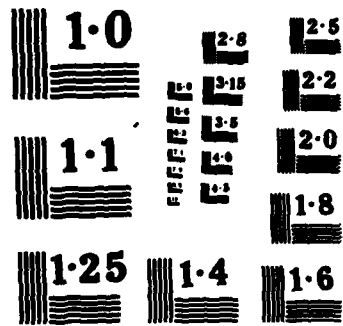
TABLE 29

GTELABS/WFAFB CELL REACTION STUDY
 "D" CELL TEST RESULTS

(AS) : C CONDITIONS : TESTED FRESH
 ELECTROLYTE : STANDARD (1.8M BALANCED)
 SEPERATOR : STANDARD (CRANE GLASS)
 CARBON : SHAWINIGAN BLACK
 TFF BINDER : 10 %

CELL #	VOLTAGE DELAY TO 3.0V (SEC)	MINIMUM VOLTS BEFORE 3.0V	AMPHRS @ 3.0V	AMPHRS @ 0.2V
1175	0	3.40	12.127	12.296
1176	0	3.50	12.091	12.404
1177	0	3.40	12.161	12.387
1178	0	3.40	12.004	12.196
1179	0	3.45	12.114	12.351
GROUP MEAN	0	3.39	12.099	12.327
GROUP STD.DEV.	0	0.055	0.059	0.064

TABLE 30



GTELABS/WPAFB CELL REACTION STUDY
 "D" CELL TEST RESULTS

TEST : C CONDITIONS : 1 MO. STORED @ 55.C
 ELECTROLYTE : STANDARD (1.8M BALANCED)
 SEPERATOR : STANDARD (CRANE GLASS)
 CARBON : SHAWINIGAN BLACK
 PTFE BINDER : 10%

CELL #	VOLTAGE DELAY TO 3.0V (SEC)	MINIMUM VOLTS BEFORE 3.0V	AMPHRS @ 3.0V	AMPHRS @ 0.2V
1180	15.9	2.55	11.888	11.889
1181	10.8	2.48	11.785	11.881
1182	12.8	2.55	11.846	11.985
1183	25.2	2.38	11.848	11.916
1184	8.4	2.35	11.523	11.682
GROUP MEAN	14.86	2.43	11.762	11.855
GROUP STD. DEV.	6.54	0.115	0.136	0.0974

TABLE 31

3TELABS/MPAFB CELL REACTION STUDY
 TEST CELL TEST RESULTS

AGE : 0 HOURS : TESTED FRESH
 ELECTROLYTE : 1.8M BURNED 70.91% EXCESS AMMONIUM CHLORIDE
 SEPARATOR : STANDARD (CRANE GLASS)
 CARBON : SHAWINIGAN BLACK
 TFE BINDER : STANDARD (4% TFE)

CELL #	VOLTAGE DELAY TO 3.0V (SEC)	MINIMUM VOLTS BEFORE 3.0V	AMPHRS @ 3.0V	WHHRS @ 0.2V
1030	0	3.5	12.189	12.582
1031	0	3.5	12.544	12.745
1032	0	3.5	12.790	12.959
1033	0	3.5	11.935	12.124
1034	0	3.5	12.076	12.355
GROUP MEAN	0	3.5	12.291	12.513
GROUP STD. DEV.	0	0	0.361	0.334

TABLE 32

GIELARS/WPAFB CELL REACTION STUDY
 "D" CELL TEST RESULTS

TASK : D CONDITIONS : STORED 1 MO. @ 30°C
 ELECTROLYTE : 1.5M BALANCED (0.01% EXCESS ALUMINUM CHLORIDE)
 SEPERATOR : STANDARD (CRANE GLASS)
 CARBON : SHAWINIGAN BLACK
 TFE BINDER : STANDARD (4% TFE)

CELL #	VOLTAGE DELAY TO 3.0V (SEC)	MINIMUM VOLTS BEFORE 3.0V	AMPHRS @ 3.0V	AMPHRS @ 0.2V
1025	15.0	2.40	12.179	12.358
1026	18.4	2.40	12.132	12.421
1027	17.6	2.50	11.962	12.590
1028	14.2	2.30	11.866	12.200
1029	25.7	2.70	11.905	12.258
GROUP MEAN	17.82	2.46	12.000	12.335
GROUP STD. DEV.	3.706	0.152	0.141	0.150

TABLE 33

GTCLABS/MPAFB CELL REACTION STUDY
 "D" CELL TEST RESULTS

TEST : D CONDITIONS : TESTED FRESH
 ELECTROLYTE : 1.0M BALANCED /0.05% EXCESS ALUMINUM CHLORIDE
 SEPERATOR : STANDARD (CRANE GLASS)
 CARBON : SHAWINIGAN BLACK
 TFE BINDER : STANDARD (4% TFE)

CELL #	VOLTAGE DELAY TO 3.0V (SEC)	MINIMUM VOLTS BEFORE 3.0V	AMP-HRS @ 3.0V	AMP-HRS @ 0.2V
1040	0	3.50	12.155	12.580
1041	0	3.45	12.033	12.540
1042	0	3.50	12.065	12.550
1043	0	3.45	11.945	12.245
1044	0	3.50	11.932	12.367
GROUP MEAN	0	3.48	12.026	12.292
GROUP STD. DEV.	0	0.027	0.092	0.074

TABLE 34

GTCLABS/WFAFB CELL REACTION STUDY
 "D" CELL TEST RESULTS

TASK : D CONDITIONS : STORED @ 10.0 ± 0.5°C
 ELECTROLYTE : 1.0M BALANCED 10.0% ETHYLENE ALUMINUM CHLORIDE
 SEPERATOR : STANDARD (CRANE GLASS)
 CARBON : SHAWINIGAN BLACK
 TFE BINDER : STANDARD (4% TFE)

CELL #	VOLTAGE DELAY TO 3.0V (SEC)	MINIMUM VOLTS BEFORE 3.0V	AMPHRS @ 3.0V	AMPHRS @ 0.2V
1045	25.6	2.60	11.973	12.367
1046	29.6	2.40	11.073	12.200
1047	32.2	2.50	11.750	12.116
1048	13.6	2.40	11.956	12.275
1049	9.0	2.20	11.169	11.550
GROUP MEAN	21.06	2.42	11.746	12.102
GROUP STD. DEV.	10.40	0.140	0.333	0.322

TABLE 35

STELABS/WPAFB CELL REACTION STUDY
 "D" CELL TEST RESULTS

TEMP : 0 CONDITIONS : TESTED FRESH
 ELECTROLYTE : 1.0M BALANCED / 0.10% EXCESS ALUMINUM CHLORIDE
 SEPERATOR : STANDARD (CRANE GLASS)
 CARBON : SHAWINIGNH BLACK
 TFE BINDER : STANDARD (4% TFE)

CELL #	VOLTAGE DELAY TO 3.0V (SEC)	MINIMUM VOLTS BEFORE 3.0V	AMPHRS @ 3.0V	AMPHRS @ 0.2V
1050	0	3.40	10.293	12.011
1051	0	3.50	11.986	12.450
1052	0	3.55	11.569	12.220
1053	0	3.50	11.925	12.230
1054	0	3.50	11.012	12.360
GROUP MEAN	0	3.49	11.517	12.257
GROUP STD. DEV.	0	0.055	0.703	0.160

TABLE 36

GTCLABS/WPAFB CELL REACTION STUDY
 "D" CELL TEST RESULTS

TASK : D CONDITIONS : STORED 1 MO. @ 55.C
 ELECTROLYTE : 1.0M BALANCED / 0.10% EXCESS ALUMINUM CHLORIDE
 SEPERATOR : STANDARD (CRANE GLASS)
 CARBON : SHAWINIGAN BLACK
 TFE BINDER : STANDARD (4% TFE)

CELL #	VOLTAGE DELAY TO 3.0V (SEC)	MINIMUM VOLTS BEFORE 3.0V	AMPHRS @ 3.0V	AMPHRS @ 0.2V
1055	11.6	2.30	11.700	12.011
1056	11.0	2.40	12.284	12.450
1057	8.6	2.50	12.037	12.220
1058	8.0	2.30	11.979	12.230
1059	6.8	2.50	12.016	12.360
GROUP MEAN	9.36	2.40	12.019	12.257
GROUP STD. DEV.	2.233	0.100	0.100	0.160

TABLE 37

STELABS WFA/B CELL REACTION STUDY
 10" CELL TEST RESULTS

TASK : 0 CONDITIONS : TESTED FRESH
 ELECTROLYTE : 1.9M BALANCED 71.00% EXCESS ALUMINUM CHLORIDE
 SEPERATOR : STANDARD (CRANE GLASS)
 CARBON : SHAWINIGAN BLACK
 TFE BINDER : STANDARD (4% TFE)

CELL #	VOLTAGE DELAY TO 3.0V (SEC)	MINIMUM VOLTS BEFORE 3.0V	AMPHRS @ 3.0V	AMPHRS @ 0.2V
1060	0	3.20	12.002	12.440
1061	0	3.40	11.842	12.478
1062	0	3.35	11.816	12.225
1063	0	3.40	12.235	12.462
1064	0	3.40	12.158	12.803
GROUP MEAN	0	3.35	12.011	12.444
GROUP STD.DEV.	0	0.087	0.186	0.222

TABLE 38

STELADIS/MPWFB CELL REACTION STUDY
 "D" CELL TEST RESULTS

TASK : D CONDITIONS : STORED 1 MO. @ 95.C
 ELECTROLYTE : 1.0M BALANCED 1.00% EXCESS ALUMINUM CHLORIDE
 SEPERATOR : STANDARD (CRANE GLASS)
 CARBON : SHAWINIGAN BLACK
 TFE BINDER : STANDARD (4% TFE)

CELL #	VOLTAGE DELAY TO 3.0V (SEC)	MINIMUM VOLTS BEFORE 3.0V	AMPHRS @ 3.0V	AMPHRS @ 0.2V
1065	10.6	2.50	11.540	11.966
1066	7.4	2.40	11.776	12.104
1067	9.3	2.40	11.489	11.865
1068	8.5	2.50	11.964	12.320
1069	8.5	2.50	12.100	12.417
GROUP MEAN	8.86	2.42	11.791	12.150
GROUP STD. DEV.	1.185	0.084	0.288	0.233

TABLE 39

GTCLABS/WPAFB CELL REACTION STUDY
 "D" CELL TEST RESULTS

TASK : D CONDITIONS : TESTED FRESH
 ELECTROLYTE : 1.8M BALANCED /2.00% EXCESS ALUMINUM CHLORIDE
 SEPERATOR : STANDARD (CRANE GLASS)
 CARBON : SHAWINIGAN BLACK
 TFE BINDER : STANDARD (4% TFE)

CELL #	VOLTAGE DELAY TO 3.0V (SEC)	MINIMUM VOLTS BEFORE 3.0V	AMPHRS @ 3.0V	AMPHRS @ 0.2V
1070	0	3.30	11.838	12.114
1071	0	3.30	11.320	11.684
1072	0	3.35	12.340	12.520
1073	0	3.30	12.159	12.287
1074	0	3.30	11.391	11.502
GROUP MEAN	0	3.31	11.810	12.027
GROUP STD. DEV.	0	0.022	0.453	0.413

TABLE 40

GTCLANS/WPAFB CELL REACTION STUDY
 "D" CELL TEST RESULTS

TEST : D CONDITIONS : STORED 1 MO. @ 55.C
 ELECTROLYTE : 1.8M BALANCED / 2.00% EXCESS ALUMINUM CHLORIDE
 SEPERATOR : STANDARD (CRANE GLASS)
 CARBON : SHAWINIGAN BLACK
 TFE BINDER : STANDARD (4% TFE)

CELL #	VOLTAGE DELAY TO 3.0V (SEC)	MINIMUM VOLTS BEFORE 3.0V	AMPHRS @ 3.0V	AMPHRS @ 0.2V
1075	17.5	2.50	11.556	12.020
1076	13.3	2.50	11.685	12.070
1077	17.4	2.50	12.087	12.320
1078	12.2	2.60	11.710	12.143
1079	13.7	2.50	11.537	11.800
GROUP MEAN	14.82	2.52	11.700	12.087
GROUP STD. DEV.	2.463	0.045	0.188	0.162

TABLE 41

TELRS/WHIPS CELL REACTION STUDY
 707 CELL TEST RESULTS

TEST : 0 CONDITIONS : TESTED FRESH
 ELECTROLYTE : 1.6M BALANCED 4.20% EXCESS ALUMINUM CHLORIDE
 SEPERATOR : STANDARD (CRANE GLASS)
 CARBON : SHAWINIGAN BLACK
 TFE BINDER : STANDARD (4% TFE)

CELL #	VOLTAGE DELAY TO 3.0V (SEC)	MINIMUM VOLTS BEFORE 3.0V	AMPHRS @ 3.0V	AMPHRS @ 0.2V
1080	0	3.30	12.102	12.237
1081	0	3.20	12.118	12.328
1082	0	3.10	12.585	12.833
1083	0	3.35	12.865	12.307
1084	0	3.40	12.136	12.269
GROUP MEAN	0	3.27	12.281	12.395
GROUP STD.DEV.	0	0.120	0.216	0.247

TABLE 42

GTCLABS/WPFB CELL REACTION STUDY
 "D" CELL TEST RESULTS

TEST : D CONDITIONS : STORED 1 MO. @ 25°C
 ELECTROLYTE : 1.0M BALANCED /4.00% EXCESS ALUMINUM CHLORIDE
 SEPERATOR : STANDARD (CRANE GLASS)
 CARBON : SHAWINIGAN BLACK
 TFE BINDER : STANDARD (4% TFE)

CELL #	VOLTAGE DELAY TO 3.0V (SEC)	MINIMUM VOLTS BEFORE 3.0V	AMPHRS @ 3.0V	AMPHRS @ 0.2V
1005	37.9	2.40	11.814	12.290
1006	26.3	2.40	11.903	12.166
1007	24.5	2.30	11.510	12.167
1008	22.2	2.30	11.090	11.575
1009	14.4	2.10	11.500	12.176
GROUP MEAN	25.06	2.30	11.579	12.075
GROUP STD.DEV.	8.493	0.122	0.3178	0.204

TABLE 43

GTCLABS/WPAFB CELL REACTION STUDY
 "D" CELL TEST RESULTS

TABLE : D CONDITIONS : TESTED FRESH
 ELECTROLYTE : 1.8M BALANCED 8.00% EXCESS ALUMINUM CHLORIDE
 SEPERATOR : STANDARD (CRANE GLASS)
 CARBON : SHAWINIGAN BLACK
 TFE BINDER : STANDARD (4% TFE)

CELL #	VOLTAGE DELAY TO 3.0V (SEC)	MINIMUM VOLTS BEFORE 3.0V	AMPHRS @ 3.0V	AMPHRS @ 0.2V
1090	0	3.50	12.211	12.303
1091	0	3.50	12.008	12.070
1092	0	3.55	12.144	12.231
1093	0	3.55	11.899	11.987
1094	0	3.50	12.213	12.338
GROUP MEAN	0	3.52	12.095	12.186
GROUP STD. DEV.	0	0.027	0.138	0.152

TABLE 44

GTCLABS/MFAFB CELL REACTION STUDY
 "D" CELL TEST RESULTS

TEST : D CONDITIONS : STORED @ 55.0
 ELECTROLYTE : 1.0M BALANCED 0.00% EXCESS ALUMINUM CHLORIDE
 SEPERATOR : STANDARD (CRANE GLASS)
 CARBON : SHAWINIGAN BLACK
 TFE BINDER : STANDARD (4% TFE)

CELL #	VOLTAGE DELAY TO 3.0V (SEC)	MINIMUM VOLTS BEFORE 3.0V	AMPHRS @ 3.0V	AMPHRS @ 0.2V
1095	162.4	2.30	11.984	12.194
1096	132.4	2.30	11.784	12.833
1097	719.0	---	11.796	12.383
1098	0	---	11.755	12.145
1099	539.0	---	11.614	12.233
GROUP MEAN	548.3	2.30	11.755	12.198
GROUP STD. DEV.	518.61	0	0.187	0.128

TABLE 45

GTE LABS/WPAFB CELL REACTION STUDY
 "D" CELL TEST RESULTS

TEST : E CONDITIONS : TESTED FRESH
 ELECTROLYTE : STANDARD (1.0M BALANCED)
 SEPERATOR : STANDARD (CRANE GLASS)
 CARBON : GULF TEXAS CARBON
 TFE BINDER : STANDARD (4 % TFE)

CELL #	VOLTAGE DELAY TO 3.0V (SEC)	MINIMUM VOLTS BEFORE 3.0V	AMPERES @ 3.0V	AMPERES @ 0.2V
1130	0	3.35	12.478	12.620
1131	0	3.35	12.141	12.240
1132	0	3.35	11.821	12.070
1133	0	3.30	11.800	12.135
1134	0	3.30	12.452	12.638
GROUP MEAN	0	3.33	12.153	12.341
GROUP STD. DEV.	0	0.015	0.306	0.270

TABLE 46

GTCL/MS/WF/FFB CELL REACTION STUDY
 "D" CELL TEST RESULTS

TASK : E CONDITIONS : STORED 1 MO. @ 55.C
 ELECTROLYTE : STANDARD (1.8M BALANCED)
 SEPERATOR : STANDARD (CRANE GLASS)
 CARBON : GULF TEXAS CARBON
 TFE BINDER : STANDARD (4 % TFE)

CELL #	VOLTAGE DELAY TO 3.0V (SEC)	MINIMUM VOLTS BEFORE 3.0V	AMPHRS @ 3.0V	AMPHRS @ 0.2V
1260	50.4	2.70	11.972	12.010
1261	0	2.30	11.934	12.155
1262	15.6	2.25	11.893	11.998
1263	15.6	2.40	11.691	11.828
1264	21.6	2.30	11.669	11.748
GROUP MEAN	20.68	2.59	11.832	11.943
GROUP STD. DEV.	18.54	0.434	0.142	0.164

TABLE 47

Cell Type	(PSIG) At End of Discharge Average (Std. Dev.)	(PSIG) Maximum During Discharge	(PSIG) Four Weeks After Discharge
Baseline	10.07 (.57)	14.19 (.01)	19.24 (5.32)
Low Nitrogen Lithium	14.88 (1.27)	19.71 (.61)	16.18 (.30)
Lydall Paper	10.86 (.41)	14.38 (2.30)	15.16 (.80)
SO ₂ Purged	10.75 (.34)	14.82 (1.32)	17.67 (.80)
Gulf Carbon	10.05 (.11)	14.90 (.78)	14.75 (.46)

Summary of Pressure Results Continuous Discharge

Table 48

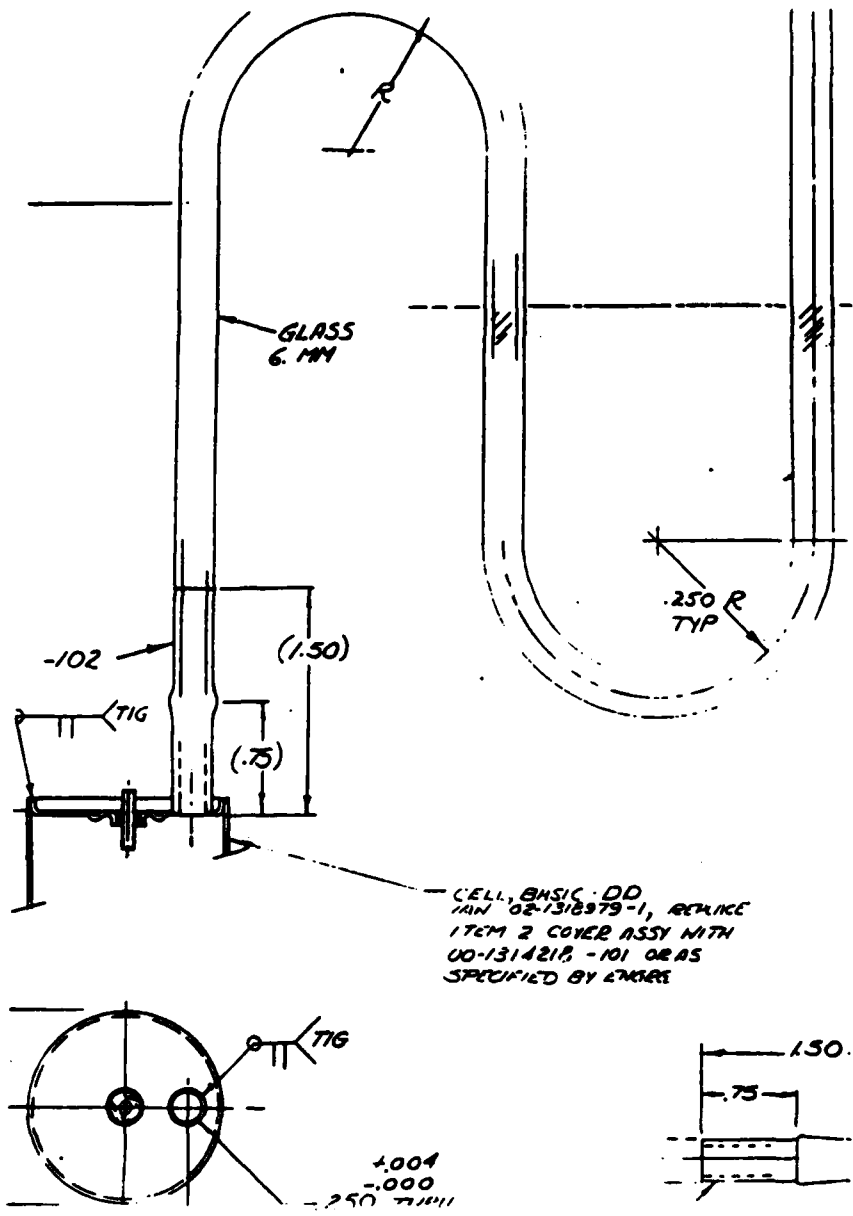
Cell Type	PSIG 1st 24 Hr. Discharge	PSIG 1 Week OCV	PSIG 2nd 24 Hr. Discharge	PSIG 5 Week OCV	PSIG 3rd 24 Hr. Discharge	PSIG 3 Week OCV	PSIG Contin. Discharge	PSIG 4 Weeks After Discharge	PSIG 8 Weeks After Discharge
Baseline	-78 (35)	0.31 (.46)	0.64 (.85)	3.34 (1.24)	3.45 (.77)	5.15 (.88)	11.20 (.86)	14.30 (.40)	14.84 (1.96)
Low Nitrogen Lithium	-26 (61)	1.22 (.63)	2.25 (.36)	6.78 (2.28)	10.60 (2.84)	12.08 (3.35)	17.82 (5.09)	20.23 (1.20)	19.52 (1.82)
Lydall Paper	-79 (39)	-62 (.63)	-34 (.79)	2.95 (0.11)	6.10 (.03)	8.20 (1.34)	14.30 (5.82)	15.82 (1.16)	13.58 (0.36)
SO ₂ Purge	-95 (39)	.42 (1.4)	1.03 (.62)	13.30 (3.00)	11.55 (7.14)	11.94 (1.01)	18.79 (6.68)	22.24 (8.18)	19.14 (3.87)
Gulf Carbon	-46 (74)	-08 (.40)	.29 (.68)	2.70 (1.87)	2.40 (2.21)	6.18 (1.17)	9.47 (2.91)	14.42 -	13.1 (1.84)

Summary of Pressure Results Following Each Segment of Intermittent Discharge

Table 49

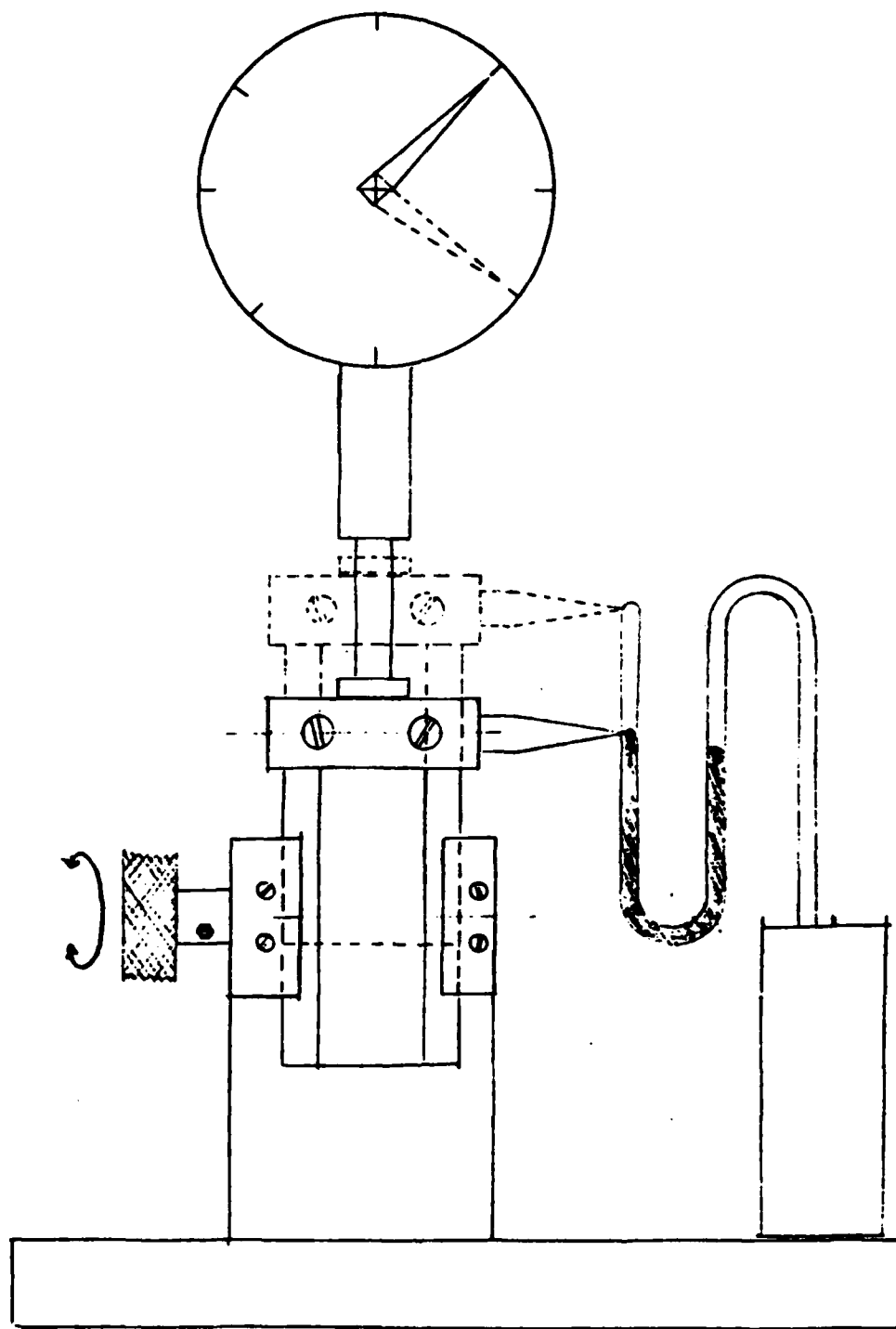
TABLE 50
Physical Comparison of the MESP (10,000Ah) and DD (28Ah) Cells

Ratio	DD Cell	MESP Cell
Void Volume: Capacity		
Initial	0.161 cc/Ah	0.910 cc/Ah
Final	0.661 cc/Ah	0.590 cc/Ah
Interfacial Area: Capacity		
Initial	0.261 cm ² /Ah	0.079 cm ² /Ah
Cathode Volume: Capacity	1.72 cc/Ah	1.61 cc/Ah
Cathode Weight: Capacity	0.482 gm/Ah	0.603 gm/Ah
Electrolyte Volume: Capacity		
Initial	2.39 cc/Ah	2.20 cc/Ah
Final	1.89 cc/Ah	1.70 cc/Ah
Lithium Surface Area: Separator Weight	215.0 cm ² /gm	115.5 cm ² /gm
Electrolyte Volume: Lithium Surface Area	0.753 1.19 cm	0.485 2.00 cm



MANOMETER ASSEMBLY

FIGURE 51



MERCURY HEIGHT MEASURING APPARATUS

TASK C TEFLON BINDER CONTENT 3.0 VOLT CAPACITIES

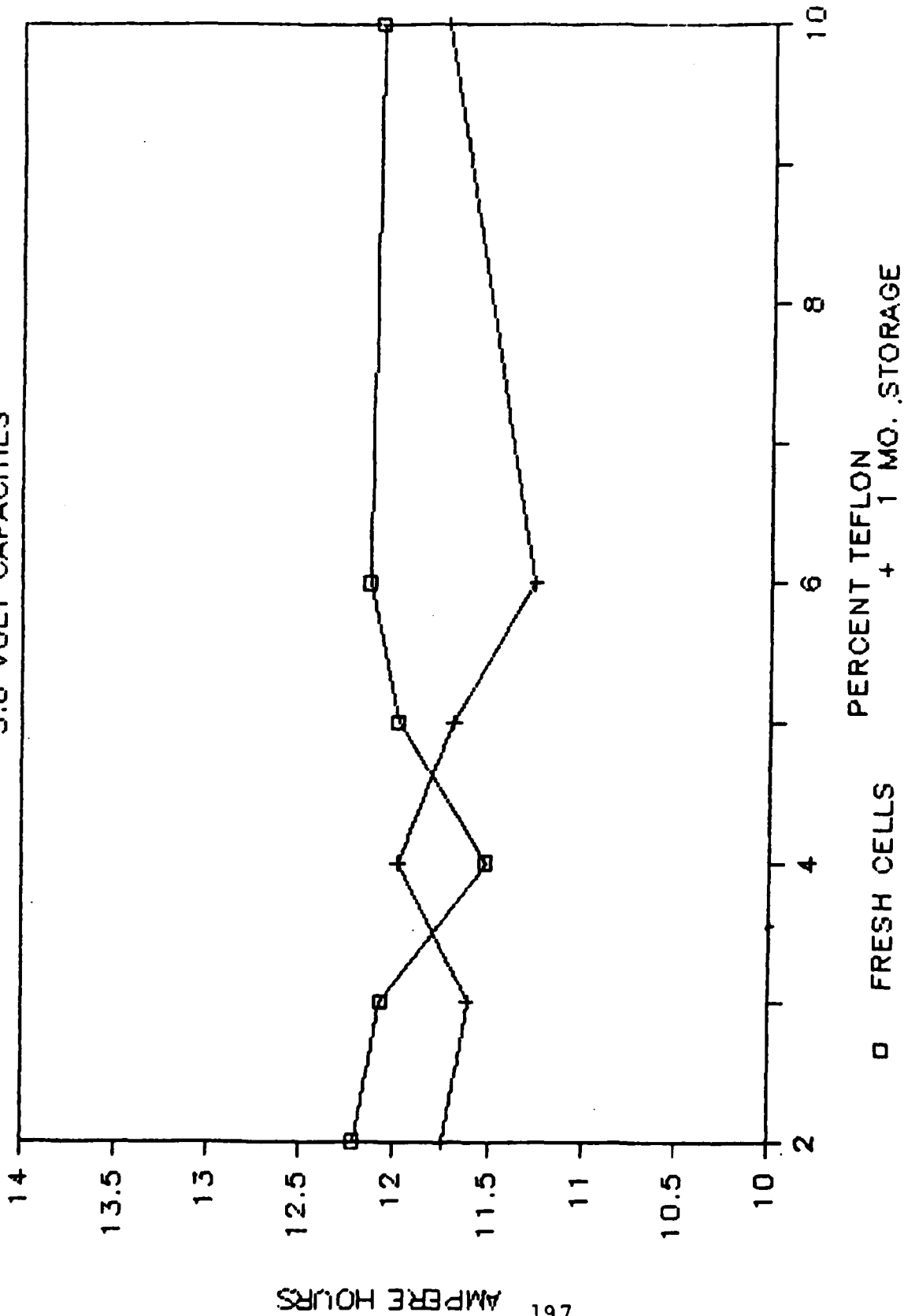


FIGURE 53

TEFLON BINDER

0.20 VOLT CAPACITIES FRESH VS. STORED

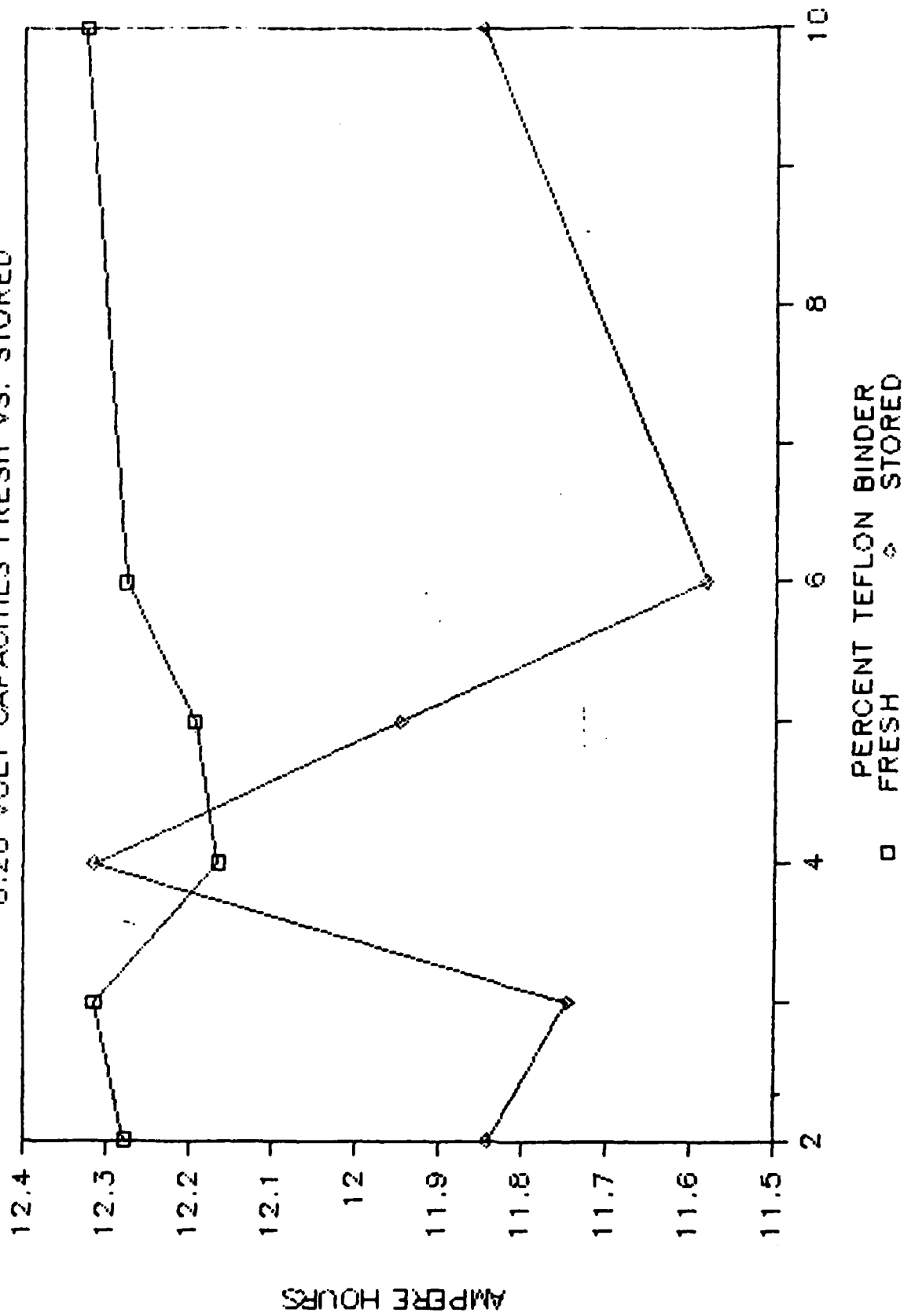


FIGURE 54

TEFLON BINDER VOLTAGE DELAY AFTER STORAGE

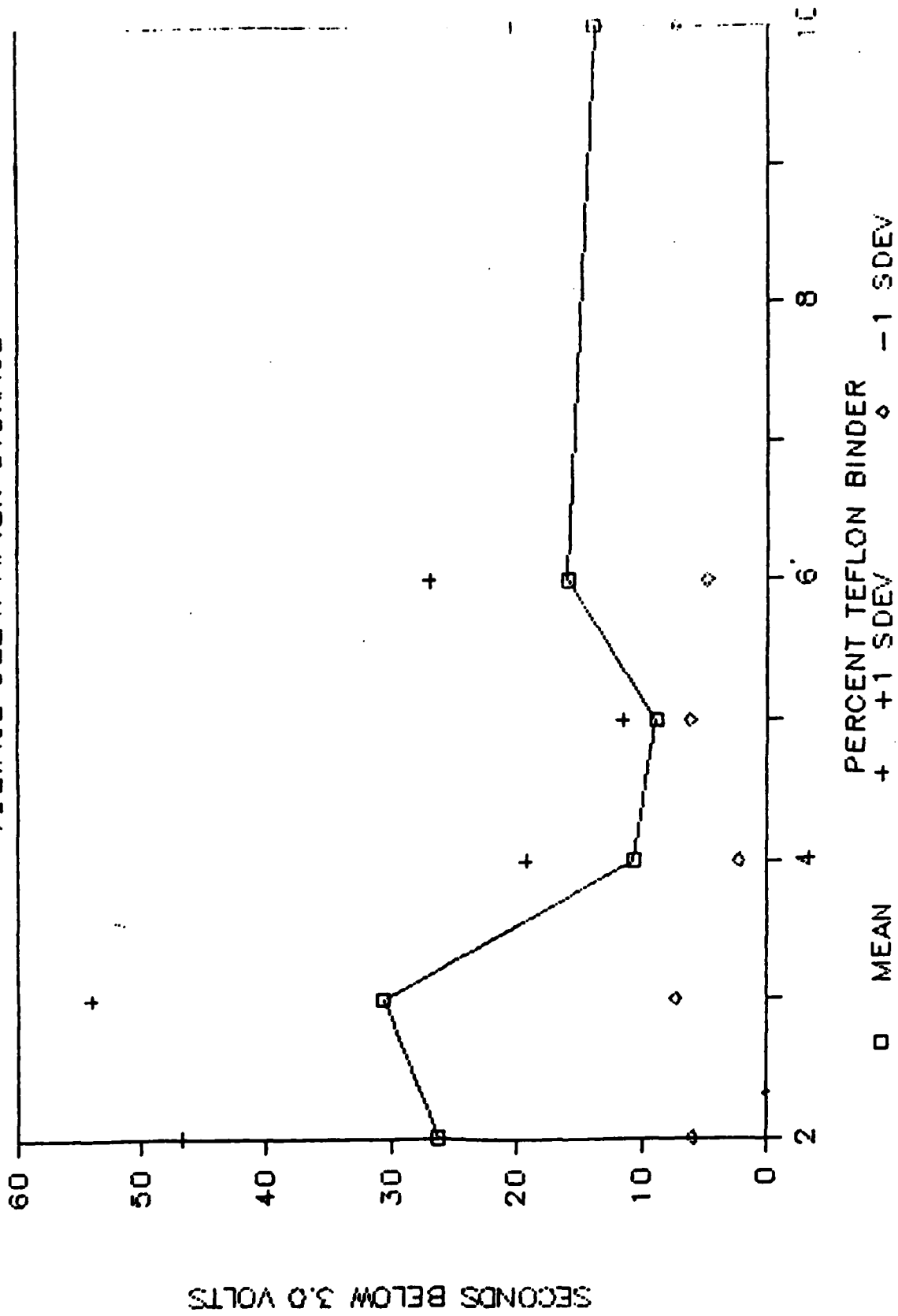


FIGURE 55

TEFLON BINDER

MIN VOLTAGE DURING DELAY PERIOD

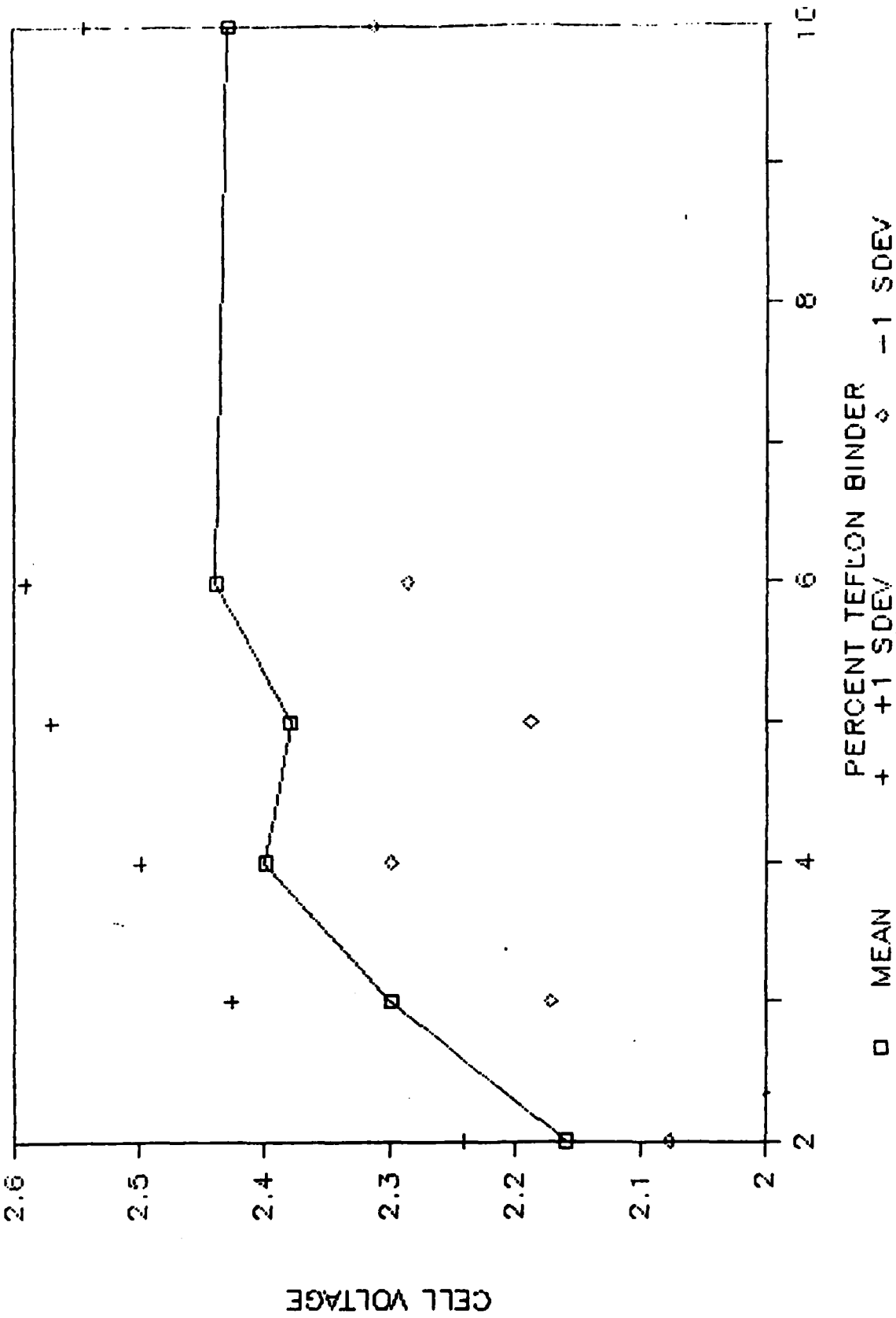


FIGURE 56

EXCESS ALUMINUM CHLORIDE STORED VS. FRESH CELLS

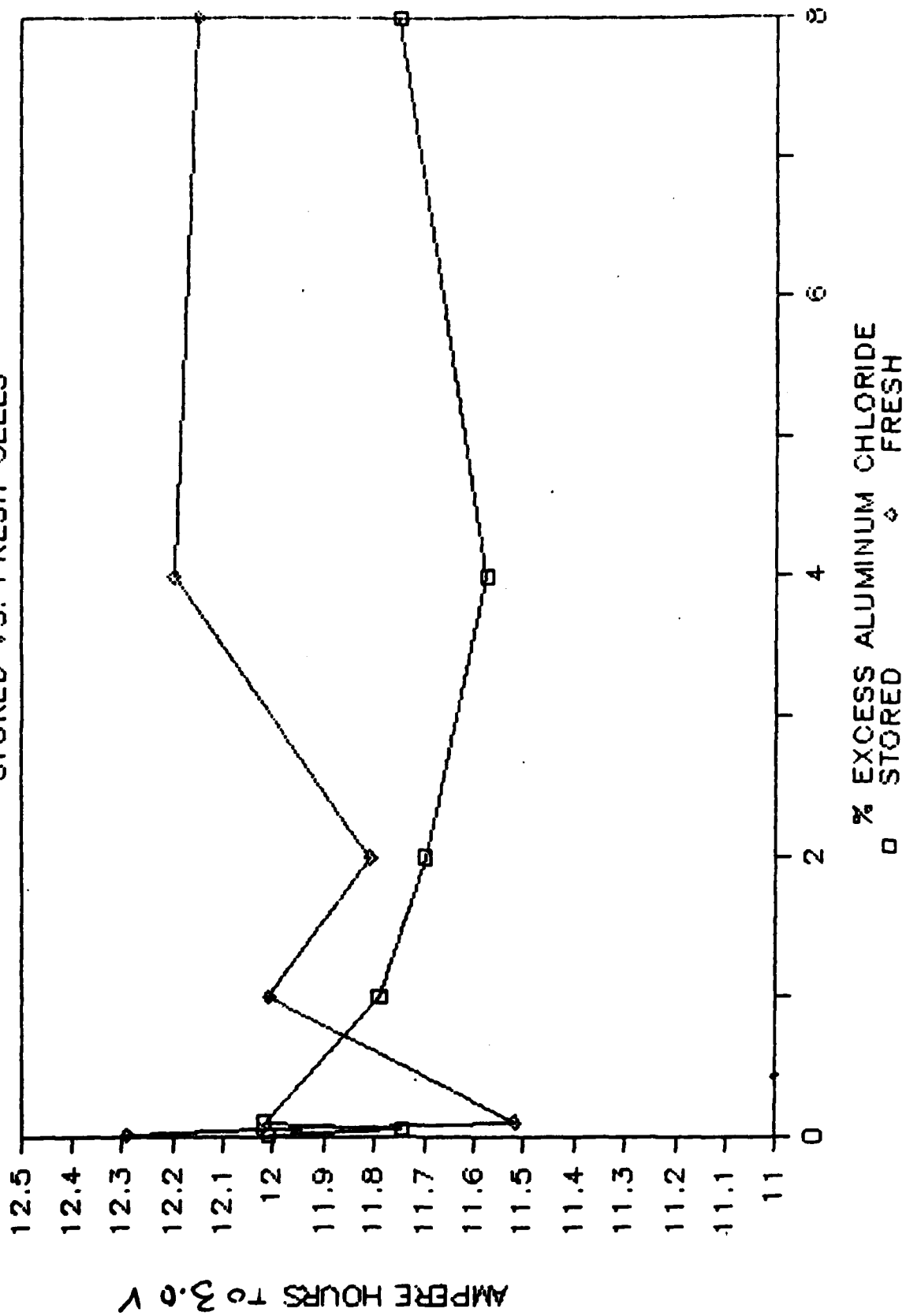


FIGURE 57

EXCESS ALUMINUM CHLORIDE FRESH VS. STORED CELLS

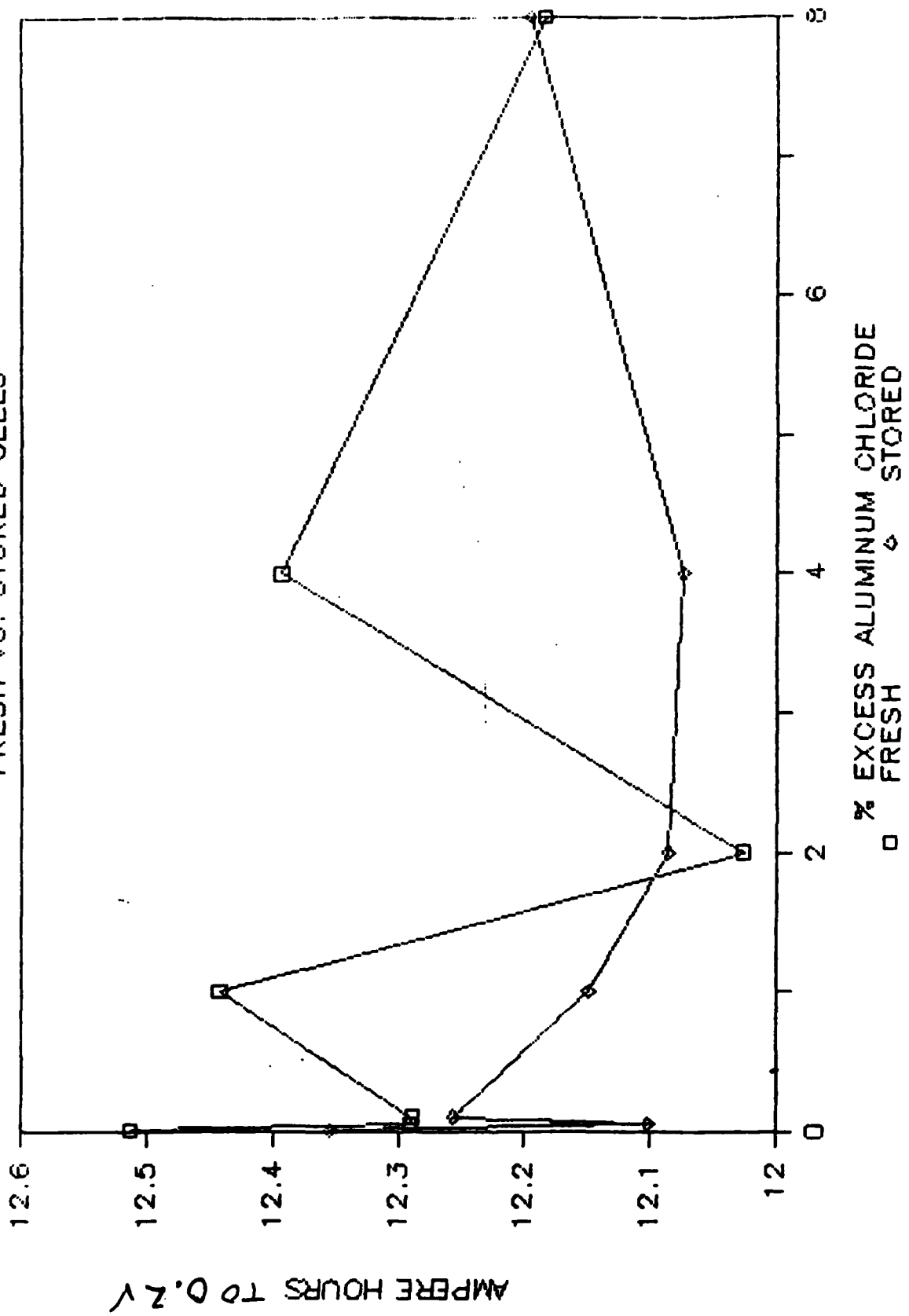


FIGURE 58

EXCESS ALUMINUM CHLORIDE

VOLTAGE DELAY AFTER STORAGE

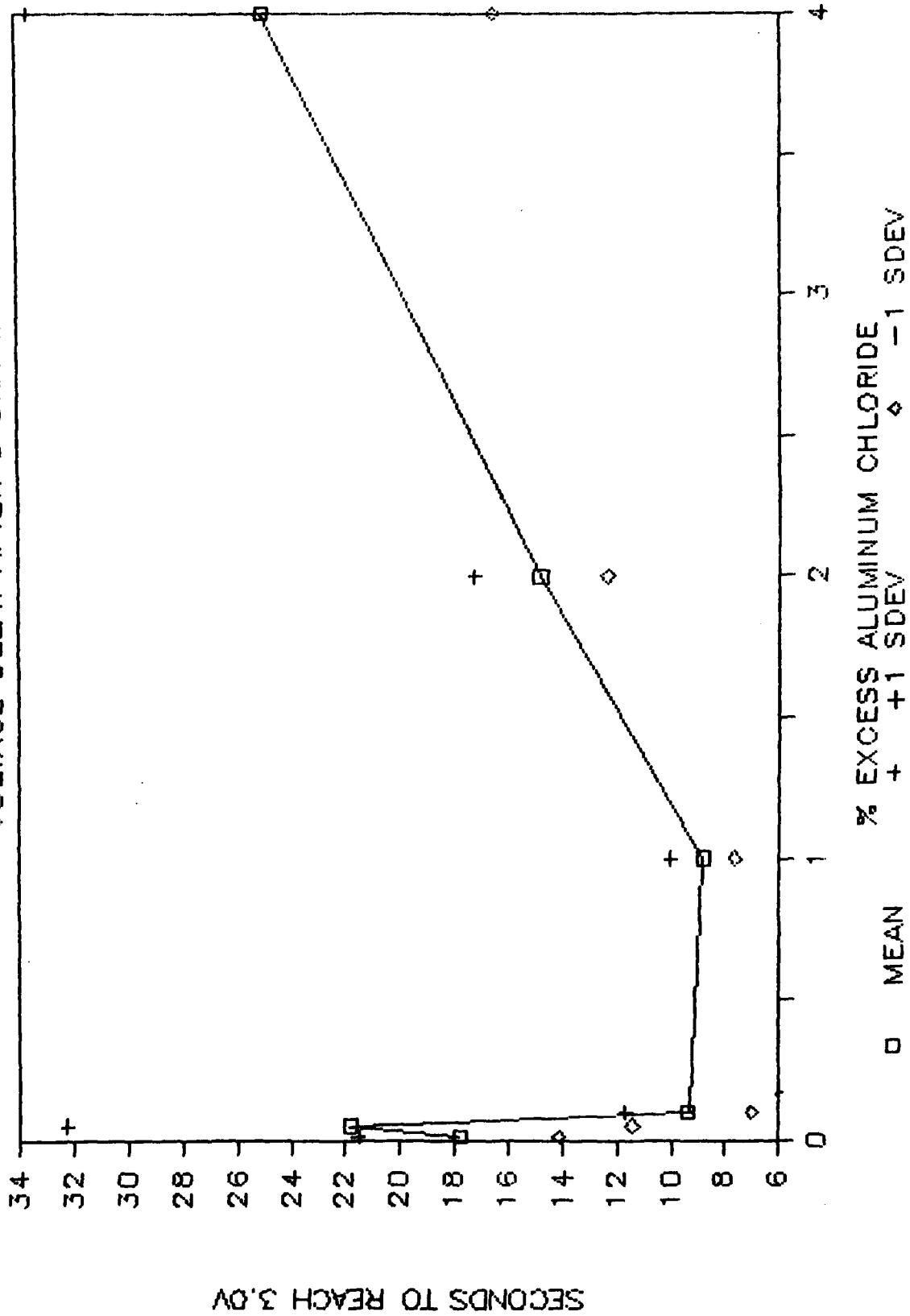


FIGURE 59

EXCESS ALUMINUM CHLORIDE

MIN VOLTAGE DURING DELAY PERIOD

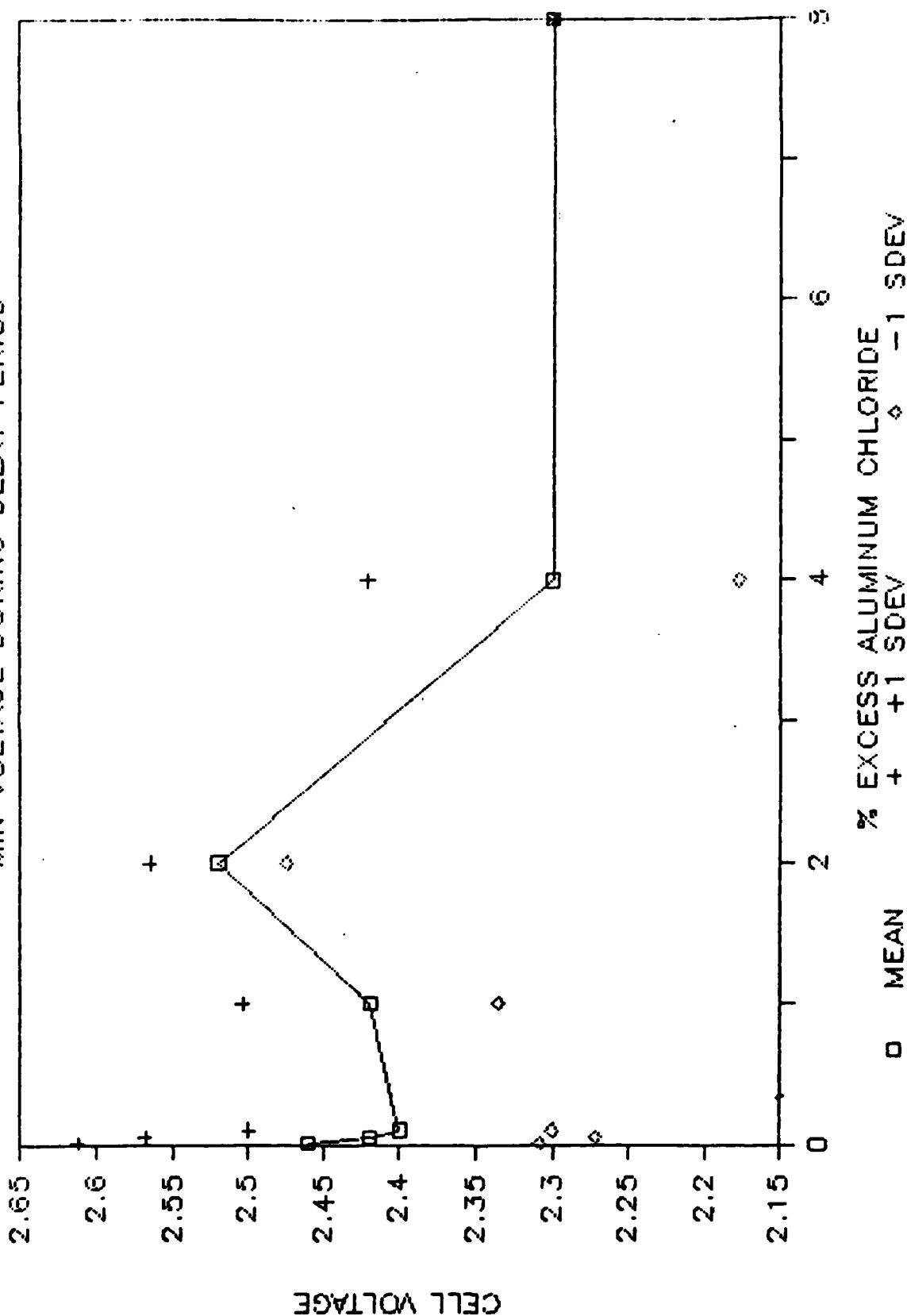


FIGURE 60

CELL REACTIONS TASK III / PRESSURE STUDY

CONTINUOUS DISCHARGE / BASELINE

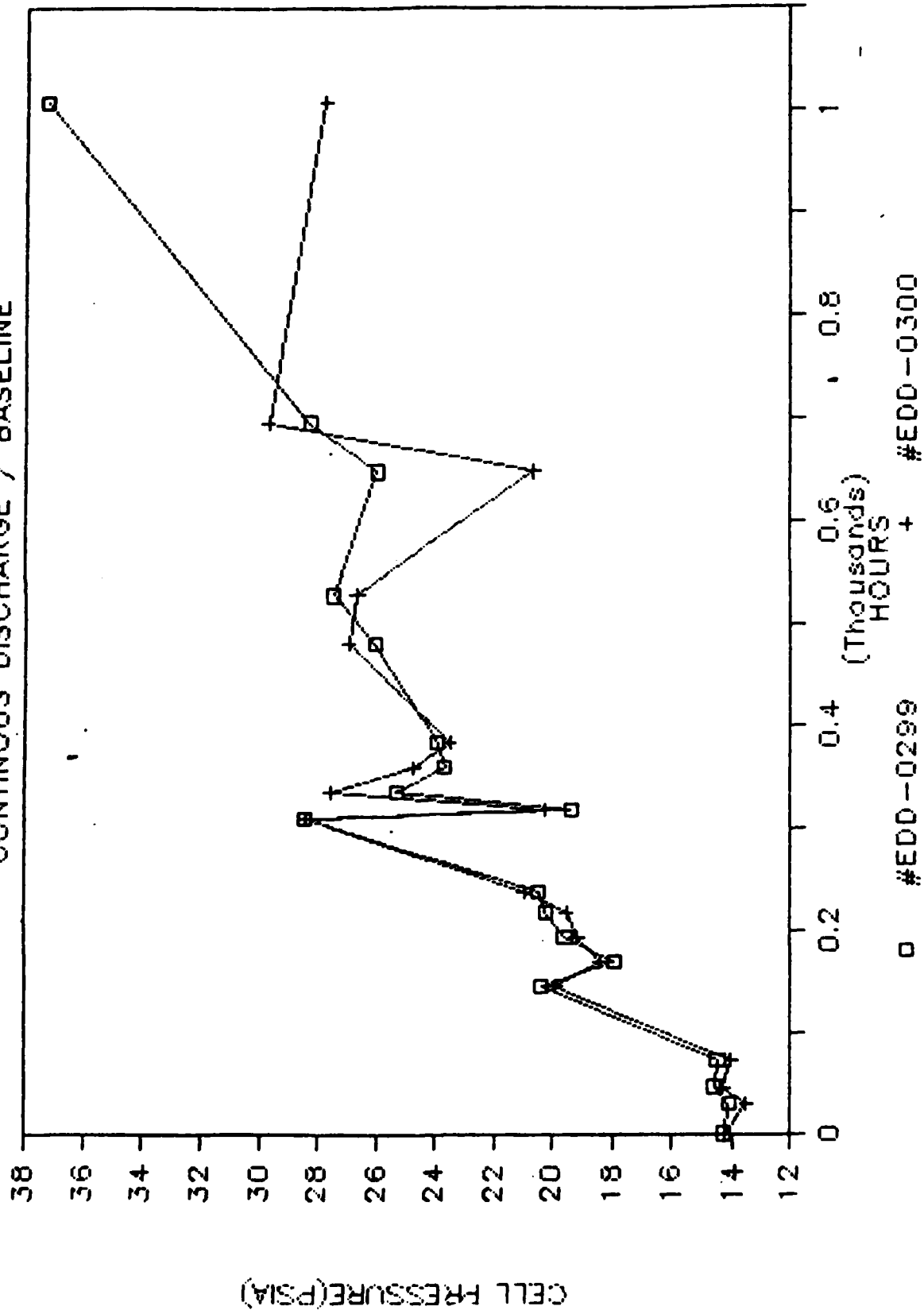


FIGURE 61

CELL REACTIONS TASK III/PRESSURE STUDY

CONTINUOUS DISCHARGE/LYDALL PAPER

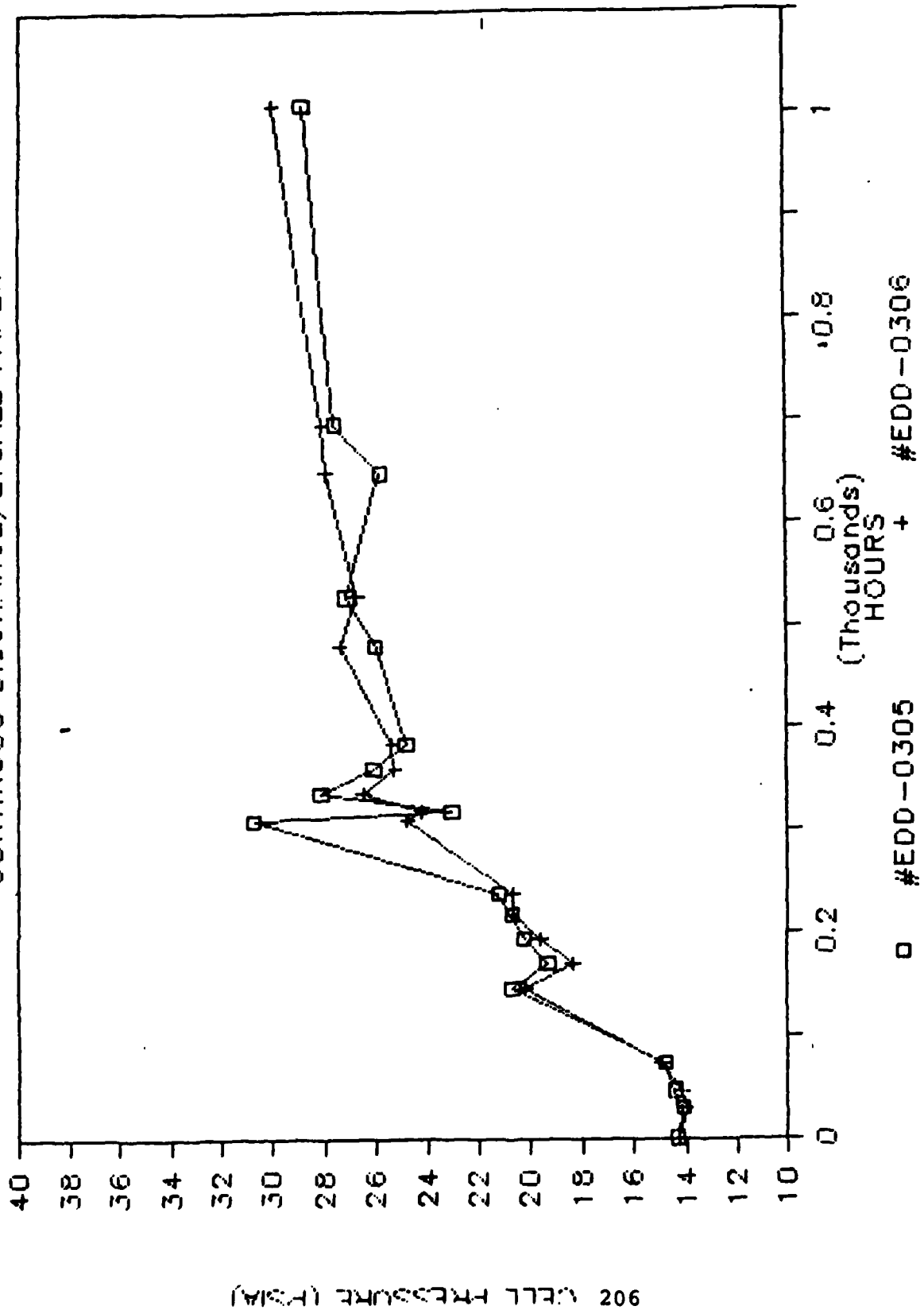


FIGURE 62

CELL REACTIONS TASK III/PRESSURE STUDY

CONTINUOUS DISCHARGE / SO2 PURGED

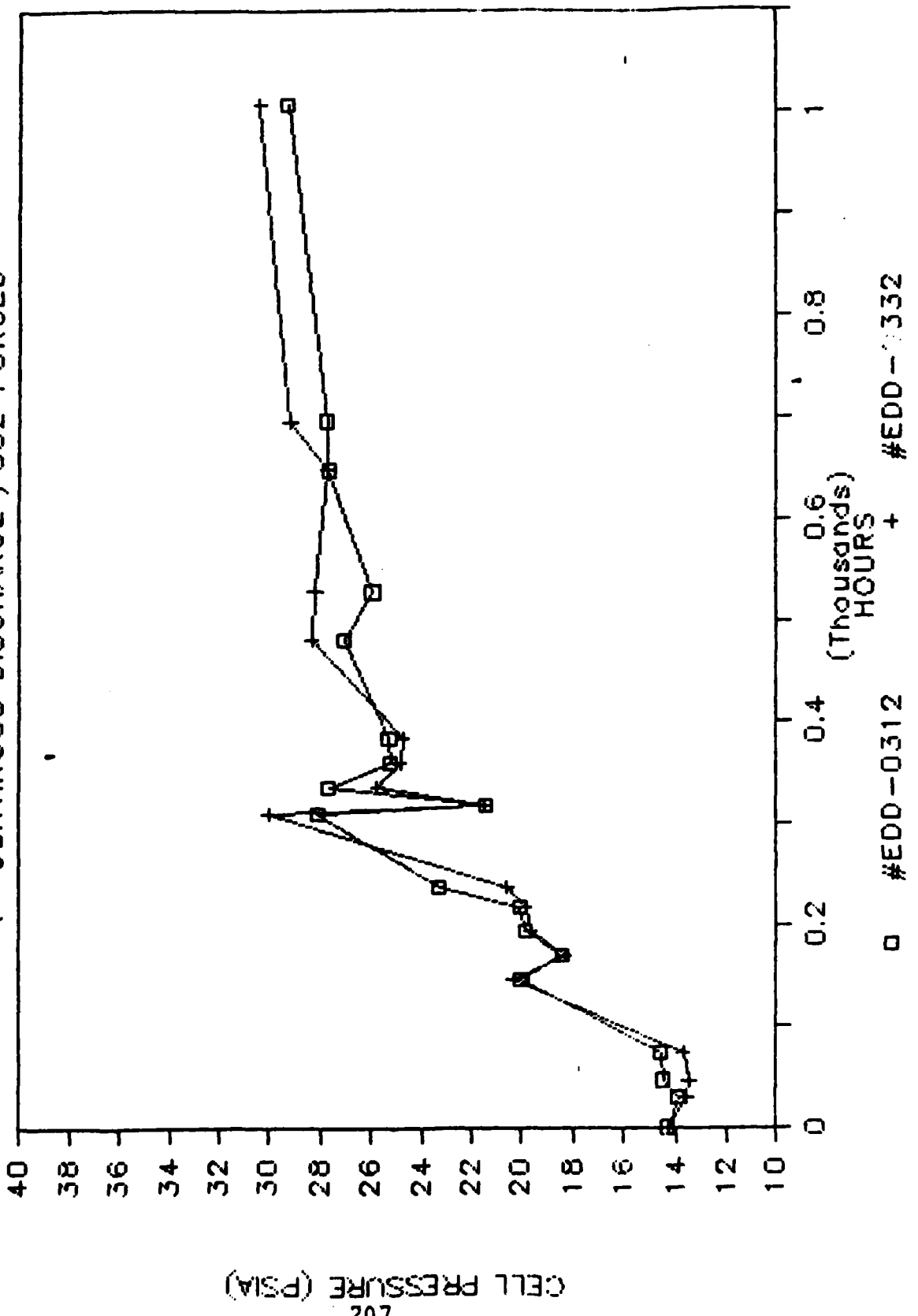


FIGURE 63

CELL REACTIONS TASK III/PRESSURE STUDY

CONTINUOUS DISCHARGE/LOW N2 LITHIUM

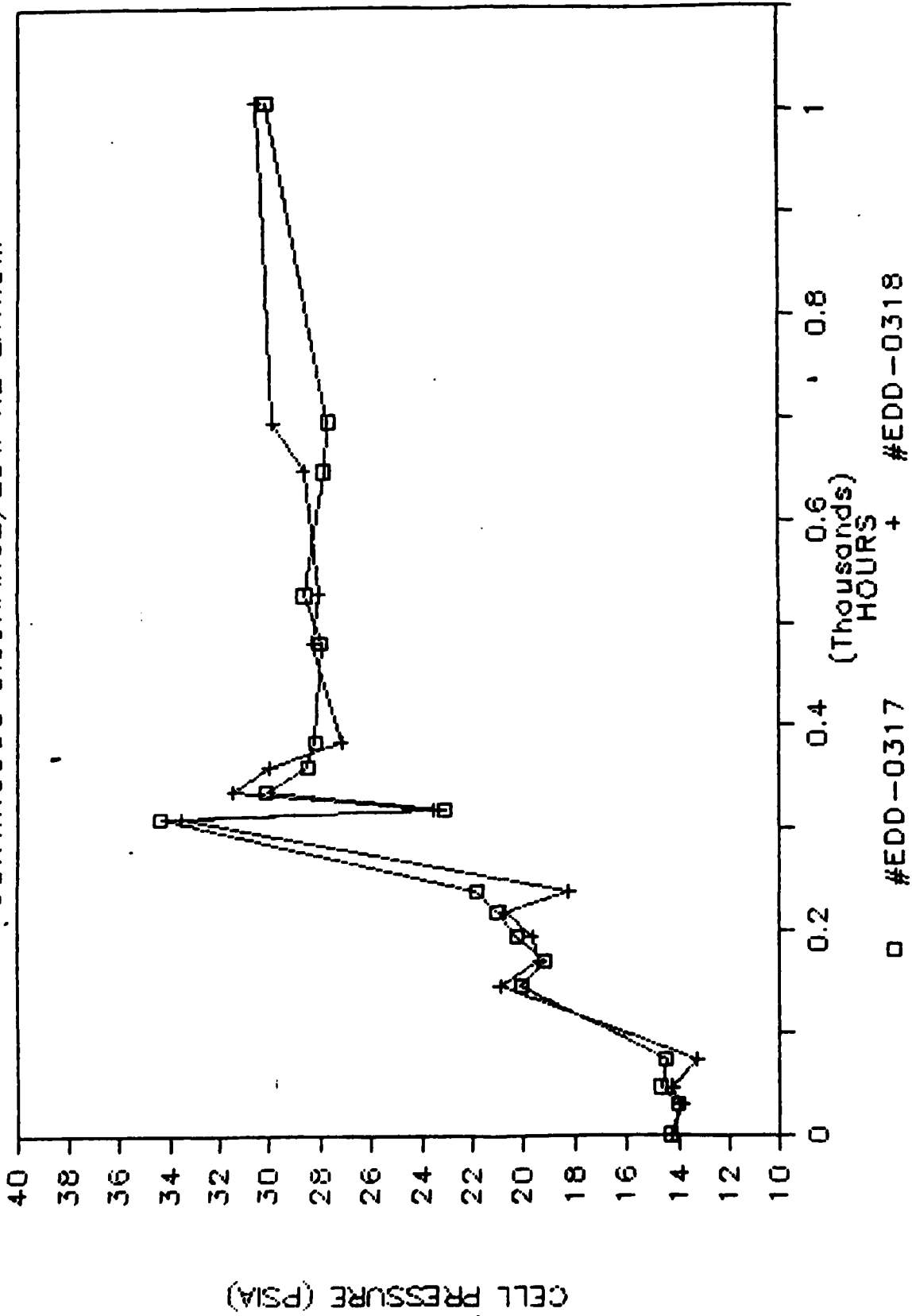


FIGURE 64

CELL REACTIONS TASK III/PRESSURE STUDY

CONTINUOUS DISCHARGE / GULF CARBON

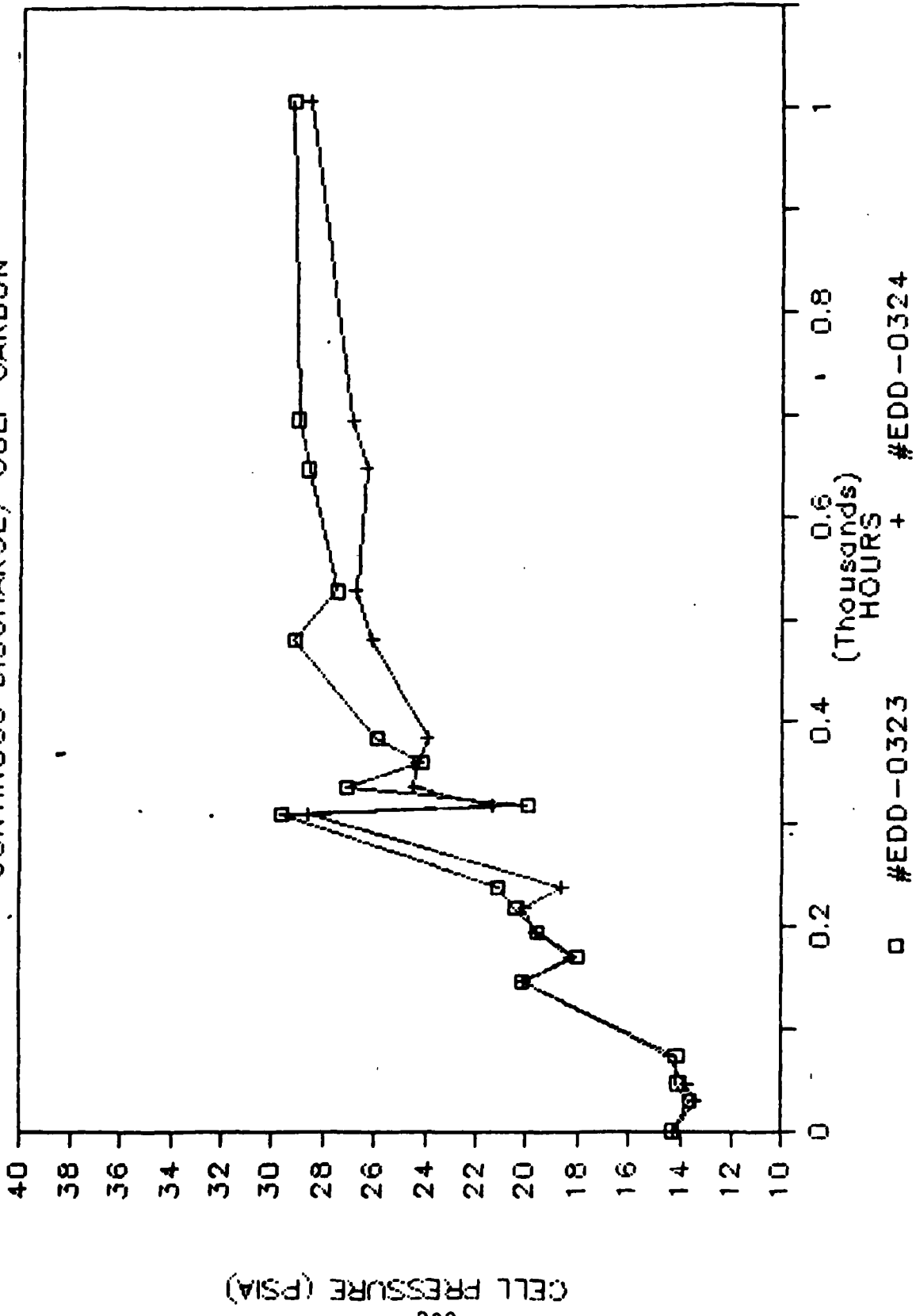


FIGURE 65

CELL REACTIONS TASK III/PRESSURE STUDY

INTERMITTENT DISCHARGE/BASELINE CELLS

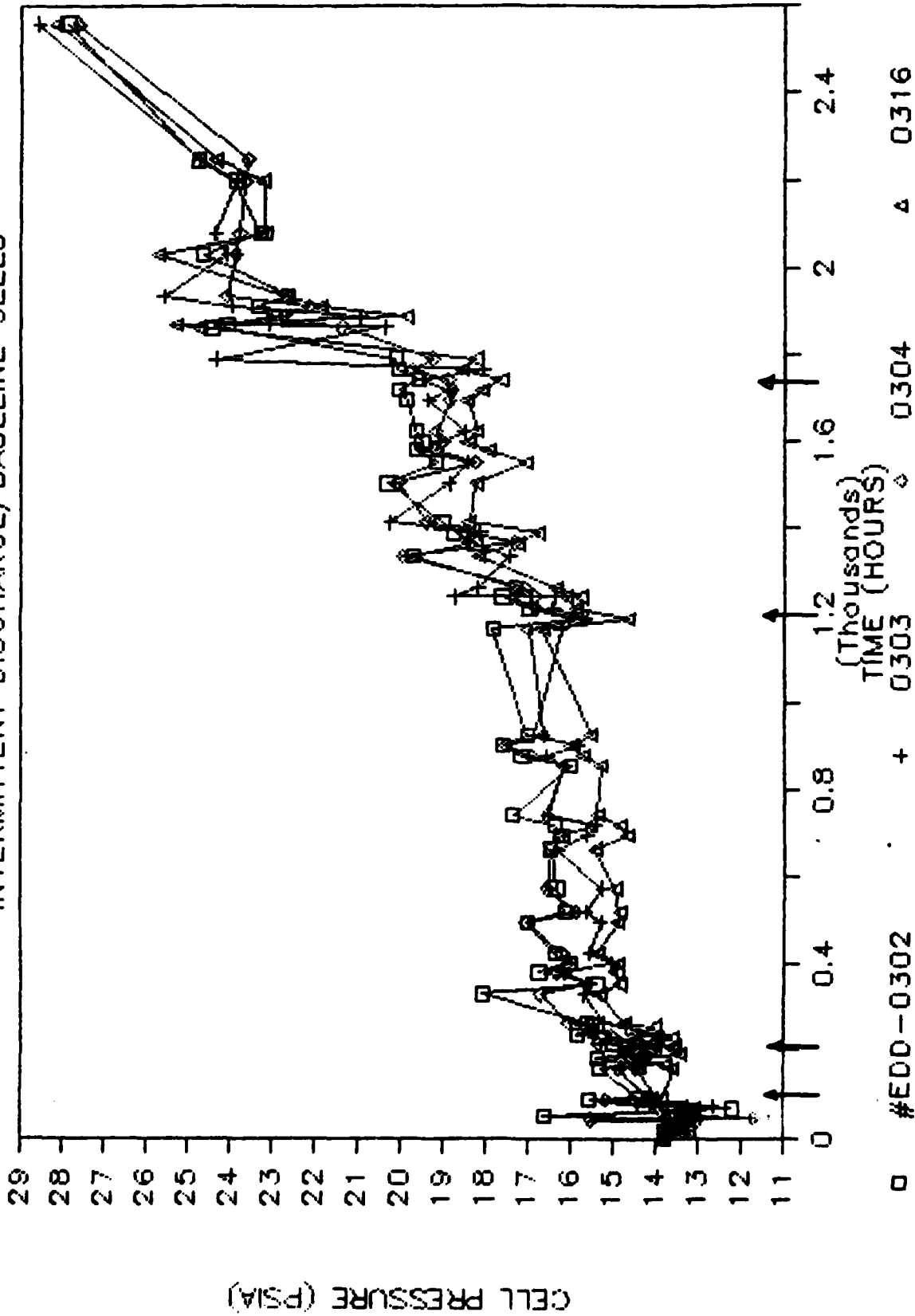


FIGURE 66

CELL REACTIONS TASK III/PRESSURE STUDY

INTERMITTENT DISCHARGE/LOW N2 LITHIUM

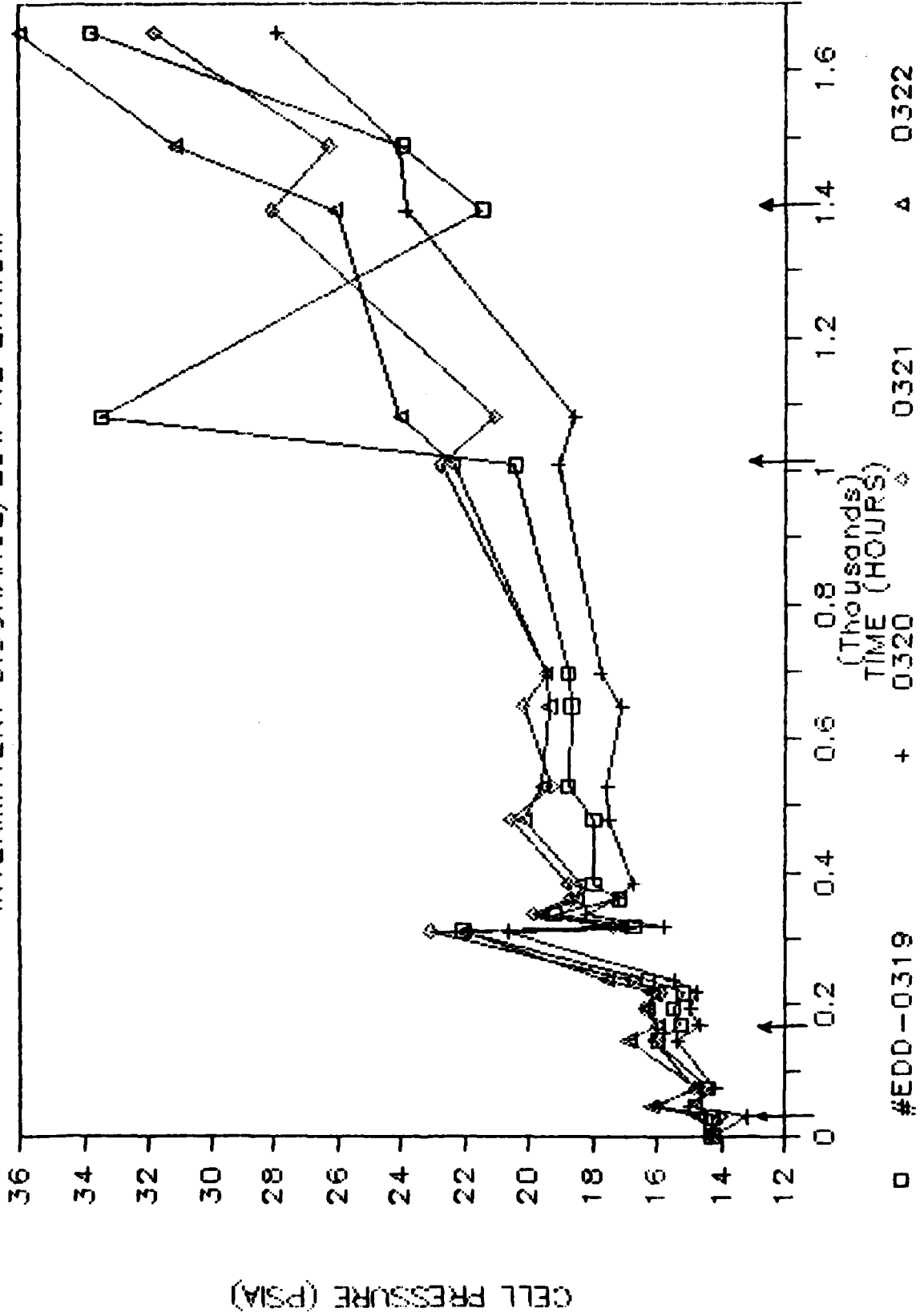


FIGURE 67

CELL REACTIONS TASK III/PRESSURE STUDY

INTERMITTENT DISCHARGE/BINDERLESS PAPER

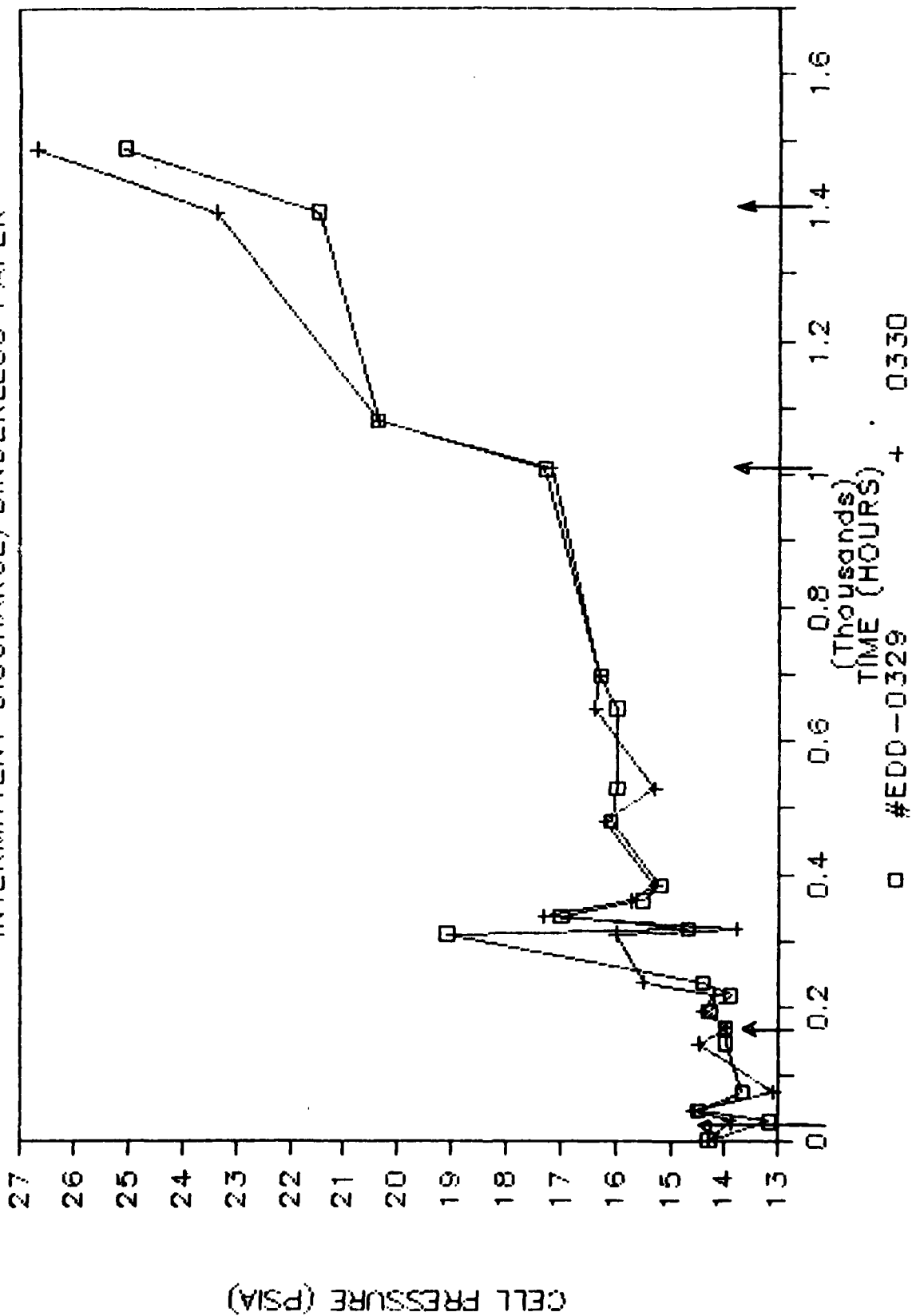


FIGURE 68

CELL REACTIONS TASK III/PRESSURE STUDY

INTERMITTENT DISCHARGE/SO2 PURGED

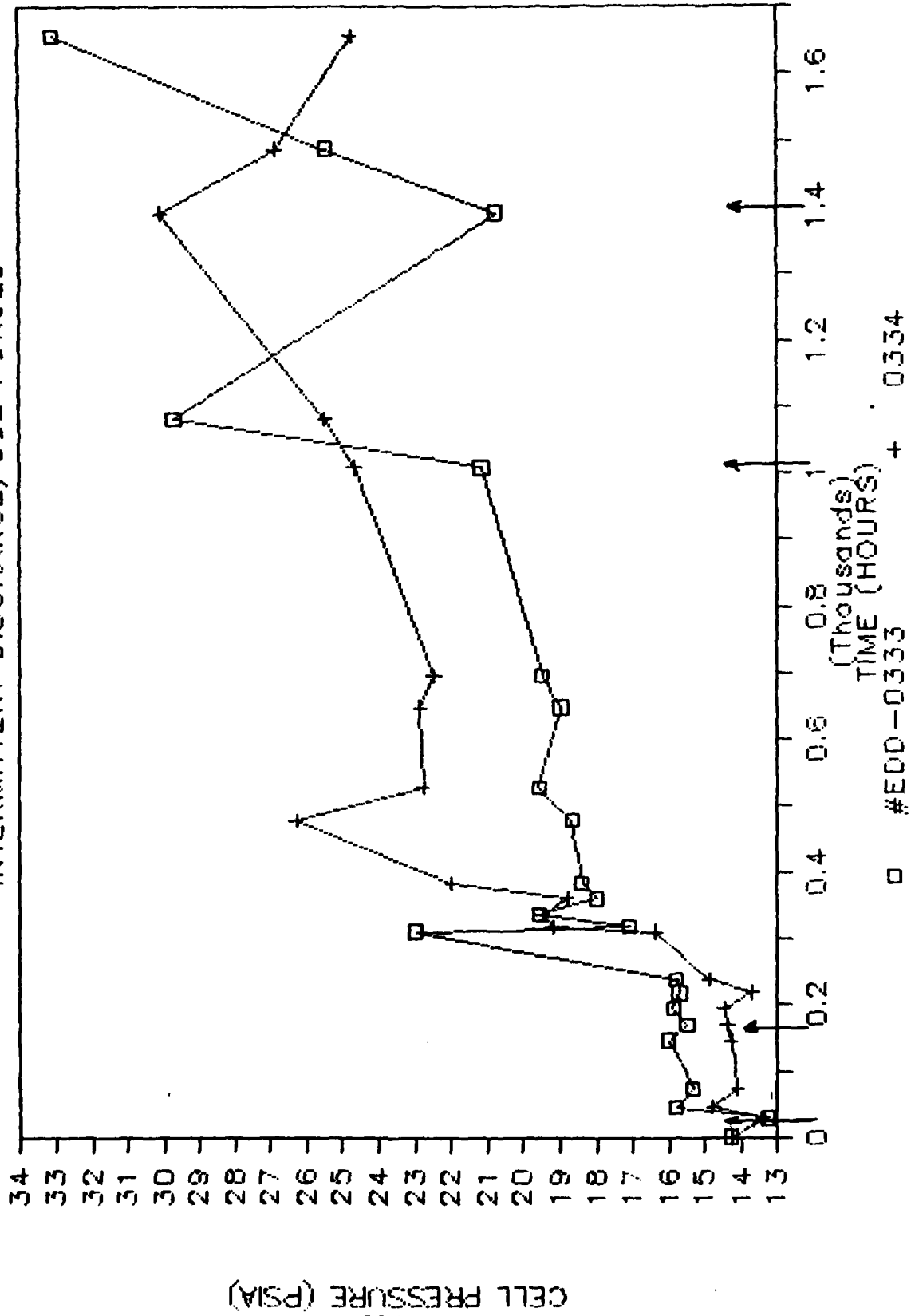


FIGURE 69

TASK III / PRESSURE STUDY

INTERMITTENT DISCHARGE GULF CARBON

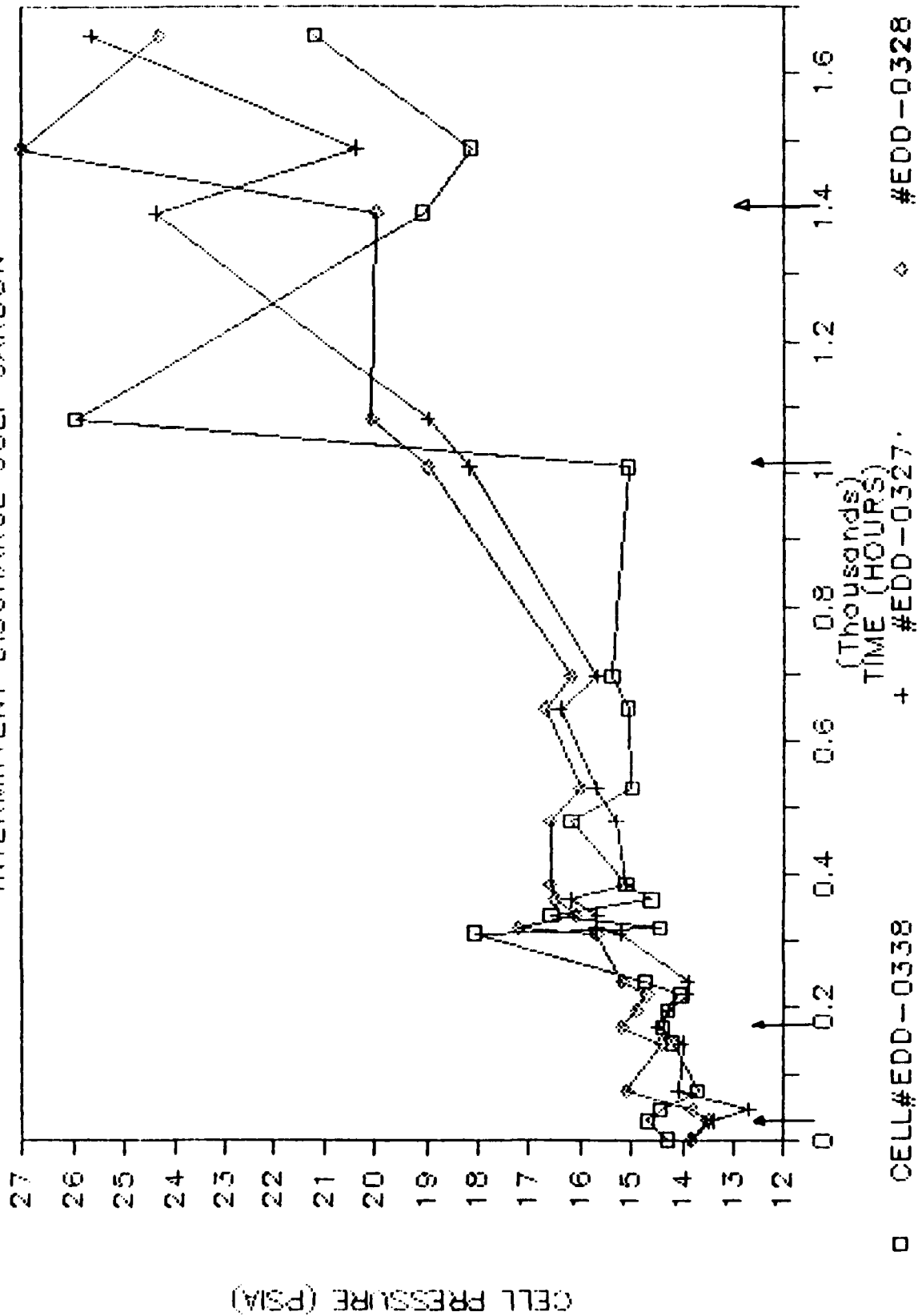


FIGURE 70

ROOM TEMP VS TIME

MEASURED @ TIME OF PRESS READINGS

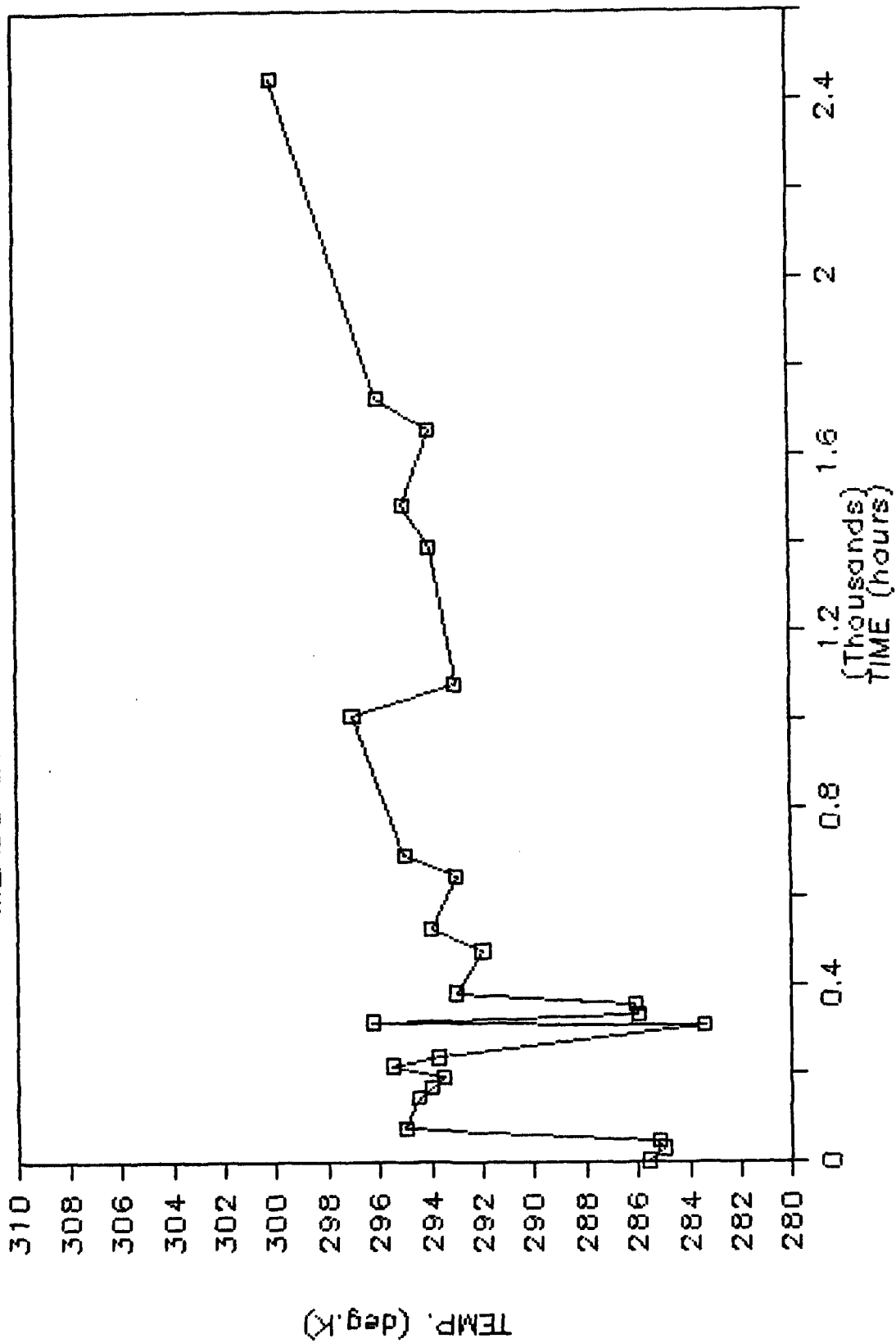


Figure 71

Variation in Ambient Temperature

FIGURE 72. Cell Pressure During and After Continuous Discharge

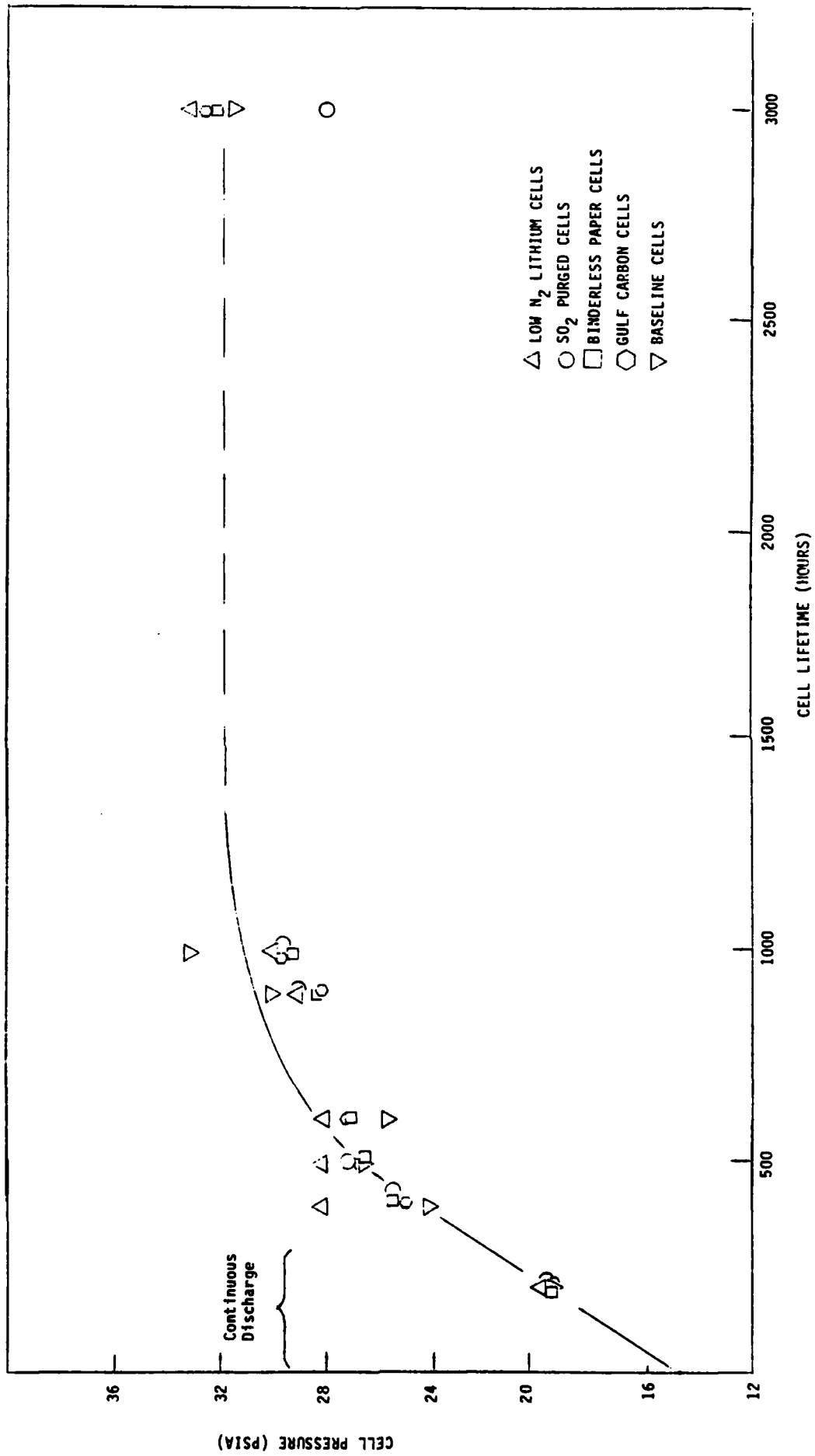
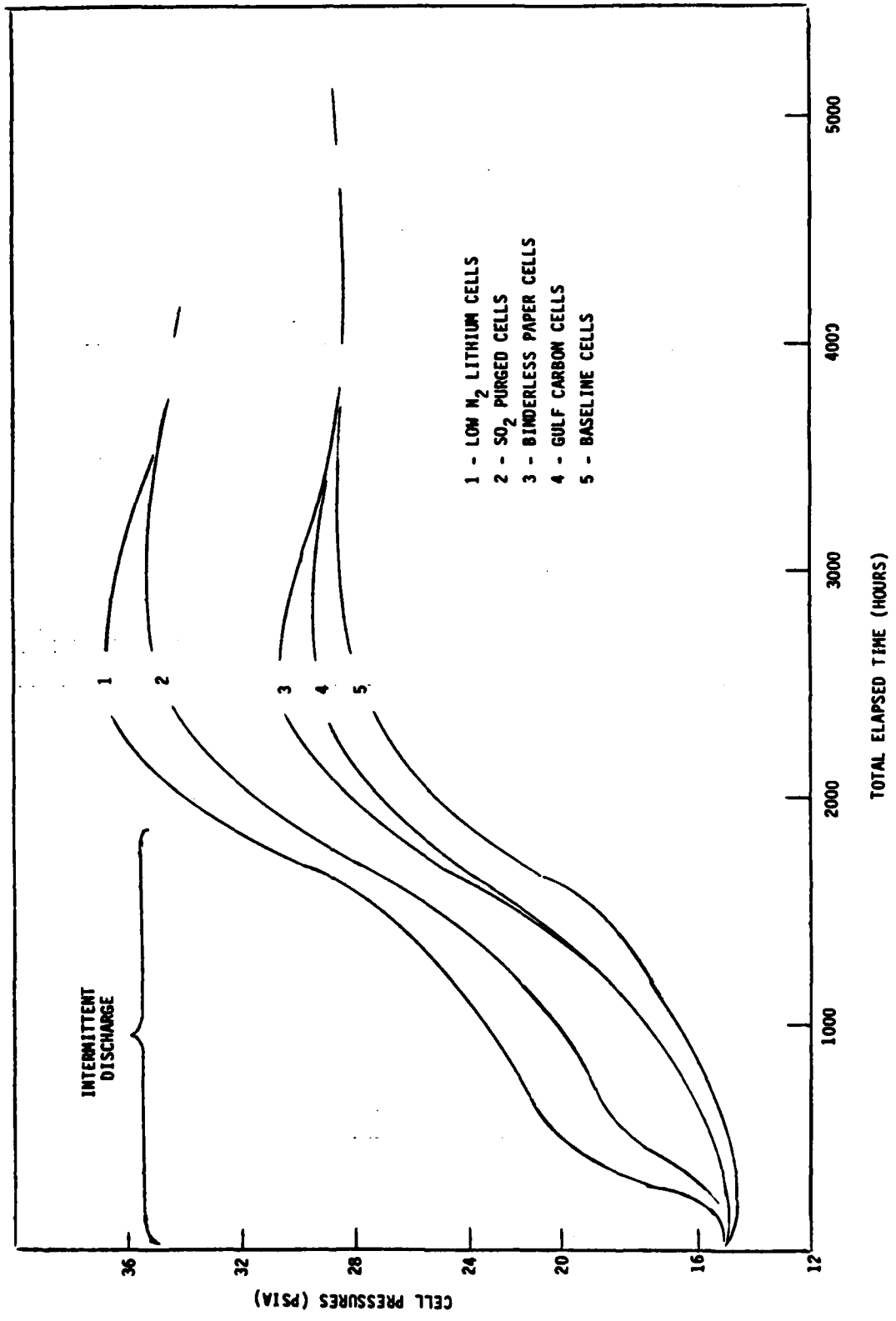


FIGURE 73. Averaged, Smoothed Pressure Curves For Each Cell Type



REFERENCES

1. W. Clark, F. Dampier, A. Lombardi and T. Cole, U.S. Air Force Systems Command, Wright Patterson AFB, Ohio, Interim Report, No. AFWAL-TR-83-2083, Dec. (1983).
2. A.I. Attia, K.A. Gabriel and R.P. Burns, Naval Surface Weapons Center, Report No. 838-012, January 1983.
3. R. Williams, F. Tsay, S. Kim, M. Evans, Q. Kim, A. Rodriguez, B.J. Carter and H. Frank. Proc. of the Symposium on Lithium Batteries, The Electrochem. Soc. Proceedings Volume 84-1,60 (1984).
4. A.J. Bard and L.R. Faulkner, 'Electrochemical Methods, Fundamentals and Applications', John Wiley & Sons, New York, Pg. 218 (1980).
5. A.N. Dey, Thin Solid Films, 43, 131 (1977)
6. C.R. Schlaijker, F. Goebel, and N. Marincic, J. Electrochem. Soc. 126, 513 (1979).
7. W.L. Bowden and A.N. Dey, J. Electrochem. Soc. 127, 1419 (1980).
8. N. Marincic and A. Lombardi, U.S. Army, Final Report No. ECOM-74-0108-F, April (1977).
9. A.N. Dey, U.S. Army Quarterly Report, ECOM-74-0109-1, July (1974).
10. J. Bressan, G. Feuillade, and R. Wiart, J. Electrochem. Soc. 129, 2649 (1982).

REFERENCES

11. R.P. Martin, W.H. Doub, J.L. Roberts and D.T. Sawyer, *Inorg. Chem.* 12, 1921 (1973).
12. K.A. Klinedinst and M.L. McLaughlin, *J. Chem. Eng Data* 24, 203 (1979).
13. D.F. Burow in, The Chemistry of Nonaqueous Solvents, Vol. III, Ed. J.J. Lagowski, P. 144 (1970).
14. H.V. Venkatesetty, Final Report, Naval Ocean Systems Center, Contract No. N00123-81-C-0443, December 1982.
15. Y. Bedfer, J. Corset, M.C. Dhamelinourt, F. Wallart and P. Barbier, *J. Power Sources*, 9, 267 (1983).
16. M.C. Day and J. Selbin, *Theoretical Inorganic Chemistry*, Reinhold Publ. Corp. New York (1962).
17. R. Keller, J.N. Foster, D.C. Hanson, J.F. Hon, and J.S. Muirhead, NASA Report No. CR-1425 August (1969).
18. J.J. Auburn and N. Marincic, Proc. 9th International Power Sources Symposium, Brighton, 683 (1975).
19. C.R. Schlaijker, "Lithium Oxyhalide Cells" in "Lithium Batteries", J.P. Gabano, ed., Academic Press, New York (1983).
20. A.W. Adamson, "Physical Chemistry of Surfaces", Interscience Publ. (1967).
21. D. Kivelson, *J. Chem. Phys.* 22, 904 (1954).
22. D.F. Burow, in "The Chemistry of Nonaqueous Solvents", Vol. III, Ed. J.J. Lagowski, P. 138 (1970).

REFERENCES

23. M.C. Day and J. Selbin, "Theoretical Inorganic Chemistry", Reinhold Pub. Co., P 209 (1962).
24. N. Doddapaneni, Proc. 30th Power Sources Symposium, The Electrochem. Soc., P. 169 (1982).
25. N. Doddapaneni, U.S. Army, ERADCOM, Final Report No. DELET-TR-81-0381-F (August 1982).
26. F. Walsh, R.S. Morris and M. Yaniv, Abstract 33, Electrochemical Society, Fall Meeting (1983).
27. J.R. Driscoll and S. Szpak, Proc. 30th Power Sources Symposium, The Electrochem Soc., P. 166 (1982).
28. S. Szpak and J.R. Driscoll, J. Power Sources 10, 343 (1983).
29. A.N. Dey, Proc. 27th Power Sources Symposium, Atlantic City, N.J. 42 (1976).
30. A.N. Dey, U.S. Army, ERADCOM, Final Report No. DELET-TR-74-0109 F, July (1978).
31. H.A. Frank, Jet Propulsion Laboratory, Pasadena, CA, Publication 80-6 (1980).
32. F. Goebel, R. McDonald, G. Younger, U.S. Air Force, Wright-Patterson AFB, Ohio, Technical Report No. AFWAL-TR-80-2121, January 1981.
33. D.I. Chua, J.O. Crabb and S.L. Deshpande, Proceedings of the 28th Power Sources Symposium, P. 247 (1978).
34. K.M. Abraham and R.M. Mank, J. Electrochem. Soc. 127, 2091 (1980).

REFERENCES

35. F.W. Dampier and R.C. McDonald, Proc. Symposium on Lithium Batteries, The Electrochem. Soc., Vol 84-1, 154 (1984).
36. R.C. McDonald and F.W. Dampier, Naval Surface Weapons Center, Final Report, No. N60921-81-C-C229 (AD-A--12930216), January 1983.
37. A.N. Dey, Proc. 28th Power Sources Symposium, Atlantic City, N.J. 251 (1978).
38. W.P. Kilroy and S.D. James, J. Electrochem. Soc. 128, 934 (1981).
39. GTE Laboratories, Inc., Office of Naval Research, Contract No. N00014-76-C-0524, Final Report, Jan (1979).
40. J. Bene, NASA Goddard Flight Center Battery Workshop, Greenbelt, Maryland, 111 (1980).
41. V.O. Catanzarite, U.S. Patent 4,331,745, May 25 (1982).
42. R.L. Ake, D.M. Oglesby and W.P. Kilroy, J. Electrochem. Soc. 131, 968 (1984).
43. K.A. Klinedinst and M.L. McLaughlin, J. Chem. and Eng. Data 24, 203 (1979).
44. GTE Sylvania Inc., Document No. 00-1319104, Contract No. F 33615-77-C-2021, U.S. Air Force, Needham Heights, MA, Oct. 18 (1978).
45. TRW Inc., Defence and Space Systems Group, Ballistic Missiles Division, Qualification Testing Status Report Minuteman Extended Survival Program, February 1981.
46. K.F. Garoutte and D.L. Chua, Proc. 29th Power Sources Symposium, The Electrochem. Soc., 153 (1980).

REFERENCES

47. R.L. Zupancic, L.F. Urry and V.S. Alberto, Proc. 29th Power Sources Symposium, The Electrochem. Soc. 157 (1980).
48. F.A. Cotton and G. Wilkinson, "Advanced Inorganic Chemistry", Third Edition, P. 440, John Wiley & Sons, New York (1972).
49. B.J. Carter, R.M. Williams, M. Evans, Q. Kim, S. Kim, F.D. Tsay, H. Frank and I. Stein, Proc. Symposium on Lithium Batteries, The Electrochemical Soc., Proceedings Volume 84-1, 162 (1984).
50. D.J. Salmon, M.E. Peterson, L.L. Henricks, L.L. Abels, and J.C. Hall, J. Electrochem. Soc. 129, 2496 (1982).
51. C.R. Schlaijker, P.G. Garvy and A. Lombardi, Progress in Batteries and Solar Cells, 5, 302 (1984).
52. K.A. Klinedinst; J. Electrochem. Soc., 131, 492 (1984).
53. G.E. Blomgren, V.Z. Leger, T. Kalnoki-kis, M.L. Kronenberg and R.J. Brodd, Proc. 11th International Power Sources Symposium, Brighton, P. 583, Sept. 1978.
54. D.R. Cogley, M.J. Turchan, G.L. Holleck, J.R. Driscoll and D.E. Toland, S.B. Brummel and P.G. Gudrais, Contract No. DAAB 07-74-C-0030, U.S. Army, ECOM Ft. Monmouth, Second Quarterly (May, 1974); Fifth Quarterly (April, 1975); Sixth Quarterly Report (July, 1975).
55. J.C. Bailey and J.P. Kohut, Proc. 12th International Power Sources Symp. P.17, Academic Press, New York (1981).
56. N. Doddapaneni, Abstract No. 83, Electrochemical Society Meeting, Minneapolis, Minnesota, May (1981).
57. W.K. Istone and R.J. Brodd, J. Electrochem. Soc. 129, 1853 (1982).

REFERENCES

58. A.I. Attia, C. Sarrazin, K. A. Gabriel and R.P. Burns, J. Electrochem. Soc., 131, 2523 (1984).
59. W.K. Istone and R.J. Brodd, J. Electrochem. Soc. 131, 2467 (1984).
60. D. Chua, W.C. Merz, W.S. Bishop, Proceedings of the 27th Power Sources Symposium, Atlantic City, N.J., pp 33-37, The Electrochemical Soc. (1977).
61. R.C. MacDonald, J. Electrochem. Soc. 129, 2453 (1982).

END

FILMED

6-85

DTIC